מידע זה מפורסם לפי הוראות סעיף 6א לחוק חופש המידע, התשנ"ח – 1998, והוראות תקנות חופש המידע (העמדת מידע על איכות הסביבה לעיון הציבור), התשס"ט – 2009.
המידע דווח למשרד להגנת הסביבה, וטרם נבדק על ידי גורמי המקצוע שלו.

Environmental Monitoring Program
Leviathan Production Platform
Offshore Israel

December 2020 Marine Environmental Monitoring Report

June 2021

Prepared for:

Noble Energy Mediterranean Ltd.
1 Arik Einstein, Herzliya
4659070 Israel

Prepared by:

Marine Ventures International Inc.
147 Bar-Yehuda Road, Nesher
3688306 Israel

Environmental Monitoring Program
Leviathan Production Platform
Offshore Israel
December 2020 Marine Environmental Monitoring Report

DOCUMENT NO. MVI-NOBLE-IL-21-3630-07C-REP-01-FIN

Internal review process					
Version	Date	Description	Prepared by:	Reviewed by:	Approved by:
INT-01	06/02/2021	Initial draft for science review	[NAME]	[NAME] [NAME]	[NAME]
INT-02	06/03/2021	TE review	[NAME]	[NAME]	[NAME]

Client deliverable			
Version	Date	Description	Project Manager Approval
01	06/09/2021	Client deliverable	[NAME]
FIN	06/28/2021	Final client deliverable	[NAME]

The electronic PDF version of this document is the Controlled Master Copy at all times. A printed copy is considered to be uncontrolled and it is the holder's responsibility to ensure that they have the current version. Controlled copies are available upon request from the CSA Document Production Department.

Author Certification Signature

[NAME], M.Sc.
Project Scientist | Project Manager [SIGNATURE]
CSA Ocean Sciences Inc.
E-mail: [E-MAIL]

[NAME], Ph.D.
Senior Scientist | Energy Programs Director [SIGNATURE]
CSA Ocean Sciences Inc.
E-mail: [E-MAIL]

[NAME], M.Sc.
Senior Scientist | Managing Director [SIGNATURE]
Marine Ventures International Inc.
E-mail: [E-MAIL]

[NAME], B.Sc.
Project Scientist
Marine Ventures International Inc. [SIGNATURE]
E-mail: [E-MAIL]

Executive Summary

Noble Energy Mediterranean Ltd. (Noble Energy) is developing a gas production and transportation system connecting the Leviathan Field to the Israeli gas market off the northern coast of Israel. This project is herein referred to as the Leviathan Field Development Project. Natural gas from the North and South Leviathan lease blocks is being produced from subsea wells in the Leviathan Field and transported through subsea production flowlines to the offshore Leviathan Production Platform (LPP) and then to a landing location in the vicinity of Dor through a transportation system (pipelines). The LPP is located approximately 10 km offshore Dor, Israel, in a water depth of 86 m. Noble Energy commenced operation of the LPP in December 2019.

Noble Energy engaged Marine Ventures International, Inc. (MVI) and CSA Ocean Sciences Inc. (CSA) to conduct an environmental baseline survey (2019 LPP EBS) in July and August 2019. The main objectives of the 2019 LPP EBS were to determine environmental conditions (i.e., chemical, physical, and biological) at the LPP location, to enable assessment of the effects from future platform operations, identify parameters within the ecosystem that may be sensitive to change, and provide a reference point to evaluate future claims of impacts. Subsequently, after commencement of operation of the LPP, Noble Energy engaged MVI and CSA to conduct an environmental monitoring survey (2020 LPP EMS) during active production at the LPP. The main objectives of the LPP EMS were to:

- Determine environmental conditions (i.e., chemical, physical, and biological) at the LPP location after installation to assess the effects from platform operations; and
- Identify parameters within the ecosystem that may be sensitive to change and provide a reference point to evaluate future claims of impacts.

The 2020 LPP EMS utilized the same survey design and scope as was approved for the 2019 LPP EBS. The sampling effort for the 2020 LPP EMS consisted of sampling physical and chemical components. Water column profiles of conductivity-temperature-depth, dissolved oxygen, pH, fluorescence, and turbidity as well as seawater samples were collected at 20 stations, including four stations in each distance strata (Near-Platform [50 to 150 m from the LPP], Near-Field [150 to 350 m], Mid-Field [350 to 500 m], Far-Field [500 to 1,000 m] and Reference [3,000 m]), and at two additional stations east of the LPP towards the Israeli shoreline. Seawater samples were collected within the near-surface (i.e., 10 m water depth), mid-water (i.e., 40 m water depth), and near-bottom (approximately 1 m above the seafloor) at each station.

Sediment sampling stations were positioned using a stratified random sampling pattern with stratification based on both distance and direction (northeast, northwest, southeast, and southwest quadrants) from the LPP. A total of 46 sediment stations (including reference stations) were sampled for chemical and infauna analysis. This sampling design allows for the statistical assessment of impacts both in a directional and/or distance-based manner.

Where applicable, results from the 2020 LPP EMS were compared with results from samples collected during the 2019 LPP EBS and with samples from the 2014 Leviathan Field Development EBS which were collected in the vicinity of the LPP prior to installation. Six samples were collected in the vicinity of the LPP during the 2014 survey for most analytes. For the 2020 LPP EMS data, a three-way analysis of variance (3ANOVA) was performed on sediment chemistry and infauna parameters to determine overall impacts within sediments based on distance, direction, survey, and all interaction terms.

Hydrographic profiles of the water column at the seawater sampling stations locations showed that surface waters were cool and isothermal (approximately 21°C) throughout the water column. Salinity was stable throughout the water column at approximately 39 PSU. pH was also stable throughout the water column at approximately 8.2. Turbidity was low (<1 nephelometric turbidity units) throughout the water column all stations; a near-seafloor turbidity spike at Station NP-NW-44 was likely caused

by remotely operated vehicle (ROV) thrusters. Fluorescence was generally homogeneous throughout the water column, with values of approximately 0.6 mg^{-3}. Due to the winter season, there was no photosynthetic maximum. The water column was well oxygenated (6.7 mg L^{-1}) throughout the water column with values generally homogeneous from the surface to the seafloor.

All total petroleum hydrocarbons (TPH), phenols, and benzene, toluene, ethylbenzene, and xylenes (BTEX) concentrations were below the analytical laboratory's method reporting limit in all seawater samples. Because TPH was not detected in any sample, polycyclic aromatic hydrocarbons (PAHs) were not analyzed. Concentrations of nutrients were either below the laboratory's method reporting limit (nitrate and ammonium) or low (total nitrogen, total phosphorus, total organic carbon [TOC]). Total suspended solids concentrations were low in all samples (2.4 to 9.1 mg L^{-1}). All concentrations of radionuclides (except one) in seawater (^{226}Ra, ^{228}Ra, and ^{228}Th) were well below the analytical laboratory's minimum detectable concentration. One value for ^{228}Th at station REF-NE-37 was just above the laboratory's minimum detectable concentration.

Sediment samples were analyzed for grain size and were classified as sand silt clay (27 stations), sandy clay (8 stations), clayey sand (9 stations), or silty sand (3 stations). Grain size was generally similar by distance and direction from the platform. While several Near Platform samples were among the sandiest collected during the 2020 LPP EMS, there was no substantial clustering of samples by distance strata based on grain size structure. Sediment TOC concentrations ranged from 0.12% to 0.81% and were general similar across directional strata. TOC concentrations were slightly lower in the Near Platform strata as compared with other distance strata. A 3ANOVA revealed significantly lower TOC concentrations in the Near Platform strata as compared with the Mid-Field strata, but statistically similar to other distance strata.

Sediment samples were analyzed for aluminum, arsenic, barium, cadmium, chromium, copper, iron, lead, mercury, nickel, and zinc. Metals concentrations were compared to the effects range low (ERL) and effects range media (ERM) benchmark values. Additionally, 2020 results were assessed in context to those of sediments collected during the 2019 LPP EBS and the 2014 Leviathan Field Development EBS. Sediment metals concentrations for the current survey were generally low and generally similar to background conditions as measured during the 2014 Leviathan Field Development EBS and the 2019 LPP EBS.

All concentrations of cadmium were below the laboratory's method reporting limit. All concentrations of aluminum, lead, mercury, and zinc were below the ERL. Concentrations of arsenic, chromium, and some concentrations of copper were above the ERL, but below the ERM. Most of the concentrations of nickel were above the ERL, with approximately one third above the ERM. Elevated concentrations of arsenic, chromium, copper, and nickel also occurred during the 2019 LPP EBS and the 2014 Leviathan Field Development EBS and are considered ambient for the region. A 3ANOVA analysis was completed where the main effects were distance, direction, and survey year. Sediment barium concentrations significantly differed among distance strata. Barium concentrations collected from within the Near-Platform strata were significantly higher when compared against the Mid-Field, Far-Field, and Reference strata. Sediment concentrations of other metals did not significantly differ among distance strata, where statistical analysis was applicable.

Sediment concentrations of chromium, copper, iron, nickel, and zinc differed among directional quadrants. Concentrations of these metals in sediments were significantly higher within the northwest and southwest platform quadrants relative to the northeast and southeast quadrants. Arsenic concentrations were significantly higher within the southwest quadrant relative to the southeast quadrant; but were otherwise statistically similar to one another. Sediment concentrations of barium, iron, and lead did not significantly differ among platform strata. Sediment concentrations of chromium and mercury collected around the LPP had significantly higher concentrations during the 2019 LPP EBS relative to the 2020 LPP EMS. Sediment concentrations of other metals did not significantly differ between survey years, where statistical analysis was applicable.

Sediment samples were analyzed for TPH, PAHs, and phenols. TPH concentrations ranged from 14 to 26 µg g^{-1} with an overall average of 19.6 ± 3.3 µg g^{-1}. Average TPH concentrations were similar by distance and direction. Total PAH concentrations ranged from 44.3 to 188 ng g^{-1} with an overall average of 80.9 ± 28.0 ng g^{-1}. Concentration of phenols was below the laboratory's method reporting limit for all samples except for one (0.44 µg kg^{-1} at Station MF-SE-19).

A 3ANOVA was performed on TPH and total PAHs where the main effects were distance, direction, and survey year. There was no significant three-way interaction among the main effects for TPH, but there was a significant interactive effect for distance and survey year. There was no significant difference in TPH concentration among the distance strata. All Near Platform TPH concentrations were significantly lower during the 2020 LPP EMS as compared with the 2019 LPP EBS. There were no significant differences in sediment total PAH concentrations, which indicate concentrations are statistically similar within the region surrounding the LPP both spatially (i.e., distance and direction) and temporally (i.e., survey year).

All sediment concentrations of radionuclides (^{226}Ra, ^{228}Ra, and ^{228}Th) were below the laboratory's method reporting limit.

Video data were collected near the LPP to assess species composition and abundance of fish assemblages and epibenthic fouling communities associated with the LPP. Using the ROV, video data were collected from all vertical and horizontal structural components (legs and cross members) on the up-current and down-current sides of the LPP. The epibenthic fouling community was primarily composed of sponges, bryozoans, ascidians, and bivalves. The vertical distribution of taxa across the different sampling depths was generally similar at all platform legs. Serpulids, bivalves, and a form of branching bryozoa were prevalent and found at all depths. The encrusting ascidian *Didemnum* sp. was also prevalent and found from 10 to 60 m depth, while the solitary ascidian *Herdmania momus* was found from 15 to 70 m depth, and the solitary ascidian *Phallusia nigra* was found sporadically down to a maximum depth of 50 m. Various sponge species of the class Demospongia were found from 10 m depth all the way down to the bottom of the platform legs while the calcareous sponge *Leucosolenida* sp. were observed between depths of 15 and 60 m. Hydrozoans and barnacles were found at the shallow end of the water column on the northeastern side (and down to a maximum depth of 40 and 20 m, respectively) while at the southwest side both groups extended their range further down the water column. The crinoid *Antedon mediterranea* was the most abundant of the motile benthic fauna and occurred from a depth of 40 m down to 80 m with the highest density found at 60 m depth on the northeastern side.

Analysis of the video of the LPP legs revealed a total of eight fish species. Six of the eight species were observed on the northeast side and were distributed among most strata along the vertical extent of the platform. No fish were observed at the 40 m and 50 m depths. The shallow water depths (10 m to 30 m) were numerically dominated by the blue runner (*Caranx crysos*) and white trevally (*Pseudocaranx dentex)*. White trevally were the most ubiquitous, found among half of the strata, ranging from 10 m to 30 m depth and amassing the greatest abundance overall on the northeast side with 18 individuals. The fishes observed at the LPP were typical of those found in the region and within the habitat preferences (temperature, clarity, depth) of individual species.

Video data were also collected from 12 sites approximately 3.5 km north of the LPP on exposed kurkar hardbottom formations. The locations were characterized by a weak near-bottom westerly current, poor near-bottom visibility, and a large amount of anthropogenic debris including monofilament line, weighted nets, steel cables, and nets. Despite an official government decision made on regional banning of fishing activities north of Dor-HaBonim area at all water depths within the Israeli territorial waters (2016 update to fishing regulations), trawling vessels are still sighted around the LPP deploying nets and potentially causing additional damages to these kurkar hardbottom formations and associated benthic communities. Trawl fishing activities with potential impacts could confound a continuous assessment of any impact potentially caused by the LPP. Similar to previous surveys, the hardbottom formations had variable biological coverage, ranging from <1% to

approximately 25% for horizontal surfaces and up to approximately 75% for vertical surfaces. Reduced sediment cover on several of the horizontal surfaces of the kurkar hardbottom features resulted in biological cover qualitatively estimated at the higher end of this range. Epifauna mainly consisted of encrusting and bulky sponges, but cnidarians, annelids, echinoderms, bryozoans, and decapod shrimp and lobsters were also observed. Several species of fish were also observed, including gobies, lionfish, wrasses, porgies, amberjacks, scorpionfish, and eels. Overall, the biotic assemblage was similar between the 2020 LPP EMS and surveys conducted at the kurkar hardbottom formations in 2018-2019, and no detectable temporal changes were noted among surveys.

Benthic grab samples were collected from 46 stations during the 2020 LPP EMS. The 46 samples yielded a total of 65,599 individuals from 120 taxa. Abundance was high at all stations and ranged from 499 to 2,845 individuals with an overall average of 1,361 ± 497 individuals per station. Infauna density ranged from 2,661 to 15,173 individuals m^{-2}. The most numerically dominant group were nematodes (n = 39,172) followed by Nephtyidae polychaetes (n = 2,703) and *Prionospio* sp. (n = 2,617). Overall, identified taxa included individuals from the phyla Annelida, Arthropoda, Cnidaria, Echinodermata, Hemichordata, Mollusca, Nematoda, Nemertea, Phoronida, Platyhelminthes, Porifera, and Sipincula. Species richness was moderate at all stations, ranging from 25 to 76 species per station. Values of Margalef's richness index (D) were moderate to high, ranging from 3.4 to 10.2, with an overall average of 7.5 ± 2.4. Calculated values of Peilou's Evenness (J') were variable, with values ranging from 0.12 to 0.70 and an overall average value across all stations of 0.46 ± 0.14. Shannon-Wiener Diversity Index (H') values were low to moderate, ranging from 0.46 to 3.99. These results indicate that the infauna community in the vicinity of the LPP has low to moderate diversity. However, it should be noted that H' values are likely skewed too low given the index considers the numerically dominant unidentified nematodes as a single species.

Two types of passive sampling devices (PSDs were deployed at five locations: four down-current from the LPP (200, 500, 1,000, and 3,500 m from the LPP), and one at the kurkar hardbottom site 3.5 km north of the LPP. The PSDs use a synthetic material to mimic biotic tissue to measure uptake of bioavailable compounds. Semipermeable membrane devices (SPMDs) were used to mimic the passive uptake of organic compounds (such as PAHs), while diffuse gradient in thin film (DGT) samplers were used to assess the mass of bioavailable metals (cadmium, chromium, lead, manganese, mercury, nickel, and zinc). The samplers were deployed on fabricated monopods and left in place on the seafloor for 43-days after which they were retrieved and analyzed.

The SPMDs were analyzed for 76 PAHs. Mean total PAH masses were slightly higher at the Near Platform (1,028 ± 28 ng) and Hardbottom location (977 ± 38) as compared to the other deployment locations, which ranged from 852 ± 40 ng (Reference) to 914 ± 41 ng (Mid-Field). Of the 16 USEPA priority PAHs, phenathrene and fluoranthene were found with the highest mean mass (57.2 ± 5.2 and 49.5 ± 4.4 ng, respectively) across all deployment locations. This result is the same as was observed during a 2019 deployment of SPMDs at the LPP location prior to commencement of operations at the LPP. Using an empirical model, the time-weighted average concentration of each of the 16 USEPA priority PAHs was calculated. Naphthalene was the PAH with the highest concentration, with average values ranging from approximately 1.3 to 1.5 ng L^{-1}. There were no obvious trends in PAH concentrations by deployment location except for a small spike in fluorene in the Near Platform deployment location. Mean PAH concentrations across all deployment locations were similar to values observed during the 2019 LPP EBS SPMD deployment, with the exception of naphthalene which was somewhat higher during the current study.

DGT samplers were analyzed for accumulated masses of cadmium, chromium, lead, manganese, mercury, nickel, and zinc. Chromium, cadmium, and lead were not detected on any sampler. Nickel was detected only on two Near Platform samplers and zinc was detected on a single Far-Field sampler. Mercury masses ranged from 60.7 to 151 ng, while manganese masses ranged from 0.275 to 3.2 µg. The time weighted average concentrations (TWAC) were calculated for all samplers where mass was detected. Mercury TWACs ranged from 0.098 to 0.175 ng mL^{-1}, with an overall average of 0.138 ± 0.02 ng mL^{-1}. The mean TWAC of the three samplers deployed at the Near Platform

deployment area (0.165 ± 0.05 ng mL^{-1}) was slightly elevated as compared with other deployment areas.

Mean manganese TWACs were similar across deployment locations, ranging from 1.71 ± 1.14 ng mL^{-1} (Far-Field) to 2.87 ± 1.91 ng mL^{-1} (Reference). Manganese TWACs showed no obvious trend by deployment location. Nickel was only detected on two of the Near Platform DGT samplers and therefore nickel TWACs could only be calculated for those two samplers. The nickel TWAC was similar on the two samplers (0.337 and 0.401 ng mL^{-1}). Zinc was only detected on a single DGT sampler at the Far-Field deployment location. The TWAC for that sample was calculated to be 0.777 ng mL^{-1}.

Overall, results from the 2020 LPP EMS indicate that sediment and water quality parameters in the vicinity of the LPP are ecologically similar to those found during the 2019 LPP EBS prior to commencement of operations at the LPP and are similar to reference areas. Results from the 2020 LPP EMS indicate that there were no substantial ecological effects on the marine environment from LPP operations.

Table of Contents

Page

Author Certification Signature ..... **c**
Executive Summary **ES-1**
List of Tables ..... **viii**
List of Figures ..... **xi**
List of Images ..... **xvi**
List of Acronyms and Abbreviations ..... **xix**

1 Introduction **1**
1.1 BACKGROUND 1
1.2 HYDROGRAPHIC REGIME 7
1.2.1 Winds 7
1.2.2 Currents 7
1.2.3 Waves 7

2 Survey Design **9**
2.1 PROGRAMMATIC SURVEY SAMPLING DESIGN 9
2.2 SEAWATER SAMPLING 9
2.3 SEDIMENT SAMPLING 11
2.4 HARDBOTTOM MONITORING 14
2.5 PLATFORM FOULING AND FISH COMMUNITIES 16
2.6 BIOACCUMULATION PASSIVE SAMPLING DEVICES 16

3 Field Methods **19**
3.1 SURVEY PERSONNEL 19
3.2 SURVEY VESSEL, REMOTELY OPERATED VEHICLE, AND OPERATIONS 19
3.3 PLATFORM FOULING AND FISH COMMUNITIES 20
3.4 WATER COLUMN SAMPLING 21
3.5 SEDIMENT AND INFAUNAL SAMPLING 22
3.5.1 Infaunal Samples 23
3.6 HARDBOTTOM MONITORING 23
3.7 BIOACCUMULATION PASSIVE SAMPLING DEVICES 24
3.8 QUALITY ASSURANCE 26
3.8.1 Quality Control Measures 26
3.8.2 Sampling Handling and Transport 27
3.8.3 Document and Data Security 27
3.8.4 Data and Document Review 28

4 Laboratory Methods, Data Processing, and Analysis **29**
4.1 HYDROGRAPHIC PROFILES 29
4.2 SEAWATER AND SEDIMENT SAMPLES 29
4.2.1 Seawater 31
4.2.2 Sediment 32
4.3 INFAUNA 34
4.4 STATISTICAL ANALYSIS 34
4.4.1 Sediment 34
4.4.2 Infauna 35
4.5 VIDEOGRAPHY 35
4.5.1 Fouling Community 35
4.5.2 Fish Community 36
4.6 BIOACCUMULATION PASSIVE SAMPLING DEVICES 36
4.6.1 DGT Samplers 36

Table of Contents (Continued)

Page

4.6.2 Semipermeable Membrane Devices 37

5 Results and Discussion 41
5.1 LOCAL WEATHER AND SEA STATE CONDITIONS 41
5.2 HYDROGRAPHIC PROFILES 41
5.3 SEAWATER ANALYSES 44
5.3.1 Hydrocarbons 44
5.3.2 Total Nitrogen, Total Phosphorous, Total Organic Carbon, Nutrients and Total Suspended Solids 44
5.3.3 Radionuclides 47
5.4 SEDIMENT ANALYSES 48
5.4.1 Grain Size Composition 48
5.4.2 Total Organic Carbon 56
5.4.3 Metals 58
5.4.4 Hydrocarbons 80
5.4.5 Radionuclides 86
5.5 VIDEO ANALYSIS 87
5.5.1 Fouling Community 87
5.5.2 Fish Community 99
5.5.3 Hardbottom Analysis 106
5.6 INFAUNA ANALYSIS 132
5.6.1 Taxonomy 134
5.6.2 Infauna Statistical Analysis 137
5.7 BIOACCUMULATION PASSIVE SAMPLING DEVICES ANALYSIS 139
5.7.1 Metals – DGT Samplers 139
5.7.2 Hydrocarbons – SPMD Samplers 143

6 References 153

Appendices 158
APPENDIX A 2019 LEVIATHAN PRODUCTION PLATFORM ENVIRONMENTAL BASELINE SURVEY SCOPE OF WORK A-1
APPENDIX B DISCHARGE REPORTS B-1
APPENDIX C SAMPLING STATION GEOGRAPHIC COORDINATES C-1
APPENDIX D NOR NAOMI VESSEL SPECIFICATIONS D-1
APPENDIX E WATER COLUMN PROFILES E-1
APPENDIX F ANALYTICAL DATASHEETS: SEAWATER HYDROCARBONS F-1
APPENDIX G ANALYTICAL DATASHEETS: SEAWATER TOTAL NITROGEN, TOTAL PHOSPHOROUS, TOTAL ORGANIC CARBON, NUTRIENTS AND TOTAL SUSPENDED SOLIDS G-1
APPENDIX H ANALYTICAL DATASHEETS: SEAWATER RADIONUCLIDES H-1
APPENDIX I ANALYTICAL DATASHEETS: SEDIMENT GRAIN SIZE I-1
APPENDIX J ANALYTICAL DATASHEETS: SEDIMENT TOTAL ORGANIC CARBON J-1
APPENDIX K ANALYTICAL DATASHEETS: SEDIMENT METALS K-1
APPENDIX L ANALYTICAL DATASHEETS: SEDIMENT HYDROCARBONS L-1
APPENDIX M ANALYTICAL DATASHEETS: SEDIMENT RADIONUCLIDES M-1
APPENDIX N ANALYTICAL DATASHEETS: INFAUNA N-1
APPENDIX O ANALYTICAL DATASHEETS: DGT SAMPLERS O-1
APPENDIX P ANALYTICAL DATASHEETS: SPMD SAMPLERS P-1

List of Tables

Table		Page
1	Daily mean and monthly discharge of effluents from the Leviathan Production Platform for one year prior to and including the month of the December 2020 Leviathan Production Platform Environmental Monitoring Survey	3
2	Yearly total discharges of effluents from the Leviathan Production Platform	4
3	Daily discharge activity from the Leviathan Production Platform one month prior to the first day of seawater sampling (26 December 2020), and during water sampling for the 2020 Leviathan Production Platform Environmental Monitoring Survey	5
4	Minimum, maximum, and mean (± standard deviation) concentrations of pollutants in produced water at the Leviathan Production Platform during 2020	6
5	2020 produced water discharge volumes, mean total organic carbon, and calculated annual organic load in produced water discharges from the Leviathan Production Platform for 2020	7
6	Significant wave heights and their frequency of occurrence at a buoy offshore Israel from 1 December to 16 December 2020	8
7	Designation of distance and directional stratification within the Leviathan Production Platform (LPP) survey area	11
8	Summary of the sampling depths and depth strata used to characterize the fouling and fish communities	16
9	Names and roles of the staff members who conducted the 2020 Leviathan Production Platform Environmental Monitoring Survey	19
10	Date and times of sampling and the sample depths for each platform leg sampled using the remotely operated vehicle (ROV) for the fouling and fish community analysis	21
11	Guidelines for water sample collection (From: U.S. Geological Survey, 2000)	21
12	Processing and storage requirements for sediment chemistry sampling parameters	22
13	Analytical parameters, analysis methods, reporting units, reporting/limits of quantification, Mediterranean environmental water quality standards (MEWQS), and analytical laboratory for seawater samples	29
14	Analytical parameters, analysis methods, reporting units, reporting/limits of quantification, sediment quality guidelines, and analytical laboratory for sediment samples	30
15	Wentworth size class nomenclature and Folk scale grain sizes	32
16	Braun-Blanquet (BB) ordinal scale classifications and the corresponding range of percent cover used for analysis of the fouling community	36
17	Scale of Log^4 abundance categories used to estimate fish abundance	36
18	Intermediate values used to calculate the sampling rate of each performance reference compound on each deployed semipermeable passive membrane device (SPMD)	39
19	Summary of weather conditions during the 2020 Leviathan Production Platform Environmental Monitoring Survey	41

List of Tables (Continued)

Table		Page
20	Results of total nitrogen, total phosphorous, total organic carbon, nutrients and total suspended solids analyses in seawater during the 2020 Leviathan Production Platform Environmental Monitoring Survey	45
21	Mean (± standard deviation) total organic carbon, total nitrogen, total phosphorous, and nutrient concentrations by distance and directional strata in seawater samples collected during the 2020 Leviathan Production Platform Environmental Monitoring Survey	47
22	Radioactive compound concentrations (pCi g^{-1}) ± total propagated analytical uncertainty in seawater samples during the 2020 Leviathan Production Platform Environmental Monitoring Survey	48
23	Sediment type and percentages of major (total clay, silt, and sand) and individual (very fine, fine, medium, and coarse) grain size classes at sampling stations during the 2020 Leviathan Production Platform Environmental Monitoring Survey	49
24	Mean (± standard deviation) sediment percentages of major (total clay, silt, and sand) and individual (very fine, fine, medium, and coarse) grain size classes by distance and directional strata during the 2020 Leviathan Production Platform Environmental Monitoring Survey	54
25	Total organic carbon concentrations (%) in sediment samples collected during the 2020 Leviathan Production Platform Environmental Monitoring Survey	56
26	Mean total organic carbon concentrations (% ± standard deviation) in sediment samples by distance and directional strata collected during the 2020 Leviathan Production Platform Environmental Monitoring Survey (2020 LPP EMS)	57
27	Total metals concentrations (mg kg^{-1} unless noted otherwise) in sediment samples collected during the 2020 Leviathan Production Platform Environmental Baseline Survey	59
28	Mean metals concentrations (mg kg^{-1} unless noted otherwise) ± standard deviation) by distance and directional strata in sediment samples collected during the 2020 Leviathan Production Platform Environmental Baseline Survey	61
29	Analysis of variance (ANOVA) results for differences in sediment metals concentrations by distance, direction, and survey year	71
30	Post-hoc Tukey's Multiple Means Comparison Test results for differences in metals concentrations for the interactive effect of distance × survey year specific to the comparison with Near-Platform samples from the 2020 Leviathan Production Platform Environmental Monitoring Survey (2020 LPP EMS)	71
31	Post-hoc Tukey's Multiple Means Comparison Test results for differences in metals concentrations among directional strata (platform quadrants)	77
32	Hydrocarbon concentrations in sediment samples collected during the 2020 Leviathan Production Platform Environmental Monitoring Survey	81
33	Mean (± standard deviation) total petroleum hydrocarbons (TPH) and total polycyclic aromatic hydrocarbon (PAHs) concentrations by distance and directional strata in sediment samples collected during the 2020 Leviathan Production Platform Environmental Monitoring Survey	82

List of Tables (Continued)

Table		Page
34	Individual polycyclic aromatic hydrocarbon concentrations in sediment samples during the 2020 Leviathan Production Platform Environmental Monitoring Survey	83
35	Post-hoc Tukey's Multiple Means Comparison Test result matrix for differences in total petroleum hydrocarbons for the interactive effect of distance strata × survey year specific to the comparisons between 2019 (column) and 2020 (row) survey results	85
36	Radioactive compound concentrations (pCi g^{-1}) in sediment samples collected during the 2020 Leviathan Production Platform Environmental Monitoring Survey	86
37	Taxonomic list of the fouling community identified organisms from the Leviathan Production Platform (LPP) northeast and southeast legs during the 2020 LPP Environmental Monitoring Survey	87
38	Taxonomic list of fish identified from the Leviathan Production Platform (LPP) northeast and southwest legs during the 2020 LPP Environmental Monitoring Survey (names follow Carpenter and De Angelis, 2016)	100
39	Diversity metrics for benthic infauna collected during the 2020 Leviathan Production Platform (LPP) Environmental Monitoring Survey	132
40	Mean (± standard deviation) infauna diversity metrics by distance and directional strata in sediment samples collected during the 2020 Leviathan Production Platform Environmental Monitoring Survey	133
41	Measured mass of metals from the DGT samplers after a 43-day deployment near the Leviathan Production Platform	140
42	Mean metals mass by deployment location on DGT samplers after a 43-day deployment near the Leviathan Production Platform	140
43	Calculated time-weighted average concentrations for selected metals (ng mL^{-1}) on deployed DGT samplers during a 43-day deployment near the Leviathan Production Platform	142
44	The accumulated masses of polycyclic aromatic hydrocarbons (PAHs) on the semi-permeable passive membrane devices (SPMDs) after the 43-day deployment near the Leviathan Production Platform	144
45	Calculated sampling rates of the 16 United States Environmental Protection Agency priority polycyclic aromatic hydrocarbons for each of the 15 deployed semi-permeable passive membrane devices	148
46	Calculated seawater concentrations of the 16 United States Environmental Protection Agency priority polycyclic aromatic hydrocarbons for each of the 15 deployed semi-permeable passive membrane devices	149
47	Calculated mean seawater concentrations (± standard deviation) of the 16 United States Environmental Protection Agency priority polycyclic aromatic hydrocarbons for each of the 15 deployed semi-permeable passive membrane devices (SPMDs) and reference concentrations of PAHs in seawater taken from three published literature sources and MVI (2020)	151

List of Figures

Figure		Page
1	Location of the Leviathan Production Platform, Leviathan Pipeline, and Israeli Natural Gas Lines (INGL) pipeline relative to Dor along the Israeli coast	2
2	Hourly all-year mean wind speed percentage by direction (From: Fugro GEOS, 2001)	7
3	Location of seawater stations during the 2020 Leviathan Production Platform Environmental Monitoring Survey	10
4	Locations of sediment and infauna samples collected during the 2020 Leviathan Production Platform Environmental Monitoring Survey	12
5	Locations of sampling stations during the 2014 Leviathan Field Development Environmental Baseline Survey, the 2019 Leviathan Production Platform (LPP) Environmental Baseline Survey and the 2020 LPP Environmental Monitoring Survey	13
6	Hardbottom locations selected for monitoring (colored triangles) are distributed throughout the survey area located between 3.5 and 5 km from the Leviathan Production Platform	15
7	Deployment locations of passive sampler devices (semipermeable membrane devices and diffuse gradient in thin film samplers) during the 2020 Leviathan Production Platform Environmental Monitoring Survey	18
8	Example of the first-order kinetic uptake process of semipermeable passive membrane devices	38
9	Hydrographic profiles of the water column collected at Station NF-SW-10 on 26 December 2020: temperature, salinity, and pH (left) and dissolved oxygen (mg L^{-1}), dissolved oxygen (% saturation), fluorescence, and turbidity (right)	41
10	Hydrographic profiles of the water column collected in August 2019 at Station REF-SW-42 during the 2019 Leviathan Production Platform Environmental Baseline Survey: temperature, salinity, and pH (left) and dissolved oxygen (mg L^{-1}), dissolved oxygen (% saturation), fluorescence, and turbidity (right)	42
11	Hydrographic profile of the water column collected at in the vicinity of the Leviathan Production Platform during the 2014 Leviathan Field Development Environmental Baseline Survey	43
12	Ternary diagram showing grain size distribution from sediment samples (grouped by directional strata) collected during the 2020 Leviathan Production Platform Environmental Monitoring Survey	51
13	Ternary diagram showing grain size distribution from sediment samples (grouped by distance strata) collected during the 2020 Leviathan Production Platform Environmental Monitoring Survey	51
14	Ternary diagram showing grain size distribution from sediment samples (grouped by survey) from the 2014 Leviathan Field Development Environmental Baseline Survey (EBS), the 2019 Leviathan Production Platform EBS, and the 2020 Leviathan Platform Environmental Monitoring Survey (EMS)	52

List of Figures (Continued)

Figure **Page**

15 Mean individual grain size classes (± standard deviation [SD]) for samples collected within the Leviathan Production Platform survey area during the 2014 Leviathan Field Development Environmental Baseline Survey (EBS), the 2019 Leviathan Production Platform EBS, and the 2020 Leviathan Production Platform Environmental Monitoring Survey (EMS) 53

16 Mean percent (± standard deviation [SD]) of major grain size classes for samples collected within the Leviathan Production Platform survey area by directional strata during the 2020 Leviathan Production Platform Environmental Monitoring Survey 55

17 Mean percent (± standard deviation [SD]) of major grain size classes for samples collected within the Leviathan Production Platform survey area by distance strata during the 2020 Leviathan Production Platform Environmental Monitoring Survey 55

18 Statistical least square means (± standard error) of sediment total organic carbon concentrations (%) by distance strata as computed by the analysis of variance (ANOVA) model 58

19 Plot of aluminum versus arsenic during the 2020 Leviathan Production Platform Environmental Monitoring Survey (EMS) as compared to 2019 Leviathan Production Platform Environmental Baseline Survey (EBS) and the 2014 Leviathan Field Development EBS 62

20 Plot of aluminum versus barium during the 2020 Leviathan Production Platform Environmental Monitoring Survey (EMS) as compared to 2019 Leviathan Production Platform Environmental Baseline Survey (EBS) and the 2014 Leviathan Field Development EBS 63

21 Plot of aluminum versus chromium during the 2020 Leviathan Production Platform Environmental Monitoring Survey (EMS) as compared to 2019 Leviathan Production Platform Environmental Baseline Survey (EBS) and the 2014 Leviathan Field Development EBS 64

22 Plot of aluminum versus copper during 2020 Leviathan Production Platform Environmental Monitoring Survey (EMS) as compared to 2019 Leviathan Production Platform Environmental Baseline Survey (EBS) and the 2014 Leviathan Field Development EBS 65

23 Plot of aluminum versus iron during the 2020 Leviathan Production Platform Environmental Monitoring Survey (EMS) as compared to 2019 Leviathan Production Platform Environmental Baseline Survey (EBS) and the 2014 Leviathan Field Development EBS 66

24 Plot of aluminum versus lead during the 2020 Leviathan Production Platform Environmental Monitoring Survey (EMS) as compared to 2019 Leviathan Production Platform Environmental Baseline Survey (EBS) and the 2014 Leviathan Field Development EBS 67

25 Plot of aluminum versus mercury during the 2020 Leviathan Production Platform Environmental Monitoring Survey (EMS) as compared to 2019 Leviathan Production Platform Environmental Baseline Survey (EBS) and the 2014 Leviathan Field Development EBS 68

List of Figures (Continued)

Figure		Page
26	Plot of aluminum versus nickel during the 2020 Leviathan Production Platform Environmental Monitoring Survey (EMS) as compared to 2019 Leviathan Production Platform Environmental Baseline Survey (EBS) and the 2014 Leviathan Field Development EBS	69
27	Plot of aluminum versus zinc during the 2020 Leviathan Production Platform Environmental Monitoring Survey (EMS) as compared to 2019 Leviathan Production Platform Environmental Baseline Survey (EBS) and the 2014 Leviathan Field Development EBS	70
28	Statistical least square means (± standard error) of arsenic concentrations (parts per million [ppm]) analyzed within the significant distance strata × survey year interaction as computed by the analysis of variance (ANOVA) model	72
29	Statistical least square means (± standard error) of copper concentrations (parts per million [ppm]) analyzed within the significant distance strata × survey year interaction as computed by the analysis of variance (ANOVA) model	72
30.	Statistical least square means (± standard error) of nickel concentrations (parts per million [ppm]) analyzed within the significant distance strata × survey year interaction as computed by the analysis of variance (ANOVA) model	73
31	Statistical least square means (± standard error) of zinc concentrations (parts per million [ppm]) analyzed within the significant distance strata × survey year interaction as computed by the analysis of variance (ANOVA) model	73
32	Statistical least square means (± standard error) of barium concentrations (parts per million [ppm]) analyzed for significant differences among distance strata as computed by the analysis of variance (ANOVA) model	74
33	Statistical least square means (± standard error) of chromium concentrations (parts per million [ppm]) analyzed for significant differences among directional strata (platform quadrants) as computed by the analysis of variance (ANOVA) model	75
34	Statistical least square means (± standard error) of copper concentrations (parts per million [ppm]) analyzed for significant differences among directional strata (platform quadrants) as computed by the analysis of variance (ANOVA) model	75
35	Statistical least square means (± standard error) of iron concentrations (parts per million [ppm]) analyzed for significant differences among directional strata (platform quadrants) as computed by the analysis of variance (ANOVA) model	76
36	Statistical least square means (± standard error) of nickel concentrations (parts per million [ppm]) analyzed for significant differences among directional strata (platform quadrants) as computed by the analysis of variance (ANOVA) model	76
37	Statistical least square means (± standard error) of zinc concentrations (parts per million [ppm]) analyzed for significant differences among directional strata (platform quadrants) as computed by the analysis of variance (ANOVA) model	77
38	Statistical least square means (± standard error) of arsenic concentrations (parts per million [ppm]) analyzed for significant differences among directional strata (platform quadrants) as computed by the analysis of variance (ANOVA) model	78

List of Figures (Continued)

Figure **Page**

39 Statistical least square means (± standard error) of chromium concentrations (parts per million [ppm]) analyzed for significant differences among survey years as computed by the analysis of variance (ANOVA) model 78

40 Statistical least square means (± standard error) of mercury concentrations (parts per billion [ppb]) analyzed for significant differences among survey years as computed by the analysis of variance (ANOVA) model 79

41 Statistical least square means (± standard error) of sediment total petroleum hydrocarbon concentration ($\mu g\ g^{-1}$) within the significant survey year by distance strata interaction as computed by the analysis of variance (ANOVA) model 85

42 Mean depth distribution of taxa identified from the video survey on the northeastern side of the Leviathan Production Platform 89

43 Mean depth distribution of taxa identified from the video survey on the southeastern side of the Leviathan Production Platform 89

44 Mean number of *Antedon mediterranea* individuals m^{-2} (± standard deviation), at each sampling depth on the (A) northeastern side and (B) southwestern side of the Leviathan Production Platform 93

45 Mean number of *Arbacia lixula* and *Diadema* sp. individuals m^{-2} (± standard deviation), at each sampling depth on the (A) Northeastern side and (B) Southwestern side of the Leviathan Production Platform 94

46 Mean percent cover of Bryozoa, encrusting Ascidia (*Didemnum* sp.) and Solitary Ascidia (*Herdmania momus* / *Phallusia nigra*) from all sampling depths recorded on the (A) northeastern side and (B) northwestern side of the Leviathan Production Platform 95

47 Mean percent cover of Hydrozoa and Bivalvia from all sampling depths recorded on the (A) northeastern side and (B) southwestern side of the Leviathan Production Platform 96

48 Mean percent cover of tube worms (Families: *Serpulidae* and *Sabelidae*) and barnacles (Infraclass: Cirripedia) from all sampling depths recorded on the (A) northeastern side and (B) southwestern side of the Leviathan Production Platform 97

49 Mean percent cover of Porifera from the classes Calcarea (Order: Leucosolenida) and Demospongiae from all sampling depths recorded on the (A) northeastern side and (B) southwestern side of the Leviathan Production Platform 98

50 Proportional abundance and depth distribution of fish species found at the northeast side of the Leviathan Production Platform 101

51 Proportional abundance and depth distribution of fish species found at the southwest side of the Leviathan Production Platform 103

52 Percentage of total individuals within each of the dominant phyla collected during the 2014 Leviathan Field Development Environmental Baseline Survey (EBS), the 2019 Leviathan Production Platform EBS, and the 2020 Leviathan Production Platform Environmental Monitoring Survey (EMS) 135

List of Figures (Continued)

Figure **Page**

53 Multi-dimensional scaling ordination of infauna samples by distance during the 2020 Leviathan Production Platform Environmental Monitoring Survey 137

54 Multi-dimensional scaling ordination of infauna samples by direction (quadrant) during the 2020 Leviathan Production Platform Environmental Monitoring Survey 138

55 Multi-dimensional scaling ordination of infauna samples by survey 139

56 Average (± standard deviation [SD]) accumulated mercury mass on the diffuse gradient in thin film sampler devices by deployment location and blank devices after the 43-day deployment near the Leviathan Production Platform 141

57 Average (± standard deviation [SD]) accumulated manganese mass on the diffuse gradient in thin film sampler devices by deployment location after the 43-day deployment near the Leviathan Production Platform 141

58 Average (± standard deviation [SD]) accumulated total polycyclic aromatic hydrocarbon (PAH) mass on the semi-permeable passive membrane devices by deployment location after the 43-day deployment near the Leviathan Production Platform 147

59 Average (± standard deviation [SD]) calculated concentrations (ng L^{-1}) of the seven highest-concentration PAHs as detected by the semi-permeable passive membrane devices after the 43-day deployment near the Leviathan Production Platform. 150

60 Average (± standard deviation [SD]) calculated concentrations (ng L^{-1}) of the seven highest-concentration PAHs as detected by the semi-permeable passive membrane devices during the 2019 and 2020 deployments in the vicinity of the Leviathan Production Platform 152

List of Images

Image		Page
1	The M/V *Nor Naomi*, the vessel used for the 2020 Leviathan Production Platform Environmental Monitoring Survey	20
2	A DeepOcean Schilling remotely operated vehicle and associated tether management system used during the 2020 Leviathan Production Platform Environmental Monitoring Survey	20
3	Macrobenthic infaunal sieving apparatus	23
4	Self-fabricated stainless-steel monopod with attached mounting cage for semipermeable membrane device deployment	25
5	Acrylic holder with diffuse gradient in thin film samplers	26
6	Representative image of organisms found on the northeastern side of the Leviathan Production Platform legs	90
7	Representative organisms (red circles) found on the northeastern side of the Leviathan Production Platform legs	90
8	Representative organisms found on the northeastern side of the Leviathan Production Platform legs	91
9	Representative organisms (red circles) found on the northeastern side of the Leviathan Production Platform legs	91
10	Representative organisms (red arrows) found on the northeastern side of the Leviathan Production Platform legs	92
11	White trevally, *Pseudocaranx dentex* at 10 m water depth on the Leviathan Production Platform's F-2 northeastern leg	101
12	An unidentified grouper (red circle), *Epinephelus* sp., *at* 70 m water depth on the Leviathan Production Platform's G-2 northeastern leg	102
13	A comber, *Serranus cabrilla,* at 80 m water depth on the Leviathan Production Platform's C-2 northeastern leg	102
14	A lionfish, *Pterois miles,* at 70 m water depth on the Leviathan Production Platform's F-2 northeastern leg	103
15	A school of greater amberjack (*Seriola dumerili*) near 80 m water depth on the Leviathan Production Platform's C-4 northeastern leg	104
16	A gray triggerfish (red circle), *Balistes capriscus,* at 60 m water depth on the Leviathan Production Platform's B-4 southwestern leg	104
17	A scorpionfish (red circle) (*Scoropaena* sp.) at 70 m water depth on the Leviathan Production Platform's C-4 southwestern leg	105
18	The more vertical and underside of overhanging features of the hardbottom appears to support generally higher biological coverage and occurrence of less sediment tolerant biota (e.g. corals)	107
19	Anthropogenic debris, primarily related to commercial fishing, was commonly observed during the 2020 Leviathan Production Platform Environmental Monitoring Survey	108
20	Faces of the kurkar hardbottom features. a) horizontal surface (topside) of kurkar hardbottom feature showing biological coverage of up to 25% from Location 7	109

List of Images (Continued)

Image		Page
21	Some of the sponge morphologies observed across the kurkar hardbottom features. a) bulky sponge (red arrow) from Location 6, b) encrusting sponges (orange arrows) from Location 4, and c) erecting sponge (blue arrow) from Location 7	110
22	Cnidarians observed across the kurkar hardbottom features. a) cup corals (red arrows) from Location 8, b) sea anemone (orange arrow) from Location 12, and c) hydroids (blue arrows) from Location 4	111
23	Annelida taxa observed across the kurkar hardbottom features. a) spoon worms (Polychaeta: *Bonellia viridis*) (red arrows) from Location 3, and b) tube worms (Serpulidae) (orange arrow) from Location 12	112
24	Echinodermata taxa observed across the kurkar hardbottom features. a) Sea star (Asterroidea: *Echinaster sepositus*) (red arrow), and b) sea urchin (Echinoidea: *Centrostephanus longispinus*) (orange arrow)	113
25	The green algae, *Caulerpa* sp. (red arrows). The dual laser beams (red oval) (10 cm apart) in are displayed for size reference	114
26	Planktivorous fishes (*Anthias* sp.) (red arrows), and Mediterranean rainbow wrasses (*Coris julis*) (orange arrow)	115
27	A leopard spotted goby (*Thorogobius ephippiatus*) (red arrow)	115
28	A common lionfish (*Pterois miles*) (red arrow)	116
29	A red porgy (*Pagrus pagrus*)	116
30	Greater amberjacks (*Seriola dumerili*). As can be seen in the image, the amberjacks were responsible for suspending sediments from the seafloor and increasing turbidity at this location, as well as at several other locations	117
31	The large-scaled scorpionfish (*Scorpaena scrofa*) (red arrow)	117
32	The Mediterranean moray eel (*Muraena helenae*) (red arrow)	118
33	The European conger eel (*Conger conger*)	118
34	A comparative view of the seafloor at Location 1 with a) taken during the pre-installation survey, b) taken during the post-installation survey, and c) taken during the 2020 Leviathan Platform Environmental Monitoring Survey	120
35	A comparative view of the seafloor at Location 2 with a) taken during the pre-installation survey, b) taken during the post-installation survey, and c) taken during the 2020 Leviathan Platform Environmental Monitoring Survey	121
36	A comparative view of the seafloor at Location 3 with a) taken during the pre-installation survey, b) taken during the post-installation survey, and c) taken during the 2020 Leviathan Platform Environmental Monitoring Survey	122
37	A comparative view of the seafloor at Location 4 with a) taken during the pre-installation survey, b) taken during the post-installation survey, and c) taken during the 2020 Leviathan Platform Environmental Monitoring Survey	123
38	A comparative view of the seafloor at Location 5 with a) taken during the pre-installation survey, b) taken during the post-installation survey, and c) taken during the 2020 Leviathan Platform Environmental Monitoring Survey	124
39	A comparative view of the seafloor at Location 6 with a) taken during the pre-installation survey, b) taken during the post-installation survey, and c) taken during the 2020 Leviathan Platform Environmental Monitoring Survey	125

List of Images (Continued)

Image		Page
40	A comparative view of the seafloor at Location 7 with a) taken during the pre-installation survey, b) taken during the post-installation survey, and c) taken during the 2020 Leviathan Platform Environmental Monitoring Survey	126
41	A comparative view of the seafloor at Location 8 with a) taken during the pre-installation survey, b) taken during the post-installation survey, and c) taken during the 2020 Leviathan Platform Environmental Monitoring Survey	127
42	A comparative view of the seafloor at Location 9 with a) taken during the pre-installation survey, b) taken during the post-installation survey, and c) taken during the 2020 Leviathan Platform Environmental Monitoring Survey	128
43	A comparative view of the seafloor at Location 10 with a) taken during the pre-installation survey, b) taken during the post-installation survey, and c) taken during the 2020 Leviathan Platform Environmental Monitoring Survey	129
44	A comparative view of the seafloor at Location 11 with a) taken during the pre-installation survey, b) taken during the post-installation survey, and c) taken during the 2020 Leviathan Platform Environmental Monitoring Survey	130
45	A comparative view of the seafloor at Location 12 with a) taken during the pre-installation survey, b) taken during the post-installation survey, and c) taken during the 2020 Leviathan Platform Environmental Monitoring Survey	131

List of Acronyms and Abbreviations

3ANOVA	three-way analysis of variance
ALS	ALS Environmental
BB	Braun-Blanquet
BTEX	benzene, toluene, ethylbenzene, xylenes
CoC	chain of custody
CSA	CSA Ocean Sciences Inc.
CTD	conductivity-temperature-depth (water quality profiler)
DGT	diffuse gradient in thin film
EBS	environmental baseline survey
EMS	environmental monitoring survey
ERL	effects range low
ERM	effects range median
IOLR	Israel Oceanographic and Limnological Research Institute
LPP	Leviathan Production Platform
LPTL	lowest practical taxonomic level
MDC	minimum detectable concentration
MDL	method detection limit
MDS	multidimensional scaling
MRL	method reporting limit
MVI	Marine Ventures International, Inc.
Noble Energy	Noble Energy Mediterranean Ltd.
PAH	polycyclic aromatic hydrocarbons
PRC	performance reference compound
PSD	passive sampling device
QA	quality assurance
QC	quality control
Ra	radium
Rn	radon
ROV	remotely operated vehicle
SBE	Sea-Bird Electronics, Inc.
SD	standard deviation
SIMPER	similarity percentages
SPMD	semipermeable membrane device
TN	total nitrogen
TOC	total organic carbon
TP	total phosphorus
TPH	total petroleum hydrocarbons
TPU	total propagated uncertainty
TSS	total suspended solids
TWAC	time weighted average concentration
USBL	ultra-short baseline
USEPA	U.S. Environmental Protection Agency
USGS	U.S. Geological Survey
VOC	volatile organic compounds

1 Introduction

1.1 BACKGROUND

Noble Energy Mediterranean Ltd. (Noble Energy) has developed a gas production and transportation system connecting the Leviathan Field to the Israeli gas market off the northern coast of Israel. This project is herein referred to as the Leviathan Field Development Project. Natural gas from the North and South Leviathan lease blocks is being produced from subsea wells in the Leviathan Field and transported through subsea production flowlines to the offshore Leviathan Production Platform (LPP) and then to a landing location in the vicinity of Dor through a transportation system (pipelines). The LPP is located approximately 10 km offshore Dor, Israel, in a water depth of approximately 86 m (**Figure 1**). Noble Energy commenced operation of the LPP in December 2019.

Noble Energy engaged Marine Ventures International, Inc. (MVI) and CSA Ocean Sciences Inc. (CSA) to conduct an environmental baseline survey (2019 LPP EBS) in July and August 2019. The main objectives of the 2019 LPP EBS were to determine environmental conditions (i.e., chemical, physical, and biological) at the LPP location to enable assessment of the effects from future platform operations, identify parameters within the ecosystem that may be sensitive to change, and provide a reference point to evaluate future claims of impacts. Subsequently, after commencement of operation of the LPP, Noble Energy engaged MVI and CSA to conduct an environmental monitoring survey (2020 LPP EMS) during active production at the LPP. The main objectives of the 2020 LPP EMS were to:

- Assess the potential effect from LPP production operations on selected environmental components (i.e., chemical, physical, and biological);
- Determine temporal and spatial variation of selected chemical environmental standards within the LPP survey area; and
- Compare concentrations of selected environmental components with environmental standards.

The 2020 LPP EMS utilized the same survey design and scope as was approved for the 2019 LPP EBS. The scope of work/sampling analysis plan for the 2019 LPP EBS is presented in **Appendix A**. This SOW/SAP document describes field methods, data processing and laboratory methods, and reporting requirements used for the 2020 LPP EMS effort.

A summary of the daily mean and monthly discharges from the LPP for one year prior to the start of the 2020 LPP EMS is provided in **Table 1**. A summary of the annual discharges for the LPP is provided in **Table 2**. A summary of the daily discharge activity for 30 days prior to the beginning of sampling for the 2020 LPP EMS is provided in **Table 3**. Using the discharge volume classification scheme of Veil et al. (2005), the LPP would be characterized as low volume produced water discharger. Further details of discharges are provided in the Discharge Report provided by Noble in **Appendix B**.

Produced water started being discharged from the LPP in June 2020. Concentrations of contaminants in produced water are summarized in **Table 4** and calculated annual organic load from produced water discharges is presented in **Table 5**. Annual organic loads were calculated by multiplying the annual produced water discharge volume by the annual mean total organic carbon (TOC) concentration in the produced water discharge. Further details of concentrations of analytes in produced water are provided in the Discharge Report provided by Noble in **Appendix B**. The Discharge Report documented that oil and grease levels were below the analytical laboratory's detection limit of 4 mg L^{-1} and were therefore well below the limit for platform discharges as outlined by the World Bank (30-day average should not exceed 29 mg L^{-1}), U.S. Environmental Protection Agency (USEPA) National Pollutant Discharge Elimination System (30-day average should not exceed 29 mg L^{-1}), and the Barcelona Convention (monthly mean should not exceed 40 mg L^{-1}). TOC concentrations were all well below platform discharge permit thresholds of average 2,100 mg L^{-1} and maximum 10,000 mg L^{-1} during the first 12 months of operations. Polycyclic aromatic hydrocarbon (PAH) concentrations were below the detection limit in all produced water samples tested.

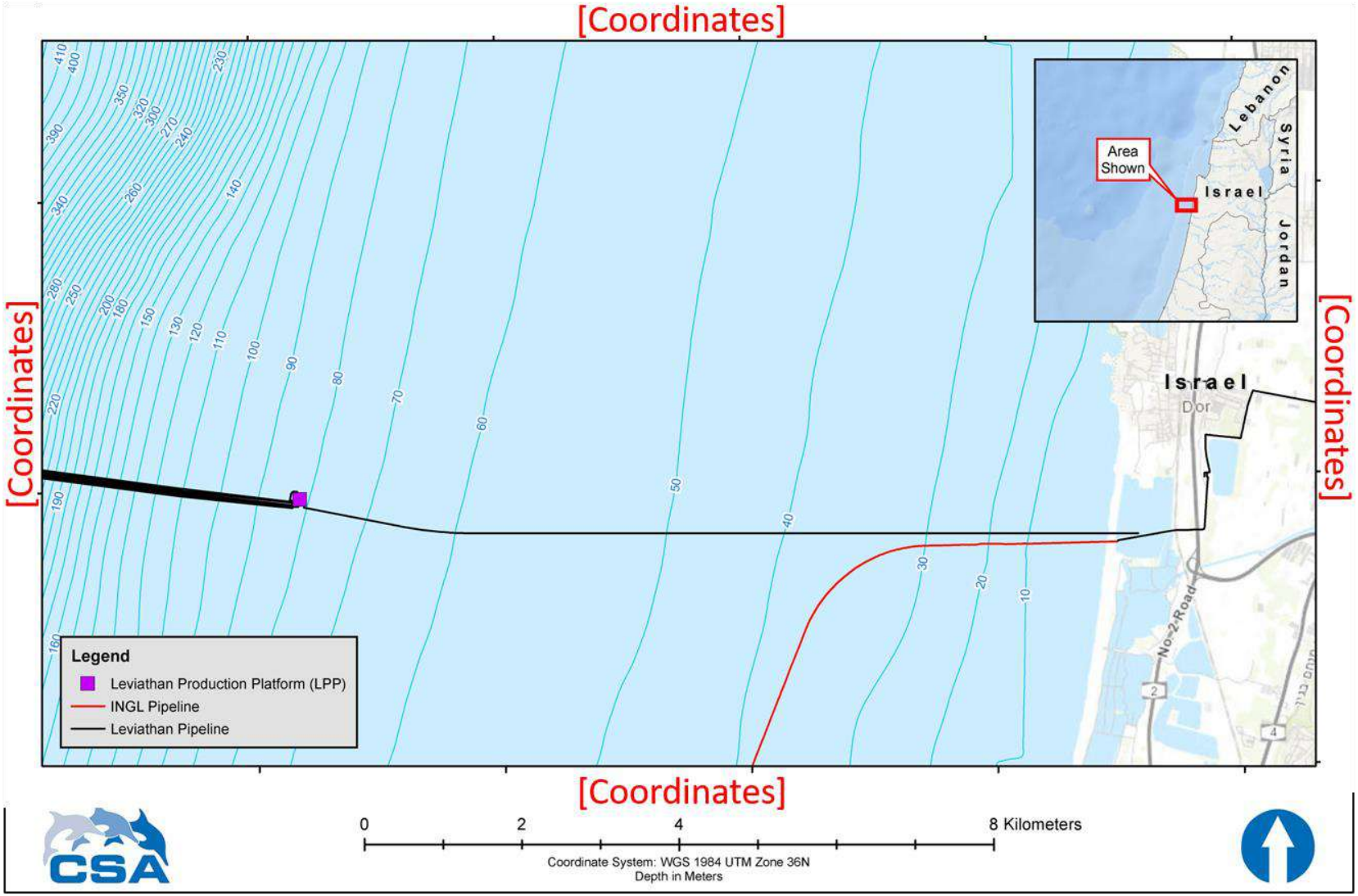


Figure 1. Location of the Leviathan Production Platform, Leviathan Pipeline, and Israeli Natural Gas Lines (INGL) pipeline relative to Dor along the Israeli coast.

Table 1. Daily mean and monthly discharge of effluents from the Leviathan Production Platform for one year prior to and including the month of the December 2020 Leviathan Production Platform Environmental Monitoring Survey. Data was provided by Noble Energy.

Indicator	Units	2019	2020											
		December	January	February	March	April	May	June	July	August	September	October	November	December
Leviathan Production Platform Daily Mean Discharge														
Produced water	m^3	0	0	0	0	0	0	18.1	35.1	31.5	0	11.1	46.0	57.8
Total open drain	m^3	91.9	68.2	17.2	11.5	3.0	2.1	3.3	2.6	15.1	26.7	13.6	45.0	24.1
Black water	m^3	0.1	4.0	0	0	0	0	0	0	0	0	0	0	0
Gray water	m^3	0	0	0	0	0	0	0	0	0	0	0	0	0
Freshwater Watermaker No. 1	gallons	1,293	1,834	1,975	391	295	601	596	374	27.4	28.3	323	323	0
Freshwater Watermaker No. 2	gallons	1,461	2,313	1,378	720	731	152	157	310	735	751	563	563	0
Watermaker No. 1 brine	m^3	14.7	20.8	22.4	4.4	3.3	6.8	6.8	4.2	0.3	0.3	3.7	2.3	1.6
Watermaker No. 2 brine	m^3	16.6	26.3	15.6	8.2	8.3	1.7	1.8	3.5	8.3	8.5	6.4	10.6	2.7
Cooling water	m^3	693	13,981	37,551	51,410	47,157	25,674	27,882	29,129	34,137	46,730	47,049	37,256	38,765
Jockey pump	m^3	1,252	1,264	1,250	1,258	1,236	1,264	1,264	1,262	1,264	1,264	1,264	1,264	1,264
Fire water	m^3	434	747	206	134	259	444	332	233	67.5	237	144	281	105
Leviathan Production Platform Monthly Total Discharge														
Produced water	m^3	0	0	0	0	0	0	544	1,087	975	0	343	1,379	1,792
Total open drain	m^3	2,849	2,114	498	357	89.8	65.4	97.6	81.9	469	800	423	1,349	748
Black water	m^3	4.3	123	0	0	0	0	0	0	0	0	0	0	0
Gray water	m^3	0	0	0	0	0	0	0	0	0	0	0	0	0
Freshwater Watermaker No. 1	gallons	40,082	56,840	57,264	12,104	8,840	18,635	17,869	11,599	850	850	10,004	10,004	0
Freshwater Watermaker No. 2	gallons	45,304	71,693	39,954	22,328	21,927	4,717	4,717	9,614	22,769	22,521	17,448	17,448	0
Watermaker No. 1 brine	m^3	455	646	650	138	100	212	203	132	9.7	9.7	114	68.4	50.6
Watermaker No. 2 brine	m^3	515	814	454	254	249	53.6	53.6	109	259	256	198	317	83.7
Cooling water	m^3	21,497	433,408	1,088,969	1,593,707	1,414,709	795,890	836,467	902,984	1,058,246	1,401,900	1,458,516	1,117,672	1,201,725
Jockey pump	m^3	38,825	39,181	36,244	38,983	37,087	39,194	37,930	39,115	39,194	37,930	39,194	37,930	39,194
Fire water	m^3	13,446	23,157	5,976	4,140	7,757	13,748	9,973	7,230	2,092	7,113	4,307	8,436	3,261

Table 2. Yearly total discharges of effluents from the Leviathan Production Platform. Data was provided by Noble Energy.

Indicator	Units	2019	2020
Produced water	m^3	0	6,121
Total open drain	m^3	2,951	7,092
Black water	m^3	224	123
Gray water	m^3	119	0
Freshwater Watermaker No. 1	gallons	2,494,513	204,859
Freshwater Watermaker No. 2	gallons	2,301,660	255,136
Watermaker No. 1 brine	m^3	1,521	2,332
Watermaker No. 2 brine	m^3	1,398	3,100
Cooling water	m^3	150,052	13,304,193
Jockey pump	m^3	108,363	461,174
Fire water	m^3	102,474	97,189

Table 3. Daily discharge activity from the Leviathan Production Platform one month prior to the first day of seawater sampling (26 December 2020), and during water sampling for the 2020 Leviathan Production Platform Environmental Monitoring Survey. Data was provided by Noble Energy.

Date	Produced Water (m^3)	Total Open Drain (m^3)	Black Water (m^3)	Gray Water (m^3)	Freshwater Watermaker No. 1 (gallons)	Freshwater Watermaker No. 2 (gallons)	Water Maker No. 1 Brine (m^3)	Water Maker No. 2 Brine (m^3)	Cooling Water (m^3)	Jockey Pump (m^3)	Fire Water (m^3)
26-Nov-2020	83.8	269.4	0	0	982	0	0	13.9	44,718	1,264	1,209
27-Nov-2020	86.2	13.2	0	0	1,272	90	0	13.1	42,021	1,264	0
28-Nov-2020	53.1	8.7	0	0	447	430	0	13.4	42,811	1,264	0
29-Nov-2020	53.0	7.6	0	0	107	377	0	14.1	44,758	1,264	1,920
30-Nov-2020	58.5	6.7	0	0	0	1,149	0	8.2	45,273	1,264	0
1-Dec-2020	48.6	6.2	0	0	--	--	13.6	0.0	24,824	1,264	3.2
2-Dec-2020	46.6	5.69	0	0	--	--	14.3	0.0	22,320	1,264	0
3-Dec-2020	47.3	6.3	0	0	--	--	8.2	0.0	22,968	1,264	0
4-Dec-2020	44.7	5.2	0	0	--	--	12.0	0.0	23,712	1,264	0
5-Dec-2020	45.6	101.1	0	0	--	--	0.8	10.8	24,096	1,264	0
6-Dec-2020	45.8	92	0	0	--	--	0.0	9.7	23,640	1,264	341.7
7-Dec-2020	49.3	10	0	0	--	--	0.1	8.4	24,768	1,264	0
8-Dec-2020	55.5	11	0	0	--	--	0.7	0.9	24,288	1,264	123.8
9-Dec-2020	67.5	25.4	0	0	--	--	0.0	0.6	22,488	1,264	49.9
10-Dec-2020	70.0	6.2	0	0	--	--	0.0	1.5	19,464	1,264	0
11-Dec-2020	70.0	4	0	0	--	--	0.0	12.7	41,544	1,264	0
12-Dec-2020	67.9	3.6	0	0	--	--	0.0	14.1	42,568	1,264	0
13-Dec-2020	67.4	3.2	0	0	--	--	0.0	0.9	42,480	1,264	343.3
14-Dec-2020	53.9	32	0	0	--	--	0.0	1.0	37,920	1,264	0
15-Dec-2020	62.0	138.2	0	0	--	--	0.0	1.4	45,360	1,264	0
16-Dec-2020	68.2	150.5	0	0	--	--	0.0	0.0	47,829	1,264	0
17-Dec-2020	67.5	124.6	0	0	--	--	0.0	1.1	45,696	1,264	20.7
18-Dec-2020	75.5	5.89	0	0	--	--	0.0	0.0	45,744	1,264	8.0
19-Dec-2020	66.6	2.71	0	0	--	--	0.0	0.9	46,632	1,264	0
20-Dec-2020	63.7	2.38	0	0	--	--	0.0	0.9	46,776	1,264	405.7
21-Dec-2020	68.2	2.01	0	0	--	--	0.1	1.1	48,792	1,264	0
22-Dec-2020	60.9	0.67	0	0	--	--	0.0	1.2	46,896	1,264	0

Table 3. (Continued).

Date	Produced Water (m^3)	Total Open Drain (m^3)	Black Water (m^3)	Gray Water (m^3)	Freshwater Watermaker No. 1 (gallons)	Freshwater Watermaker No. 2 (gallons)	Water Maker No. 1 Brine (m^3)	Water Maker No. 2 Brine (m^3)	Cooling Water (m^3)	Jockey Pump (m^3)	Fire Water (m^3)
23-Dec-2020	61.6	3.68	0	0	--	--	0.0	1.2	49,488	1,264	0
24-Dec-2020	77.9	3.54	0	0	--	--	0.0	0.9	49,776	1,264	1.3
25-Dec-2020	71.7	0.76	0	0	--	--	0.0	0.9	47,736	1,264	0
26-Dec-2020*	68.5	0.29	0	0	--	--	0.0	1.0	48,288	1,264	0
27-Dec-2020*	62.8	0.32	0	0	--	--	0.0	1.0	40,872	1,264	1,963.4
28-Dec-2020*	63.3	0.15	0	0	--	--	0.0	0.9	47,880	1,264	0
Pre-Survey Total†	**1,858.5**	**1,052.4**	**0**	**0**	**2,808**	**2,046**	**49.8**	**132.9**	**1,137,386**	**37,920**	**4,426.6**

-- = data not provided.
*Dates of December 2020 marine environmental monitoring sampling; †total from 26 November 2020 to 25 December 2020.

Table 4. Minimum, maximum, and mean (± standard deviation) concentrations of pollutants in produced water at the Leviathan Production Platform during 2020. Units are expressed as mg L^{-1}. In some cases, a mean could not be calculated because data were below detection limits. Data was provided by Noble Energy.

Year	pH	TOC	Mineral Oil	Oil & Grease	PAH	Total N	P	Al	As	Cd	Cr	Cu	Fe	Hg	Ni	Pb	Zn
2020 *	5.97-9.33; 7.40 ± 0.89	17.9-1,537; 260 ± 292	<4; --	<4; --	0; --	14.1-30.7; 19.8 ± 4.8	0.195-0.72; 0.10 ± 0.12	0.013-0.99; 0.38 ± 0.43	<0.05; --	<0.01; --	<0.02; --	>0.02-0.035; --	0.128-0.345; 0.237 ± 0.153	<0.001; --	<0.02; --	<0.05; --	<0.02-0.032; --

-- = no mean; Al = aluminum; As = arsenic; Cd = cadmium; Cr = chromium; Cu = copper; Fe = iron; Hg = mercury; N = nitrogen; N = nitrogen; Ni = nickel; P = phosphorus; PAH = polycyclic aromatic hydrocarbons; Pb = lead; TOC = total organic carbon; Zn = zinc.
Data are expressed as minimum-maximum (or the highest detection limit); mean ± standard deviation.
*Data is inclusive from June through December 2020.

Table 5. 2020 produced water discharge volumes, mean total organic carbon, and calculated annual organic load in produced water discharges from the Leviathan Production Platform for 2020. Calculations based on data provided by Noble Energy.

Year	2020 Produced Water Discharge (m^3)	Mean Total Organic Carbon (grams $m^{3\ -1}$)	2020 Organic Load (kilograms $year^{-1}$)s
2020*	6,121	260	1,591

* = Produced water discharged began in June 2020.

1.2 HYDROGRAPHIC REGIME

1.2.1 Winds

Wind speed and direction data in the regional vicinity of the LPP was described in Fugro GEOS (2001) were hindcast models created by the UK Meteorological Office using the distribution of atmospheric pressure. Winds out of the west, northwest, and north comprised more than 70% of all modeled samples (**Figure 2**). Winds are generally moderate in speed, averaging between 2.86 and 6.12 m s^{-1}. There is some seasonal variability with stronger winds occurring in the winter months (December through March).

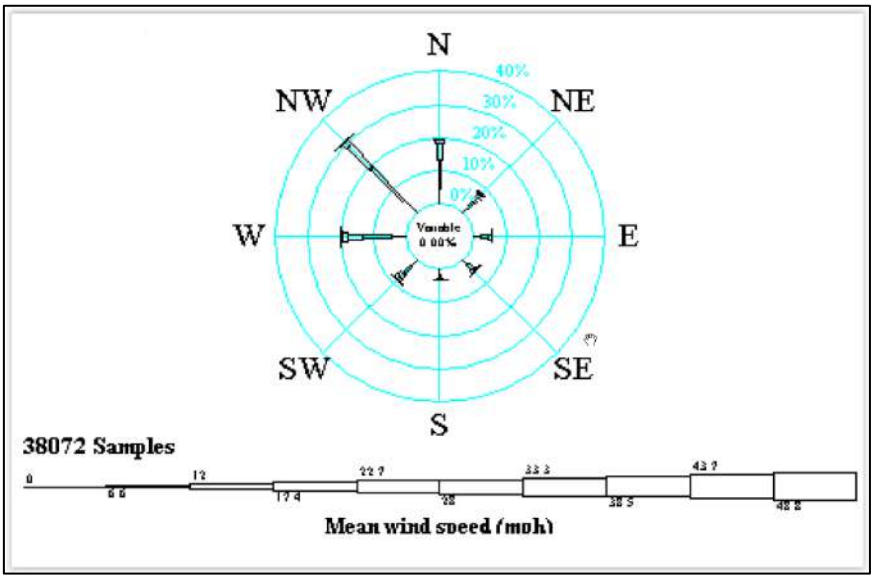


Figure 2. Hourly all-year mean wind speed percentage by direction (From: Fugro GEOS, 2001).

1.2.2 Currents

Currents within the vicinity of the LPP are generally slow (20 cm s^{-1}). A prevailing current offshore Dor, Israel flows northward parallel to both coast and bathymetric contours for the majority of the year (Rosen et al., 2013). The strongest currents generally recorded in the winter and early spring months between December and April and are associated with storm events and very strong westerly winds.

1.2.3 Waves

There is no publicly available wave height data from the vicinity of the LPP. However, data from the University of Haifa – Eastern Mediterranean (THEMO) project deepwater buoy (University of Haifa, 2021) include wave data. The buoy is located approximately 80 km west-northwest of the LPP and 50 km due west of Haifa. Wave heights for the month of December 2020 (data inclusive from 1 December to 16 December) ranged from 0.38 to 4.39 m. The majority of waves in December 2020

were less than 2 m in height (72.7% of all measurements) and nearly half of all measurements (46%) were between 0.51 and 0.75 m in height) (**Table 6**). Annual wave height data for all of 2020 (through 16 December 2020) show that wave heights ranged from 0.07 to 4.39 m, with the tallest waves typically observed in the winter months (University of Haifa, 2021). Wave height data collected during the 2020 LPP EMS by the survey vessel are presented in **Section 5.1**.

Table 6. Significant wave heights and their frequency of occurrence at a buoy offshore Israel from 1 December to 16 December 2020. (Data from: University of Haifa, 2021).

Wave Height Range (m)	Frequency (Occurrences over Period of Record)	Percentage (%)*
0 to 0.25	0	0%
0.26 to 0.50	142	11.1%
0.51 to 0.75	590	46.0%
0.76 to 1.00	200	15.6%
1.01 to 1.25	179	14.0%
1.26 to 1.50	57	4.4%
1.51 to 1.75	10	0.78%
1.76 to 2.00	6	0.47%
2.01 to 2.25	8	0.62%
2.26 to 2.50	14	1.1%
2.51 to 2.75	15	1.2%
2.76 to 3.00	13	1.0%
3.01 to 3.25	13	1.0%
3.26 to 3.50	13	1.0%
3.51 to 3.75	10	0.78%
3.76 to 4.00	8	0.62%
4.01 to 4.25	3	0.23%
>4.25	2	0.16%

* Total does not exactly equal 100% due to rounding.

2 Survey Design

2.1 PROGRAMMATIC SURVEY SAMPLING DESIGN

LPP survey sampling stations were positioned using a stratified random sampling pattern with stratification based on both distance and direction from the LPP (**Figure 3**). This sampling design allows for the statistical assessment of impacts both in a directional (i.e. northeast, northwest, southeast, southwest) and/or distance-based manner (i.e., Near-Platform, Near-Field, Mid-Field, Far-Field, Reference).

Samples collected at each station are considered within-strata replicates that provides for a statistical summary of mean and variance for each sampling parameter. The sampling design ensures statistically defensible data within area-wide estimates of the spatial variability. The same sampling design was used during the 2019 LPP EBS, enabling statistically defensible comparisons of fine-scale temporal variability within the survey area. The results obtained from the stratified random approach are more representative of the conditions within each stratum and, consequently, are more informative concerning the extent of potential impacts than from fixed station designs; thereby providing a broader spatial and temporal context for regulatory decisions. The sampling design is compliant with international standards (i.e., International Organization for Standardization 5667-19, International Organization for Standardization 16665; Joint Monitoring and Assessment Programme guidelines).

2.2 SEAWATER SAMPLING

Four seawater samples were collected within each distance strata; these samples were allocated so that one sample from each distance strata was located in each directional quadrant. Additionally, one seawater sample was collected from the upstream reference zone (**Figure 3**) to enable comparison with previous seawater samples collected in the area. One seawater sample was also collected from the downstream reference zone; however, no seawater samples were previously collected from the downstream reference zone during the 2019 LPP EBS over concerns that vessels working in the vicinity of the LPP could have caused sample contamination. Two seawater samples were also collected approximately 3.5 km east of the LPP (**Figure 3**). Seawater samples were collected within the near-surface (i.e., 10 m water depth), mid-water (i.e., 40 m water depth), and near-bottom (approximately 1 m above the seafloor) at each station.

Actual seawater station positioning was determined during the survey based upon prevailing current conditions. The current direction and velocity was estimated *in situ* based on the drift of the remotely operated vehicle (ROV) at 10, 15, 40, and 80 m water depths. Based on ROV drift at various water depths, the current velocity and direction was estimated at 0.3 kn from the northeast (opposite from the prevalent current). Based on this direction, seawater stations did not need to be relocated from their pre-plotted locations along the southeast-northeast axis relative to the LPP.

In addition to the seawater sampling design described above, a Noble representative collected a sample of produced water directly from the LPP's discharge pipe on the same day as the previously described water sampling occurred. All seawater samples were collected in the final days of the survey when sea conditions were calm (i.e., <1 m wave height). Full water column *in situ* hydrographic profiles were collected at each seawater station on the day of sampling. Each profile included temperature, salinity, dissolved oxygen, pH, fluorescence, and turbidity. Geographic coordinates for the seawater sampling stations are listed in **Appendix C**.

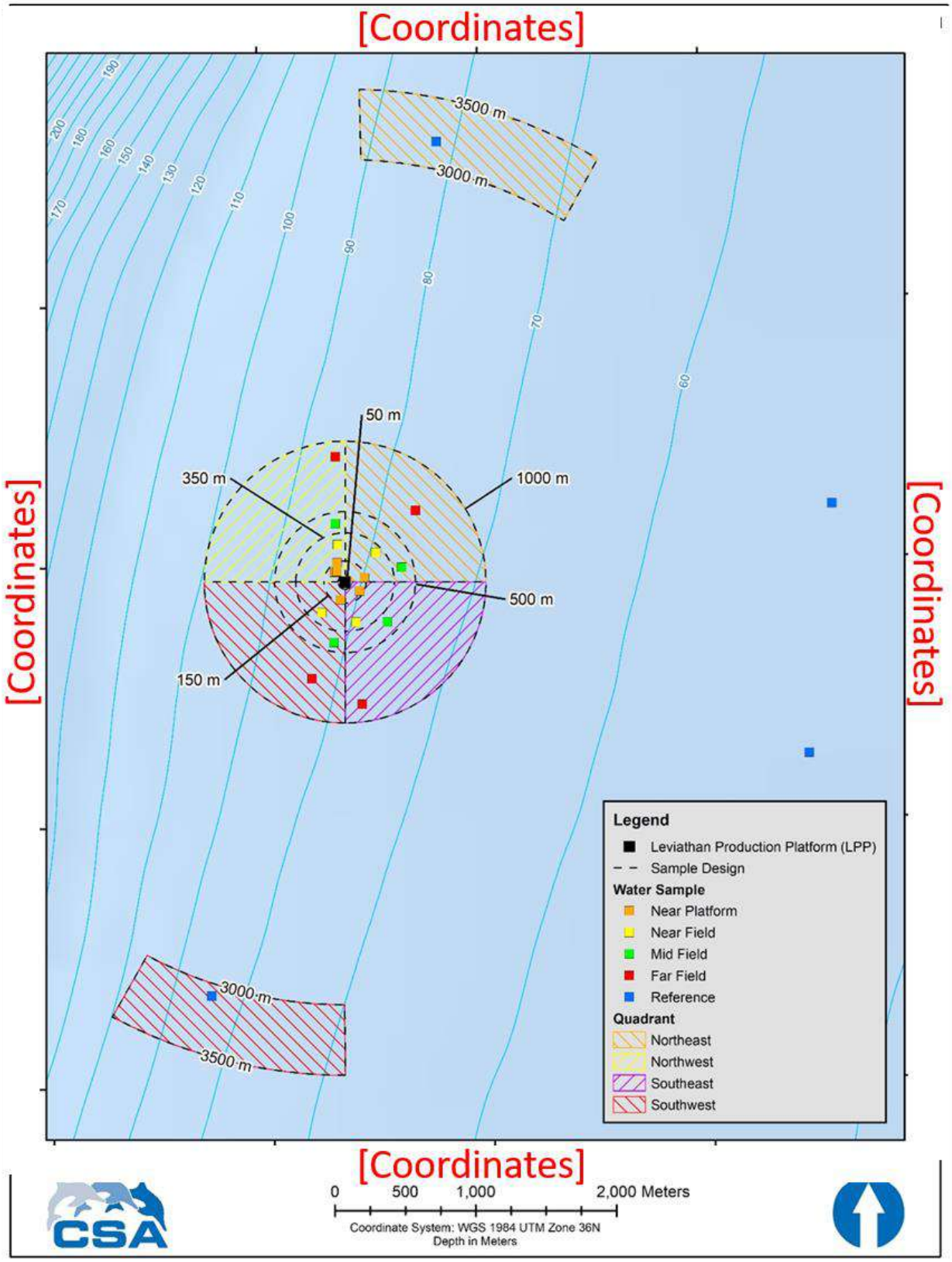


Figure 3. Location of seawater stations during the 2020 Leviathan Production Platform Environmental Monitoring Survey.

2.3 SEDIMENT SAMPLING

Sediment sampling stations were also positioned using a stratified random sampling pattern with stratification based on both distance and direction from the LPP (**Table 7**; **Figure 4**). Due to vessel safety considerations and platform safety procedures, it was not possible to conduct sediment sampling at distances of less than 50 m from the LPP structure; therefore, the first distance stratum (i.e., Near-Platform) included an area from 50 to 150 m from the edge of the LPP topside. Geographic coordinates for the sediment sampling stations are listed in **Appendix C**.

The locations of three sediment sampling stations were randomly selected within each of the strata for a total of 46 sediment stations. One infauna sample was collected at each of the sediment sampling stations. **Figure 5** shows a comparison of the sample stations in the vicinity of the LPP for the 2014 Leviathan Field Development EBS, the 2019 LPP EBS, and the 2020 LPP EMS.

Table 7. Designation of distance and directional stratification within the Leviathan Production Platform (LPP) survey area. The number of sediment sampling stations within each stratum are also provided.

LPP Distance Strata (m)	LPP Directional Strata				
	Northwest	Northeast	Southeast	Southwest	Sediment Stations within Directional Strata
	Number of Sediment Stations				
Near-Platform (50–150 m)	1	1	1	1	*4*
Near-field (150–350 m)	3	3	3	3	*12*
Mid-field (350–500 m)	3	3	3	3	*12*
Far-field (500–1000 m)	3	3	3	3	*12*
Reference (3,000 m)	--	3	--	3	*6*
Sediment Stations within Distance Strata	*10*	*13*	*10*	*13*	--
Total Number of Sediment Stations					**46**

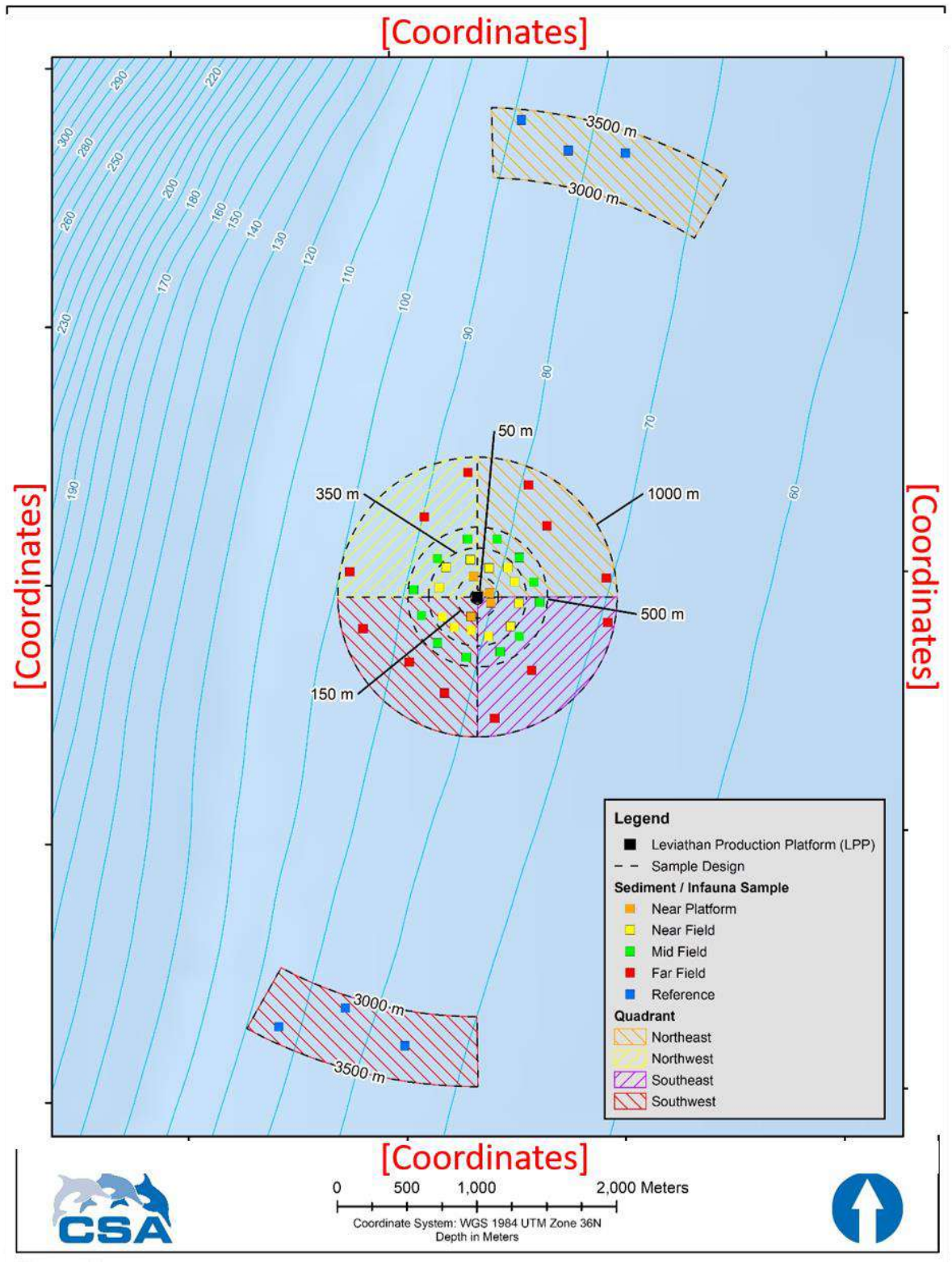


Figure 4. Locations of sediment and infauna samples collected during the 2020 Leviathan Production Platform Environmental Monitoring Survey. Strata are organized both by distance (i.e., different colored stations) and direction (i.e., different colored crosshatch).

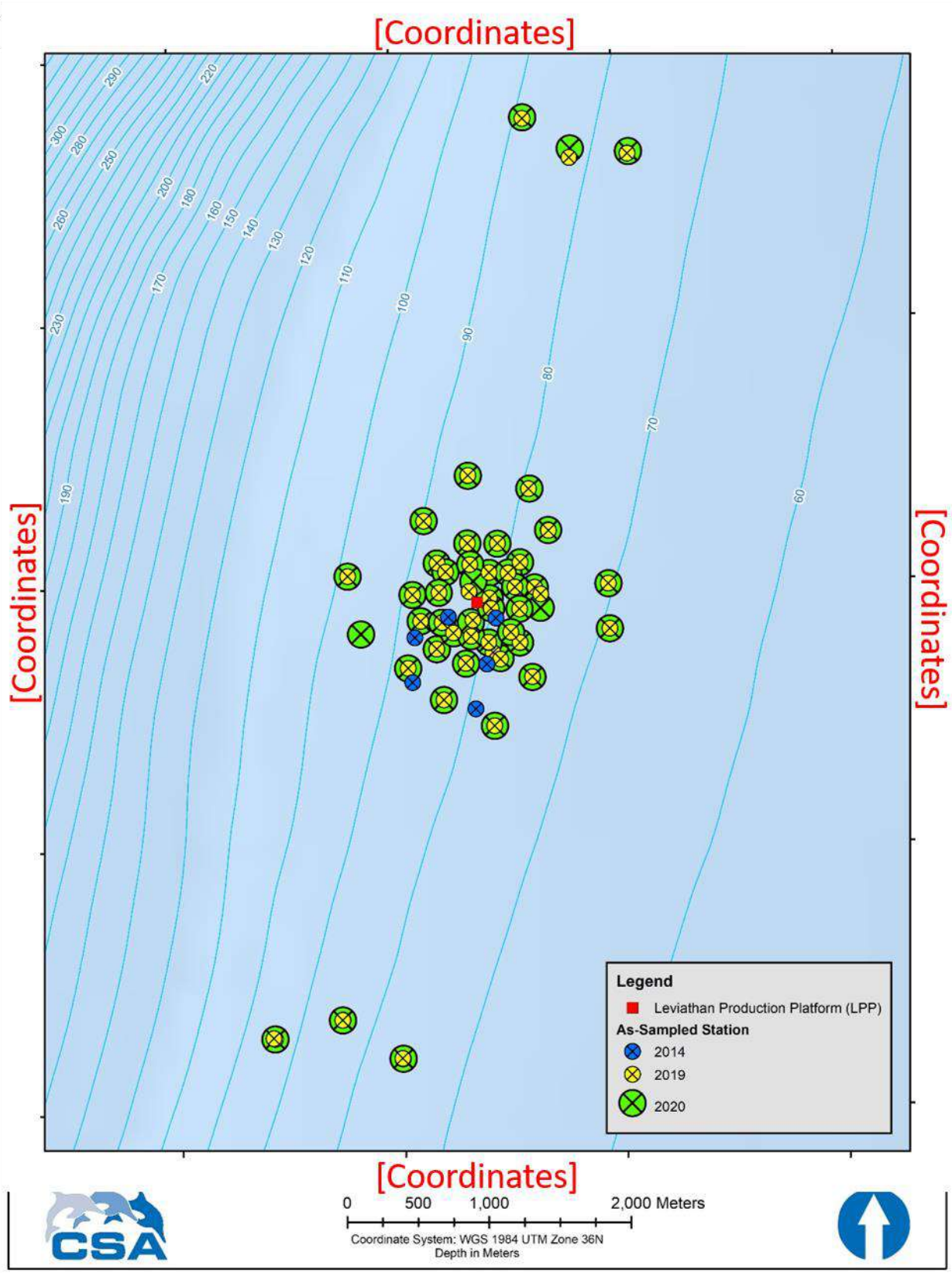


Figure 5. Locations of sampling stations during the 2014 Leviathan Field Development Environmental Baseline Survey, the 2019 Leviathan Production Platform (LPP) Environmental Baseline Survey and the 2020 LPP Environmental Monitoring Survey.

2.4 HARDBOTTOM MONITORING

A naturally occurring hardbottom trend located approximately 3.5 km north of the LPP was identified during a pre-installation seafloor survey. After installation of the LPP jacket, a post-installation qualitative environmental survey was conducted in March 2019 to assess general conditions and visually obvious temporal changes to the hardbottom benthic and ichthyofaunal assemblages. Based on the qualitative visual data (still and video imagery) collected during the pre- and post-installation environmental surveys, there was no detectable temporal changes to the hardbottom benthic environment in relatively close proximity to the LPP.

Twelve hard-bottom locations selected during the March 2019 post-installation survey were investigated during the 2020 LPP EMS (**Figure 6**). Geographic coordinates of the 12 stations are listed in **Appendix C**. The placement of the 12 stations was deliberate in order to create a distance gradient for down-current observations over time. At each station, a 360-degree view of the existing hard-bottom was recorded, and close-up still photographs of epibenthic cover and demersal fishes were taken. Qualitative difference between surveys were noted in order to evaluate potential impacts resulting from platform activities over time. On-board marine scientists recorded a narrative of seafloor observations to characterize presence and condition of substrates and associated biota.

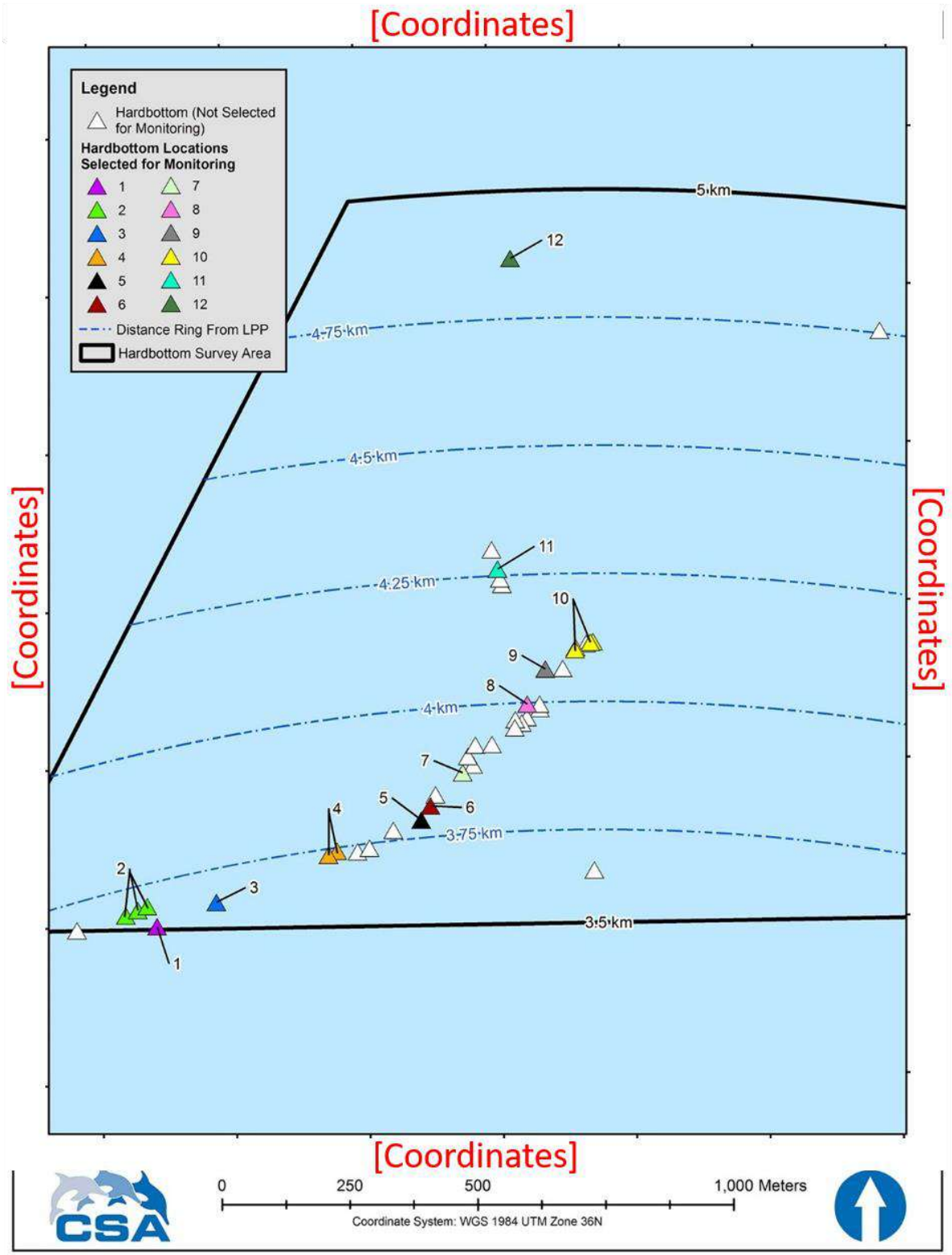


Figure 6. Hardbottom locations selected for monitoring (colored triangles) are distributed throughout the survey area located between 3.5 and 5 km from the Leviathan Production Platform.

2.5 PLATFORM FOULING AND FISH COMMUNITIES

Video data were collected from the LPP to assess species composition and abundance of fish assemblages and fouling communities associated with the platform. A systematic video survey of the vertical structural units (legs) on the down-current and up-current sides of the platform and the water column immediately surrounding them was conducted by a remotely operated vehicle (ROV; **Section 3.2**) with illuminated digital video capabilities to characterize the fouling and fish communities associated with the LPP. For the purposes of this survey, the fouling communities refer to attached, sessile organisms, as well as associated motile invertebrates (e.g., echinoderms). The fish community survey included any fish that was observed associated with the platform and recorded by the ROV video.

A depth-stratified method was conducted to characterize the fouling and fish communities associated with the platforms (Stanley and Wilson, 2000, Wilson et al., 2006). The ROV continuously recorded the LPP support legs and the adjacent water column from a depth of 10 m to the seafloor. Sampling at depths shallower than 10 m was not possible due to safety concerns. To characterize the fouling community, the ROV hovered alongside and zoomed-in on each LPP support leg at every 5 m water depth until reaching a depth of 30 m (**Table 8**). After 30 m water depth, the ROV hovered alongside and zoomed-in on each LPP support leg at every subsequent 10 m water depth until reaching the seafloor. Concurrently, the fish community was characterized within the same depth strata, which are listed in **Table 8**.

The ROV continuously recorded video within each depth strata. At the end of each depth stratum (those corresponding to the fouling community water depths [e.g., at 20 m, 25 m, 30 m, 40 m, etc.]) the ROV was held stationary a few meters from the structure with the video camera facing toward the structure for a 1-minute period. During this period, the ROV shifted laterally around the platform leg. After each 1-minute survey of the platform leg, the ROV was turned away from the platform to record video of the water column for a 1-minute period to characterize fish not specifically associated with the platform legs. ROV operations were conducted on a 12 hours per day basis.

Table 8. Summary of the sampling depths and depth strata used to characterize the fouling and fish communities.

Sampling Depths (m)	Fouling Community Depths (m)
10 to 30	Every 5
30 to Seafloor	Every 10
Sampling Depths (m)	**Fish Community Depth Strata (m)**
10 to 30	10 to 15 15 to 20 20 to 25 25 to 30
30 to Seafloor	30 to 40 40 to 50 55 to 60 60 to 70 70 to 80 80 to 86

2.6 BIOACCUMULATION PASSIVE SAMPLING DEVICES

Bioaccumulation consists of small amounts of contaminants capable of building up in the tissues of exposed organisms such as fishes and invertebrates over time. For offshore oil and gas operations these contaminants, primarily PAHs and trace metals, are introduced through effluents such as produced water discharges. Bioaccumulation in organisms, usually sessile invertebrates (e.g., clams or mussels) and fishes, associated with actively discharging platforms is studied by examining

contaminant levels in tissues, viscera, or whole animals (e.g., Harman et al., 2011; Hale et al., 2016). Organisms for testing may be collected around the platform or may be held in cages or on racks at varying distances from the discharge point. Bioaccumulation studies for PAHs and metals in the marine environment have historically been conducted with in-situ deployment of live biota, usually mussels or fish (e.g., Green et al., 1986; Roper et al., 1997; Salazar and Salazar, 1995). However, this method can be controversial due to ethical issues with using live animals for testing, interference in results from lipids naturally present in the test organisms (Gert-Jan de Maagd, 2009), and logistic issues with keeping caged animal alive and free of predation or other health issues for the length of the deployment. Additionally, collecting sufficient numbers of organisms of different species may be difficult and the unknown extent of movements by fishes, even those species presumed to be site-attached, results in considerable uncertainty with respect to contaminant sources. Caged organisms can provide a more controlled situation (e.g., placement of organism relative to the contaminant source) for assessing bioaccumulation but seasonal and environmental conditions affecting well-being and survivorship of those organisms can confound the efficiency of accurate data collection.

Another approach for estimating potential bioaccumulation is to deploy passive sampling devices (PSDs) that use synthetic material such as semipermeable membrane devices (SPMDs). Passive samplers have been in use for decades and their use with offshore oil and gas operations has increased recently (e.g., Harman et al., 2011; Hale et al., 2016). SPMDs are designed to mimic the passive uptake of organic compounds such as PAHs, across biological membranes (e.g., gills). The synthetic membranes are made of polyethylene and filled with a triolein film. Triolein is a lipid-based material that will accumulate PAHs and other organic compounds over time. SPMDs as a stand-alone option or a complement to caged organisms, can produce more standard measures of contamination risk over a broader area. SPMDs were deployed to monitor small concentrations (ng L^{-1}) of low-molecular weight hydrocarbons (PAHs) in the vicinity of the LPP. These data allows for the assessment of the risk for bioaccumulation of PAHs around the LPP.

Diffuse gradient in thin film (DGT) samplers, another type of PSD that differs from the SPMDs, was used to assess bioavailable metals (cadmium, chromium, lead, manganese, mercury, nickel, and zinc). DGT samplers measure the accumulated mass of labile metal species (i.e., free metal cations, inorganic, and some small organic metal complexes). These labile metal species are the most likely to be bioavailable. Using the analytically determined metal mass and Fick's law of diffusion, a concentration of bioavailable metals can be calculated. This concentration is reported as the mean time weighted average concentration (TWAC) at the interface between the sampler and the deployment matrix (e.g., seawater). The sampler uses a binding agent within a hydrogel, overlain by a filter membrane. The known rate of diffusion across this membrane allows for the quantification of the TWAC of the targeted dissolved substance. DGT membranes have extensive published literature relating to investigation of trace metals concentrations in estuarine/seawater (e.g., Wallner-Kersanach et al., 2009; Kim et al, 2016; Schintu et al., 2009).

It should be noted that two types of DGT samplers were utilized depending on the target analyte: 1) samplers with a Chelex (iminodiacetate) binding layer for measuring cadmium, chromium, lead, manganese, nickel, and zinc; and 2) samplers with a 3-mercaptopropyl silica binding layer for mercury. It has been shown that mercury does not bind well to Chelex (e.g., Docekalová and Divis, 2005).

SPMDs and DGT samplers were deployed at five locations: four down-current from the LPP (200, 500, 1,000, and 3,500 m from the LPP), and one at the kurkar hardbottom site. The deployed locations for the PSDs samplers relative to the LPP are provided in **Figure 7**.

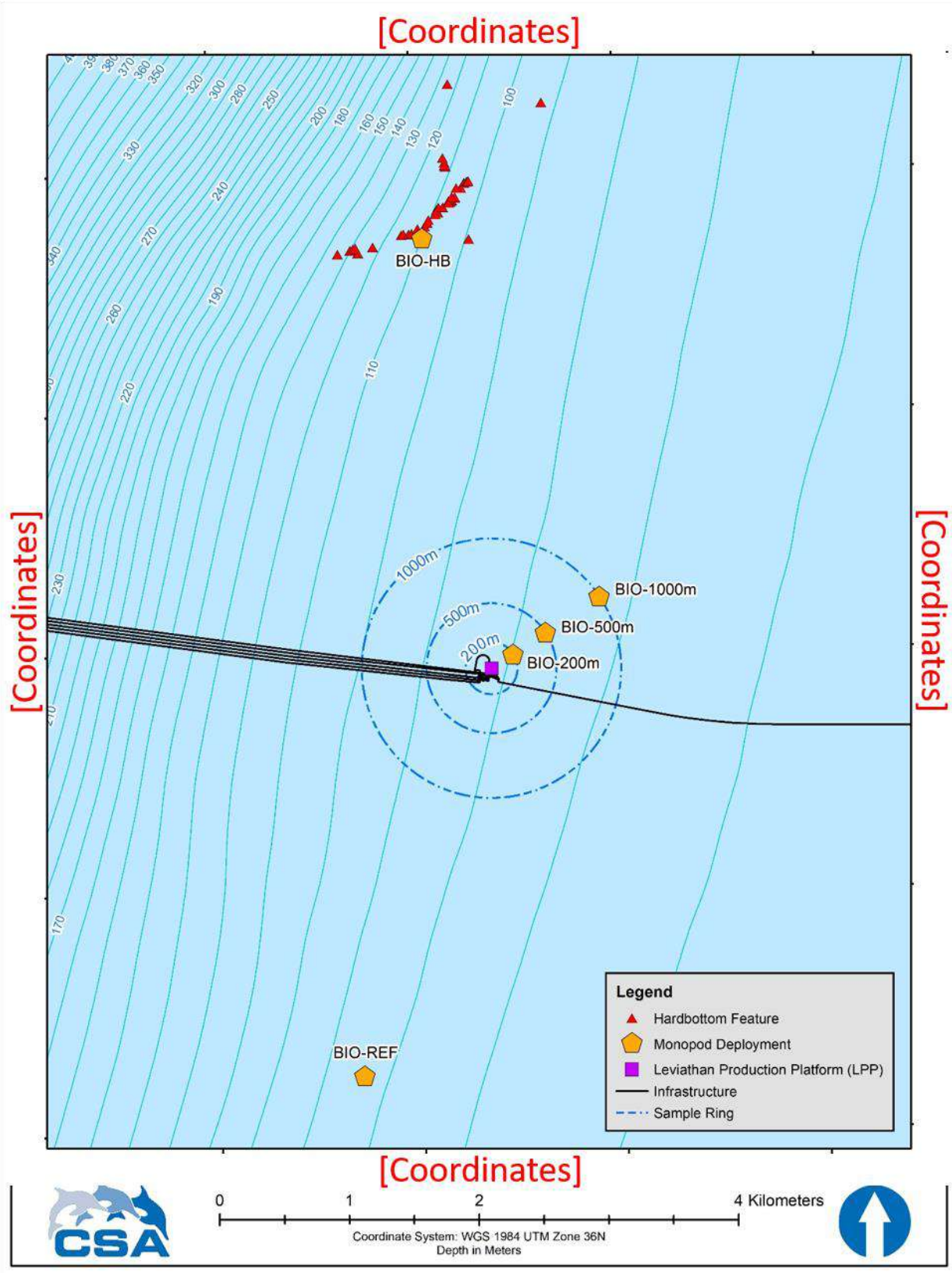


Figure 7. Deployment locations of passive sampler devices (semipermeable membrane devices and diffuse gradient in thin film samplers) during the 2020 Leviathan Production Platform Environmental Monitoring Survey.

3 Field Methods

3.1 SURVEY PERSONNEL

This survey involved 24-hour operations during the field sampling effort. MVI/CSA provided six survey personnel (four scientists and two operational technicians) to conduct in-country mobilization of survey equipment and supplies, outfit the vessel to conduct sediment sampling, and process collected samples. The names and roles of MVI/CSA staff are provided in **Table 9**.

Table 9. Names and roles of the staff members who conducted the 2020 Leviathan Production Platform Environmental Monitoring Survey.

Staff Name	Staff Role
Mr. [NAME]	Chief Scientist
Ms. [NAME]	Project Scientist/Health and Safety Officer
Ms. [NAME]	Project Scientist
Ms. [NAME]	Project Scientist
Mr. [NAME]	Operations Manager
Mr. [NAME]	Operations Technician

3.2 SURVEY VESSEL, REMOTELY OPERATED VEHICLE, AND OPERATIONS

The survey vessel and navigational equipment were provided by Noble Energy. M/V *Nor Naomi*, owned and operated by NorTrans Offshore II PTE LTD and under contract to Noble Energy, was used for the 2020 LPP EMS (**Image 1**). The survey vessel was mobilized with personnel and equipment from Haifa Port, Israel. Vessel specifications are found in **Appendix D**.

Video data was collected using a Schilling HD 150 HP ROV that was contracted by Noble Energy and owned and operated by DeepOcean (**Image 2**). The ROV system installed on the M/V *Nor Naomi* included the vehicle, a dedicated tether management system, launch and recovery system, and an ROV control center. An ultra-short baseline transponder was attached to the ROV to record its position relative to the vessel, using differential global positioning system. The positions of the ROV track and sample collection locations were recorded and stored by the ultra-short baseline transponder navigation software. The ROV was equipped with an altimeter reporting height above the bottom that allowed the operator to maintain the ROV at a desired vertical position. The ROV's computer control system provided automatic heading, altitude, depth, pitch, and roll control. Digital video data were collected continuously during sediment and seawater sample collection with a high-definition color zoom camera mounted on hydraulic pan-and-tilt units with multiple 250-watt lamps for illumination. Dual parallel laser beams with a known distance apart (10 cm), were placed in the camera field of view, and were used as a scale bar for the visual monitoring components.



Image 1. The M/V *Nor Naomi*, the vessel used for the 2020 Leviathan Production Platform Environmental Monitoring Survey.

3.3 PLATFORM FOULING AND FISH COMMUNITIES

Using the methods described in **Section 2.5**, the ROV systematically surveyed all LPP legs on the down-current and up-current sides of the platform. The interior and up-current side of the platforms were avoided to reduce the risk of entanglement. Video was collected along the lengths of the four northeastern platform legs (B-2, C-2, F-2, and G-2), and the two southwestern platform legs closest to the LPP discharge point (B-4 and C-4) to assess potential differences between the platform sides resulting from proximity to the discharge point. **Table 10** summarizes the sampling dates and the start and end times of the video surveys recorded with the ROV. Notes on the fouling community and fish associated with the legs and cross-members were recorded in the field by MVI/CSA scientists. Community analysis was conducted in the MVI office (Nesher, Israel) and is described below in **Section 4.5**.



Image 2. A DeepOcean Schilling remotely operated vehicle and associated tether management system used during the 2020 Leviathan Production Platform Environmental Monitoring Survey.

Table 10. Date and times of sampling and the sample depths for each platform leg sampled using the remotely operated vehicle (ROV) for the fouling and fish community analysis. Times indicate the start and end of ROV video recording.

Date Sampled (dd/mm/yy)	Platform Side	Platform Leg	Time Start to End (hh:mm)	Depth of Sampling (m) (<30 m: 5-m depths/strata >30 m: 10-m depths/strata)
30/12/20	Northwest	B-2	08:15 – 09:49	10 to 30
				40 to 80
		C-2	10:03 – 11:26	10 to 30
				40 to 80
		F-2	11:30 – 12:38	10 to 30
				40 to 80
		G-2	12:43 – 13:46	10 to 30
				40 to 80
	Southwest	B-4	15:32 – 16:43	10 to 30
				40 to 80
		C-4	16:47 – 18:11	10 to 30
				40 to 80

3.4 WATER COLUMN SAMPLING

Vertical hydrographic profiles of the water column from the surface to approximately 1 m above the seabed were conducted using a conductivity-temperature-depth (CTD) water quality profiler mounted to the ROV. Measurements of salinity, temperature, pH, turbidity, chlorophyll a (as measured by fluorescence), and dissolved oxygen (concentration and percent saturation) were collected continuously throughout the water column during each profile at each station using a Sea-Bird Electronics, Inc. (SBE) 19*plus* CTD profiler.

Water samples were collected with clean Go-Flo water sampling bottles mounted on a fabricated ROV rack and manually activated using the ROV's manipulators. Water samples were transferred from the collection bottles into pre-cleaned sample containers, processed on board, and stored as recommended by the USEPA protocols (U.S. Geological Survey [USGS], 2000). Water parameters and sampling protocols are summarized in **Table 11**. Radioactive compounds were only collected within the near-surface and near-bottom samples of the four seawater stations located within 50 m of the platform, four seawater stations located within the mid-field stratum, and both reference stations (10 total stations).

Table 11. Guidelines for water sample collection (From: U.S. Geological Survey, 2000).

Parameter/ Analyte(s)	Minimum Sample Volume	Container Type and Size	Handling, Storage Conditions, and/or Preservation Method	Holding Time
TOC/TN/TP	250 mL	250-mL HDPE plastic bottle	Frozen; ship on ice	28 days
NO_2/ NO_3/NH_4/PO_4	250 mL	250-mL HDPE plastic bottle	Filter; Freeze filtrate; ship on ice	28 days
TPH (and PAH if TPH is detected)	1 L	1-L amber glass bottle	Dichloromethane; cool to 4°C; ship on ice	28 days
TSS	1 L	Pre-weighed filter	Filter, store frozen, ship on ice	indefinite
BTEX	40 ml	2 × 40-mL VOA	HCl; cool to 4°C; ship on ice	28 days
$Radium^{226}$, $Radium^{228}$, $Thorium^{228}$	4 L	4-L plastic jug	HCl; cool to 4°C; ship on ice	28 days
Phenols	1 L	1-L amber glass bottle	Ship on ice	7 days

BTEX = phenols, and benzene, toluene, ethylbenzene, and xylenes; HCl = hydrochloric acid; HDPE = high-density polyethylene; NO_2 = nitrite; NO_3 = nitrate, NH_4 = ammonium; PAH = polycyclic aromatic hydrocarbons; PO_4 = phosphate; TN = total nitrogen; TOC = total organic carbon; TP = total phosphorus; TPH = total petroleum hydrocarbons; TSS = Total suspended solids; VOA = volatile organic compounds.

3.5 SEDIMENT AND INFAUNAL SAMPLING

Sediment and infaunal samples were collected using a stainless steel 0.5-meter × 0.5-meter modified Gray O'Hara box corer. Each box core sample was evaluated for acceptability on return to deck using standard USEPA (2001) sediment grab sampling criteria as follows:

- No sediment touching the top of the sampler or overflowing from the sampler;
- Clear, overlying water present in the sampler;
- No sign of channeling or sample washout; and
- No evidence of sediment loss.

Box core samples were subsampled for sediment chemical and geological analyses and infauna. The box core sample was partitioned using a 0.35-meter × 0.35-meter stainless steel insert to separate the chemical and geological subsample from the infaunal sample. Box core samples were subsampled for chemical and geological analytes by collecting sediment from the top 0.5 cm (but not greater than 1.0 cm) of the sediment. Processing for infauna is described in greater detail in **Section 3.5.2**. Pre-cleaned stainless sampling spatula were used to collect the top 0.5 cm of the sediment.

The top 0.5 to 1 cm of the box core was subsampled for sediment physio-chemical analyses including grain size distribution/particle size analysis, TOC, metals, phenols, volatile organic compounds (VOCs), and hydrocarbons (alkanes and PAHs). Radionuclides were analyzed from 14 sediment stations. Analyses were conducted to determine the concentrations of various USEPA priority pollutant and hydrocarbon-associated metals including arsenic, barium, cadmium, chromium, copper, lead, mercury, nickel, and zinc. Sediments were also analyzed for aluminum and iron. These metals occur naturally within the environment and can be used as reference metals to detect unnatural concentrations of hydrocarbon-associated metals through correlation. Sediment samples were transferred into precleaned sample containers, frozen, and handled/stored as recommended by USEPA protocols. Sediment sampling protocols are summarized in **Table 12**.

Table 12. Processing and storage requirements for sediment chemistry sampling parameters.

Parameter/ Analyte(s)	Sampling Procedure	Container Type and Size	Storage Conditions and/or Preservation Method	Holding Time
Grain size distribution/particle size analysis; total organic carbon	Box core sample; collect in pre-cleaned plastic jar	250-mL wide-mouth plastic jar	Freeze, ship on ice, and store frozen	Indefinite when frozen
Metals*	Box core sample; collect in pre-cleaned plastic jar	250-mL wide-mouth plastic jar	Freeze, ship on ice, and store frozen	Indefinite when frozen
TPH/PAH	Box core sample; collect in glass container with Teflon-lined caps	125-mL wide-mouth glass jar	Freeze, ship on ice, and store frozen	28 days
VOCs	Box core sample; collect in glass vial with Teflon septa	2 × 20-mL glass vial with septa	Freeze, ship on ice, and store frozen	28 days
Phenols	Box core sample; collect in glass container with Teflon-lined caps	125-mL wide-mouth glass jar	Freeze, ship on ice, and store frozen	14 days
$Radium^{226}$, $Radium^{228}$, $Thorium^{228}$	Box core sample; collect in pre-cleaned plastic jar	500-mL wide-mouth plastic jar	Freeze, ship on ice, and store frozen	indefinite
Infauna	Box core sample; collect in pre-cleaned plastic jar	1-L wide mouth plastic jar	Preserve with 8% buffered formalin (duplicate samples at selected stations were be preserved in ethanol)	N/A

*Metal analyses include aluminum, arsenic, barium, cadmium, chromium, copper, iron, mercury, nickel, lead, and zinc.
PAH = polycyclic aromatic hydrocarbons; TPH = total petroleum hydrocarbons; VOCs = volatile organic compounds.

3.5.1 Infaunal Samples

Infaunal samples collected from within the box corer were wet-sieved through a mesh sieve with a technique that minimizes trauma to infaunal organisms and facilitates resuspension of sediment (including clay fractions) and separation of infaunal organisms from the sediment. The apparatus consisted of a sample mixing barrel fitted with a spillover drain, and was positioned above a large spillover barrel. A 12-in. diameter stainless steel 0.25-mm sieve was mounted between the spillover drain and over the lower spillover sink (**Image 3**). The flow rate from the mixing barrel was monitored to prevent overloading on the sieve screen. The sieved sample (containing infaunal organisms, residual sediment, and debris) was consolidated and transferred to a labelled sample container, preserved with an 8% borax-buffered formalin solution and thoroughly percolated. Appropriately sized sample jars were labeled and properly stored aboard the vessel; the lids were sealed with electrical tape to prevent leakage of preservative during shipment.

At four stations, an additional sample was collected and preserved in 90% ethanol to allow for potential genetic identification of infauna organisms. These samples will be provided to the Israel Oceanographic and Limnological Research Institute (IOLR).



Image 3. Macrobenthic infaunal sieving apparatus. The apparatus consists of an upper mixing barrel and sieve table over a lower spillover sink.

3.6 HARDBOTTOM MONITORING

The patchily distributed hardbottom discussed in **Section 2.4** is composed of discrete kurkar outcrops separated by a softbottom habitat. These hardbottom features are in water depths ranging from 107 to 130 m and have variable vertical relief visually estimated to be in excess of 2 m. The observed kurkar hardbottom features supported an epibenthic biotic assemblage visually dominated by sponges. Pre- and Post-LPP installation surveys indicated benthic cover at the hardbottom targets on horizontal surfaces to be between <1% to 25%, with most features having between 5% to 10% benthic coverage (Marine Ventures International, Inc., 2018, 2019a).

The hardbottom trend was visually assessed using ROV-based video and still imagery. This task assessed the condition of the habitat and qualitatively documented taxa of epibenthos and fishes associated with the hardbottom. A high-definition color zoom video camera (Insite Pacific, model number 005-8681) mounted on a controllable pan and tilt motor on the ROV was used to collect visual survey data. Underwater photographic data was collected to document the conditions of the substrate and associated biological communities within the immediate area of the revisited hardbottom features. The ROV-mounted camera was aimed slightly above vertical to provide a field

of view that includes the bottom substrate in front of the system. The ROV was maneuvered at relatively slow speeds around the station and close to the seafloor to ensure the collection of photographic data that best meet the study objectives. At each station, The ROV completed a 360-degree view of the existing hardbottom and took close-up still photographs of the epibenthic cover and demersal fishes. Video observations were recorded continuously, and representative qualitative photographs were collected as determined by the directing scientist.

3.7 BIOACCUMULATION PASSIVE SAMPLING DEVICES

Fabricated monopod devices (**Image 4**) were used to deploy the SPMD and DGT samplers on the seafloor at a total of five locations, including four down-current from the LPP at varying distances (Near-Platform, 200 m; Mid-Field, 500 m; Far-Field, 1,000 m and an up-current Reference, 3,500 m), as well as at one location near the hardbottom are approximately 3,600 m north of the LPP (as discussed in **Section 2.4**). At each location, triplicate SPMDs and DGT samplers were deployed for redundancy. The PSDs were deployed for a 43-day soak period prior to retrieval. The monopods were deployed and retrieved using the ROV on the M/V *Nor Naomi*.

The DGT samplers were shipped in cooled sealed containers directly from the manufacturer. The DGT membranes were fitted into a custom-made acrylic holder (**Image 5**) immediately prior to attaching them to the monopod devices for deployment. The analysis of DGT sampler data requires a known water temperature to accurately calculate TWACs. Therefore, deepwater temperature loggers (HOBO TidbiT) manufactured by Onset Computer Corporation were deployed on the Near-Platform monopod, the Reference monopod, and on the monopod located at the hardbottom location. The loggers collected a temperature reading every two minutes for the duration of the 43-day deployment.

The SPMDs were shipped on ice in sealed containers and frozen prior to deployment. SPMDs were fitted onto aluminum canisters, attached to the monopod, and then deployed at the sampling locations. Before fitting the membranes, all canisters were cleaned with soap and de-ionized water followed by a hexane rinse. Because the SPMDs absorb PAHs from the air, a field blank was exposed to the air at each deployment site then stored frozen pending SPMDs retrievals. Following retrieval, the SPMDs were recovered from the canisters, placed back into the shipping container, and sealed. These sealed sample containers were stored frozen and shipped on ice. The same field blank was re-exposed to the air and ambient conditions at the time of SPMD retrieval.



Image 4. Self-fabricated stainless-steel monopod with attached mounting cage for semipermeable membrane device deployment. Height of monopod is approximately 1.5 m.



Image 5. Acrylic holder with diffuse gradient in thin film samplers. The left column contains samplers measuring cadmium, chromium, lead, manganese, nickel, and zinc, and the right column contains samplers for mercury. Below the acrylic holder is a unit of the HOBO TidbiT temperature logger.

3.8 QUALITY ASSURANCE

A quality assurance (QA) program was implemented in this survey to verify that collected samples and data met required specifications and expectations. Quality control (QC) measures were implemented in the field as fundamental components of the project QA program. These QC measures included the collected representative samples and the implementation of sample management procedures to minimize sample loss, and ensure collection of requisite samples and data, such as the preparation of checklists and data checks, and the use of qualified/certified equipment, personnel, and laboratories; chain-of-custody (CoC) process; and detailed documentation of sample and data analysis steps and results. QC measures are discussed in the following sections.

3.8.1 Quality Control Measures

Cleaning Procedures

Sediment samplers and sample processing equipment were thoroughly cleaned prior to use in the field. Sampling equipment was cleaned with Alconox detergent and raw seawater before the start of the sampling effort, then thoroughly scrubbed and hosed out between sampling stations according to

accepted procedures. Pre-cleaned sample containers processed by the distributor following appropriate USEPA protocols as specified in the Office of Solid Waste and Emergency Response (OSWER) Directive 9240.0-05A "Specifications and Guidance for Contaminant-Free Sample Containers" (USEPA, 1992) were used for all sample collections.

Data and Sample Collection Checklists

Prior to the survey, data and sample checklists were prepared by the Lead Scientist and completed in the field as appropriate for QC. Prior to departing each sampling station, the Lead Scientist or his designee reviewed the checklist and physically examined and confirmed data files, logbooks, and sample containers to ensure that the data and required samples were properly collected and labelled.

Sample Preservation, Storage, and Holding Times

Samples were preserved according to specifications from applicable regulations or standard industry practice. Samples were shipped to the laboratories for analysis within prescribed sample holding times and under appropriate preservation and handling conditions.

3.8.2 Sampling Handling and Transport

To ensure proper management of the baseline survey activities and sample and data collection and handling, all stages of field sampling, and sample and data storage and handling were documented in a field logbook. All pertinent information concerning field activities and sampling were recorded in the logbook by an MVI/CSA field scientist, including problems encountered and necessary deviations from the proposed scope of work. Collected samples were packaged within shipping containers in a manner to avoid contamination or loss (leakage or breakage). The sample shipping containers themselves were secured to be leak proof and were clearly marked with shipping information and labels indicating content and fragility. Sample analysis instructions were prepared to accompany all samples shipped to the laboratories or were sent separately.

All samples were transported or shipped under a CoC process. Proper CoC was maintained for all samples, and a CoC record accompanied all samples. Each person involved with the custody of the sample(s) signed the appropriate forms and ensured that the samples were properly handled, stored, and transported to the analytical laboratories. The Lead Scientist or their designee confirmed by telephone or e-mail that all samples were delivered and logged in at each designated laboratory.

3.8.3 Document and Data Security

During field operations, all data collected (e.g., navigation and positioning) were saved to a field computer and backed up on separate, removable medium (e.g., backup computer, flash memory/data stick, or external hard drive). While on site, all backup media were stored separately from the field computer. Securing the primary data and backup copies occurred as soon as possible after the backups were created but within the same watch or day depending on the field deployment. Either the Lead Scientist or Operations Manager oversaw the collection and securing of the primary data as well as the creation and securing of all backup copies.

Following completion of the field survey, the field computer and all backup media were transported separately by the Lead Scientist or the Operations Manager under the direction of the Lead Scientist with at least one copy travelling in personal possession. Upon return to CSA's corporate headquarters in Stuart, Florida, the Lead Scientist ensured that all data were properly delivered, cataloged, and transferred to CSA's local data delivery file server. Field notebooks and datasheets were then copied and scanned into files that were then associated with the project data and placed on the CSA server Once the delivery of the project data was finalized, the data was secured to read-only status, a copy of all project data was created on CSA's project data server, and a link to the location of these data was shared with the Project Manager to ensure redundant knowledge and to secure future access. The Lead Scientist, working with CSA's Database Administrator verified that all the data were transferred

to CSA's project data server and individual datasets transferred into CSA's Enterprise SQL Server database management system as appropriate. CSA currently maintains three copies of the data; one live working copy on CSA's data server, one protected copy on CSA's data delivery file server and one on magnetic tape (off campus bank vault) for disaster recovery purposes.

3.8.4 Data and Document Review

Standardized sample description nomenclature was utilized throughout the project and with laboratories for consistent reporting and seamless incorporation of reported results MVI/CSA's data servers. Data review and QC procedures were implemented to ensure that sample and data collections from the field and analytical results from laboratories were accurate and accompanied by required metadata. A CSA scientist with requisite experience and background reviewed all datasets prior to data analysis and inclusion into the report. The draft report was subject to in-house technical and editorial review and copy proofing.

4 Laboratory Methods, Data Processing, and Analysis

4.1 HYDROGRAPHIC PROFILES

Digital data files from the SBE 19*plus* V2 CTD profiler were processed using Sea-Bird Electronics, Inc. (SBE) proprietary data processing software, to convert the raw data to a text file, extract the desired sections, and import the file into a spreadsheet prior to plotting. Further processing prepared the data as diagrammatic vertical hydrographic profiles using SigmaPlot and tabular spreadsheet summaries. The hydrographic data collected during the previous Leviathan Field Development EBS and 2019 LPP EBS were compared by visual inspection to identify any substantive differences or trends between surveys.

4.2 SEAWATER AND SEDIMENT SAMPLES

Laboratories with established quality assurance programs that have provided analytical services for several MVI/CSA projects involving seawater and marine sediments were used to conduct the sample analyses. Chesapeake Biological Laboratory (Solomons, Maryland, U.S.) performed the analysis of seawater nutrients, TOC, and total suspended solids (TSS). TDI-Brooks/B&B Laboratories (College Station, Texas, U.S.), a research and contract laboratory with extensive experience in the analysis of hydrocarbons and other organics in seawater and marine sediments, performed the analyses of seawater and sediment hydrocarbons. Stratum Reservoir (formerly Weatherford Laboratories) (Houston, Texas, U.S.) performed the analyses for sediment grain size distribution/particle size analysis. Bactochem Ltd. (Ness Ziona, Israel) performed the analysis of sediment TOC. ALS Environmental (Kelso, Washington, U.S.) performed the analysis of sediment metals, phenols, and VOCs, as well as seawater phenols, and benzene, toluene, ethylbenzene, and xylenes (BTEX). ALS Environmental (Ft. Collins, Colorado, U.S.) performed the analysis of radioactive compounds for seawater and sediment samples. **Tables 10** and **11** outline the analytical parameters, analysis methods, reporting limits, and reporting units of seawater and sediment samples, respectively.

Laboratory results are reported as either method reporting limits (MRLs) or laboratory method detection limits (MDLs). The MRL is defined as the lowest level that can be reliably achieved within specified limits of precision and accuracy during routine laboratory operating conditions. The MDL is defined as the minimum concentration of a substance that can be measured and reported with 99% confidence that the analyte concentration is greater than zero and is determined from analysis of a sample in a given matrix containing the analyte. Methods for analyzing seawater and sediment and the corresponding quantification limits are summarized in **Tables 13** and **14** (limits of detection and resolution for the various analyses are approximate and are dependent upon sample type and volume).

Table 13. Analytical parameters, analysis methods, reporting units, reporting/limits of quantification, Mediterranean environmental water quality standards (MEWQS), and analytical laboratory for seawater samples.

Parameter/ Analyte	Digestion/ Extraction Method	Analytical/Detection/ Quantification Method	Quantification Limit	MEWQS [a]		Units	Analytical Laboratory
				Mean	Max.		
TPH	Hexane	USEPA/SW-846 Modified 8100/8015C	13	--	--	µg L^{-1}	TDI Brooks
PAH (only if TPH is detected)	Hexane	USEPA/SW-846/8269/GC-MS	0.74–2.91	--	--	ng L^{-1}	
TN	Persulfate digestion	Diazo colorimetric method	0.15	1.0		mg L^{-1}	Chesapeake Biological Laboratory
TP	Persulfate digestion	Ascorbic acid colorimetric method	0.0045	0.1		mg L^{-1}	
TOC	N/A	Sugimura and Suzuki 1988	0.50	--		mg L^{-1}	
Nitrite	N/A	Diazo colorimetric method	0.0022	--		mg L^{-1}	

Table 13. (Continued).

Parameter/ Analyte	Digestion/ Extraction Method	Analytical/Detection/ Quantification Method	Quantification Limit	MEWQS [a]		Units	Analytical Laboratory
				Mean	Max.		
Nitrate	Cadmium reduction	Diazo colorimetric method	N/A[b]	--		mg L^{-1}	Chesapeake Biological Laboratory cont'd
Ammonium	N/A	Indophenol colorimetric method	0.039	0.50	2.4	mg L^{-1}	
TSS	N/A	Analytical balance	0.01	--		mg L^{-1}	
BTEX	Hexane	USEPA 8260C/GC-MS	0.50	--		µg L^{-1}	ALS Kelso
Phenols	Chloroform	USEPA 9065	0.01	--		mg L^{-1}	ALS Kelso
Radioactive Compounds	N/A	USEPA Method 903.1/904.0	1	--		pCi L^{-1}	ALS Ft. Collins

[a] Mediterranean Environmental Water Quality Standards proposed by the Ministry of Environmental Protection (2002).
[b] Computed by calculation.
BTEX = phenols, and benzene, toluene, ethylbenzene, and xylenes; GC-MS = gas chromatography-mass spectrometry; N/A = not applicable; PAH = polycyclic aromatic hydrocarbons; TN = total nitrogen; TOC = total organic carbon; TP = total phosphorus; TPH = Total Petroleum Hydrocarbons; TSS = Total suspended solids; USEPA = U.S. Environmental Protection Agency.

Table 14. Analytical parameters, analysis methods, reporting units, reporting/limits of quantification, sediment quality guidelines, and analytical laboratory for sediment samples. Quantification limit is the method reporting limit.

Parameter/Analyte	Digestion/ Extraction Method	Analytical/Detection/ Quantification Method	Quantification Limit	ERL	ERM	Units	Analytical Laboratory
Grain size distribution/particle size analysis	N/A	Laser diffraction particle size analysis	0.1	--	--	µm	Stratum Reservoir
TOC	N/A	In-house method based on European Standard Norm 1484	5	--	--	ppm	Bactochem
Aluminum	HF digestion[a]	ICP-OES (200.7)	25	--	--	ppm	ALS Kelso
Arsenic	HF digestion	ICP-MS (200.8)	4	8.2	70	ppm	
Cadmium	HF digestion	ICP-MS (200.8)	0.16	1.2	9.6	ppm	
Chromium	HF digestion	ICP-MS (200.8)	1.6	81	370	ppm	
Copper	HF digestion	ICP-MS (200.8)	0.8	34	270	ppm	
Iron	HF digestion	ICP-OES (200.7)	50	--	--	ppm	
Lead	HF digestion	ICP-MS (200.8)	0.4	46.7	218	ppm	
Nickel	HF digestion	ICP-MS (200.8)	1.6	20.9	51.6	ppm	
Zinc	HF digestion	ICP-MS (200.8)	4	150	410	ppm	
Mercury	HF digestion	USEPA 1631 (P&T/ICP-AFS)	0.001	0.15	0.71	ppm	
Phenols	Chloroform	USEPA 9065 Modified	0.20–0.46	--	--	ppm	
VOC	Hexane	USEPA SW-846/8260B/GC-MS	1	--	--	ppb	
Radioactive Compounds	N/A	USEPA Method 903.1/904.0	1	--	--	pCi g^{-1}	
TPH	Hexane	USEPA 1664/8100/8015/ GC-MS	1.4	--	--	ppm	TDI-Brooks
PAH	Hexane	USEPA SW-846/8260/ GC-MS	0.04–0.342	552b[b] 4,002[c]	3160[b] 44,792[c]	ppb	

a HF digestion results in the release of nearly all the metal content of a sample and it is believed to be a more accurate estimate of the metal concentrations in all sample matrices.
b PAHs = low molecular weight.
c Total PAHs.
ERL = effects range low; ERM = effects range median; GC-MS = gas chromatography-mass spectrometry; GSD/PSA = grain size distribution / particle size analysis; HF = hydrofluoric acid; ICP-MS = inductively coupled plasma-mass spectrometry; ICP-AFS = Inductively Coupled Atomic-Fluorescence Spectrometry; ICP-OES = inductively coupled plasma optical emission spectroscopy; N/A = not-available; PAH = polycyclic aromatic hydrocarbon; ppb = parts per billion; ppm = parts per million; P&T = purge and trap; SW = solid waste test method; TOC = total organic carbon; TPH = total petroleum hydrocarbons; USEPA = U.S. Environmental Protection Agency; VOC = volatile organic compounds; "--" = no benchmark value available.

4.2.1 Seawater

The following subsection provide a brief summary of the analytical methods used for each seawater sample parameter as summarized in **Table 13**.

Hydrocarbons

Hydrocarbon components in seawater were analyzed using solvent extraction and gas chromatographic techniques. The analytical method for total petroleum hydrocarbons (TPH) is USEPA/SW-846 Modified 8100/8015C. Analytical methods for PAHs include USEPA SW-846/8260, 8270, or equivalent, using an Agilent Model 6890/5973 gas chromatograph-mass spectrometer. Samples for phenols were analyzed using USEPA 9065 Phenolic material was reacted with 4-aminoantipyrine in the presence of potassium ferricyanide at a pH of 10 which produces an antipyrine dye. The amount of color produced is a function of the concentration of phenolic material. BTEX were analyzed by USEPA method 8260C using a gas chromatograph-mass spectrometer.

Total Organic Carbon

TOC was determined in a Shimadzu TOC-5000 analyzer using a high temperature combustion method. Samples were treated with hydrochloric acid and sparged with ultra-pure carrier grade air to drive off inorganic carbon. High temperature (680°C) combustion on a catalyst bed of platinum coated alumina balls breaks down organic carbon into carbon dioxide. The carbon dioxide was carried by ultra-pure air to a nondispersive infrared detector for quantification.

TSS, TN, TP, Nutrients

TSS concentrations in seawater samples were determined by pouring a known volume of seawater (~1 L) through a pre-weighed glass fiber filter of a specified pore size and then weighing the filter again after rinsing with deionized water to remove salts and drying in an oven to remove residual water. Seawater nutrient analyses included total nitrogen (TN), total phosphorus (TP), nitrate, and nitrite. TN and TP were determined through colorimetric methods in a segmented flow analyzer. TN was determined by the diazo colorimetric method after alkaline persulfate digestion, and TP was determined by the molybdo phosphoric blue colorimetric method after alkaline persulfate digestion. Initial analysis of samples for the determination of nitrogen bound in nitrate and nitrite was conducted by the enzyme-catalyzed reduction method, followed by the cadmium reduction method if the concentration was low. Nitrate and nitrite were measured by the colorimetric method. To determine the concentration of nitrogen bound in ammonium, filtered samples were complexed with sodium potassium tartrate and sodium citrate. The complexed sample reacted with alkaline phenol and hypochlorite, catalyzed by sodium nitroprusside, and then was measured by a photometric method. Concentrations of nitrite, nitrate, and ammonium are presented as mg N L^{-1}. To determine the concentration of phosphorous bound in phosphate, filtered samples were mixed with a sulfuric acid-antimony-molybdate solution, and subsequently with an ascorbic acid solution, then measured by a photometric method. Phosphate concentrations are presented as mg P L^{-1}.

Radioactive compounds

The radium (Ra) 226 in aqueous samples is concentrated and separated by co-precipitation with barium sulfate. Prior to separation, a portion of the sample is removed for inductively coupled plasma atomic emission spectroscopy determination of the preparation concentration of Ba in the sample. The Ba[Ra]SO_4 precipitate is dissolved in basic ethylenediaminetetraacetic acid solution, placed in a 40-mL volatile organic analysis vial, purged of any existing radon (Rn) 222, and stored to allow quantitative in-growth of Rn 222. After in-growth, the Rn is purged into an alpha scintillation cell. The short-lived Rn 222 progeny are allowed to come to equilibrium with the parent Rn (approximately 4 hours) before the scintillation cell is counted for alpha activity. The 4-hour in-growth period also allows for the decay of other Rn isotopes.

The radium isotopes in a water sample are collected by co-precipitation of barium and lead sulfate and purified by re-precipitation out of a basic ethylenediaminetetraacetic acid solution. This technique is devised so that the beta activity from actinium 228, which is produced by decay of Ra 228, can be determined and related to the activity concentration of Ra 228 present in the sample. After a 36-hour period to allow for the in-growth of actinium 228, lead is removed as lead (II) sulfide, and actinium is carried on yttrium as the hydroxide and mounted as the oxalate, and quickly beta-counted on a gas flow proportional counter to minimize decay of the short-lived actinium 228 (approximately 6 hours).

Environmental Benchmarks Comparisons

Results were compared with proposed Environmental Quality Standards for the Mediterranean Sea in Israel (also referred to as the Mediterranean Environmental Water Quality Standards [MEWQS]) (Ministry of the Environment, 2002). Water quality standards for TPH are not found within the European Union Commission on Environmental Quality Standards (EUCEQS) for priority substances in the field of water policy (Directive 2008/105/EC and the proposed amendment COM[2011]876), and USEPA water quality benchmarks.

4.2.2 Sediment

The following subsections provide a brief summary of the analytical methods used for each sediment sample parameter as summarized in **Table 14**.

Grain Size Distribution / Particle Size Analysis

Sediment grain size distribution was determined by means of laser diffraction particle size analysis using a Malvern 2000 Mastersizer. Grain sizes were computed automatically within the instrument using the Mie model for light scattering and reported as percent distribution according to size classes representing sand, silt, and clay-sized particles as well as the Wentworth scale based on Folk's classification (Folk, 1954, 1974) (**Table 15**). Mean and standard deviation (SD) were calculated and analyzed by sampling strata. Sediment grain size for each grid cell was also characterized by sediment categories within a Shepard's diagram (Shepard, 1954).

Table 15. Wentworth size class nomenclature and Folk scale grain sizes.

Wentworth Size Class	Folk Scale (mm)
Granule	>1.99
Very Coarse Sand	>0.999 to ≤1.999
Coarse Sand	>0.499 to ≤0.999
Medium Sand	>0.249 to ≤0.499
Fine Sand	>0.1249 to ≤0.249
Very Fine Sand	>0.0619 to ≤0.1249
Coarse Silt	>0.0309 to ≤0.0619
Medium Silt	>0.0159 to ≤0.0309
Fine Silt	>0.0079 to ≤0.0159
Very Fine Silt	>0.0039 to ≤0.0079
Clay	≤0.0039

Total Organic Carbon

TOC was analyzed by the combustion and gravimetric methods based on European Standard Norm 1484. TOC was determined in a Shimadzu TOC-L_{CPH} Analyzer and an SSM-5000A solid sample combustion unit. Samples were treated with acid to remove carbonates and dried at 200^{o}C to quantify inorganic carbon. Samples were then dried at 900^{o}C and carbon dioxide generated by the combustion of organic matter in the samples was quantitatively measured with an infrared detector and calibrated

against prepared standard solutions. The quantity of organic matter in a sediment sample is expressed in percent of sample weight (%).

Total Metals

Analysis for total metals in sediment samples was conducted by hydrofluoric acid digestion and analyzed by either a Thermo iCAP3500 Duo-View inductively coupled plasma-atomic emission spectrometer or Thermo X-Series inductively coupled plasma-mass spectrometer, calibrated against prepared standard solutions. Mercury analysis of sediments was conducted using purge-and-trap atomic fluorescence spectroscopy (USEPA, 2002). The sediment subsample was digested in a nitric/sulfuric acid mix and diluted to volume with dilute bromine monochloride with the release of elemental mercury by the addition of stannous chloride. Mercury concentrations were measured by atomic fluorescence spectroscopy and calibrated against prepared standard solutions.

In order to normalize metals concentrations arising from sediment grain size effects, each metal was plotted against aluminum. Concentrations of aluminum and other trace metals vary naturally in ambient seafloor sediments, primarily due to differences in sediment grain sizes. Clay sediments are composed primarily of aluminosilicates and typically have higher concentrations of metals. Sediments classified as silt or sand are primarily composed of quartz and fragments of carbonate shell, which dilute ambient metals concentrations (Herut and Sandler, 2006). Aluminum concentration is assumed to correlate linearly with other metals concentrations when there is no anthropogenic input (Trefry et al., 2003, 2013). Therefore, it is reasonable to assume that a particular metal concentration may be considered enhanced above ambient seafloor concentrations by anthropogenic activity if the metal concentration of a sample deviates greatly from a prediction interval (i.e. 99% prediction interval) calculated from that seen for the linear regression of aluminum versus that metal for sediments of a particular particle size range. Samples falling greatly outside of the 99% prediction interval may indicate anthropogenic impacts on anomalous values. Thus, normalization using aluminum concentration removes the inherent effect of grain size on targeted metals and allows assessment for potential anthropogenic contributions to accumulation.

Hydrocarbons

Hydrocarbon components in sediments were analyzed by solvent extraction and gas chromatographic techniques. The analytical methods for hydrocarbons included USEPA/SW-846 Modified 8100/8015C for TPH and USEPA SW-846/8260 or 8270 using an Agilent Model 6890/5973 gas chromatograph-mass spectrometer and calibrated against prepared standard solutions for PAHs. Sediment phenols were analyzed using USEPA Method 9065 Modified. Steam-distilled phenolic material was reacted with 4-aminoantipyrine in the presence of potassium ferricyanide at a pH of 10 which produces an antipyrine dye. The amount of color produced is a function of the concentration of phenolic material. VOCs were analyzed using USEPA method 8620C using a gas chromatograph-mass spectrometer.

Radioactive compounds

For Ra 226, the method involved drying and sieving the sample, sealing the sample in a steel can, and allowing 21 days for the in-growth of the lead 214 and bismuth 214 progeny. The analysis entailed quantification of the lead 214 and bismuth 214 progeny, assuming secular equilibrium, and reporting the abundance weighted average of the lead and bismuth activities as Ra 226. Assuming secular equilibrium, the gamma emissions from actinium 228, which is produced by decay of Ra 228, are determined and related to the activity concentration of Ra 228 present in the sample. Gamma emissions from radionuclides were detected by a semiconductor germanium crystal, which provided a small electronic pulse for each gamma interaction where the pulse height was proportional to the gamma incident energy. These electronic data were converted to digital data by an analog-to-digital converter and stored in a multichannel buffer. The data collected by the multichannel buffer were subsequently interpreted by a complex software program, generating results in units of radioactivity per unit sample volume.

For thorium 228, the samples were dried and ground to a fine particle size. For cases in which there is high organic matter, the samples were placed in a muffle furnace so that any organic matter was removed by combustion. Tracers were added and dissolution was accomplished using nitric, hydrochloric, and hydrofluoric acids. When actinides were being determined, a hydroxide co-precipitation was performed to pre-concentrate actinides and remove constituents that did not form insoluble hydroxides. The hydroxide precipitate was then redissolved, and further purification was performed through various chromatography resins. The purified thorium 228 was co-precipitated with lanthanum fluoride and mounted on a filter membrane for quantification by alpha spectroscopy.

Comparisons with Environmental Benchmarks and Previous Surveys

Data were interpreted in the context of the actual values (means) relative to benchmark values to evaluate their biological relevance. A benchmark is a chemical concentration in sediment above which there is the possibility of harm to organisms in the environment. Benchmark values such as the effects range low (ERL) and effects range median (ERM) may be used to assess the potential risk to fish and other marine life (Buchman, 2008). These sediment quality guidelines are based on marine sediment chemistry paired with sediment toxicity bioassay data. The benchmarks represent points on a continuum of chemical concentrations ranked from lowest (least toxic) to highest (most toxic) concentrations, and are defined as follows:

- ERL is indicative of concentrations below which adverse effects rarely occur; and
- ERM is indicative of concentrations above which adverse effects more frequently occur (Long and Morgan, 1990).

Data were also assessed in context to the samples collected during the 2014 Leviathan Field Development EBS near the current location of the LPP in order to provide a broader context of baseline conditions within the region. Other samples collected in the Levantine basin are in different water depths and marine conditions. Therefore, results from sediment analyses during the 2019 LPP EBS were not compared to the overall Levantine basin baseline average.

4.3 INFAUNA

Samples were shipped to EcoAnalysts, Inc. (Moscow, Idaho, U.S.) for sorting and taxonomic identification. Prior to sorting each infaunal sample, the sample was transferred from formalin to ethyl alcohol. Samples were sorted into major taxonomic groups and then distributed to taxonomists for species identification and enumeration. During the taxonomic process, organisms were identified to the lowest practical taxonomic level (LPTL) by EcoAnalysts, Inc.'s in-house taxonomists. Nematodes were enumerated but not identified to LPTL, and oligochaetes, copepods, and ostracods were only enumerated as these are often not infauna but epibenthic fauna. These organisms and other meiofaunal, epibenthic, and water column species were excluded from any statistical analyses. Data were recorded on electronic datasheets within the EcoAnalysts, Inc. laboratory information management system and then later output in a Microsoft Excel format designed by MVI/CSA for integration into CSA's enterprise database.

4.4 STATISTICAL ANALYSIS

4.4.1 Sediment

A three-way analysis of variance (3ANOVA) was performed on sediment, and some select infauna parameters to determine overall impacts within sediments based on:

- Distance;
- Direction (Quadrant);
- Survey (2019 LPP EBS and 2020 LPP EMS); and
- Interaction terms.

Determinations of statistical significance on where (if any) impacts within sediments or among infaunal communities occur among individual strata were made utilizing a post-hoc Tukey multiple means comparison tests.

Sediment chemical concentrations were compared against benchmark values to evaluate their biological relevance. Some benchmark values to which chemical concentrations are compared against, as applicable, are:

- ERL;
- ERM; and
- 2002 Environmental Quality Standards for the Mediterranean Sea in Israel.

4.4.2 Infauna

A variety of statistical routines were applied to the infaunal data set using the PRIMER Version 6 software (Clarke and Gorley, 2006) to calculate diversity indices, including species richness (Margalef's D), diversity (Shannon's H′), and evenness (Pielou's J′). Infaunal density within each station were also calculated.

A non-metric multidimensional scaling (MDS) analysis was used to compare infauna assemblages and assess spatial patterns in taxonomic composition across the platform survey area. The general analytical approach taken employs non-parametric multivariate analyses as outlined by Clarke (1993). The MDS analysis was performed using PRIMER Version 6 software (Clarke and Gorley, 2006). MDS is an ordination technique that provides a two-dimensional projection of inter-sample relationships in abstract high dimensional space. Samples that are most similar in species composition and proportional abundance will cluster near one another in a two-dimensional ordination diagram. This data matrix was initially pre-treated by square root transformation of the raw data followed by application of the Bray-Curtis similarity index (Bray and Curtis, 1957) to construct the sample similarity matrix. A similarity percentages (SIMPER) analysis was also conducted to investigate clustering observed in the MDS plot to determine the contribution percentage of individual taxa to the overall dissimilarity between clusters.

4.5 VIDEOGRAPHY

4.5.1 Fouling Community

Video data of the fouling communities from platform legs were reviewed and analyzed after the survey. Still-frame images were captured from each sampling depth of each platform leg. Each image was captured so that the platform leg filled the field of view and the overall area of the image covered 1.08 m^3 (0.9 × 1.2 m), therefore enabling standardization of organisms enumerated in each image.

All fouling organisms were identified to the LPTL using relevant literature and regional field guides, as appropriate (Wirtz and Debelius, 2003). The goal was to provide an accurate inventory list of organisms recorded during the survey, however, identification of species from images can be difficult, and in many cases impossible without obtaining physical samples. In cases where identification was not possible (i.e., Porifera and Bryozoa phyla) the term "morphospecies" was used. This term describes taxa readily separated by morphological differences that are obvious to individuals without extensive taxonomic training (Oliver and Beattie, 1996). Porifera and Bryozoa morphospecies were identified to class level.

The percent cover of sessile organisms (e.g., bivalves, sponges) and the abundance of motile organisms (e.g., echinoderms) was quantified within each image. Percent cover was estimated using the Braun-Blanquet (BB) method of coverage estimation (Braun-Blanquet, 1964). The BB method employs a 6-point ordinal scale to visually assess the percent cover of sessile organisms. Each sessile taxa were given a BB category based on a range of percent coverage defined in **Table 16**. An average

BB category was calculated from the three measurements made at each depth per platform. Average BB scores were then converted to percent cover for each area to allow interpolation of averaged BB scores that fall between BB scale values (conversion was conducted by regressing the mid-point of percent cover associated within the range covered by each BB scale value (**Formula 1**; BB category as presented in **Table 16**), on the associated BB scale value. Depth distribution, mean percent cover data of sessile organisms, and density data of motile organisms were graphed separately for each inspected side of the platform (northeastern legs and southwestern legs).

Table 16. Braun-Blanquet (BB) ordinal scale classifications and the corresponding range of percent cover used for analysis of the fouling community.

BB Category	Percent Cover Range
0.5	<1%
1	1% to 5%
2	6% to 25%
3	26% to 50%
4	51% to 75%
5	76% to 100%

Formula 1:
Percent Cover = 2.8108*[BB]^2.2325

4.5.2 Fish Community

Video data of the LPP legs were analyzed to identify fishes and estimate their proportional abundances within each depth. Observed fishes were identified to the lowest possible taxonomic level and scored for categorical abundance based on a $\log^4$ scale (**Table 17**). This survey method is limited to conspicuous fishes and is likely to underestimate small and cryptic benthic dwelling species such as fishes in the families of Blennidae and Gobiidae. Within each depth, categorical abundance values by species observed were divided by the sum of categorical abundances of all species observed in that particular depth stratum to generate proportional contributions. Proportional values for all species were plotted by depth to illustrate vertical distribution patterns (e.g., Ajemian et al., 2015). Data on depth distribution and proportional abundance were graphed separately for each inspected side of the platform (northeastern legs and southwestern legs).

Table 17. Scale of Log^4 abundance categories used to estimate fish abundance. Scale adopted from English et al. (1997).

Log_4 Abundance Category	Number of Individuals
1	1
2	2 to 4
3	5 to 16
4	17 to 64
5	65 to 256
6	257 to 1024

4.6 BIOACCUMULATION PASSIVE SAMPLING DEVICES

4.6.1 DGT Samplers

The DGT samplers were analyzed for chromium, cadmium, lead, manganese, mercury, nickel and zinc by ALS Environmental (Kelso, Washington), using method 3050B (SW-846) and repeated additions of HNO_3 and hydrogen peroxide. The resulting sample was analyzed for metals content (mass) by inductively coupled plasma – mass spectrometry (USEPA Method 6020A). The DGT

samples for mercury were extracted using a HNO_3/sulfuric acid/bromine monochloride digestion and were analyzed using oxidation, purge and trap, and cold vapor atomic fluorescence spectrometry (USEPA Method 1631E). It should be noted that the digestion procedures used by ALS differed slightly from those recommended by the DGT sampler manufacturer (DGT Research Ltd., nd). However, the laboratory confirmed their digestion procedure is equivalent to that recommended by the manufacturer and the mass values reported are suitable for calculating the TWAC. Where calculable, the TWAC of each metal (in ng mL^{-1}) was calculated using the following equation:

$$TWAC = \frac{M\Delta g}{DtA}$$

where M is the mass of the metal on the binding resin gel as measured by the analytical laboratory, Δg is the thickness of the diffusive gel (0.08 cm) plus the thickness of the membrane (0.014 cm), D is the diffusion coefficient for the metal in the gel, t is deployment time (seconds), and A is the exposure area of the binding gel (3.14 cm^2). The TWAC is used as an estimate to predict bioavailability of metals since the DGT hydrogels only accumulate labile metal species.

Diffusion coefficients are temperature dependent and based on calculations presented by Davison (2016). It should be noted that diffusion coefficients for mercury have not been well established in the literature. The diffusion coefficient used for mercury for this analysis was based on an estimated value based on a critical review of data in Davison (2016). Because the water temperature at the seafloor deployment locations varied across the 43- day deployment, an average temperature was calculated for the deployment period for each of the three temperature loggers. The temperature data from the Near-Platform monopod was used to calculate TWACs for the three monopods in the vicinity of the LPP, while the temperature data from the reference area and hardbottom area were used to calculate their respective TWACs.

4.6.2 Semipermeable Membrane Devices

SPMDs were analyzed by SGS AXYS Analytical Services. As an initial step in the sample processing, the SPMDs were cleaned with water, rinsed with hydrochloric acid, and then rinsed with ultrapure water. PAHs were subsequently extracted with hexane and analyzed by gas-chromatography mass- spectrometry.

In order to calculate seawater concentrations (i.e., ng L^{-1}) of targeted PAHs, it is necessary to determine the sampling rate R_s; the amount of water per day extracted by the sampler per day for each target analyte. The preferred method for determining R_s entails measuring the dissipation of performance reference compounds (PRCs) which are non-interfering organic compounds with high fugacity (i.e., ability to dissipate) that are spiked into the samplers prior to deployment (Booij et al., 1998; Huckins et al., 2002). When conducting field surveys using SPMDs, environmental factors such as water temperature, flow rate, and fouling of the SPMD membrane can affect the uptake rate of contaminants from the environment which in turn can affect the accuracy of calculated results (Alvarez, 2010; Huckins et al., 2002; Harman et al., 2009). By determining the dissipation rate of one or more PRCs, adjustments to sampling rates for each analyte can be made to reflect site-specific conditions (Alvarez, 2010). Moreover, the equations in the PRC adjustment account for the first-order kinetic functions that passive samplers follow (i.e., linear, curvilinear, and equilibrium uptake states; **Figure 8**; Alvarez, 2019). If a sampler is retrieved prior to reaching the equilibrium state with the ambient environment, it is likely that the analytical results will be an underestimation of the true concentration of the targeted analyte. The use of PRCs accounts for each phase of the uptake process based on separate equations; based on the SPMD partition coefficient, the calculations are altered for each target analyte to choose the proper kinetic function to provide a proper estimate of the targeted analyte at an equilibrium state (Alvarez, 2010). Without the use of PRCs, it is very difficult to determine if the SPMD has reached an equilibrium state for any particular analyte, potentially compromising the accuracy of results.

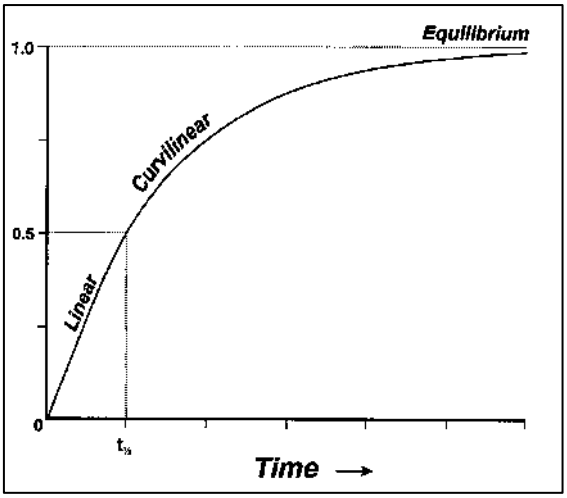


Figure 8. Example of the first-order kinetic uptake process of semipermeable passive membrane devices. From: Alvarez, 2019.

It is advantageous to spike samplers with multiple PRCs to ensure that at least one has suitable dissipation during the deployment; and to reduce variability in calculating R_s (Alvarez, 2010). For the current study, two PAHs were utilized as PRCs with relatively high fugacity: anthracene d-10 and fluoranthene d-10. SPMDs were each spiked by the manufacturer with 10 µg per SPMD. A third PAH, dibenzo(a,h)-anthracene, has a very low fugacity but degrades easily in sunlight (Alvarez, 2010); each SPMD was spiked with 1µg to account for potential PAH degradation on the SPMD membranes by sunlight. Sampling rates for each PRC were determined by the use of the following empirical model, as described in detail by Huckins et al. (2006):

$$R_s = V_s K_{sw} K_e$$

where V_s is the volume of the sampler (4.77 cm^3 for each SPMD sampler), K_{sw} is the SPMD water partitioning coefficient ($cm^3\ cm^{-3}$) and K_e is the release rate constant for each PRC (d^{-1}). K_e was determined for each of the three PRCs using an equation presented by Huckins et al. (1993):

$$K_e = -\frac{\ln(\frac{N}{N_0})}{t}$$

where N_0 and N are the concentrations of the PRC at the start and end of the deployment, respectively, and t is time (in days) of the deployment.

Subsequently, logK_{sw} was calculated using logK_{ow} of each PRC, where K_{ow} is the octano-water partitioning coefficient. The logK_{ow} values for the three PRCs were taken from Durell et al., 2006. The logK_{ow} values for the PAH surrogates anthracene d-10 and fluoranthene d-10 were substituted with the logK_{ow} values for anthracene and fluoranthene, respectively. The following quadratic equation (from Huckins et al., 2006) was used:

$$\log K_{sw} = a_0 + 2.32 \log K_{ow} - 0.1618(\log K_{ow}^2)$$

where a_0 is the constant value of -2.61 for most hydrophobic compounds (Harman et al., 2009). Thus, R_s was calculated for each of the three PRCs for each SPMD sampler (**Table 18**). The ambient concentration of each PAH in the ambient seawater (C_w) was determined using the following equation:

$$C_w = \frac{N}{Rs * t}$$

where N is the mass of the PAH accumulated in the SPMD (ng), R_s is the sampling rate (L d^{-1}), and t is the exposure time (days). These equations were completed manually and subsequently cross-checked using a calculator spreadsheet prepared by USGS (2016).

The accumulated mass for each of the 16 USEPA priority PAH on each SPMD as measured following the deployment was inserted into the USGS (2016) spreadsheet. Using a model described in Huckins et al. (2006), the calculator determined R_s for each targeted analyte and the overall concentration of each analyte in the water column using the PRC data to make appropriate adjustments in the release rate constant.

Table 18. Intermediate values used to calculate the sampling rate of each performance reference compound on each deployed semipermeable passive membrane device (SPMD).

Deployed SPMD	Performance Reference Compound	Sampler Volume (V_s) (cm^3)	logK_{sw}	Release Rate Constant (K_e)	Sampling Rate (R_s) (L d^{-1})
NP-200m-1	Anthracene d-10	4.77	4.59	0.035	6.49
	Fluoranthene d-10	4.77	5.10	0.012	6.88
	Dibenzo(a,h)-anthracene	4.77	5.68	0.002	5.30
NP-200m-2	Anthracene d-10	4.77	4.59	0.037	6.90
	Fluoranthene d-10	4.77	5.10	0.012	7.01
	Dibenzo(a,h)-anthracene	4.77	5.68	0.003	6.38
NP-200m-3	Anthracene d-10	4.77	4.59	0.038	7.12
	Fluoranthene d-10	4.77	5.10	0.013	7.62
	Dibenzo(a,h)-anthracene	4.77	5.68	0.003	7.11
MF-500m-1	Anthracene d-10	4.77	4.59	0.034	6.42
	Fluoranthene d-10	4.77	5.10	0.012	6.97
	Dibenzo(a,h)-anthracene	4.77	5.68	0.003	7.41
MF-500m-2	Anthracene d-10	4.77	4.59	0.039	7.21
	Fluoranthene d-10	4.77	5.10	0.013	7.99
	Dibenzo(a,h)-anthracene	4.77	5.68	0.004	8.22
MF-500m-3	Anthracene d-10	4.77	4.59	0.039	7.21
	Fluoranthene d-10	4.77	5.10	0.008	4.83
	Dibenzo(a,h)-anthracene	4.77	5.68	0.004	8.66
FF-1000m-1	Anthracene d-10	4.77	4.59	0.036	6.75
	Fluoranthene d-10	4.77	5.10	0.012	6.88
	Dibenzo(a,h)-anthracene	4.77	5.68	0.003	6.98
FF-1000m-2	Anthracene d-10	4.77	4.59	0.040	7.44
	Fluoranthene d-10	4.77	5.10	0.010	5.99
	Dibenzo(a,h)-anthracene	4.77	5.68	0.003	7.29
FF-1000m-3	Anthracene d-10	4.77	4.59	0.039	7.28
	Fluoranthene d-10	4.77	5.10	0.013	7.77
	Dibenzo(a,h)-anthracene	4.77	5.68	0.003	6.38
HB-3.5km-1	Anthracene d-10	4.77	4.59	0.036	6.75
	Fluoranthene d-10	4.77	5.10	0.011	6.41
	Dibenzo(a,h)-anthracene	4.77	5.68	0.003	6.13
HB-3.5km-2	Anthracene d-10	4.77	4.59	0.038	7.07
	Fluoranthene d-10	4.77	5.10	0.012	7.13
	Dibenzo(a,h)-anthracene	4.77	5.68	0.003	7.66
HB-3.5km-3	Anthracene d-10	4.77	4.59	0.034	6.32
	Fluoranthene d-10	4.77	5.10	0.009	5.64
	Dibenzo(a,h)-anthracene	4.77	5.68	0.002	5.66

Table 18. (Continued).

Deployed SPMD	Performance Reference Compound	Sampler Volume (V_s) (cm^3)	logK_{sw}	Release Rate Constant (K_e)	Sampling Rate (R_s) (L d^{-1})
REF-3.5km-1	Anthracene d-10	4.77	4.59	0.036	6.79
	Fluoranthene d-10	4.77	5.10	0.012	7.27
	Dibenzo(a,h)-anthracene	4.77	5.68	0.003	6.80
REF-3.5km-2	Anthracene d-10	4.77	4.59	0.035	6.53
	Fluoranthene d-10	4.77	5.10	0.011	6.54
	Dibenzo(a,h)-anthracene	4.77	5.68	0.003	6.38
REF-3.5km-3	Anthracene d-10	4.77	4.59	0.038	7.07
	Fluoranthene d-10	4.77	5.10	0.005	2.85
	Dibenzo(a,h)-anthracene	4.77	5.68	0.005	11.11

5 Results and Discussion

5.1 LOCAL WEATHER AND SEA STATE CONDITIONS

MVI/CSA conducted the 2020 LPP EMS from 24 to 27 December 2020, and 30 to 31 December 2020. Weather conditions during the 2020 LPP EMS were partly cloudy to sunny with light to moderate winds and were generally favorable for vessel operations. **Table 19** summarizes wind speed and sea conditions during the survey.

Table 19. Summary of weather conditions during the 2020 Leviathan Production Platform Environmental Monitoring Survey.

Date	Wind Speed and Direction	Sea State	Conditions
24 December 2020	6 kn ENE	0.8 m	Sunny
25 December 2020	25 kn E	1 m	Sunny and Windy
26 December 2020	26 kn E	0.8 m	Sunny and Windy
27 December 2020	30 kn SE	0.8 m	Sunny and Windy
30 December 2020	10 kn ENE	0.5 m	Partly Cloudy
31 December 2020	--	--	Sunny

-- = no data available.

5.2 HYDROGRAPHIC PROFILES

Hydrographic profiles of the water column were collected at 20 stations on 26 and 27 December 2020. Profiles were similar at all stations; a representative profile from Station NF-SW-10 is presented in **Figure 9** and is considered representative of the survey area. Hydrographic profiles for all stations are presented in **Appendix E**. **Figures 10** and **11** present hydrographic profiles of the water column collected in the vicinity of the LPP during the 2019 LPP EBS and the 2014 Leviathan Field Development EBS, respectively. Note the scales and colors differ between **Figures 10** and **11**. Differences in hydrographic profiles among surveys are due to seasonal differences in water column characteristics.

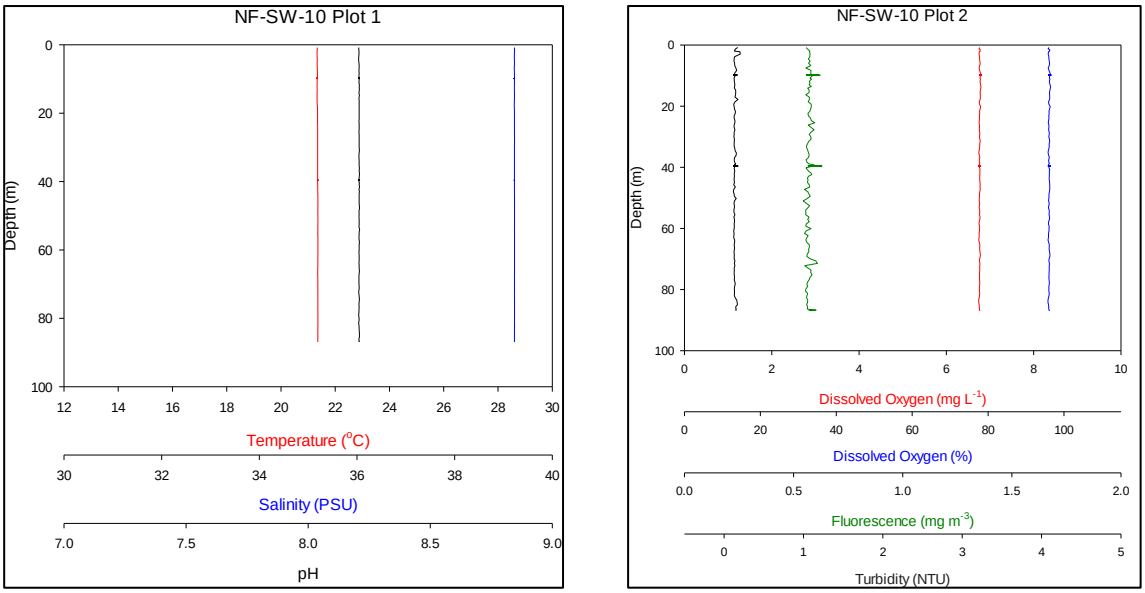


Figure 9. Hydrographic profiles of the water column collected at Station NF-SW-10 on 26 December 2020: temperature, salinity, and pH (left) and dissolved oxygen (mg L^{-1}), dissolved oxygen (% saturation), fluorescence, and turbidity (right).

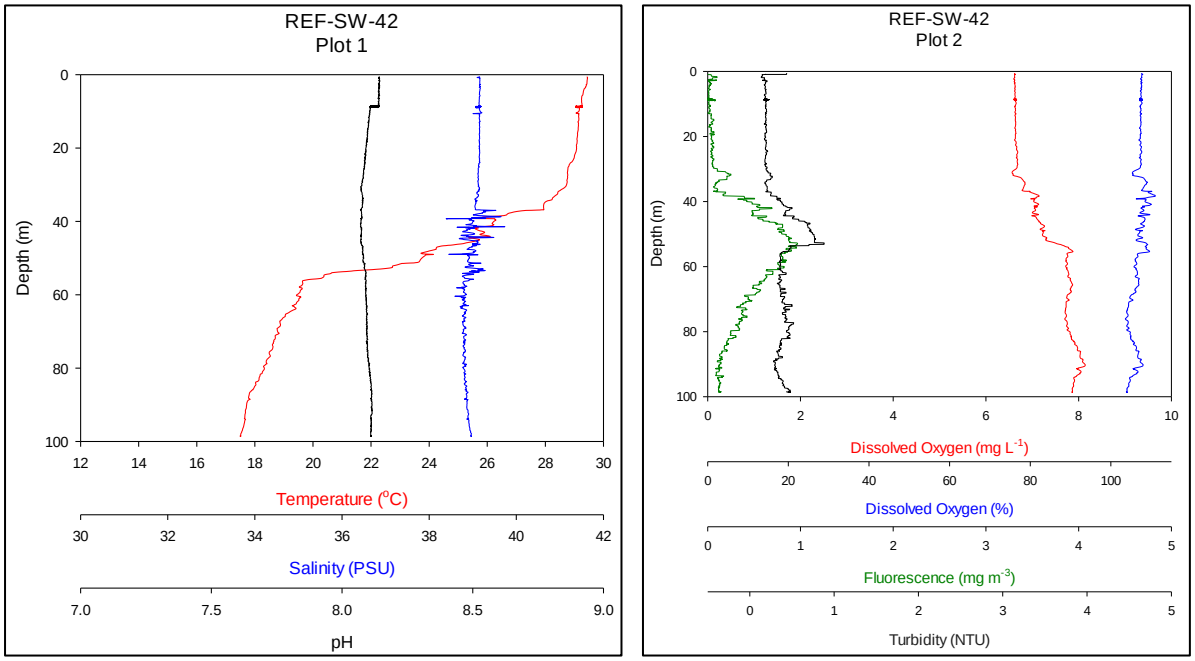


Figure 10. Hydrographic profiles of the water column collected in August 2019 at Station REF-SW-42 during the 2019 Leviathan Production Platform Environmental Baseline Survey: temperature, salinity, and pH (left) and dissolved oxygen (mg L^{-1}), dissolved oxygen (% saturation), fluorescence, and turbidity (right).

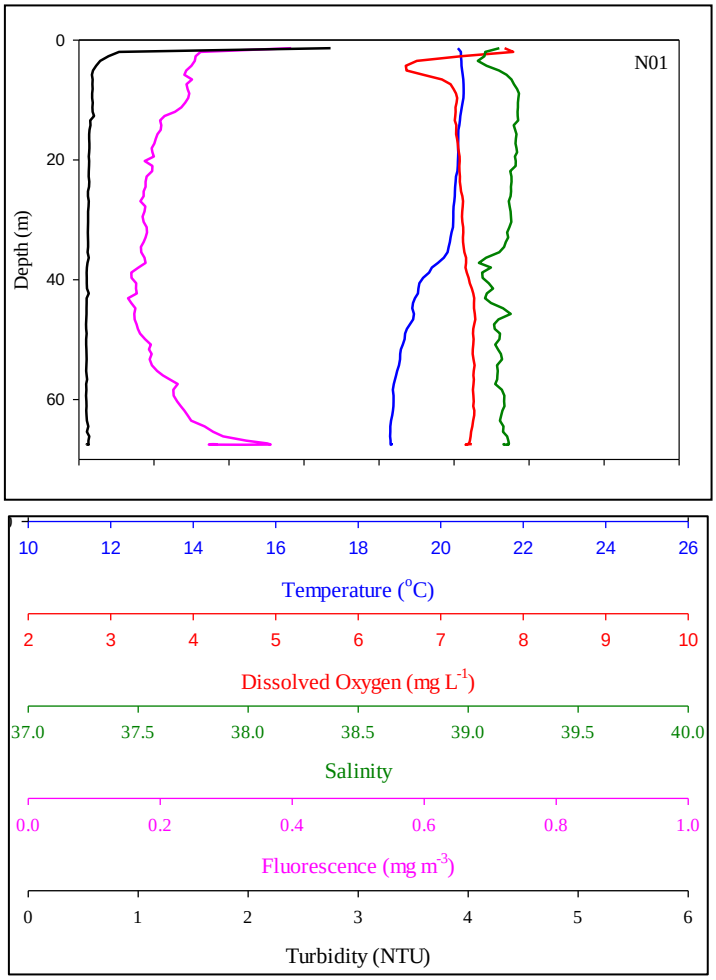


Figure 11. Hydrographic profile of the water column collected at in the vicinity of the Leviathan Production Platform during the 2014 Leviathan Field Development Environmental Baseline Survey. Data were collected in May.

Waters during the 2020 LPP EMS were cool (approximately 21°C and isothermal throughout the water column. Salinity was stable throughout the water column at approximately 39 PSU. pH was also stable throughout the water column at approximately 8.2. (**Figure 9**).

Turbidity was low (generally <1 nephelometric turbidity units) throughout the water column at every station. Station NP-NW-44 had a turbidity spike near the seafloor, but this was due to bottom disturbance caused by ROV thrusters. Photosynthetic activity, which can be used to estimate primary productivity within the water column, was measured with a fluorometer. Fluorescence was generally homogeneous throughout the water column, with values of approximately 0.6 mg^{-3}. Due to the winter season, there was no photosynthetic maximum as was observed during the 2019 LPP EBS at a depth of approximately 50 m (**Figure 10**).

The water column was well oxygenated (6.7 mg L^{-1}) throughout the water column with values generally homogeneous from the surface to the seafloor.

5.3 SEAWATER ANALYSES

5.3.1 Hydrocarbons

Analytical laboratory datasheets for TPH, phenols, and BTEX in seawater are provided in **Appendix F**. All TPH concentrations were below the analytical laboratory's method reporting limit (<13.4 µg L^{-1}). Because TPH was not detected in any sample, PAHs were not analyzed.

All BTEX concentrations were below the analytical laboratory's method reporting limit of 0.5 µg L^{-1}. All concentrations of total phenols were also below the analytical laboratory's method reporting limit of 0.01 mg L^{-1}. All TPH, BTEX, and phenols concentrations were also below the laboratory's detection limits during the 2019 LPP EBS. One near-bottom water sample was collected in the vicinity of the LPP during the 2014 Leviathan Field Development EBS; TPH was found to be below the laboratory's method reporting limit. Phenols and BTEX were not analyzed during the 2014 Leviathan Field Development EBS.

5.3.2 Total Nitrogen, Total Phosphorous, Total Organic Carbon, Nutrients and Total Suspended Solids

Analytical results for nutrients and TSS in seawater are provided in **Appendix G**. Results of the nutrient and TSS analyses are presented in **Table 20**. Concentrations of nitrate and ammonium were below the laboratory's detection limit for all samples; concentrations of TN ranged from 0.07 to 0.12 mg L^{-1} (**Table 20**). Concentrations of TP ranged from 0.0039 to 0.0109 mg L^{-1} and concentrations of TOC ranged from 0.75 to 1.51 mg L^{-1}. TN and TP from all seawater samples were below the proposed Mediterranean Environmental Water Quality Standards of 1.0 mg L^{-1} (Ministry of the Environment, 2002). TSS concentrations ranged from 2.4 to 9.1 mg L^{-1} and were generally similar to TSS concentrations from the 2019 LPP ESB and the single near-bottom TSS value collected within the vicinity of the LPP during the 2014 Leviathan Field Development EBS. Calculated concentrations of NO_3 were low, ranging from not detected to 0.0082 mg L^{-1}. Average concentrations of TN, TP, TOC, TSS, nitrite, and nitrate were similar by both distance and direction and were similar to concentrations from the single sample taken during the 2014 Leviathan Field Development EBS (**Table 21**). Because all values of nitrate dioxide and ammonium were below the laboratory's MRL, they are excluded from **Table 21**.

Table 20. Results of total nitrogen, total phosphorous, total organic carbon, nutrients and total suspended solids analyses in seawater during the 2020 Leviathan Production Platform Environmental Monitoring Survey. All units are mg L^{-1}.

Station	Distance Strata	Directional Strata	Sample	TN	TP	NO_2	NO_3	NH_4	TOC	TSS
NP-NE-43	Near Platform	Northeast	Near-surface	0.10 [a]	0.0064	<0.0007	0.0020 [c]	<0.009	1.16	4.0
			Mid-depth	0.08 [a]	0.0058	<0.0007	0.0018 [c]	<0.009	1.18	8.6
			Near-bottom	0.07 [a]	0.0067	<0.0007	0.0018 [c]	<0.009	1.16	4.0
NP-NW-44		Northwest	Near-surface	0.09 [a]	0.0081	<0.0007	0.0018 [c]	<0.009	1.11	5.1
			Mid-depth	0.10 [a]	0.0047	<0.0007	0.0082 [c]	<0.009	1.05	3.1
			Near-bottom	0.10 [a]	0.0066	<0.0007	0.0052 [c]	<0.009	1.08	6.6
NP-SW-45		Southwest	Near-surface	0.09 [a]	0.0082	<0.0007	0.0025 [c]	<0.009	1.13	9.1
			Mid-depth	0.08 [a]	0.0069	<0.0007	ND	<0.009	1.30	6.7
			Near-bottom	0.07 [a]	0.0067	<0.0007	0.0032 [c]	<0.009	1.23	7.6
NP-SE-46		Southeast	Near-surface	0.08 [a]	0.0064	<0.0007	0.0021 [c]	<0.009	1.36	3.3
			Mid-depth	0.08 [a]	0.0060	<0.0007	0.0015 [c]	<0.009	1.29	2.4
			Near-bottom	0.10 [a]	0.0051	<0.0007	0.0038 [c]	<0.009	1.44	3.8
NF-NE-02	Near-Field	Northeast	Near-surface	0.10 [a]	0.0078	<0.0007	0.0020 [c]	<0.009	1.18	3.1
			Mid-depth	0.08 [a]	0.0079	<0.0007	0.0038 [c]	<0.009	1.28	3.5
			Near-bottom	0.08 [a]	0.0084	<0.0007	0.0051 [c]	<0.009	0.95	4.1
NF-NW-06		Northwest	Near-surface	0.08 [a]	0.0070	<0.0007	ND	<0.009	1.12	7.6
			Mid-depth	0.07 [a]	0.0052	<0.0007	ND	<0.009	1.01	7.5
			Near-bottom	0.08 [a]	0.0068	<0.0007	0.0023 [c]	<0.009	1.06	6.9
NF-SE-07		Southeast	Near-surface	0.09 [a]	0.0065	<0.0007	0.0017 [c]	<0.009	0.99	6.0
			Mid-depth	0.09 [a]	0.0073	<0.0007	ND	<0.009	1.16	4.3
			Near-bottom	0.11 [a]	0.0102	<0.0007	ND	<0.009	1.17	4.4
NF-SW-10		Southwest	Near-surface	0.10 [a]	0.0109	<0.0007	0.0020 [c]	<0.009	1.31	7.3
			Mid-depth	0.08 [a]	0.0091	<0.0007	0.0023 [c]	<0.009	1.28	4.6
			Near-bottom	0.08 [a]	0.0058	<0.0007	0.0015 [c]	<0.009	1.18	9.0
MF-NE-13	Mid-Field	Northeast	Near-surface	0.08 [a]	0.0064	<0.0007	0.0017 [c]	<0.009	1.16	4.4
			Mid-depth	0.08 [a]	0.0062	<0.0007	0.0017 [c]	<0.009	1.25	8.3
			Near-bottom	0.08 [a]	0.0065	<0.0007	ND	<0.009	1.19	3.9
MF-NW-17		Northwest	Near-surface	0.09 [a]	0.0071	<0.0007	0.0030 [c]	<0.009	1.24	4.2
			Mid-depth	0.08 [a]	0.0063	<0.0007	0.0030 [c]	<0.009	1.07	5.2
			Near-bottom	0.10 [a]	0.0069	<0.0007	0.0038 [c]	<0.009	1.25	3.4
MF-SE-21		Southeast	Near-surface	0.10 [a]	0.0043 [a]	<0.0007	ND	<0.009	1.50	3.4
			Mid-depth	0.10 [a]	0.0061	<0.0007	ND	<0.009	1.05	5.6
			Near-bottom	0.08 [a]	0.0066	<0.0007	ND	<0.009	1.18	3.6
MF-SW-24		Southwest	Near-surface	0.07 [a]	0.0071	<0.0007	0.0022 [c]	<0.009	1.51	7.7
			Mid-depth	0.08 [a]	0.0077	<0.0007	0.0024 [c]	<0.009	1.18	3.2
			Near-bottom	0.07 [a]	0.0066	<0.0007	0.0018 [c]	<0.009	1.14	6.6

Table 20. (Continued).

Station	Distance Strata	Directional Strata	Sample	TN	TP	NO_2	NO_3	NH_4	TOC	TSS
FF-NE-26	Far-Field	Northeast	Near-surface	0.09 [a]	0.0081	<0.0007	ND	<0.009	1.03	7.5
			Mid-depth	0.11 [a]	0.0073	<0.0007	0.0016 [c]	<0.009	1.13	7.7
			Near-bottom	0.09 [a]	0.0068	<0.0007	0.0015 [c]	<0.009	1.16	4.7
FF-NW-28		Northwest	Near-surface	0.10 [a]	0.0050	<0.0007	0.0016 [c]	<0.009	1.32	3.6
			Mid-depth	0.08 [a]	0.0063	<0.0007	ND	<0.009	1.04	2.6
			Near-bottom	0.12 [a]	0.0061	<0.0007	ND	<0.009	1.05	4.3
FF-SE-31		Southeast	Near-surface	0.08 [a]	0.0054	<0.0007	ND	<0.009	1.02	5.7
			Mid-depth	0.10 [a]	0.0086	<0.0007	0.0024 [c]	<0.009	0.86	5.0
			Near-bottom	0.10 [a]	0.0081	<0.0007	0.0026 [c]	<0.009	0.93	3.5
FF-SW-36		Southwest	Near-surface	0.09 [a]	0.0067	<0.0007	0.0020 [c]	<0.009	1.02	3.8
			Mid-depth	0.09 [a]	0.0066	<0.0007	0.0026 [c]	<0.009	1.08	5.9
			Near-bottom	0.08 [a]	0.0075	<0.0007	0.0017 [c]	<0.009	1.04	5.7
REF-NE-37	Reference	Northeast	Near-surface	0.08 [a]	0.0075	<0.0007	0.0039 [c]	<0.009	0.86	4.5
			Mid-depth	0.09 [a]	0.0066	<0.0007	0.0077 [c]	<0.009	0.85	6.5
			Near-bottom	0.08 [a]	0.0057	<0.0007	0.0026 [c]	<0.009	0.82	5.1
REF-SW-41		Southwest	Near-surface	0.07 [a]	0.0049	<0.0007	0.0060 [c]	<0.009	0.89	3.0
			Mid-depth	0.08 [a]	0.0066	<0.0007	0.0060 [c]	<0.009	0.96	4.2
			Near-bottom	0.08 [a]	0.0068	<0.0007	0.0018 [c]	<0.009	0.90	3.4
REF-SHORE-1		N/A	Near-surface	0.08 [a]	0.0072	<0.0007	0.0023 [c]	<0.009	0.94	6.4
			Mid-depth	0.09 [a]	0.0039	<0.0007	0.0029 [c]	<0.009	0.75	4.1
			Near-bottom	0.09 [a]	0.0097	<0.0007	0.0030 [c]	<0.009	0.87	4.0
REF-SHORE-2			Near-surface	0.10 [a]	0.0083	<0.0007	0.0029 [c]	<0.009	0.94	4.1
			Mid-depth	0.10 [a]	0.0078	<0.0007	0.0101 [c]	<0.009	0.90	4.6
			Near-bottom	0.07 [a]	0.0054	<0.0007	0.0101 [c]	0.023	1.00	4.7
2020 LPP EMS Mean (± SD)				0.09 ± 0.01	0.007 ± 0.001	--	0.003 ± 0.002 [d]	--	1.1 ± 0.17	5.1 ± 1.7
2019 LPP EBS Mean (± SD)				0.08 ± 0.03	0.007 ± 0.004	0.001 ± 0.0006	0.0004 ± 0.002	0.013 ± 0	0.96 ± 0.15	10.9 ± 4.1
2014 Leviathan Field Development EBS				0.08 [b]	0.0054 [b]	0.0008 [b]	0.0022 [b c]	0.004 [b]	0.94 [b]	7.8 [b]
Method Reporting Limit (MRL)				0.15	0.0045	0.0022	-- [c]	0.027	0.50	0.01

[a] Reported value is an estimated concentration since it is below the method reporting limit.
[b] Reported value is from a single near-bottom station.
[c] Computed by calculation (TN minus NO_2).
[d] Method detection limit (0.0015 mg L^{-1}) used to calculate average for samples where NO_3 was not detected.
EBS = Environmental Baseline Survey; EMS = environmental monitoring survey; LPP = Leviathan Production Platform; TN = total nitrogen; TP = total phosphorus; ND = not detected; NO_2 = nitrate; NO_3 = nitrate; NH_4 = ammonium; SD = standard deviation; TOC = total organic carbon; TSS = total suspended solids. "--" = not calculable.

Table 21. Mean (± standard deviation) total organic carbon, total nitrogen, total phosphorous, and nutrient concentrations by distance and directional strata in seawater samples collected during the 2020 Leviathan Production Platform Environmental Monitoring Survey.

Strata Type	Strata	TN	TP	NO_3	TOC	TSS
Distance	Near-Platform	0.09 ± 0.01	0.006 ± 0.001	0.003 ± 0.002	1.21 ± 0.12	5.36 ± 2.28
	Near-Field	0.09 ± 0.01	0.008 ± 0.002	0.002 ± 0.001	1.14 ± 0.11	5.69 ± 1.93
	Mid-Field	0.08 ± 0.01	0.007 ± 0.0005	0.002 ± 0.0007	1.23 ± 0.15	4.96 ± 1.75
	Far-Field	0.09 ± 0.01	0.007 ± 0.001	0.002 ± 0.0005	1.06 ± 0.11	5.00 ± 1.58
	Reference	0.08 ± 0.01	0.007 ± 0.002	0.005 ± 0.003	0.89 ± 0.07	4.55 ± 1.05
Direction	Northeast Quadrant	0.09 ± 0.01	0.007 ± 0.0008	0.003 ± 0.002	1.09 ± 0.15	5.33 ± 1.86
	Northwest Quadrant	0.09 ± 0.01	0.006 ± 0.001	0.003 ± 0.002	1.12 ± 0.10	5.01 ± 1.76
	Southeast Quadrant	0.09 ± 0.01	0.007 ± 0.001	0.002 ± 0.0007	1.16 ± 0.20	4.25 ± 1.12
	Southwest Quadrant	0.08 ± 0.009	0.007 ± 0.001	0.003 ± 0.001	1.14 ± 0.17	5.85 ± 2.07
2020 LPP EMS Mean (± SD)		0.09 ± 0.01	0.007 ± 0.001	0.003 ± 0.002[b]	1.1 ± 0.17	5.1 ± 1.7
2019 LPP EBS Mean (± SD)		0.08 ± 0.03	0.007 ± 0.004	0.0004 ± 0.002[b]	0.96 ± 0.15	10.9 ± 4.1
2014 Leviathan Field Development EBS Mean		0.08 [a]	0.0054 [a]	0.0022 [ab]	0.94 [a]	7.8 [a]

[a] Reported value is from a single near-bottom station.
[b] Computed by calculation (TN - NO_2)
EBS = environmental baseline survey; EMS = environmental monitoring survey; LPP = Leviathan Production Platform; TN = total nitrogen; TP = total phosphorus; NO_3 = nitrate; SD = standard deviation; TOC = total organic carbon; TSS = total suspended solids.
Values of nitrate dioxide (NO_2) and ammonium (NH_4) were all below the laboratory's method reporting limit, they are excluded from this table.

5.3.3 Radionuclides

Analytical laboratory datasheets for radionuclides in seawater are provided in **Appendix H**. Results are presented in **Table 22**. Results are presented as the analytical value ± the total propagated analytical uncertainty (TPU). All results (except one) were well below the analytical laboratory's minimum detectable concentration (MDC); values presented in **Table 22** were reported by the analytical laboratory but should be considered with reduced confidence in accuracy due to being below the MDC. MDC values were sample-specific and varied within the ranges noted n **Table 22**. One near-bottom value for thorium 228 at station REF-NE-37 (0.128 ± 0.086 pCi g^{-1}) was just above the sample-specific MDC of 0.126 pCi g^{-1}. During the 2019 LPP EBS, all concentrations of radionuclides were below the laboratory's MDC. Seawater samples for radionuclide analysis were not collected in the vicinity of the LPP during the 2014 Leviathan Field Development EBS.

Table 22. Radioactive compound concentrations (pCi g^{-1}) ± total propagated analytical uncertainty in seawater samples during the 2020 Leviathan Production Platform Environmental Monitoring Survey.

Station	Sample	^{226}Ra	^{228}Ra	^{228}Th
NP-NE-43	Near-surface	0.03 ± 0.20	0.68 ± 0.45	0 ± 0.052
	Near-bottom	-0.03 ± 0.13	0.28 ± 0.41	0.053 ± 0.071
NP-NW-44	Near-surface	-0.06 ± 0.18	-0.13 ± 0.33	-0.019 ± 0.075
	Near-bottom	0.17 ± 0.22	0.13 ± 0.37	-0.05 ± 0.18
NP-SW-45	Near-surface	-0.11 ± 0.26	-0.24 ± 0.40	0.008 ± 0.075
	Near-bottom	0.10 ± 0.16	0.37 ± 0.41	0.004 ± 0.064
NP-SE-46	Near-surface	0.22 ± 0.26	0.08 ± 0.37	0.060 ± 0.079
	Near-bottom	0.07 ± 0.17	-0.01 ± 0.39	0.044 ± 0.062
MF-NE-13	Near-surface	0.18 ± 0.24	0.58 ± 0.42	0.057 ± 0.073
	Near-bottom	0 ± 0.14	0.09 ± 0.38	-0.057 ± 0.079
MF-NW-17	Near-surface	0.23 ± 0.20	0.39 ± 0.42	-0.013 ± 0.077
	Near-bottom	-0.03 ± 0.15	0.48 ± 0.38	0.026 ± 0.076
MF-SE-21	Near-surface	0.14 ± 0.20	0.15 ± 0.35	-0.05 ± 0.11
	Near-bottom	0.08 ± 0.19	0.30 ± 0.36	-0.038 ± 0.076
MF-SW-24	Near-surface	0.17 ± 0.22	0.39 ± 0.39	-0.027 ± 0.070
	Near-bottom	-0.06 ± 0.25	0.20 ± 0.38	-0.023 ± 0.080
REF-NE-37	Near-surface	0 ± 0.20	0.05 ± 0.35	-0.011 ± 0.072
	Near-bottom	0.06 ± 0.33	0.27 ± 0.40	0.128 ± 0.086
REF-SW-41	Near-surface	0.03 ± 0.14	-0.21 ± 0.37	0.051 ± 0.079
	Near-bottom	0.25 ± 0.23	0.50 ± 0.45	-0.016 ± 0.045
LPP Produced Water	From Discharge Pipe	0.26 ± 0.28	0.50 ± 0.52	0.04 ± 0.10
Minimum Detectable Concentration Range (Varies by Sample)		0.20–0.68	0.75–1.09	0.05–0.24

^{226}Ra = Radium 226; ^{228}Ra = Radium 228; ^{228}Th = Thorium 228.

5.4 SEDIMENT ANALYSES

5.4.1 Grain Size Composition

Analytical results for grain size are provided in **Appendix I**. Based on Shepard's classification, sediment types during the 2020 LPP EMS were classified as either sand/silt/clay (27 stations), sandy silt (8 stations), silty sand (8 stations), or clayey silt (3 stations) (Shepard, 1954) (**Table 23**, **Figures 12** and **13**). Percentage of clay, silt, and sand at all stations ranged from 12.6% to 30.9%, 34.9% to 56.9%, and 18.7% to 50.3%, respectively. No gravel sized grains were observed in any sample.

Compared with the 2019 LPP EBS and 2014 Leviathan Field Development EBS, grain size composition during the 2020 LPP EMS trended slightly sandier (**Figure 14**), primarily as a result of samples from the southeast and northeast quadrants (**Figure 12**). While several Near Platform samples were among the sandiest collected during the 2020 LPP EMS, there was no substantial clustering of samples by distance strata based on grain size composition (**Figure 13**).

Table 23. Sediment type and percentages of major (total clay, silt, and sand) and individual (very fine, fine, medium, and coarse) grain size classes at sampling stations during the 2020 Leviathan Production Platform Environmental Monitoring Survey.

Station	Distance Strata	Directional Strata	Total Clay	Very Fine Silt	Fine Silt	Medium Silt	Coarse Silt	Total Silt	Very Fine Sand	Fine Sand	Medium Sand	Coarse Sand	Total Sand	Sediment Type
NP-NE-43	Near-Platform	Northeast	**18.1**	7.1	7.2	7.5	17.3	**39.1**	26.0	9.1	0.5	7.2	**42.8**	Silty Sand
NP-NW-44		Northwest	**20.1**	7.8	7.8	7.9	18.9	**42.5**	28.4	9.0	0.0	0.0	**37.4**	Sand Silt Clay
NP-SW-45		Southwest	**15.7**	6.3	6.8	6.7	20.2	**40.0**	33.4	10.9	0.0	0.0	**44.4**	Silty Sand
NP-SE-46		Southeast	**16.6**	5.9	6.0	5.1	17.9	**34.9**	34.9	13.4	0.2	0.0	**48.5**	Silty Sand
NF-NE-1	Near-Field	Northeast	**12.6**	5.4	6.2	6.4	19.1	**37.1**	32.6	11.9	1.0	4.7	**50.3**	Silty Sand
NF-NE-2			**23.2**	11.3	11.9	9.5	16.2	**48.9**	22.1	5.8	0.0	0.0	**27.9**	Sand Silt Clay
NF-NE-3			**20.1**	9.2	9.9	8.3	16.4	**43.7**	26.5	9.6	0.1	0.0	**36.1**	Sand Silt Clay
NF-NW-4		Northwest	**27.6**	11.9	11.7	9.7	16.3	**49.6**	19.1	3.7	0.0	0.0	**22.8**	Sand Silt Clay
NF-NW-5			**21.5**	11.5	13.0	11.0	17.1	**52.5**	20.8	5.1	0.0	0.0	**25.9**	Sand Silt Clay
NF-NW-6			**19.3**	9.1	9.8	9.2	17.9	**46.1**	25.9	8.7	0.1	0.0	**34.6**	Sandy Silt
NF-SE-7		Southeast	**23.3**	11.8	13.0	9.7	15.4	**49.9**	21.3	5.5	0.0	0.0	**26.8**	Sand Silt Clay
NF-SE-8			**19.2**	8.6	9.4	8.1	16.9	**42.9**	27.5	10.3	0.2	0.0	**37.9**	Sandy Silt
NF-SE-9			**18.1**	9.4	10.7	8.8	16.3	**45.2**	26.6	9.9	0.1	0.0	**36.7**	Sandy Silt
NF-SW-10		Southwest	**21.6**	10.1	11.2	9.4	17.0	**47.7**	23.7	7.0	0.0	0.0	**30.7**	Sand Silt Clay
NF-SW-11			**24.0**	11.8	12.6	10.4	16.7	**51.5**	20.0	4.5	0.0	0.0	**24.6**	Sand Silt Clay
NF-SW-12			**21.5**	9.3	9.4	7.8	17.8	**44.4**	27.1	7.0	0.0	0.0	**34.1**	Sand Silt Clay
MF-NE-13	Mid-Field	Northeast	**20.4**	9.2	9.7	7.9	14.2	**41.0**	23.2	8.9	0.4	6.1	**38.6**	Sand Silt Clay
MF-NE-14			**21.4**	9.6	9.8	7.9	16.5	**43.9**	26.7	8.0	0.1	0.0	**34.8**	Sand Silt Clay
MF-NE-15			**24.6**	11.9	12.9	9.6	14.9	**49.2**	20.6	5.5	0.0	0.0	**26.1**	Sand Silt Clay
MF-NW-16		Northwest	**30.9**	12.1	10.8	8.9	16.0	**47.8**	18.4	2.9	0.0	0.0	**21.3**	Sand Silt Clay
MF-NW-17			**29.1**	11.6	10.9	9.0	15.2	**46.7**	19.4	4.8	0.0	0.0	**24.2**	Sand Silt Clay
MF-NW-18			**28.7**	12.2	12.0	9.9	15.6	**49.6**	17.8	3.9	0.0	0.0	**21.7**	Sand Silt Clay
MF-SE-19		Southeast	**19.1**	9.2	10.1	8.2	15.2	**42.7**	27.3	10.8	0.1	0.0	**38.2**	Sandy Silt
MF-SE-20			**23.6**	9.9	9.8	7.8	15.2	**42.7**	25.5	8.2	0.1	0.0	**33.7**	Sand Silt Clay
MF-SE-21			**21.3**	10.2	10.8	8.2	15.0	**44.2**	24.9	8.2	0.6	0.9	**34.5**	Sand Silt Clay
MF-SW-22		Southwest	**25.6**	14.0	15.0	10.9	15.5	**55.3**	16.5	2.5	0.0	0.0	**19.0**	Clayey Silt
MF-SW-23			**26.8**	12.5	13.1	10.3	15.3	**51.2**	18.1	3.9	0.0	0.0	**22.0**	Sand Silt Clay
MF-SW-24			**24.1**	11.8	12.3	9.3	15.5	**48.9**	21.6	5.4	0.0	0.0	**27.0**	Sand Silt Clay

Table 23. (Continued).

Station	Distance Strata	Directional Strata	Total Clay	Very Fine Silt	Fine Silt	Medium Silt	Coarse Silt	Total Silt	Very Fine Sand	Fine Sand	Medium Sand	Coarse Sand	Total Sand	Sediment Type
FF-NE-25	Far-Field	Northeast	**25.0**	10.3	9.9	7.2	13.5	**40.8**	23.8	8.6	0.9	0.9	**34.2**	Sand Silt Clay
FF-NE-26			**15.3**	7.6	8.9	6.8	13.7	**37.1**	28.8	14.5	1.9	2.4	**47.6**	Silty Sand
FF-NE-27			**16.9**	9.1	10.6	8.3	15.1	**43.2**	27.0	10.9	0.7	1.2	**39.9**	Sandy Silt
FF-NW-28		Northwest	**28.0**	11.9	11.1	9.4	15.5	**47.9**	19.3	4.7	0.0	0.0	**24.0**	Sand Silt Clay
FF-NW-29			**25.4**	12.7	13.2	9.8	14.3	**50.0**	19.4	5.2	0.0	0.0	**24.6**	Sand Silt Clay
FF-NW-30			**24.5**	14.7	16.2	11.2	14.8	**56.9**	16.1	2.6	0.0	0.0	**18.7**	Clayey Silt
FF-SE-31		Southeast	**16.7**	8.7	9.7	7.4	14.4	**40.2**	27.8	12.2	1.2	1.9	**43.1**	Silty Sand
FF-SE-32			**15.1**	7.2	7.8	6.3	15.3	**36.6**	30.8	13.6	1.8	2.1	**48.3**	Silty Sand
FF-SE-33			**16.3**	7.6	7.9	6.3	13.3	**35.1**	26.9	13.1	1.7	6.8	**48.6**	Silty Sand
FF-SW-34		Southwest	**24.3**	14.4	15.4	11.0	15.2	**56.0**	17.1	2.7	0.0	0.0	**19.7**	Clayey Silt
FF-SW-35			**26.5**	14.1	13.7	9.2	14.4	**51.4**	18.6	3.6	0.0	0.0	**22.1**	Sand Silt Clay
FF-SW-36			**22.2**	11.9	13.0	9.5	15.2	**49.6**	22.1	6.1	0.0	0.0	**28.2**	Sand Silt Clay
REF-NE-37	Reference	Northeast	**20.6**	10.8	11.4	8.8	16.7	**47.6**	24.7	7.0	0.1	0.0	**31.8**	Sand Silt Clay
REF-NE-38			**18.5**	10.0	10.7	7.8	15.5	**43.9**	28.2	9.3	0.1	0.0	**37.6**	Sandy Silt
REF-NE-39			**18.0**	8.6	9.4	8.6	17.8	**44.3**	28.0	9.6	0.1	0.0	**37.7**	Sandy Silt
REF-SW-40		Southwest	**18.4**	10.0	11.2	8.6	16.7	**46.5**	27.4	7.8	0.0	0.0	**35.2**	Sandy Silt
REF-SW-41			**30.1**	13.0	11.3	8.4	16.4	**49.0**	18.3	2.5	0.0	0.0	**20.9**	Sand Silt Clay
REF-SW-42			**22.2**	12.1	13.5	10.6	17.2	**53.4**	20.5	3.9	0.0	0.0	**24.4**	Sand Silt Clay
2020 LPP EMS Mean (± SD)			21.8 ± 4.4	10.3 ± 2.3	10.8 ± 2.3	8.7 ± 1.4	16.0 ± 1.5	45.8 ± 5.5	23.9 ± 4.7	7.4 ± 3.4	0.3 ± 0.5	0.7 ± 1.8	32.3 ± 9.1	--
2019 LPP EBS Mean (± SD)			23.3 ± 2.9	16.0 ± 1.9	15.2 ± 2.0	9.2 ± 1.2	13.4 ± 1.4	53.8 ± 4.2	18.4 ± 3.7	4.3 ± 1.9	0.1 ± 0.3	0.1 ± 0.2	22.9 ± 5.5	--
2014 EBS Mean (± SD)			25.0 ± 1.5	16.4 ± 1.6	14.4 ± 1.6	9.2 ± 0.9	13.1 ± 0.6	53.0 ± 3.7	17.4 ± 2.6	4.2 ± 1.3	0.2 ± 0.2	0.2 ± 0.3	22.0 ± 4.1	--

EBS = environmental Baseline Survey; EMS = environmental monitoring survey; --= not applicable; SD = Standard Deviation.

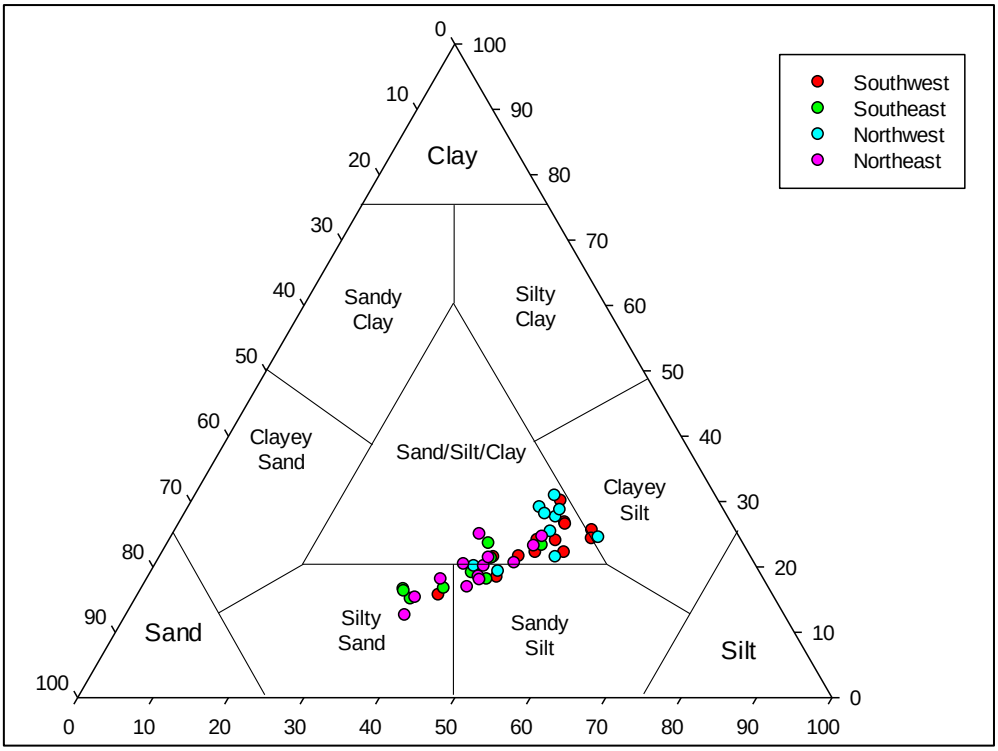


Figure 12. Ternary diagram showing grain size distribution from sediment samples (grouped by directional strata) collected during the 2020 Leviathan Production Platform Environmental Monitoring Survey.

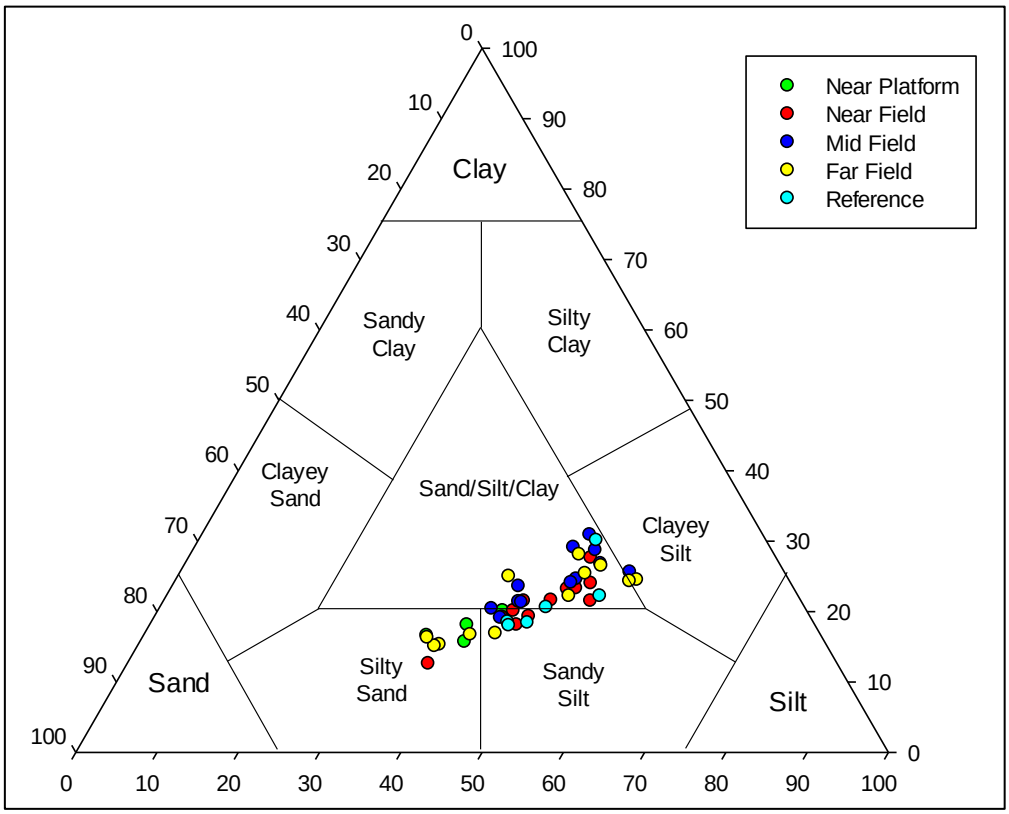


Figure 13. Ternary diagram showing grain size distribution from sediment samples (grouped by distance strata) collected during the 2020 Leviathan Production Platform Environmental Monitoring Survey.

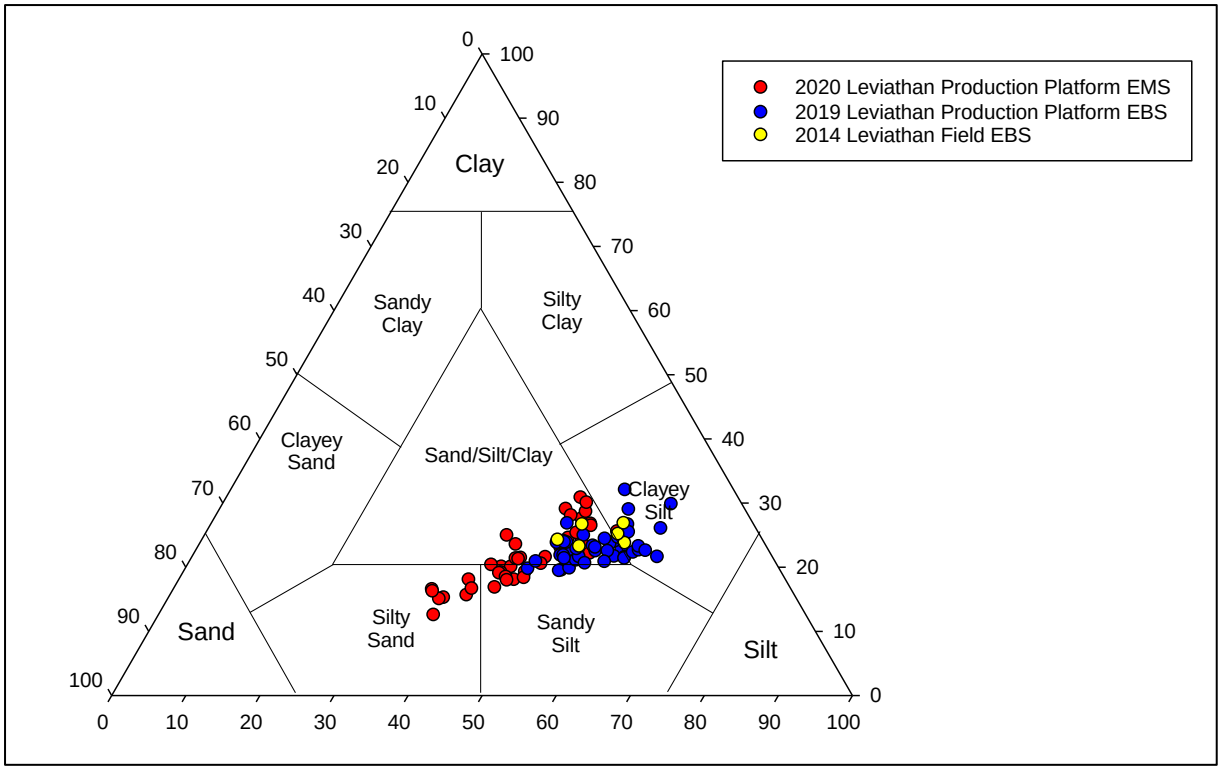


Figure 14. Ternary diagram showing grain size distribution from sediment samples (grouped by survey) from the 2014 Leviathan Field Development Environmental Baseline Survey (EBS), the 2019 Leviathan Production Platform EBS, and the 2020 Leviathan Platform Environmental Monitoring Survey (EMS).

Mean (± SD) percentages of individual grain size classes among survey years are presented in **Figure 15** and **Table 24**. Wentworth grain size fractions were generally similar among surveys, with a slight increase in very fine sand and corresponding decrease in very fine silt during the 2020 LPP EMS. Mean (± SD) percentages of each major grain size classification for each directional and distance strata for the 2020 LPP EMS are presented in **Figures 16** and **17**. Major grain size classifications were generally similar among directional strata (quadrants). Among distance strata, Near Platform stations had slightly higher fractions of sand and slightly lower fractions of silt and clay as compared with other distance strata.

A general comparison between grain size data collected near the present site of the 2014 Leviathan Field Development EBS, the 2019 LPP EBS, and the 2020 LPP EMS indicate that grain size in the area was generally similar between 2019 and 2020. In 2020, samples exhibited small increases in fine sand, very fine sand, and coarse silt fractions, and corresponding decreases in fine silt, very fine silt, and clay fractions (**Figure 16**).

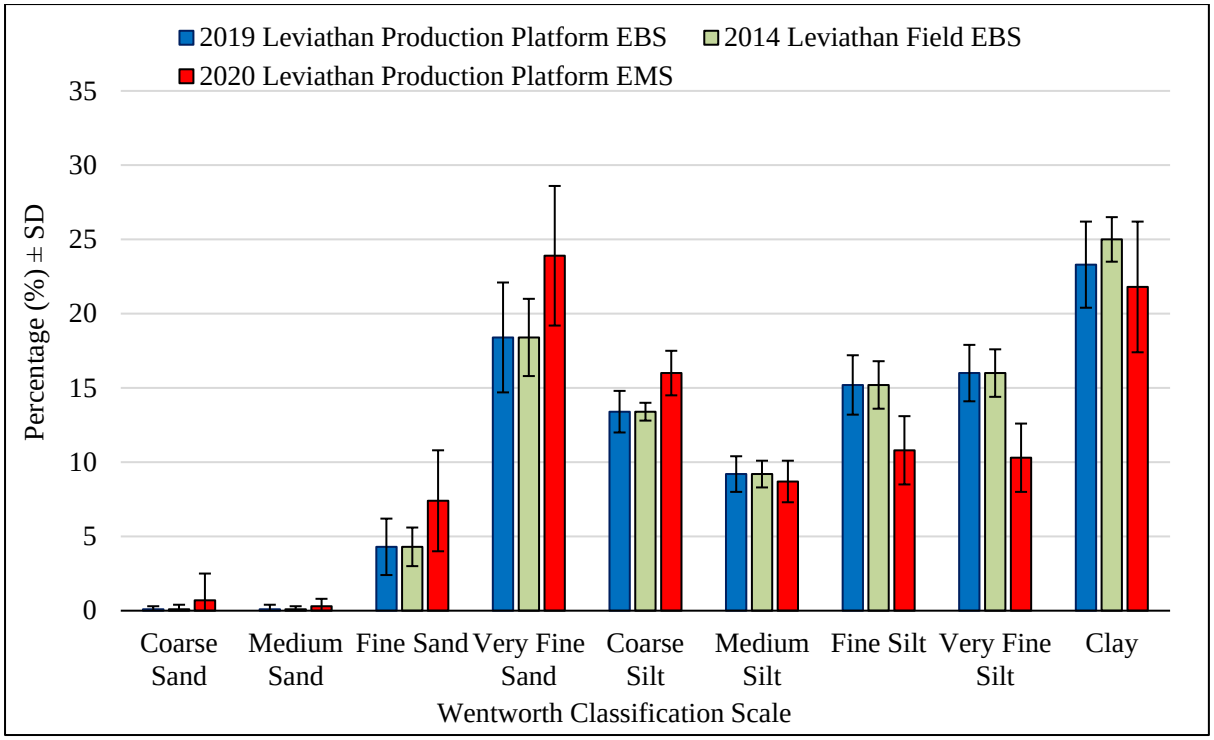


Figure 15. Mean individual grain size classes (± standard deviation [SD]) for samples collected within the Leviathan Production Platform survey area during the 2014 Leviathan Field Development Environmental Baseline Survey (EBS), the 2019 Leviathan Production Platform EBS, and the 2020 Leviathan Production Platform Environmental Monitoring Survey (EMS).

Table 24. Mean (± standard deviation) sediment percentages of major (total clay, silt, and sand) and individual (very fine, fine, medium, and coarse) grain size classes by distance and directional strata during the 2020 Leviathan Production Platform Environmental Monitoring Survey.

Strata type	Strata	Total Clay	Very Fine Silt	Fine Silt	Medium Silt	Coarse Silt	Total Silt	Very Fine Sand	Fine Sand	Medium Sand	Coarse Sand	Total Sand
Distance Strata	Near-Platform	17.6 ± 1.9	6.8 ± 0.8	7.0 ± 0.8	6.8 ± 1.2	18.6 ± 1.3	39.1 ± 3.2	30.7 ± 1.2	10.6 ± 2.1	0.2 ± 0.2	1.8 ± 3.6	43.3 ± 4.6
	Near-Field	21.0 ± 3.7	10.0 ± 1.9	10.7 ± 2.0	9.0 ± 1.2	16.9 ± 1.0	46.6 ± 4.3	24.4 ± 3.9	7.4 ± 2.6	0.1 ± 0.3	0.4 ± 1.4	32.3 ± 7.6
	Mid-Field	24.6 ± 3.7	11.2 ± 1.5	11.4 ± 1.6	9.0 ± 1.0	15.3 ± 0.6	46.9 ± 4.2	21.7 ± 3.8	6.1 ± 2.7	0.1 ± 0.2	0.6 ± 1.8	28.4 ± 7.1
	Far-Field	21.4 ± 4.9	10.9 ± 2.8	11.5 ± 2.8	8.5 ± 1.7	14.6 ± 0.7	45.4 ± 7.6	23.1 ± 5.0	8.2 ± 4.5	0.7 ± 0.8	1.3 ± 2.0	33.3 ± 11.7
	Reference	21.3 ± 4.6	10.8 ± 1.6	11.3 ± 1.3	8.8 ± 0.9	16.7 ± 0.8	47.5 ± 3.5	24.5 ± 4.2	6.7 ± 2.9	0.1 ± 0.05	0 ± 0	31.2 ± 7.1
Directional Strata	Northeast	19.6 ± 3.6	9.2 ± 1.8	9.9 ± 1.8	8.0 ± 0.9	15.9 ± 1.6	43.1 ± 4.0	26.0 ± 3.2	9.1 ± 2.4	0.5 ± 0.6	1.7 ± 2.6	37.3 ± 6.9
	Northwest	25.5 ± 4.1	11.6 ± 1.9	11.7 ± 2.2	9.6 ± 1.0	16.2 ± 1.4	49.0 ± 3.9	20.5 ± 3.8	5.1 ± 2.2	0.01 ± 0.03	0 ± 0	25.5 ± 5.9
	Southeast	18.9 ± 3.0	8.9 ± 1.7	9.5 ± 1.9	7.6 ± 1.4	15.5 ± 1.3	41.4 ± 4.8	27.4 ± 3.6	10.5 ± 2.7	0.6 ± 0.7	1.2 ± 2.1	39.6 ± 7.3
	Southwest	23.3 ± 3.7	11.6 ± 2.3	12.2 ± 2.3	9.4 ± 1.3	16.4 ± 1.5	49.6 ± 4.4	21.9 ± 4.9	5.2 ± 2.5	0 ± 0	0 ± 0	27.1 ± 7.4

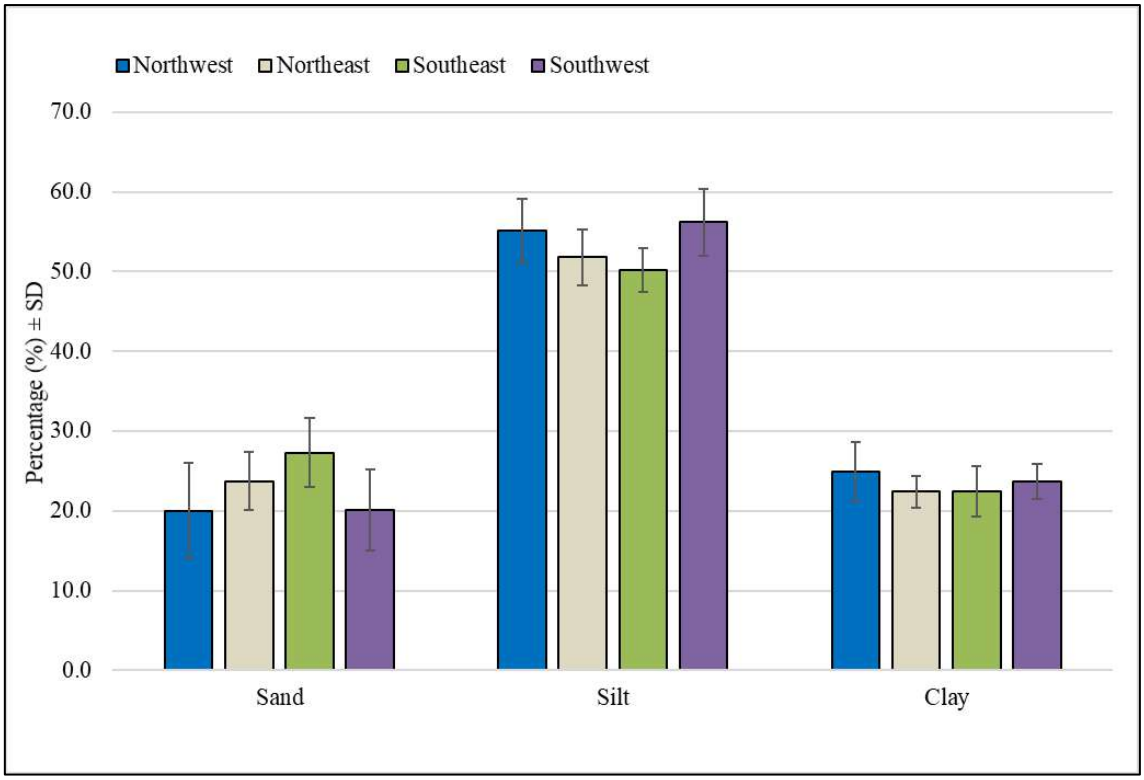


Figure 16. Mean percent (± standard deviation [SD]) of major grain size classes for samples collected within the Leviathan Production Platform survey area by directional strata during the 2020 Leviathan Production Platform Environmental Monitoring Survey.

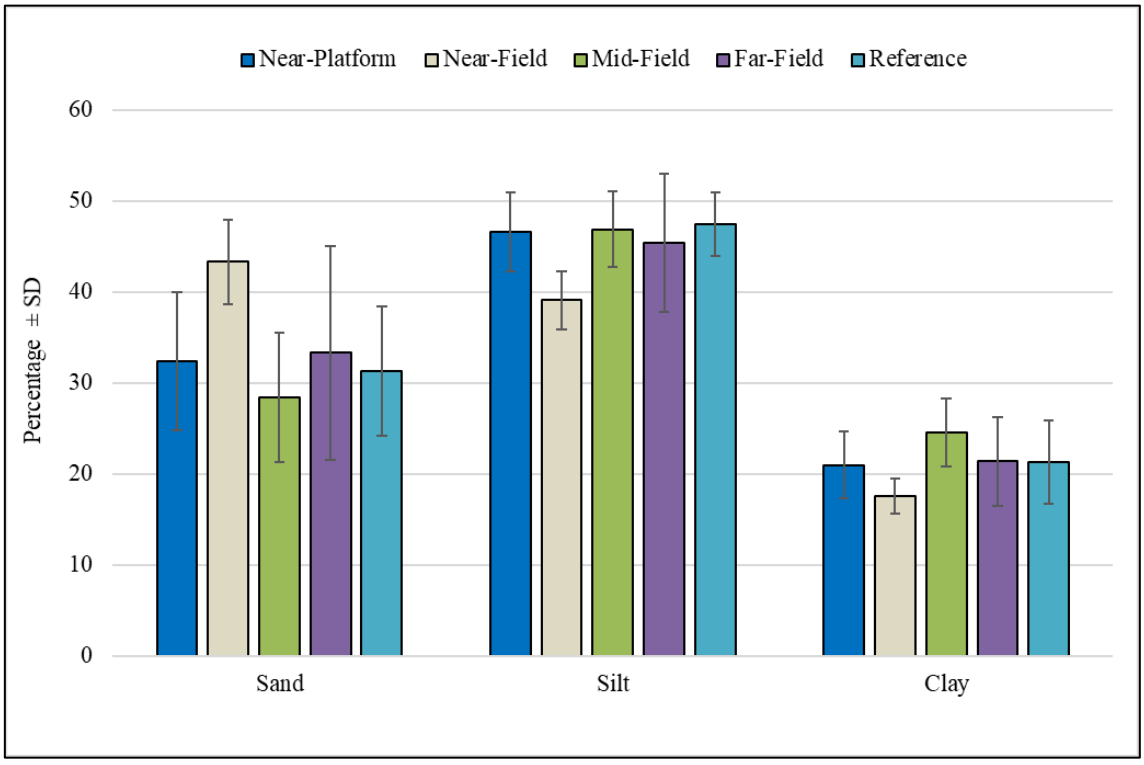


Figure 17. Mean percent (± standard deviation [SD]) of major grain size classes for samples collected within the Leviathan Production Platform survey area by distance strata during the 2020 Leviathan Production Platform Environmental Monitoring Survey.

5.4.2 Total Organic Carbon

Analytical laboratory datasheets for TOC are provided in **Appendix J**; results are presented in **Table 25** and **Table 26**. TOC concentrations in sediments ranged from 0.12% to 0.81% and averaged 0.45% ± 0.19%. There are no established toxicity thresholds for TOC in marine sediments.

Table 25. Total organic carbon concentrations (%) in sediment samples collected during the 2020 Leviathan Production Platform Environmental Monitoring Survey.

Station	Distance Strata	Directional Strata	Total Organic Carbon (%)
NP-NE-43	Near-Platform	Northeast	0.29
NP-NW-44		Northwest	0.26
NP-SW-45		Southwest	0.12
NP-SE-46		Southeast	0.13
NF-NE-1	Near-Field	Northeast	0.17
NF-NE-2			0.63
NF-NE-3			0.32
NF-NW-4		Northwest	0.56
NF-NW-5			0.39
NF-NW-6			0.35
NF-SE-7		Southeast	0.75
NF-SE-8			0.26
NF-SE-9			0.45
NF-SW-10		Southwest	0.52
NF-SW-11			0.60
NF-SW-12			0.56
MF-NE-13	Mid-Field	Northeast	0.52
MF-NE-14			0.51
MF-NE-15			0.72
MF-NW-16		Northwest	0.65
MF-NW-17			0.22
MF-NW-18			0.54
MF-SE-19		Southeast	0.41
MF-SE-20			0.39
MF-SE-21			0.61
MF-SW-22		Southwest	0.74
MF-SW-23			0.27
MF-SW-24			0.55
FF-NE-25	Far-Field	Northeast	0.42
FF-NE-26			0.38
FF-NE-27			0.40
FF-NW-28		Northwest	0.31
FF-NW-29			0.68
FF-NW-30			0.72
FF-SE-31		Southeast	0.29
FF-SE-32			0.25
FF-SE-33			0.30
FF-SW-34		Southwest	0.57
FF-SW-35			0.75
FF-SW-36			0.56

Table 25. (Continued).

Station	Distance Strata	Directional Strata	Total Organic Carbon (%)
REF-NE-37	Reference	Northeast	0.81
REF-NE-38			0.15
REF-NE-39			0.18
REF-SW-40		Southwest	0.54
REF-SW-41			0.45
REF-SW-42			0.41
2020 LPP EMS Overall Mean (± SD)			0.45 ± 0.19
2019 LPP EBS Mean (± SD)			0.50 ± 0.07
2014 EBS Mean (± SD)			0.57 ± 0.06

EBS = Environmental Baseline Survey; EMS = Environmental Monitoring Survey; SD = Standard Deviation.

Table 26. Mean total organic carbon concentrations (% ± standard deviation) in sediment samples by distance and directional strata collected during the 2020 Leviathan Production Platform Environmental Monitoring Survey (2020 LPP EMS).

Strata Type	Strata	Total Organic Carbon (%)
Distance Strata	Near-Platform	0.20 ± 0.09
	Near-Field	0.46 ± 0.17
	Mid-Field	0.51 ± 0.16
	Far-Field	0.47 ± 0.18
	Reference	0.42 ± 0.24
Directional Strata	Northeast Quadrant	0.39 ± 0.21
	Northwest Quadrant	0.47 ± 0.18
	Southeast Quadrant	0.38 ± 0.18
	Southwest Quadrant	0.51 ± 0.17
2020 LPP EMS Overall Mean (± SD)		0.45 ± 0.19
2019 LPP EBS Mean (± SD)		0.50 ± 0.07
2014 EBS Mean (± SD)		0.57 ± 0.06

EBS = Environmental Baseline Survey; EMS = Environmental Monitoring Survey; SD = Standard Deviation.

Total Organic Carbon Statistical Analysis

There was no significant three-way interactive effect among distance, direction, and survey year for sediment TOC concentrations ($F_{10,56} = 0.86$; $P = 0.58$). There were also no significant two-way interactive effects between distance and direction ($F_{10,56} = 0.68$; $P = 0.74$), direction and survey year ($F_{3,56} = 0.31$; $P = 0.81$), or distance and survey year ($F_{4,56} = 1.77$; $P = 0.15$).

Because there were no significant interactions for sediment TOC concentrations it was possible to investigate the overall main effects of distance, direction, and survey year for sediment TOC. There were no significant differences among direction ($F_{3,88} = 1.33$; $P = 0.27$) or survey year ($F_{1,90} = 3.49$; $P = 0.07$). There was, however, a significant difference in sediment TOC concentrations by distance from the LPP ($F_{4,87} = 2.64$; $P = 0.04$). Further statistical investigation showed that this difference was due to sediment TOC concentrations within the Near-Platform strata being significantly lower ($t_{87} = 3.07$; $P = 0.02$) than concentrations within the Mid-Field strata (**Table 26**; **Figure 18**). TOC concentrations in all other distance strata were statistically similar to one another.

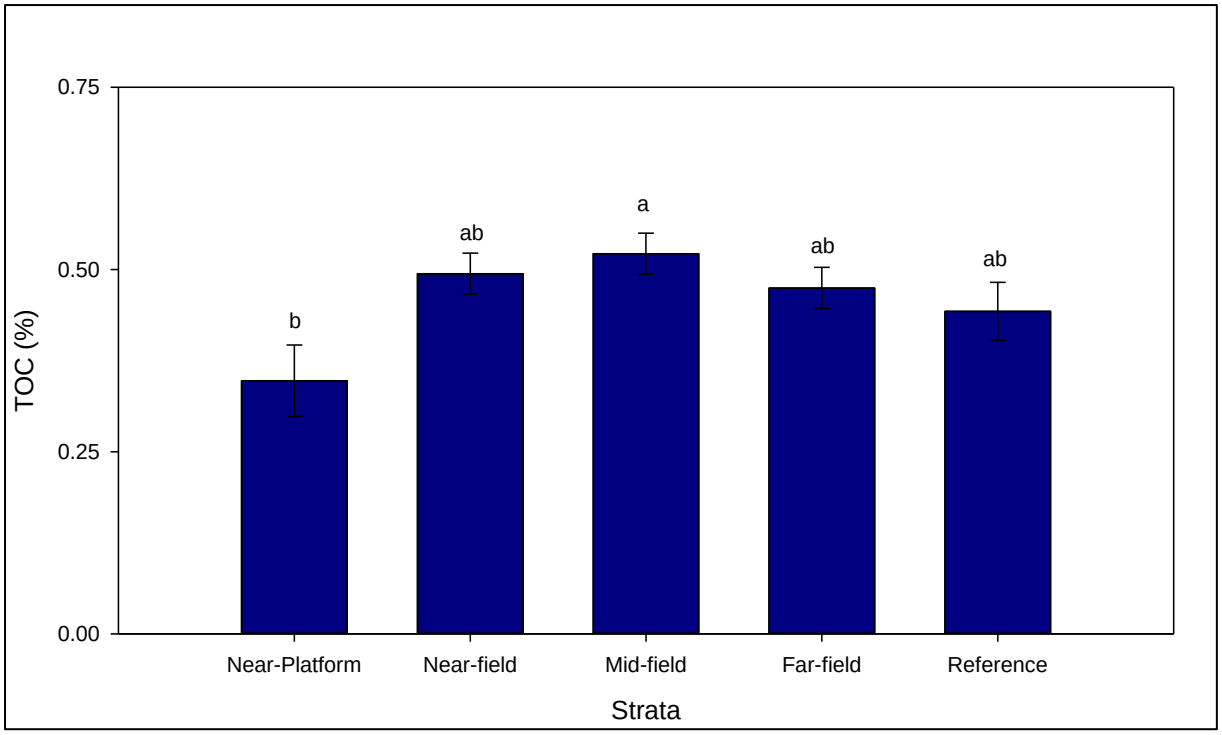


Figure 18. Statistical least square means (± standard error) of sediment total organic carbon concentrations (%) by distance strata as computed by the analysis of variance (ANOVA) model. Different letters indicate statistical significance at $P < 0.05$.

5.4.3 Metals

Analytical results for total metals in sediment samples are provided in **Appendix K**. Values for total metals concentrations from the 2020 LPP EMS are provided in **Table 27** Mean metals (± SD) concentration at each distance and directional strata are provided in **Table 28**.

Mean (± SD) metals concentrations from the 2020 LPP EMS were compared to the ERL and ERM concentrations and assessed in context to results from the 2019 LPP EBS and the six samples collected during the 2014 Leviathan Field Development EBS that are in the vicinity of the LPP (**Table 26**). Individual metals concentrations were also plotted against aluminum to normalize the metals concentrations (as discussed in **Section 4.2.2**). It should be noted that the regression used to calculate the 99% prediction interval as described in **Section 4.2.2** is based on samples collected within the vicinity of the LPP location during both the 2014 Leviathan Field Development EBS and the 2019 LPP EBS.

All concentrations of arsenic, chromium, and nickel were above the ERL. Some concentrations of copper were above the ERL and few concentrations of nickel were slightly above the ERM (**Table 27**). These elevated values are similar to previous observations in the vicinity of the LPP (MVI, 2019a), and throughout the Levantine Basin in general (CSA Ocean Sciences, 2014a); therefore, these concentrations are considered ambient for the region.

Table 27. Total metals concentrations (mg kg^{-1} unless noted otherwise) in sediment samples collected during the 2020 Leviathan Production Platform Environmental Baseline Survey. Effects range low (ERL) and effects range median (ERM) values are presented for comparison. Bold values are above the ERL; italicized values are above the ERM.

Station	Distance Strata	Directional Strata	Al (%)	As	Ba	Cd	Cr	Cu	Fe (%)	Pb	Hg (ng g^{-1})	Ni	Zn
NP-NE-43	Near-Platform	Northeast	5.35	**8.4**	349	<0.15	**86.0**	21.0	4.16	9.52	11.3	**38.3**	57.9
NP-NW-44		Northwest	7.59	**9.6**	362	<0.15	**91.4**	30.2	5.86	12.0	16.9	**47.3**	72.3
NP-SW-45		Southeast	5.82	**8.8**	329	<0.15	**85.9**	23.8	4.47	9.95	12.9	**39.7**	59.6
NP-SE-46		Southwest	5.78	**10.6**	321	<0.15	**88.3**	24.2	4.47	10.1	12.6	**42.1**	64.8
NF-NE-1	Near-Field	Northeast	5.43	**11.2**	325	>0.16	**91.9**	30.2	4.37	10.1	12.1	**40.9**	79.3
NF-NE-2			6.67	**13.4**	281	<0.16	**94.5**	31.3	5.23	11.5	16.4	**49.3**	74.9
NF-NE-3			6.14	**12.5**	300	<0.16	**90.5**	27.8	4.87	11.1	16.1	**47.7**	69.1
NF-NW-4		Northwest	7.15	**11.7**	297	<0.16	**99.7**	**34.6**	5.64	11.4	18.7	***55.1***	77.0
NF-NW-5			7.50	**12.3**	332	<0.16	**96.2**	29.9	6.00	11.0	16.8	**50.4**	74.4
NF-NW-6			6.84	**10.9**	313	<0.14	**90.8**	30.2	5.44	12.0	16.8	**49.1**	71.9
NF-SE-7		Southeast	6.49	**13.9**	285	<0.15	**96.8**	30.6	5.18	11.4	16.7	**51.3**	75.4
NF-SE-8			8.09	**12.6**	392	<0.14	**90.6**	28.4	6.37	11.2	16.1	**46.5**	68.8
NF-SE-9			6.34	**13.1**	305	<0.14	**91.0**	27.6	5.01	10.8	14.8	**47.0**	68.2
NF-SW-10		Southwest	7.22	**12.9**	309	<0.16	**93.7**	30.7	5.59	11.6	17.6	**49.8**	75.0
NF-SW-11			7.47	**13.4**	309	<0.15	**96.3**	32.6	5.79	11.6	13.6	***52.7***	76.8
NF-SW-12			6.87	**11.9**	347	<0.15	**95.1**	29.0	5.35	11.0	13.9	**47.8**	70.9
MF-NE-13	Mid-Field	Northeast	6.41	**13.1**	305	<0.14	**93.7**	28.1	4.97	10.7	16.7	**47.9**	70.1
MF-NE-14			6.70	**11.9**	290	<0.15	**94.2**	30.1	5.13	11.9	16.9	**51.1**	72.9
MF-NE-15			7.05	**13.0**	295	<0.15	**95.9**	31.3	5.31	11.7	15.0	**50.5**	72.6
MF-NW-16		Northwest	8.08	**13.2**	287	<0.14	**103**	**36.2**	6.10	10.9	14.1	***58.4***	78.1
MF-NW-17			7.77	**11.5**	279	<0.15	**102**	**36.2**	5.79	13.0	20.0	***55.4***	80.7
MF-NW-18			7.35	**12.7**	284	<0.16	**103**	**36.2**	5.53	11.5	14.8	***54.8***	79.6
MF-SE-19		Southeast	6.74	**13.9**	289	<0.15	**95.8**	30.9	5.04	11.6	15.5	**50.1**	72.0
MF-SE-20			7.80	**11.9**	351	<0.15	**86.4**	28.2	5.86	10.1	14.9	**45.9**	66.2
MF-SE-21			6.82	**12.9**	285	<0.15	**90.8**	30.2	5.12	11.1	14.3	**50.1**	70.5
MF-SW-22		Southwest	6.42	**12.2**	283	<0.15	**91.6**	29.6	4.86	11.2	13.0	**49.0**	71.5
MF-SW-23			7.74	**13.2**	271	<0.16	**99.9**	**37.1**	5.76	10.8	14.3	***58.6***	77.0
MF-SW-24			6.93	**13.2**	300	<0.15	**94.7**	30.5	5.15	11.6	15.7	**50.2**	72.4
FF-NE-25	Far-Field	Northeast	6.41	**12.5**	283	<0.14	**88.3**	28.1	4.70	10.4	16.2	**46.3**	68.2
FF-NE-26			6.10	**12.7**	284	<0.15	**91.5**	27.8	4.63	10.4	13.9	**46.4**	65.0
FF-NE-27			7.04	**13.0**	296	<0.15	**92.7**	28.7	5.32	11.4	16.1	**49.1**	72.2
FF-NW-28		Northwest	7.37	**13.3**	300	<0.15	**95.2**	31.9	5.56	11.2	13.9	**51.5**	74.5
FF-NW-29			7.65	**13.2**	272	<0.16	**97.2**	**35.8**	5.68	10.8	8.34	***58.1***	79.4
FF-NW-30			8.16	**15.1**	279	<0.14	**103**	**38.3**	6.15	13.6	20.6	***58.7***	83.1
FF-SE-31		Southeast	6.05	**12.5**	286	<0.16	**87.1**	25.5	4.57	10.3	13.1	**44.3**	65.1
FF-SE-32			8.02	**12.0**	395	<0.16	**84.7**	32.7	5.89	11.1	14.6	**48.4**	92.1
FF-SE-33			6.14	**11.4**	285	<0.15	**87.3**	28.3	4.54	9.21	12.2	**47.5**	64.4
FF-SW-34		Southwest	7.94	**15.2**	277	<0.16	**103**	**36.6**	5.90	13.1	16.0	***57.3***	82.3
FF-SW-35			8.78	**13.6**	308	<0.15	**97.5**	**35.8**	6.56	11.5	15.0	***55.1***	77.4
FF-SW-36			7.49	**13.3**	280	<0.14	**98.9**	**35.1**	5.56	11.9	13.7	***55.2***	75.3

Table 27. (Continued).

Station	Distance Strata	Directional Strata	Al (%)	As	Ba	Cd	Cr	Cu	Fe (%)	Pb	Hg (ng g^{-1})	Ni	Zn
REF-NE-37	Reference	Northeast	7.30	**13.2**	300	<0.16	**87.7**	29.9	5.41	11.5	17.3	**47.7**	71.6
REF-NE-38			6.29	**12.6**	316	<0.16	**89.8**	25.3	4.62	10.2	15.0	**43.2**	67.3
REF-NE-39			6.39	**11.0**	313	<0.14	**95.0**	27.3	4.82	9.66	11.6	**45.2**	65.4
REF-SW-40		Southwest	6.74	**13.5**	296	<0.15	**91.2**	28.8	5.14	10.5	13.1	**48.8**	69.0
REF-SW-41			7.78	**15.0**	301	<0.14	**102**	33.2	5.75	12.1	14.9	***54.8***	78.3
REF-SW-42			8.78	**14.6**	318	<0.15	**102**	**35.0**	6.32	12.3	10.8	***55.6***	79.9
2020 LPP EMS Overall Mean (± SD)			7.02 ± 0.82	**12.6 ± 1.4**	306 ± 28.8	--	**94.0 ± 5.2**	30.7 ± 3.9	5.34 ± 0.58	11.2 ± 0.91	14.9 ± 2.3	**49.8 ± 5.0**	72.8 ± 6.4
2019 LPP EBS Mean (± SD)			6.50 ± 0.51	**13.4 ± 1.3**	303 ± 17.6	--	**98.5 ± 6.2**	31.8 ± 3.5	5.25 ± 0.38	11.5 ± 3.9	17.5 ± 4.6	**51.2 ± 4.2**	76.3 ± 5.6
2014 EBS Mean (± SD)			7.20 ± 0.50	**12.2 ± 1.3**	270 ± 2.5	0.19 ± 0.02	**87.7 ± 2.9**	**34.5 ± 2.9**	5.43 ± 0.42	12.9 ± 0.73	25.4 ± 2.7	**50.3 ± 2.8**	84.0 ± 2.3
ERL			--	8.2	--	1.2	81.0	34.0	--	46.7	150	20.9	150.0
ERM			--	70.0	--	9.6	370.0	270.0	--	218.0	710	51.6	410.0

Al = aluminum; As=arsenic; Ba = barium; Cd = cadmium; Cr = chromium; Cu = copper; EBS= environmental baseline survey; EMS = environmental monitoring survey; Fe = iron; LPP = Leviathan Production Platform; Pb = lead; Hg = mercury; Ni = nickel; SD = standard deviation; Zn= zinc.

Table 28. Mean metals concentrations (mg kg^{-1} unless noted otherwise) ± standard deviation) by distance and directional strata in sediment samples collected during the 2020 Leviathan Production Platform Environmental Baseline Survey. Effects range low (ERL) and effects range median (ERM) values are presented for comparison. **Bold** values are above the ERL; *italicized* values are above the ERM.

Strata Type	Strata	Al (%)	As	Ba	Cd	Cr	Cu	Fe (%)	Pb	Hg (ng/g)	Ni	Zn
Distance Strata	Near-Platform	6.13 ± 0.99	**9.4 ± 0.97**	340 ± 18.7	--	**87.9 ± 2.6**	24.8 ± 3.9	4.74 ± 0.76	10.4 ± 1.1	13.4 ± 2.4	**41.9 ± 3.9**	63.7 ± 6.5
	Near-Field	6.85 ± 0.71	**12.5 ± 0.92**	316 ± 30.3	--	**93.9 ± 3.0**	30.2 ± 2.0	5.40 ± 0.53	11.2 ± 0.48	15.8 ± 1.9	**48.9 ± 3.5**	73.5 ± 3.6
	Mid-Field	7.15 ± 0.92	**12.7 ± 0.70**	293 ± 20.3	--	**95.9 ± 5.2**	32.1 ± 3.4	5.39 ± 0.41	11.3 ± 0.73	15.4 ± 1.8	***51.8 ± 4.0***	73.6 ± 4.3
	Far-Field	7.26 ± 0.92	**13.2 ± 1.1**	295 ± 33.0	--	**93.9 ± 6.2**	32.1 ± 4.3	5.42 ± 0.68	11.2 ± 1.2	14.5 ± 2.9	**51.5 ± 5.2**	74.9 ± 8.5
	Reference	7.21 ± 0.95	**13.3 ± 1.4**	307 ± 9.42	--	**94.6 ± 6.2**	29.9 ± 3.6	5.34 ± 0.63	11.0 ± 1.1	13.8 ± 2.4	**49.2 ± 5.0**	71.9 ± 5.9
Directional Strata	Northeast Quadrant	6.41 ± 0.58	**12.2 ± 1.4**	303 ± 19.2	--	**91.7 ± 3.1**	28.2 ± 2.8	4.89 ± 0.39	10.8 ± 0.79	14.9 ± 2.1	**46.4 ± 3.7**	69.7 ± 5.3
	Northwest Quadrant	7.55 ± 0.40	**12.4 ± 4.0**	301 ± 28.2	--	**98.2 ± 4.7**	33.9 ± 3.1	5.78 ± 0.25	11.7 ± 0.93	16.1 ± 2.6	***53.9 ± 4.1***	77.1 ± 3.7
	Southeast Quadrant	6.83 ± 0.84	**12.3 ± 1.5**	320 ± 44.6	--	**89.6 ± 4.1**	28.6 ± 2.6	5.21 ± 0.64	10.7 ± 0.76	14.5 ± 1.4	**47.1 ± 3.4**	70.2 ± 8.8
	Southwest Quadrant	7.38 ± 0.86	**13.3 ± 1.3**	302 ± 20.9	--	**96.5 ± 4.6**	32.2 ± 3.8	5.55 ± 0.57	11.5 ± 0.79	14.2 ± 1.7	***52.1 ± 4.6***	74.7 ± 4.8
2020 LPP EMS Overall Mean (± SD)		7.02 ± 0.82	**12.6 ± 1.4**	306 ± 28.8	--	**94.0 ± 5.2**	30.7 ± 3.9	5.34 ± 0.58	11.2 ± 0.91	14.9 ± 2.3	**49.8 ± 5.0**	72.8 ± 6.4
2019 LPP EBS Mean (± SD)		6.50 ± 0.51	**13.4 ± 1.3**	303 ± 17.6	--	**98.5 ± 6.2**	31.8 ± 3.5	5.25 ± 0.38	11.5 ± 3.9	17.5 ± 4.6	**51.2 ± 4.2**	76.3 ± 5.6
2014 EBS Mean (± SD)		7.20 ± 0.50	**12.2 ± 1.3**	270 ± 2.5	0.19 ± 0.02	**87.7 ± 2.9**	**34.5 ± 2.9**	5.43 ± 0.42	12.9 ± 0.73	25.4 ± 2.7	**50.3 ± 2.8**	84.0 ± 2.3
ERL		--	8.2	--	1.2	81.0	34.0	--	46.7	150	20.9	150.0
ERM		--	70.0	--	9.6	370.0	270.0	--	218.0	710	51.6	410.0

Al = aluminum; As = arsenic; Ba = barium; Cd = cadmium; Cr = chromium; Cu = copper; EBS = environmental baseline survey; EMS = environmental monitoring survey; Fe = iron; Hg = mercury; LPP = Leviathan Production Platform; Ni = nickel; Pb = lead; SD = Standard Deviation; Zn = zinc. "--" = not calculable.

Aluminum

Concentrations of aluminum were relatively consistent across all stations and ranged from 5.35 to 8.78% (**Table 27**) and the overall mean (± SD) was 7.02 ± 0.82%. Mean concentrations of aluminum were consistent among sampling distance and directional strata (**Table 28**). There is no established toxicity threshold for Al in marine sediments; however, aluminum concentrations were similar to values from the 2019 LPP EBS and the 2014 Leviathan Field Development EBS (**Table 27**).

Arsenic

Arsenic concentrations ranged from 8.4 to 15.2 mg kg^{-1} and the overall mean (± SD) was 12.6 ± 1.4 mg kg^{-1}. Arsenic concentrations were above the ERL (8.2 mg kg^{-1}) and below the ERM (70 mg kg^{-1}) at all stations. Mean arsenic concentrations were consistent among distance and directional strata (**Table 28**) and consistent with the 2019 LPP EBS and the 2014 Leviathan Field Development EBS. When normalized against aluminum all concentrations of arsenic were within the 99% prediction interval based on a regression plotted from the samples collected in the vicinity of the LPP during the 2014 Leviathan Field Development EBS and 2019 LPP EBS (**Figure 19**).

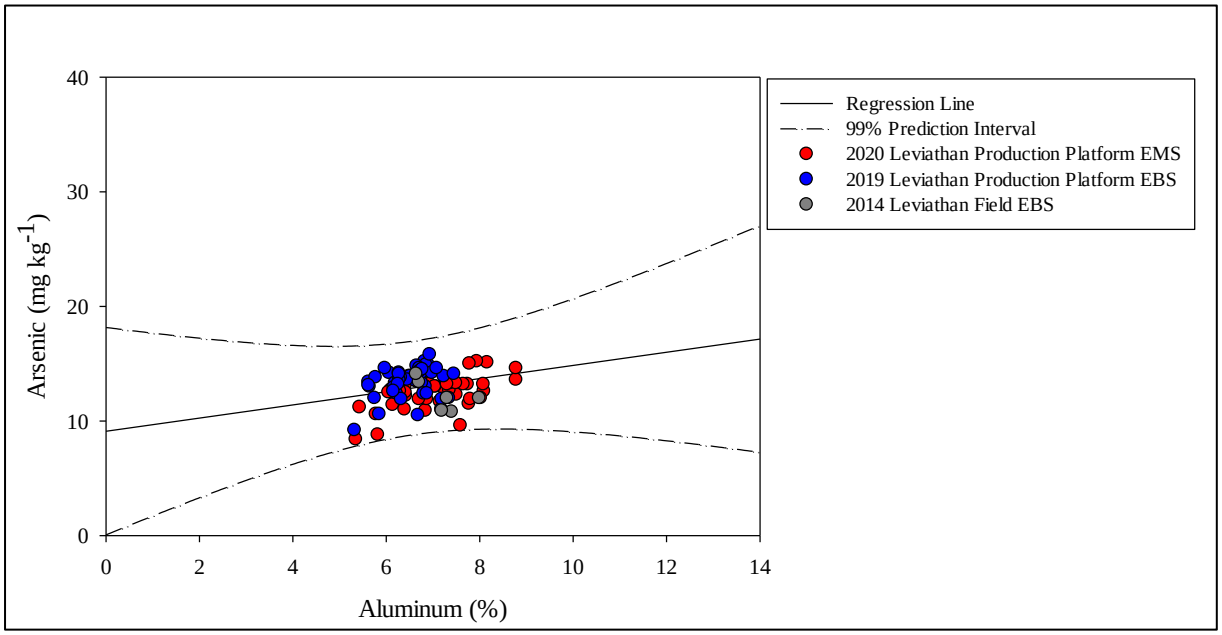


Figure 19. Plot of aluminum versus arsenic during the 2020 Leviathan Production Platform Environmental Monitoring Survey (EMS) as compared to 2019 Leviathan Production Platform Environmental Baseline Survey (EBS) and the 2014 Leviathan Field Development EBS. The 99% prediction interval based on a regression plotted from the samples collected in the vicinity of the LPP during the 2014 Leviathan Field Development EBS and 2019 LPP EBS.

Barium

Barium concentrations ranged from 271 to 395 mg kg^{-1} and the overall mean (± SD) was 306 ± 29 mg kg^{-1}. There is no established toxicity threshold for barium in marine sediments; however, barium concentrations were similar to values from the 2019 LPP EBS and the 2014 Leviathan Field Development EBS (**Table 27**).

Mean barium concentrations were consistent among distance and directional strata (**Table 28**) and consistent with the 2014 Leviathan Field Development EBS mean. When normalized against aluminum, four barium samples (stations NP-NW-44, NF-SE-8, MF-SE-20, and FF-SE-32) were above the 99% prediction interval based on a regression plotted from the samples collected in the vicinity of the LPP during the 2014 Leviathan Field Development EBS and 2019 LPP EBS (**Figure 20**).

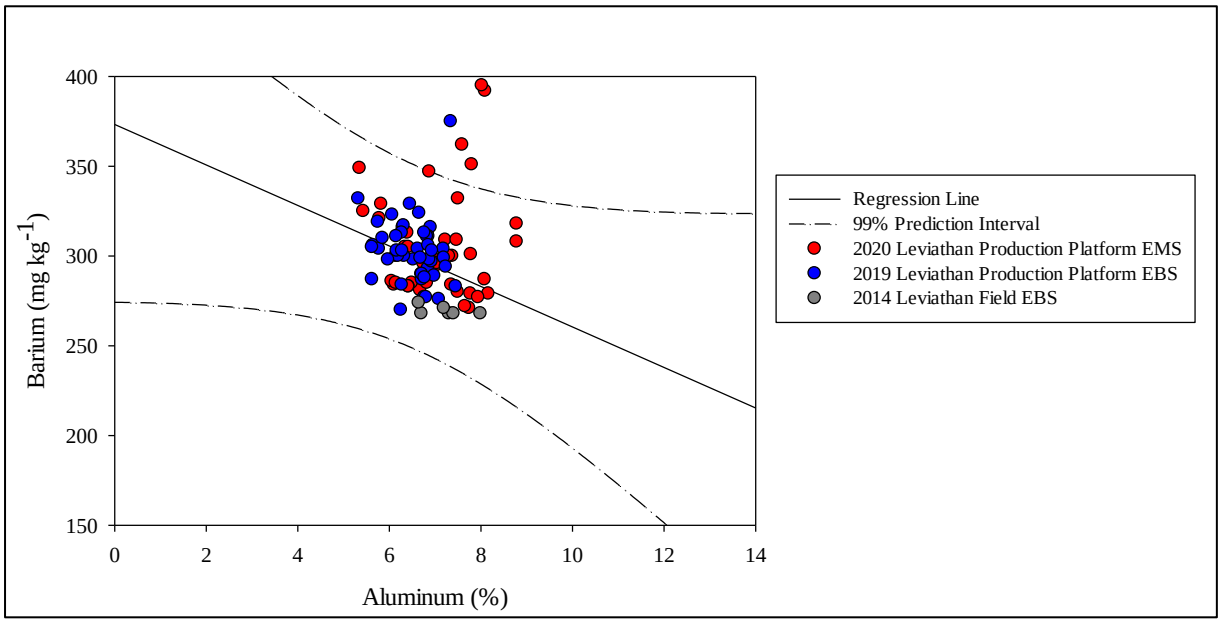


Figure 20. Plot of aluminum versus barium during the 2020 Leviathan Production Platform Environmental Monitoring Survey (EMS) as compared to 2019 Leviathan Production Platform Environmental Baseline Survey (EBS) and the 2014 Leviathan Field Development EBS. The 99% prediction interval based on a regression plotted from the samples collected in the vicinity of the LPP during the 2014 Leviathan Field Development EBS and 2019 LPP EBS.

Cadmium

Concentrations of cadmium were below the laboratory's MRL (between 0.14 and 0.16 mg kg^{-1} at all stations during the 2020 LPP EMS) (**Table 27**). During the 2019 LPP EBS, cadmium concentrations were below the laboratory's MRL (0.16 mg kg^{-1}) at all but two stations (0.18 mg kg^{-1} at station NF-NW-05 and 0.31 mg kg^{-1} at station MF-SW-22). Mean cadmium concentration from the 2014 Leviathan Field Development EBS was 0.19 ± 0.02, a result comparable with the two stations with reported cadmium values during the 2019 LPP EBS. No normalized plot of cadmium vs. aluminum was created with 2020 LPP EBS data because all cadmium concentrations were below the MRL.

Chromium

Chromium concentrations ranged from 84.7 to 103 mg kg^{-1} (**Table 27**) and the overall mean (± SD) was 94 ± 5.2 mg kg^{-1} (**Table 28**). Chromium concentrations were above the ERL (81 mg kg^{-1}) and below the ERM (370 mg kg^{-1}) at all stations. Chromium concentrations were consistent among distance and directional strata (**Table 28**) and consistent with the 2019 LPP EBS and the 2014 Leviathan Field Development EBS (**Table 27**). When normalized against aluminum, all concentrations of chromium were within the 99% prediction interval based on a regression plotted from the samples collected in the vicinity of the LPP during the 2014 Leviathan Field Development EBS and 2019 LPP EBS (**Figure 21**).

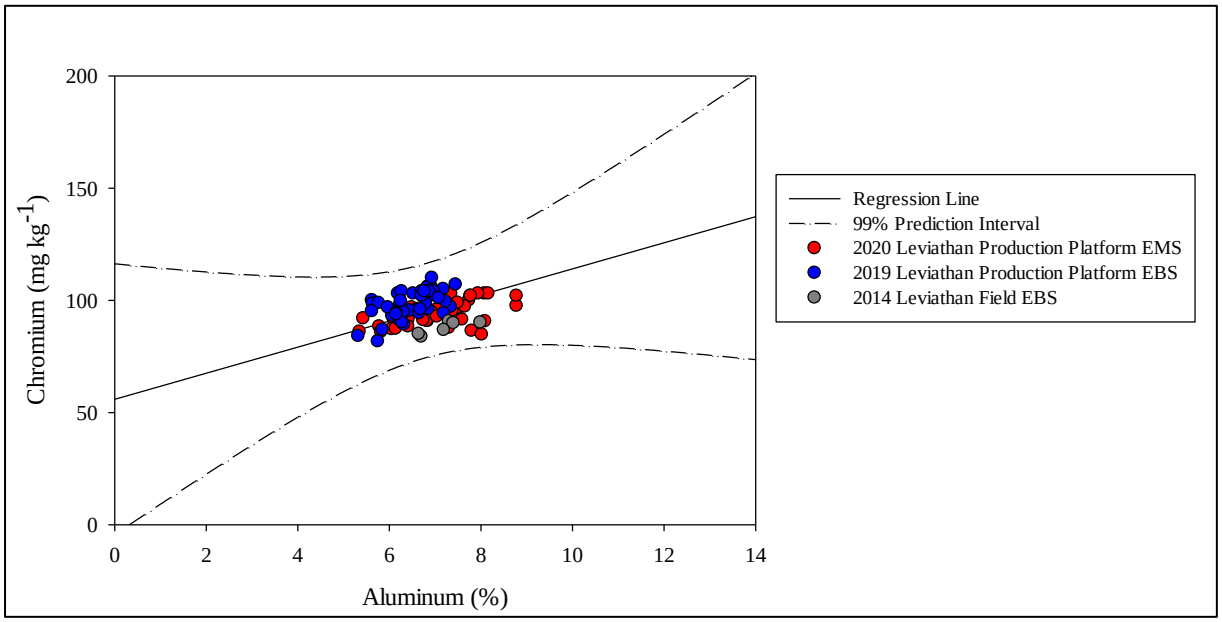


Figure 21. Plot of aluminum versus chromium during the 2020 Leviathan Production Platform Environmental Monitoring Survey (EMS) as compared to 2019 Leviathan Production Platform Environmental Baseline Survey (EBS) and the 2014 Leviathan Field Development EBS. The 99% prediction interval based on a regression plotted from the samples collected in the vicinity of the LPP during the 2014 Leviathan Field Development EBS and 2019 LPP EBS.

Copper

Copper concentrations ranged from 21.0 to 38.3 mg kg^{-1} (**Table 27**) and the overall mean (± SD) was 30.7 ± 3.9 mg kg^{-1} (**Table 28**). Copper concentrations were above the ERL (34.0 mg kg^{-1}) at 14 stations and below the ERM (270 mg kg^{-1}) at all stations. Mean concentrations of copper were similar among distance and directional strata (**Table 28**) and were consistent with the mean copper concentration from the 2019 LPP EBS and the 2014 Leviathan Field Development EBS. When normalized against aluminum, all concentrations of copper were within or slightly lower than the 99% prediction interval based on a regression plotted from the samples collected in the vicinity of the LPP during the 2014 Leviathan Field Development EBS and 2019 LPP EBS (**Figure 22**).

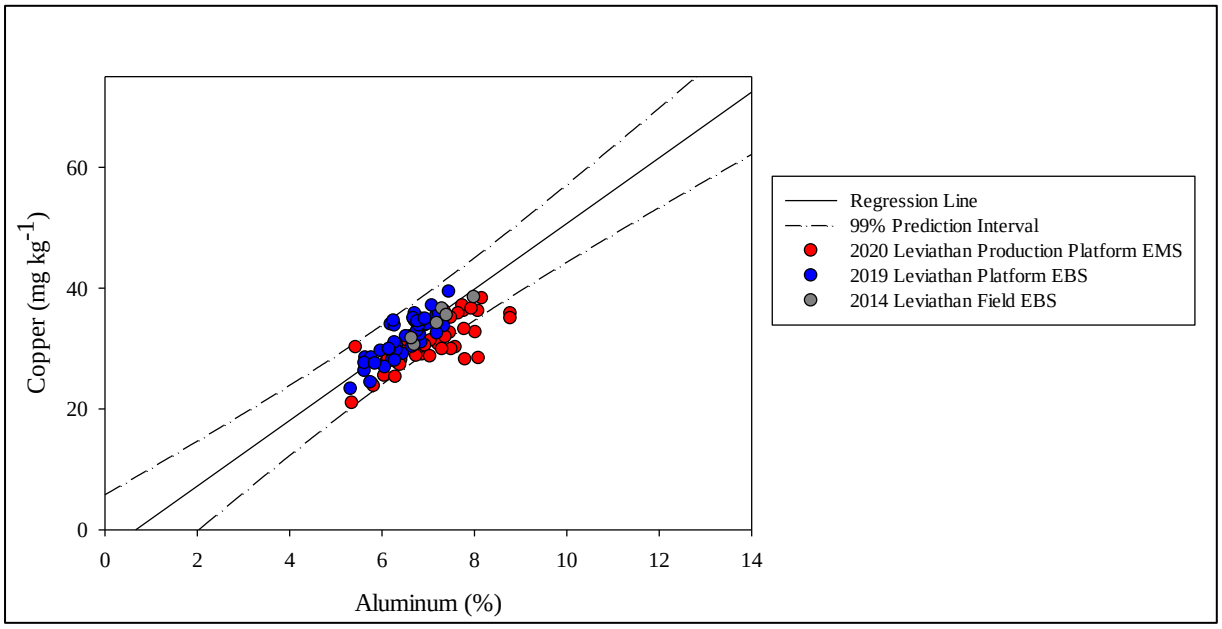


Figure 22. Plot of aluminum versus copper during 2020 Leviathan Production Platform Environmental Monitoring Survey (EMS) as compared to 2019 Leviathan Production Platform Environmental Baseline Survey (EBS) and the 2014 Leviathan Field Development EBS. The 99% prediction interval based on a regression plotted from the samples collected in the vicinity of the LPP during the 2014 Leviathan Field Development EBS and 2019 LPP EBS.

Iron

Concentrations of iron ranged from 4.16% to 6.56% and the overall mean (± SD) was 5.34% ± 0.58% (**Table 27**). Concentrations were similar to the mean 2019 LPP EBS and 2014 Leviathan Field Development EBS concentrations (**Table 27**). Iron concentrations were consistent among distance and directional strata (**Table 28**). There are no established toxicity thresholds for iron in marine sediments. When normalized against aluminum all concentrations of iron were within or similar to the upper limit of the 99% prediction interval based on a regression plotted from the samples collected in the vicinity of the LPP during the 2014 Leviathan Field Development EBS and the 2019 LPP EBS (**Figure 23**).

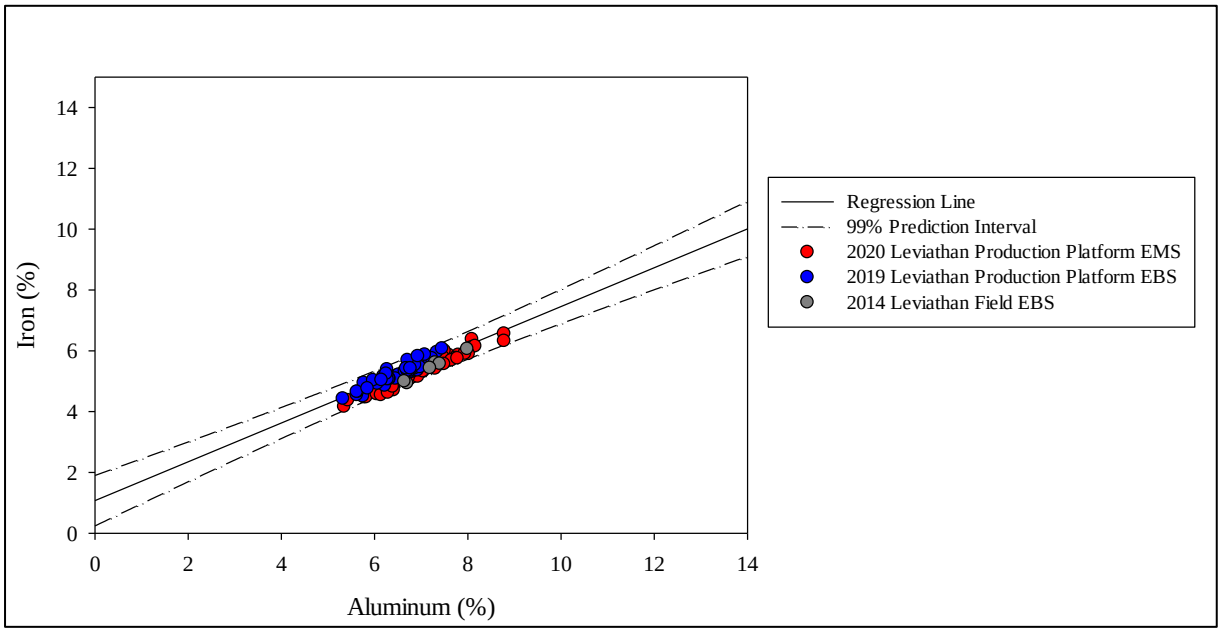


Figure 23. Plot of aluminum versus iron during the 2020 Leviathan Production Platform Environmental Monitoring Survey (EMS) as compared to 2019 Leviathan Production Platform Environmental Baseline Survey (EBS) and the 2014 Leviathan Field Development EBS. The 99% prediction interval based on a regression plotted from the samples collected in the vicinity of the LPP during the 2014 Leviathan Field Development EBS and 2019 LPP EBS.

Lead

Concentrations of lead ranged from 9.21 to 13.6 mg kg^{-1} and the overall mean (± SD) was 11.2 ± 0.91 mg kg^{-1} (**Table 27**). Concentrations at all stations were below the ERL (46.7 mg kg^{-1}). Lead concentrations were consistent among distance and directional strata (**Table 28**) and were similar to the mean lead concentration from the 2019 LPP EBS and the 2014 Leviathan Field Development EBS (**Table 27**). When normalized against aluminum, all concentrations of lead were within the 99% prediction interval based on a regression plotted from the samples collected in the vicinity of the LPP during the 2014 Leviathan Field Development EBS and 2019 LPP EBS (**Figure 24)**.

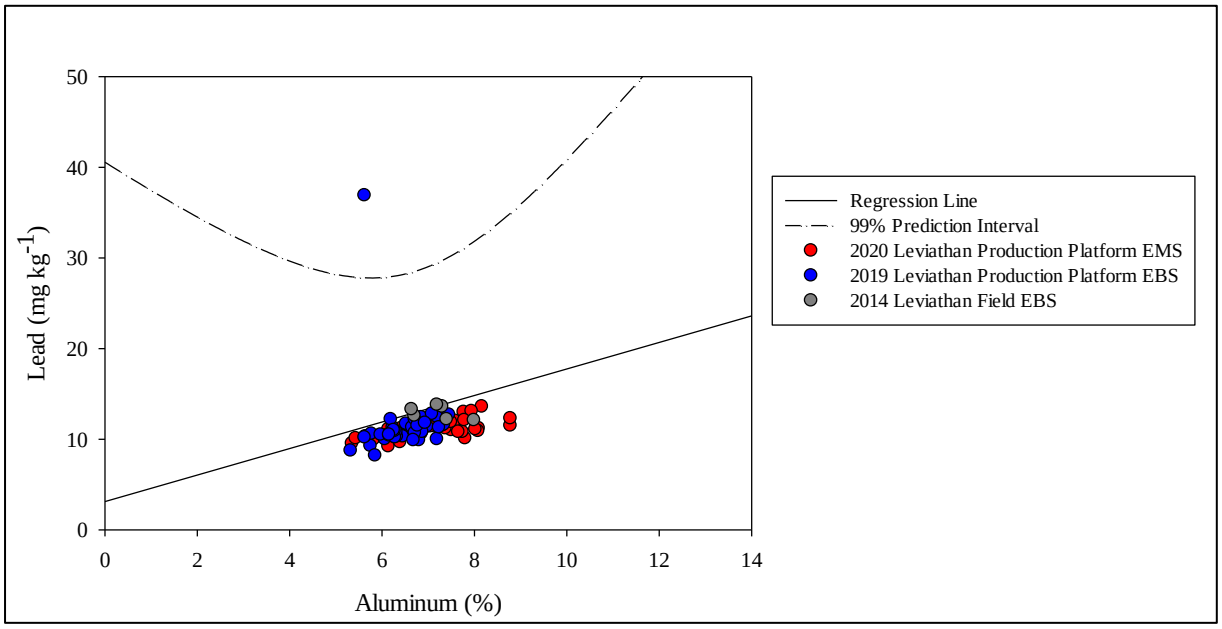


Figure 24. Plot of aluminum versus lead during the 2020 Leviathan Production Platform Environmental Monitoring Survey (EMS) as compared to 2019 Leviathan Production Platform Environmental Baseline Survey (EBS) and the 2014 Leviathan Field Development EBS. The 99% prediction interval based on a regression plotted from the samples collected in the vicinity of the LPP during the 2014 Leviathan Field Development EBS and 2019 LPP EBS.

Mercury

Mercury concentrations ranged from 8.34 to 20.6 ng g^{-1} and the overall mean (± SD) was 14.9 ± 2.3 ng g^{-1} (**Table 27**). Mean mercury concentrations were consistent among distance and directional strata (**Table 28**) and were similar to the mean mercury concentration from the 2019 LPP EBS and the 2014 Leviathan Field Development EBS (**Table 27**). When normalized against aluminum, all concentrations mercury were within or below the 99% prediction interval based on a regression plotted from the samples collected in the vicinity of the LPP during the 2014 Leviathan Field Development EBS and 2019 LPP EBS (**Figure 25**).

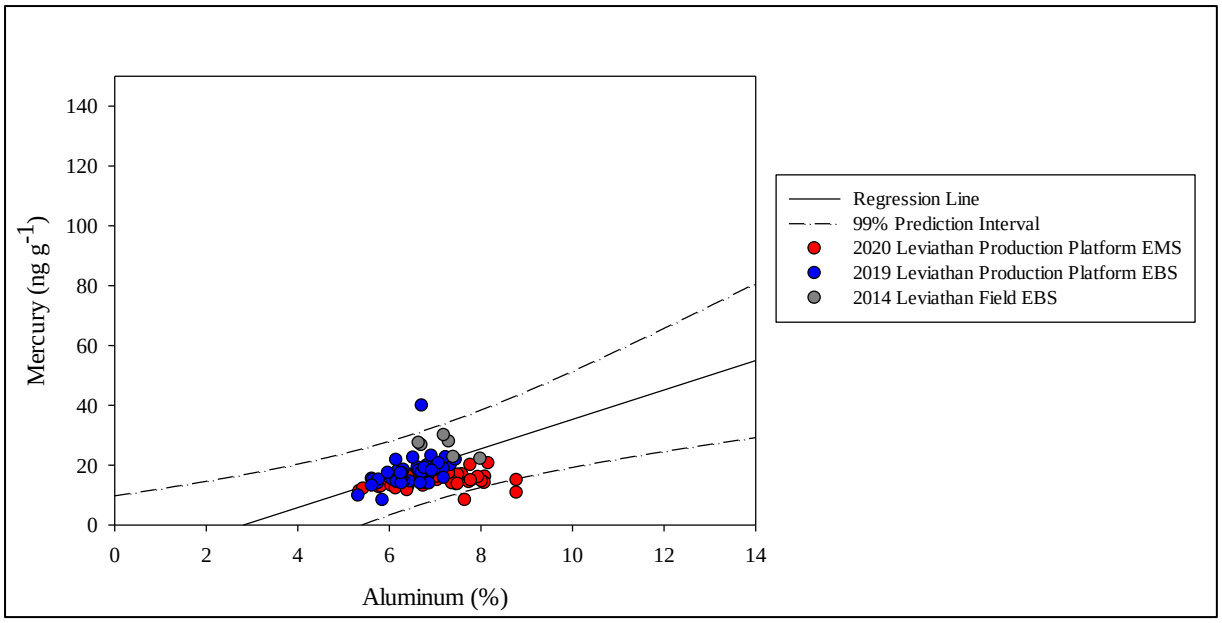


Figure 25. Plot of aluminum versus mercury during the 2020 Leviathan Production Platform Environmental Monitoring Survey (EMS) as compared to 2019 Leviathan Production Platform Environmental Baseline Survey (EBS) and the 2014 Leviathan Field Development EBS. The 99% prediction interval based on a regression plotted from the samples collected in the vicinity of the LPP during the 2014 Leviathan Field Development EBS and 2019 LPP EBS.

Nickel

Nickel concentrations ranged from 38.3 to 58.7 mg kg^{-1} and the overall mean (± SD) was 49.8 ± 5.0 mg kg^{-1} (**Table 27**). Nickel concentrations were above the ERL (20.9 mg kg^{-1}) at all stations and were above the ERM (51.6 mg kg^{-1}) at 13 stations. Mean nickel concentrations were consistent among distance and directional strata (**Table 28**) and were similar to the mean nickel concentration from the 2019 LPP EBS and the 2014 Leviathan Field Development EBS (**Table 27**). When normalized against aluminum, all concentrations of nickel were within or below the 99% prediction interval based on a regression plotted from the samples collected in the vicinity of the LPP during the 2014 Leviathan Field Development EBS and 2019 LPP EBS (**Figure 26**).

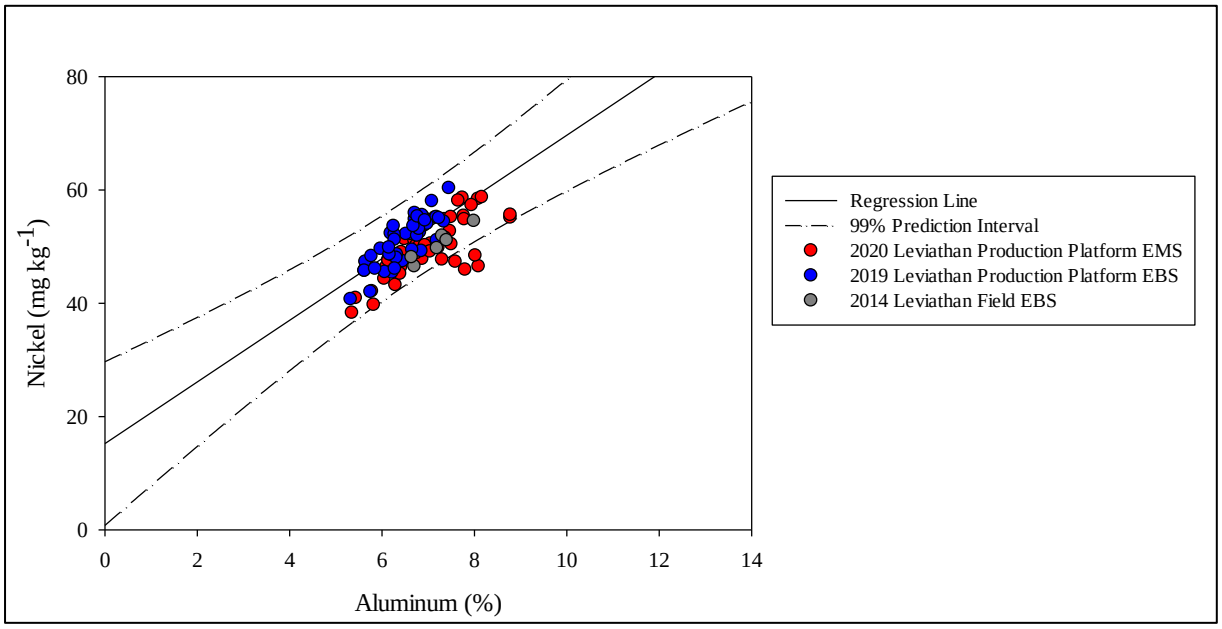


Figure 26. Plot of aluminum versus nickel during the 2020 Leviathan Production Platform Environmental Monitoring Survey (EMS) as compared to 2019 Leviathan Production Platform Environmental Baseline Survey (EBS) and the 2014 Leviathan Field Development EBS. The 99% prediction interval based on a regression plotted from the samples collected in the vicinity of the LPP during the 2014 Leviathan Field Development EBS and 2019 LPP EBS.

Zinc

Zinc concentrations ranged from 57.9 to 92.1 mg kg^{-1} and the overall mean (± SD) was 72.8 ± 6.4 mg kg^{-1} (**Table 27**). Zinc concentrations were below the ERL (150 mg kg^{-1}) at all stations. Mean Zn concentrations were consistent among distance and directional strata (**Table 28**) and were similar to the mean zinc concentration from the 2019 LPP EBS and the 2014 Leviathan Field Development EBS (**Table 27**). When normalized against aluminum, all concentrations of zinc were within or below the 99% prediction interval based on a regression plotted from the samples collected in the vicinity of the LPP during the 2014 Leviathan Field Development EBS and 2019 LPP EBS (**Figure 27**).

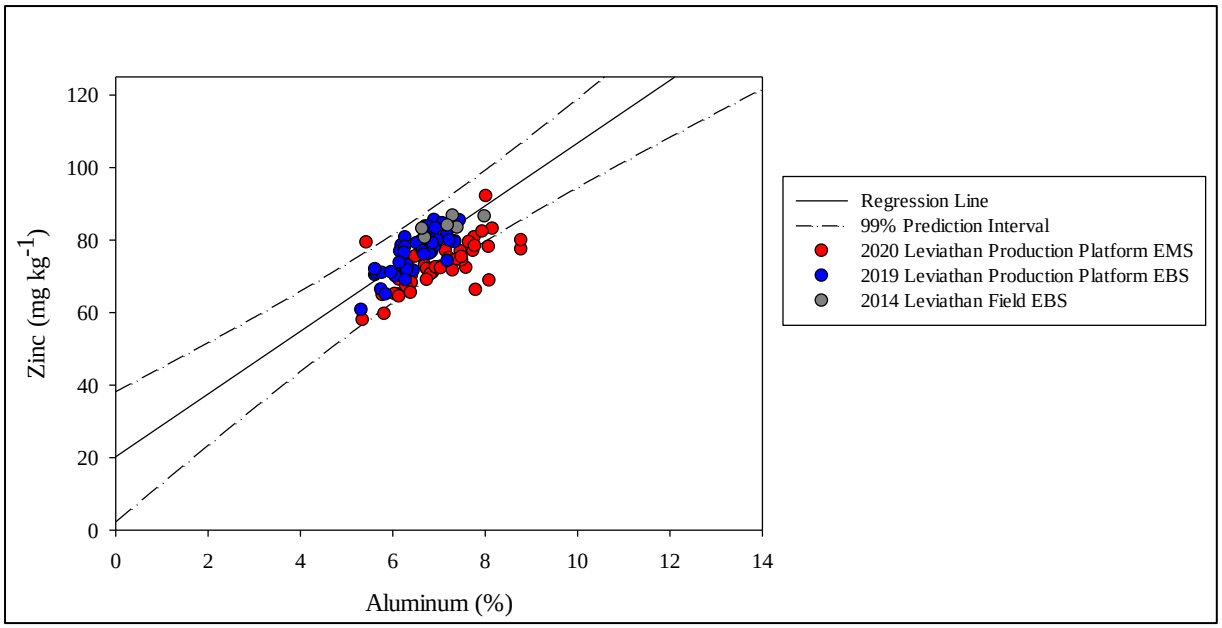


Figure 27. Plot of aluminum versus zinc during the 2020 Leviathan Production Platform Environmental Monitoring Survey (EMS) as compared to 2019 Leviathan Production Platform Environmental Baseline Survey (EBS) and the 2014 Leviathan Field Development EBS. The 99% prediction interval based on a regression plotted from the samples collected in the vicinity of the LPP during the 2014 Leviathan Field Development EBS and 2019 LPP EBS.

Metals Statistical Analyses

Interactive effects

There were no significant three-way interactive effects among distance, direction, and survey year for any of the sediment metals investigated (**Table 29**). There were also no significant two-way interactive effects between distance and direction or direction and survey year for any of the metals investigated (**Table 29**). However, there were significant two-way interactive effects between distance and survey year for sediment concentrations of arsenic, copper, nickel, and zinc (**Table 29**). Because of these significant interactions it was not possible to determine the overall main effects of distance or survey year for these particular metals. The relatively low concentration of these metals reported within the Near-Platform strata during the 2020 LPP EMS is the only factor driving these statistical interactions (**Table 30**; **Figures 28** to **31**). Concentrations of these metals collected within all other distance strata during both the 2019 LPP EBS and 2020 LPP EMS were otherwise statistically similar to one another **(Table 30**; **Figures 28** to **31**).

Table 29. Analysis of variance (ANOVA) results for differences in sediment metals concentrations by distance, direction, and survey year. Interactive and main effects for each factor is examined. P-values of tests indicating a statistically significant difference ($P < 0.05$) are shown in **bold**. F-values and degrees of freedom are provided for reference. "--" indicates that a statistical test for the applicable main effects could not be performed due to a significance within applicable interactive effects.

Metal	Interactive Effects				Main Effects		
	Distance × Direction × Survey Year	Distance × Direction	Distance × Survey Year	Direction × Survey Year	Distance	Direction	Survey Year
Arsenic	$F_{10,56} = 1.38$; P = 0.21	$F_{10,74} = 1.63$; P = 0.12	**$F_{4,82} = 5.75$; P = 0.0004**	$F_{3,56} = 0.72$; P = 0.55	--	**$F_{3,88} = 3.16$; P < 0.03**	--
Barium	$F_{10,56} = 0.77$; P = 0.65	$F_{10,56} = 0.62$; P = 0.79	$F_{4,56} = 0.86$; P = 0.49	$F_{3,56} = 1.18$; P = 0.33	**$F_{4,87} = 5.58$; P = 0.0005**	$F_{3,56} = 0.76$; P = 0.52	$F_{1,56} = 1.23$; P = 0.27
Chromium	$F_{10,56} = 0.41$; P = 0.94	$F_{10,56} = 1.69$; P = 0.11	$F_{4,56} = 1.43$; P = 0.24	$F_{3,56} = 0.54$; P = 0.65	$F_{4,56} = 1.37$; P = 0.26	**$F_{3,88} = 9.87$; P < 0.0001**	**$F_{1,90} = 14.48$; P = 0.0003**
Copper	$F_{10,56} = 0.31$; P = 0.98	$F_{10,56} = 1.45$; P = 0.18	**$F_{4,82} = 2.65$; P = 0.04**	$F_{3,56} = 0.79$; P = 0.50	--	**$F_{3,88} = 13.52$; P < 0.0001**	--
Iron	$F_{10,56} = 0.79$; P = 0.64	$F_{10,56} = 1.46$; P = 0.18	$F_{4,82} = 1.94$; P = 0.11	$F_{3,56} = 2.25$; P = 0.09	--	**$F_{3,88} = 11.68$; P < 0.0001**	--
Lead	$F_{10,56} = 0.75$; P = 0.68	$F_{10,56} = 0.75$; P = 0.68	$F_{4,56} = 0.65$; P = 0.63	$F_{3,56} = 0.63$; P = 0.60	$F_{4,56} = 0.85$; P = 0.50	$F_{3,56} = 0.63$; P = 0.60	$F_{1,56} = 0.13$; P = 0.72
Mercury	$F_{10,56} = 0.61$; P = 0.80	$F_{10,56} = 0.66$; P = 0.75	$F_{4,56} = 0.99$; P = 0.42	$F_{3,56} = 2.12$; P = 0.11	$F_{4,56} = 0.92$; P = 0.46	$F_{3,56} = 1.6$; P = 0.20	**$F_{1,90} = 12.24$; P = 0.0007**
Nickel	$F_{10,56} = 0.24$; P = 0.99	$F_{10,56} = 1.31$; P = 0.25	**$F_{4,82} = 3.29$; P = 0.02**	$F_{3,56} = 1.01$; P = 0.40	--	**$F_{3,88} = 15.09$; P < 0.0001**	--
Zinc	$F_{10,56} = 0.29$; P = 0.98	$F_{10,56} = 1.25$; P = 0.28	**$F_{4,82} = 2.93$; P = 0.03**	$F_{3,56} = 0.46$; P = 0.71	--	**$F_{3,88} = 8.19$; P < 0.0001**	--

Table 30. Post-hoc Tukey's Multiple Means Comparison Test results for differences in metals concentrations for the interactive effect of distance × survey year specific to the comparison with Near-Platform samples from the 2020 Leviathan Production Platform Environmental Monitoring Survey (2020 LPP EMS). P-values of tests indicating a statistically significant difference ($P < 0.05$) are shown in **bold**. t-values and degrees of freedom are provided for reference. Results for any non-significant interactive comparisons ($P \geq 0.05$) among other distance strata and survey year are not shown. Metals that had no significant interactions ($P \geq 0.05$) are also not shown.

Metal	Statistical Comparison to Near-Platform Samples from 2020 LPP EMS								
	Near-Platform	Near-Field		Mid-Field		Far-Field		Reference	
	2019	2019	2020	2019	2020	2019	2020	2019	2020
Arsenic	**$t_{82} = 5.12$; P < 0.0001**	**$t_{82} = 5.90$; P < 0.0001**	**$t_{82} = 4.52$; P = 0.0008**	**$t_{82} = 5.95$; P < 0.0001**	**$t_{82} = 4.87$; P = 0.0002**	**$t_{82} = 5.99$; P < 0.0001**	**$t_{82} = 5.48$; P < 0.0001**	**$t_{82} = 4.24$; P = 0.002**	**$t_{82} = 5.12$; P < 0.0001**
Copper	$t_{82} = 3.24$; P = 0.05	**$t_{82} = 3.47$; P = 0.03**	$t_{82} = 2.69$; P = 0.20	$t_{82} = 3.14$; P = 0.07	**$t_{82} = 3.58$; P = 0.02**	**$t_{82} = 3.64$; P = 0.02**	**$t_{82} = 3.58$; P = 0.02**	$t_{82} = 3.20$; P = 0.06	$t_{82} = 2.26$; P = 0.42
Nickel	**$t_{82} = 3.54$; P = 0.02**	**$t_{82} = 3.67$; P = 0.02**	$t_{82} = 2.83$; P = 0.14	**$t_{82} = 3.31$; P = 0.04**	**$t_{82} = 3.97$; P = 0.006**	**$t_{82} = 3.90$; P = 0.007**	**$t_{82} = 3.83$; P = 0.009**	**$t_{82} = 3.35$; P = 0.04**	$t_{82} = 2.62$; P = 0.23
Zinc	**$t_{82} = 4.05$; P = 0.004**	**$t_{82} = 3.77$; P = 0.01**	$t_{82} = 2.92$; P = 0.12	**$t_{82} = 3.45$; P = 0.03**	$t_{82} = 2.98$; P = 0.10	**$t_{82} = 3.78$; P = 0.01**	**$t_{82} = 3.35$; P = 0.04**	$t_{82} = 3.19$; P = 0.06	$t_{82} = 2.20$; P = 0.46

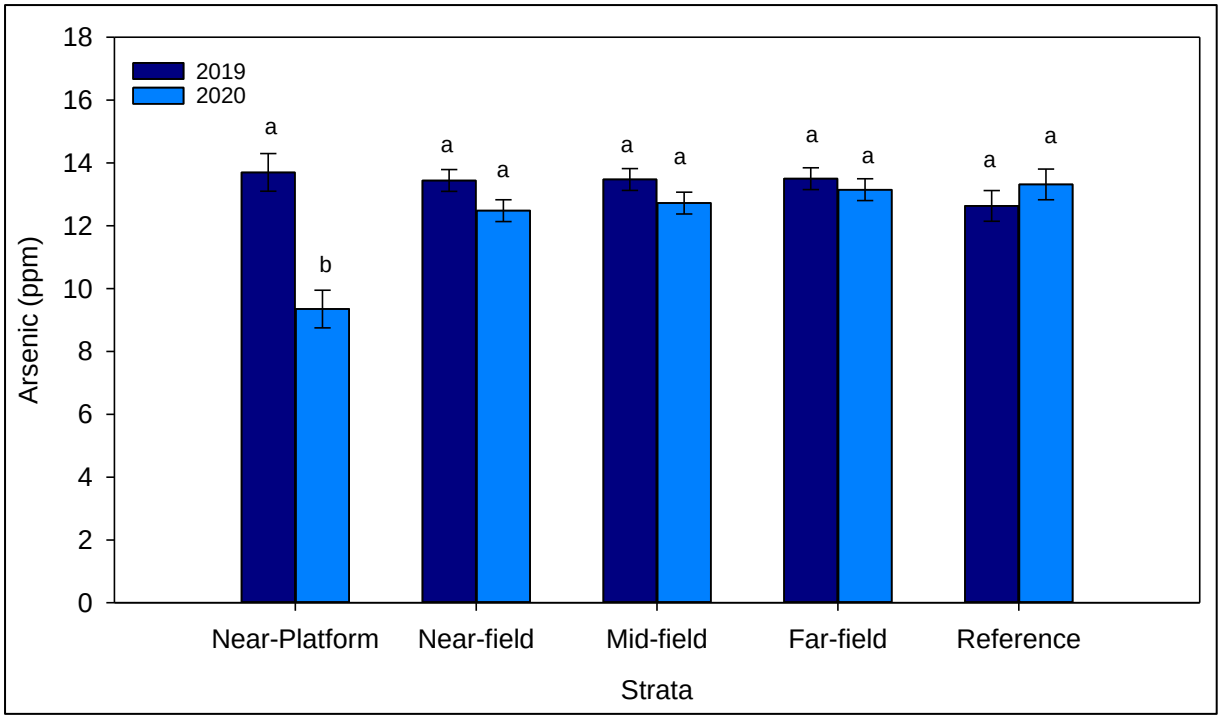


Figure 28. Statistical least square means (± standard error) of arsenic concentrations (parts per million [ppm]) analyzed within the significant distance strata × survey year interaction as computed by the analysis of variance (ANOVA) model. Different letters indicate statistical significance at P <0.05 using a post-hoc Tukey Multiple Means Comparison Test.

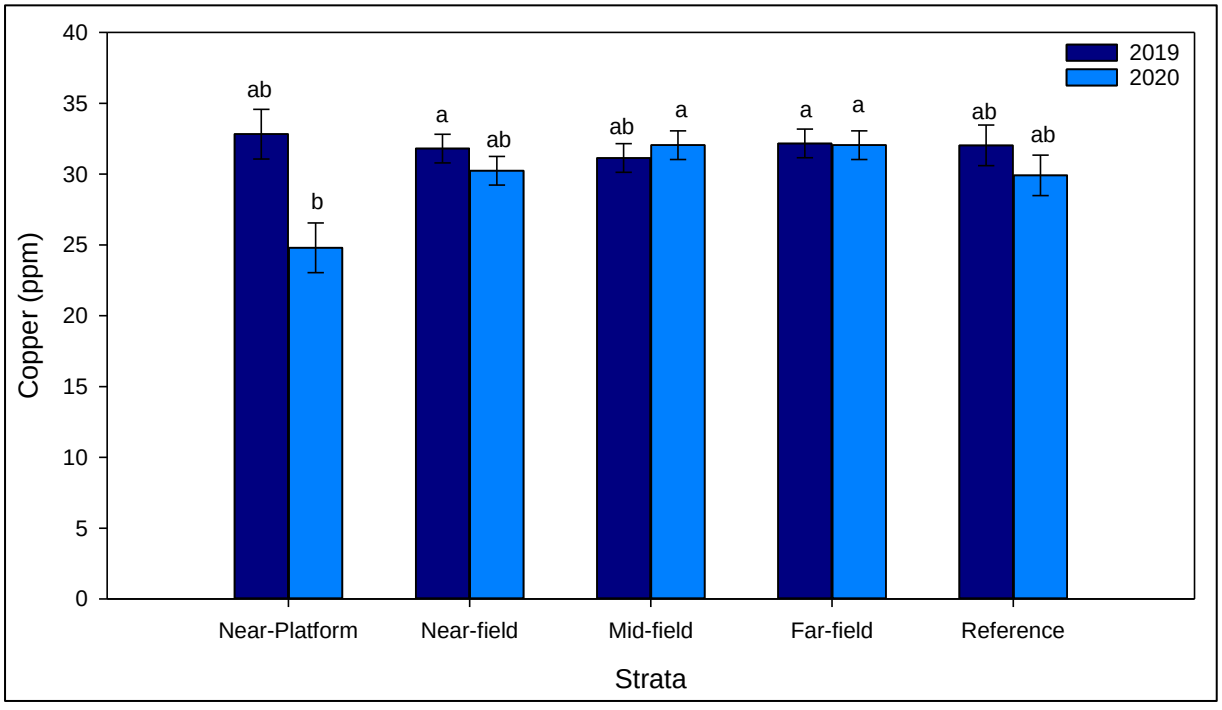


Figure 29. Statistical least square means (± standard error) of copper concentrations (parts per million [ppm]) analyzed within the significant distance strata × survey year interaction as computed by the analysis of variance (ANOVA) model. Different letters indicate statistical significance at P <0.05 using a post-hoc Tukey Multiple Means Comparison Test.

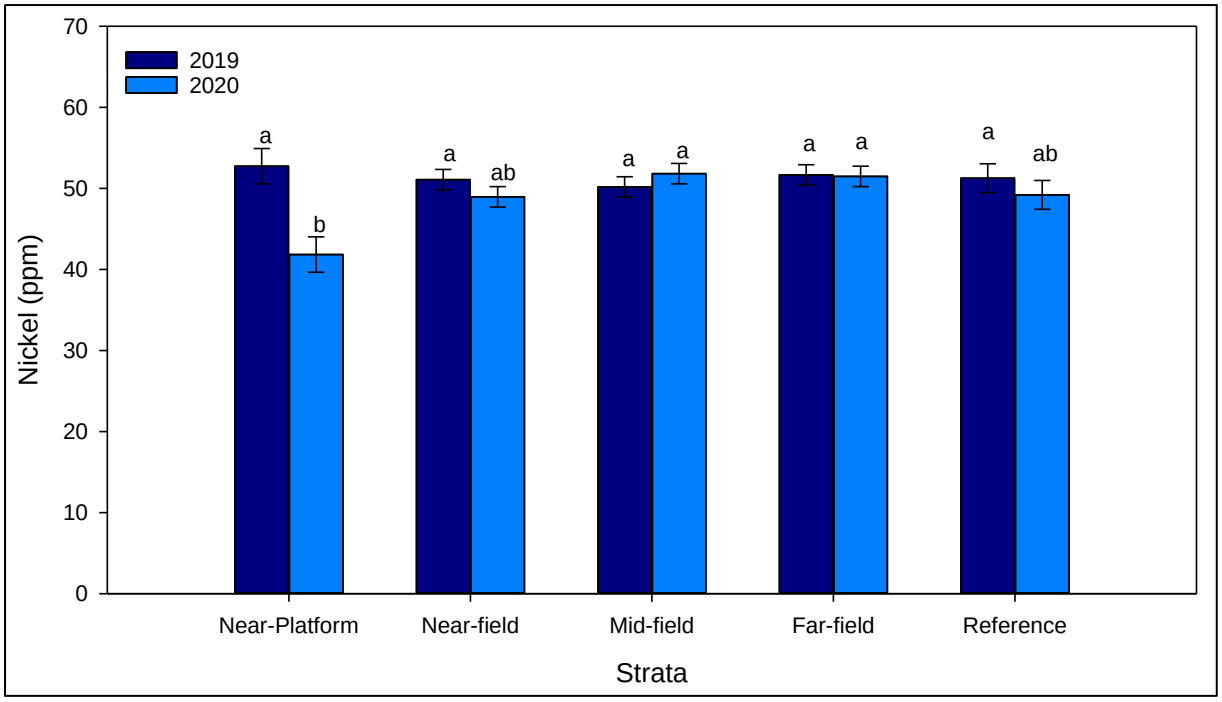


Figure 30. Statistical least square means (± standard error) of nickel concentrations (parts per million [ppm]) analyzed within the significant distance strata × survey year interaction as computed by the analysis of variance (ANOVA) model. Different letters indicate statistical significance at P <0.05 using a post-hoc Tukey Multiple Means Comparison Test.

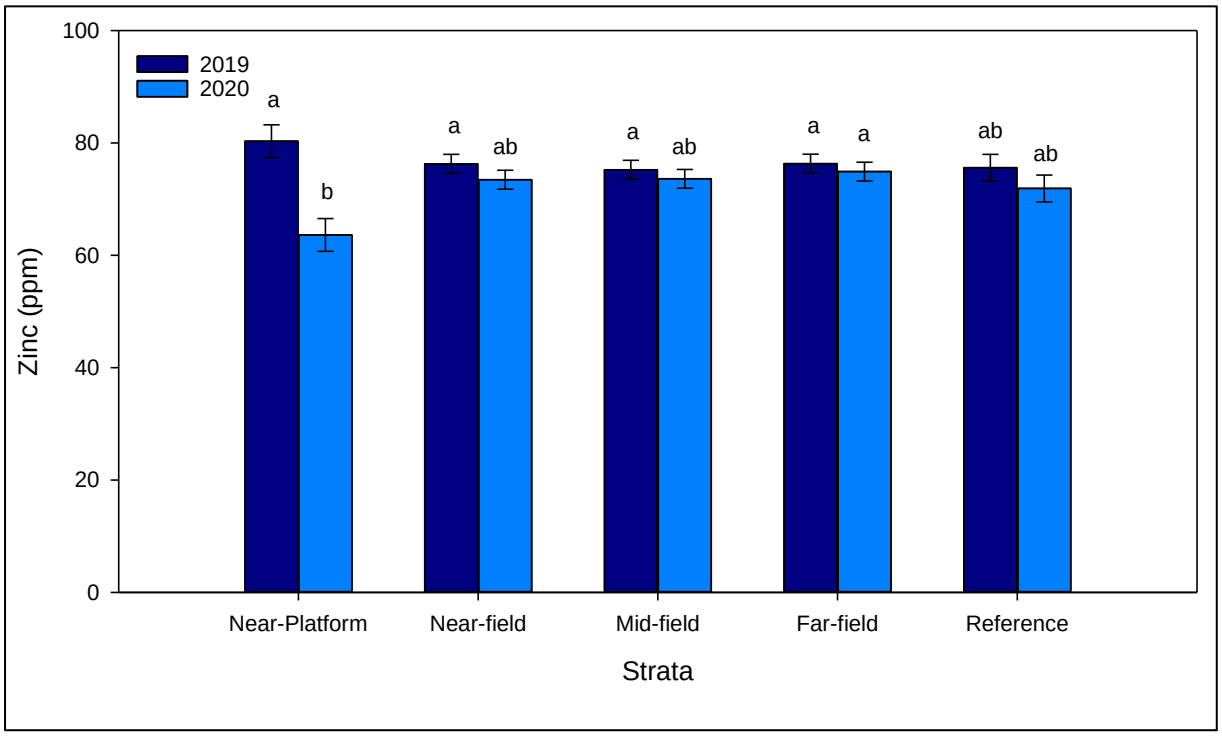


Figure 31. Statistical least square means (± standard error) of zinc concentrations (parts per million [ppm]) analyzed within the significant distance strata × survey year interaction as computed by the analysis of variance (ANOVA) model. Different letters indicate statistical significance at P <0.05 using a post-hoc Tukey Multiple Means Comparison Test.

Main effects

Distance

Sediment barium concentrations significantly differed among distance strata. Barium concentrations collected from within the Near-Platform strata were statistically significantly higher when compared against the Mid-Field (t_{87} = 4.24; P = 0.0005), Far-Field (t_{87} = 4.07; P = 0.001), and Reference (t_{87} = 2.97; P = 0.03) strata (**Table 29**; **Figure 32**). Sediment concentrations of other metals did not significantly differ among distance strata (P ≥0.05), where statistical analysis was applicable (**Table 29**). It should be noted that while statistically different, it is unlikely that the higher barium concentrations in the Near-Platform strata are environmentally significant.

Direction

Sediment concentrations of chromium, copper, iron, nickel, and zinc differed among directional quadrants (**Table 29 Figures 33** to **37**). Concentrations of these metals in sediments were significantly higher within the northwest and southwest platform quadrants relative to the northeast and southeast quadrants (**Table 31**; **Figures 33** to **37**). Arsenic concentrations were significantly higher within the southwest quadrant relative to the southeast quadrant (t_{87} = 2.75; P = 0.04); but were otherwise statistically similar to one another (**Figure 38**). Sediment concentrations of barium, iron, and lead did not significantly differ among platform strata (**Table 29**).

Survey Years

Sediment concentrations of chromium and mercury collected around the platform had significantly higher concentrations during the 2019 LPP EBS relative to the 2020 LPP EMS (**Table 29**; **Figures 39** and **40**). Sediment concentrations of other metals did not significantly differ between survey years, where statistical analysis was applicable (**Table 29**).

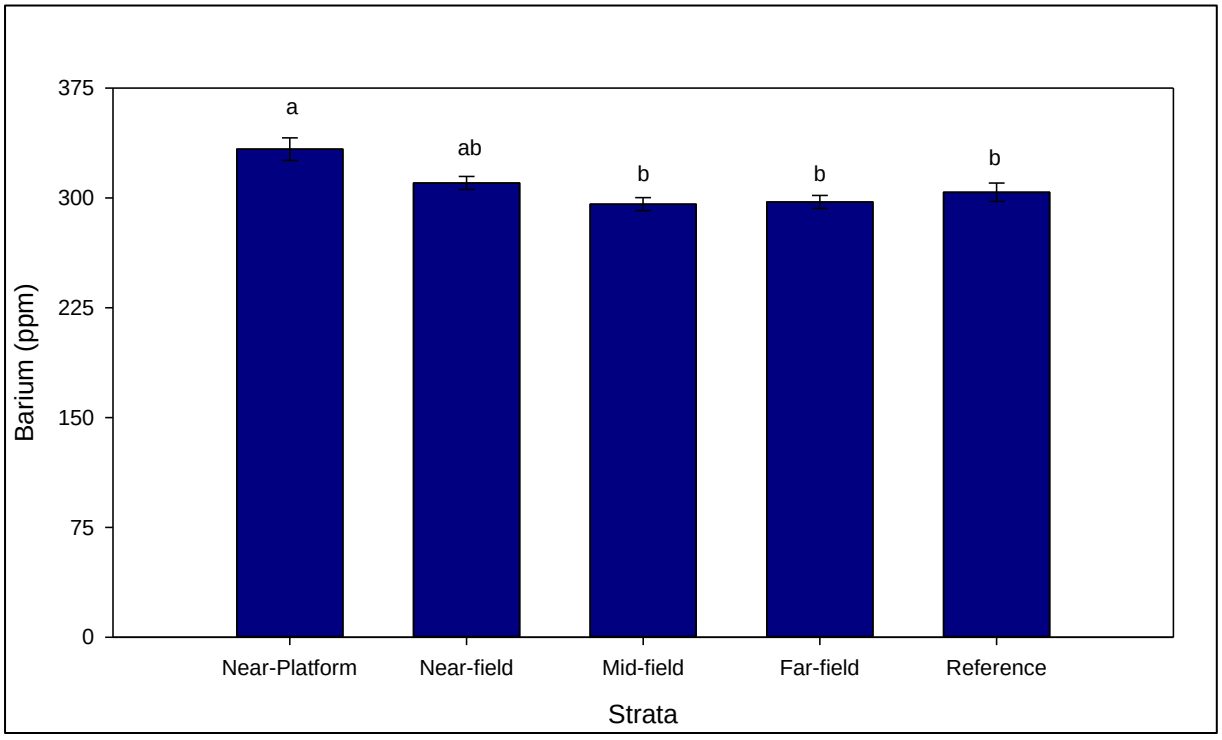


Figure 32. Statistical least square means (± standard error) of barium concentrations (parts per million [ppm]) analyzed for significant differences among distance strata as computed by the analysis of variance (ANOVA) model. Different letters indicate statistical significance at P <0.05 using a post-hoc Tukey Multiple Means Comparison Test.

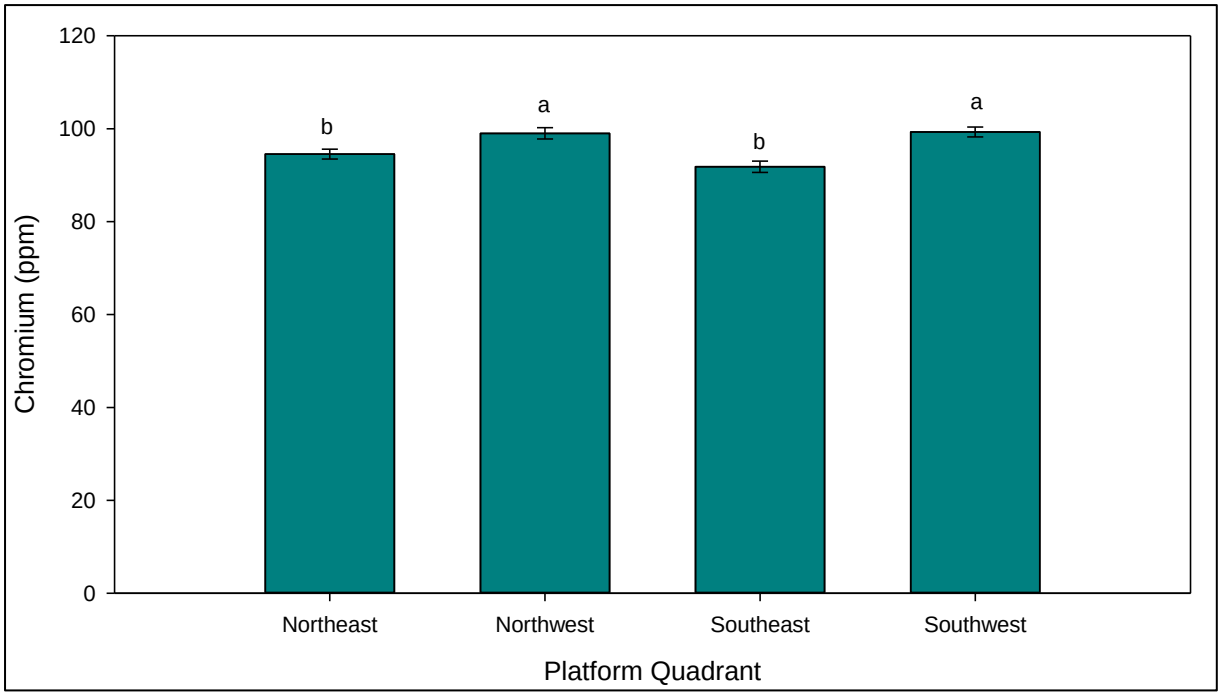


Figure 33. Statistical least square means (± standard error) of chromium concentrations (parts per million [ppm]) analyzed for significant differences among directional strata (platform quadrants) as computed by the analysis of variance (ANOVA) model. Different letters indicate statistical significance at P <0.05 using a post-hoc Tukey Multiple Means Comparison Test.

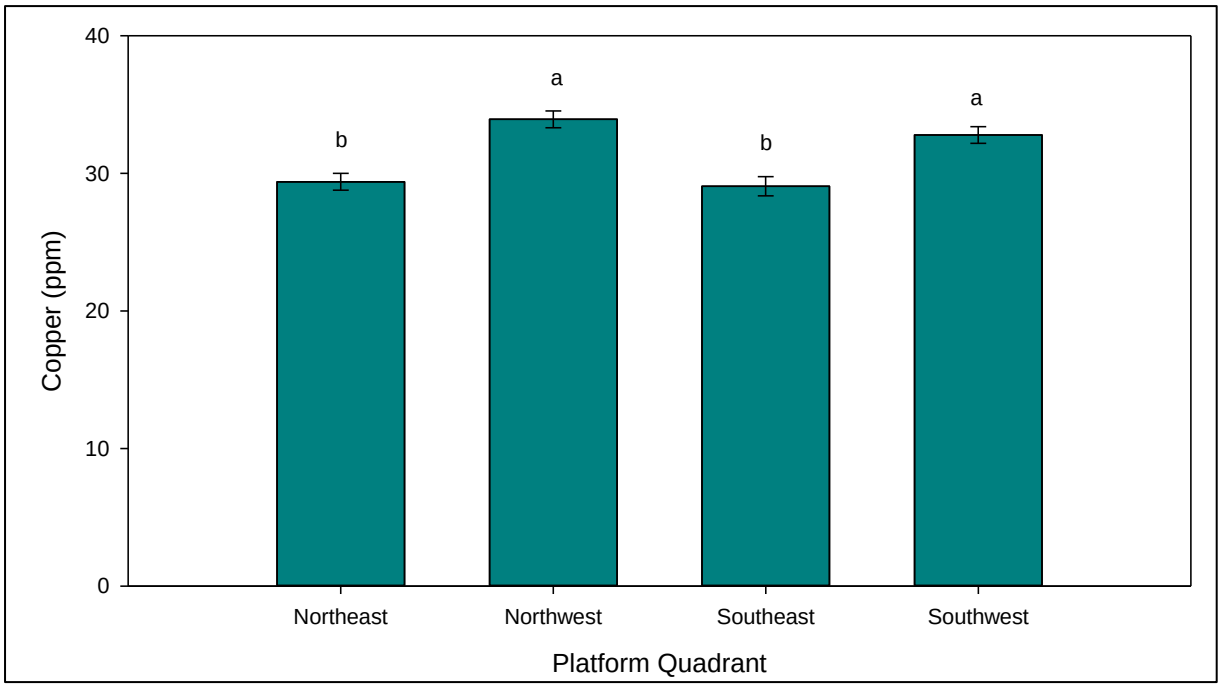


Figure 34. Statistical least square means (± standard error) of copper concentrations (parts per million [ppm]) analyzed for significant differences among directional strata (platform quadrants) as computed by the analysis of variance (ANOVA) model. Different letters indicate statistical significance at P <0.05 using a post-hoc Tukey Multiple Means Comparison Test.

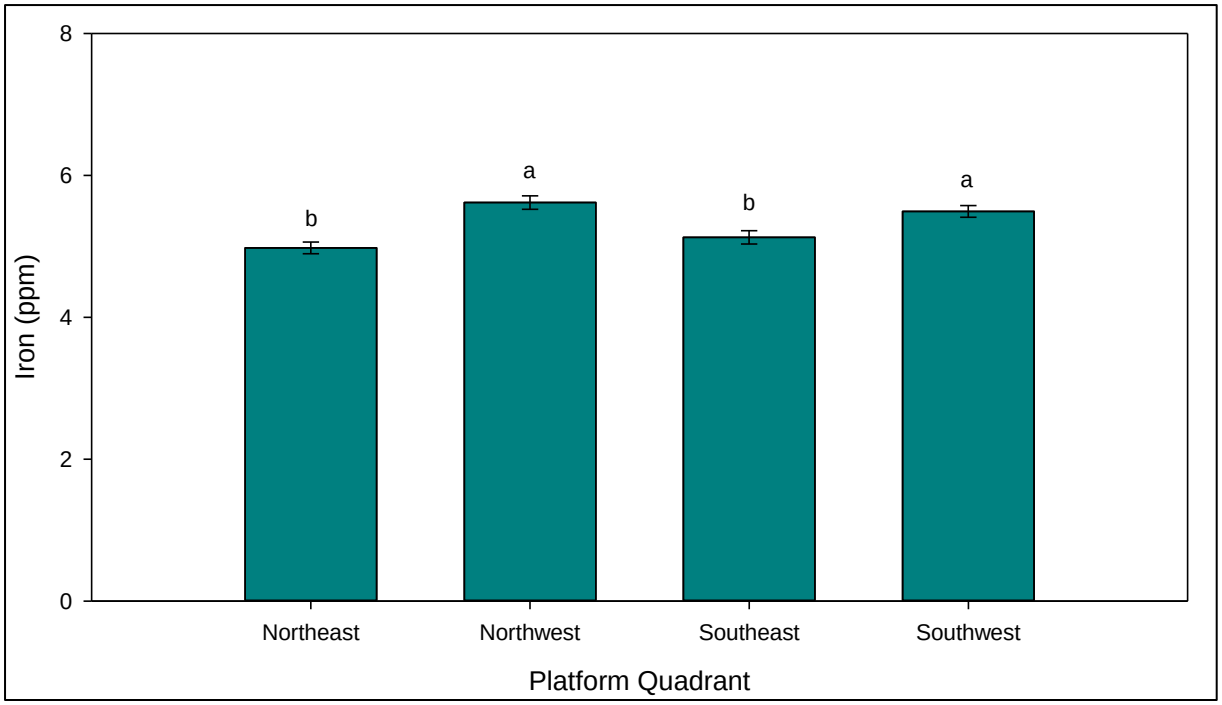


Figure 35. Statistical least square means (± standard error) of iron concentrations (parts per million [ppm]) analyzed for significant differences among directional strata (platform quadrants) as computed by the analysis of variance (ANOVA) model. Different letters indicate statistical significance at P <0.05 using a post-hoc Tukey Multiple Means Comparison Test.

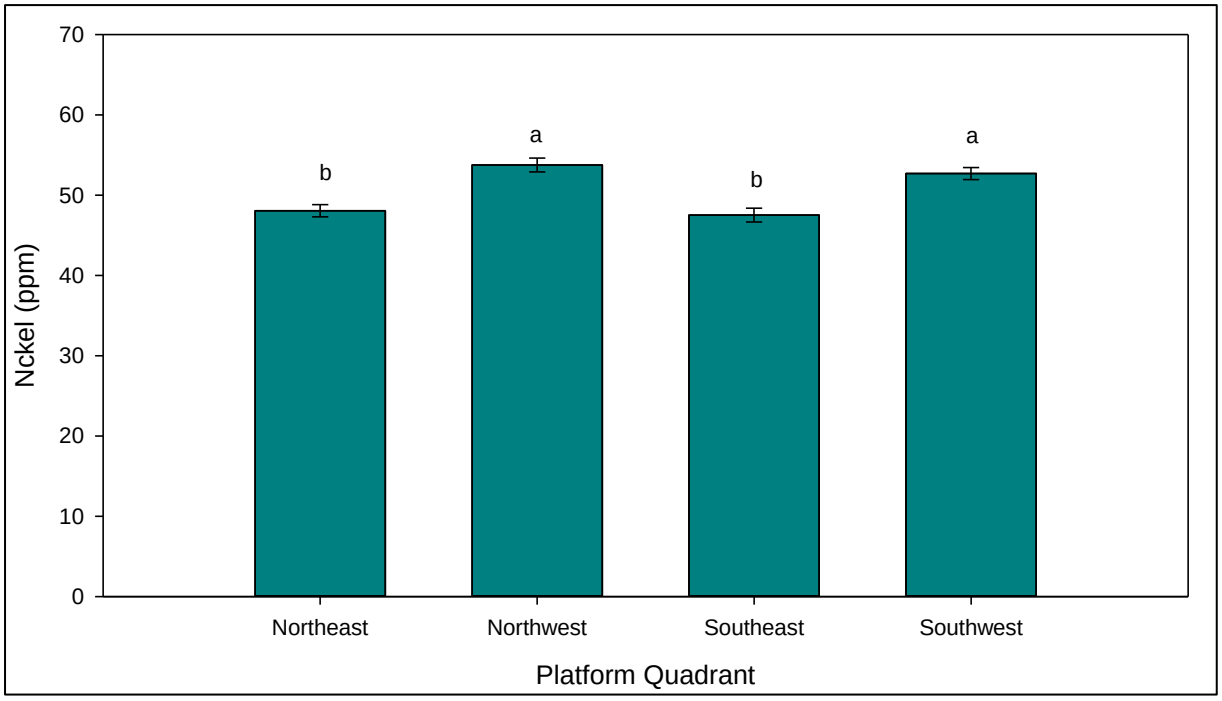


Figure 36. Statistical least square means (± standard error) of nickel concentrations (parts per million [ppm]) analyzed for significant differences among directional strata (platform quadrants) as computed by the analysis of variance (ANOVA) model. Different letters indicate statistical significance at P <0.05 using a post-hoc Tukey Multiple Means Comparison Test.

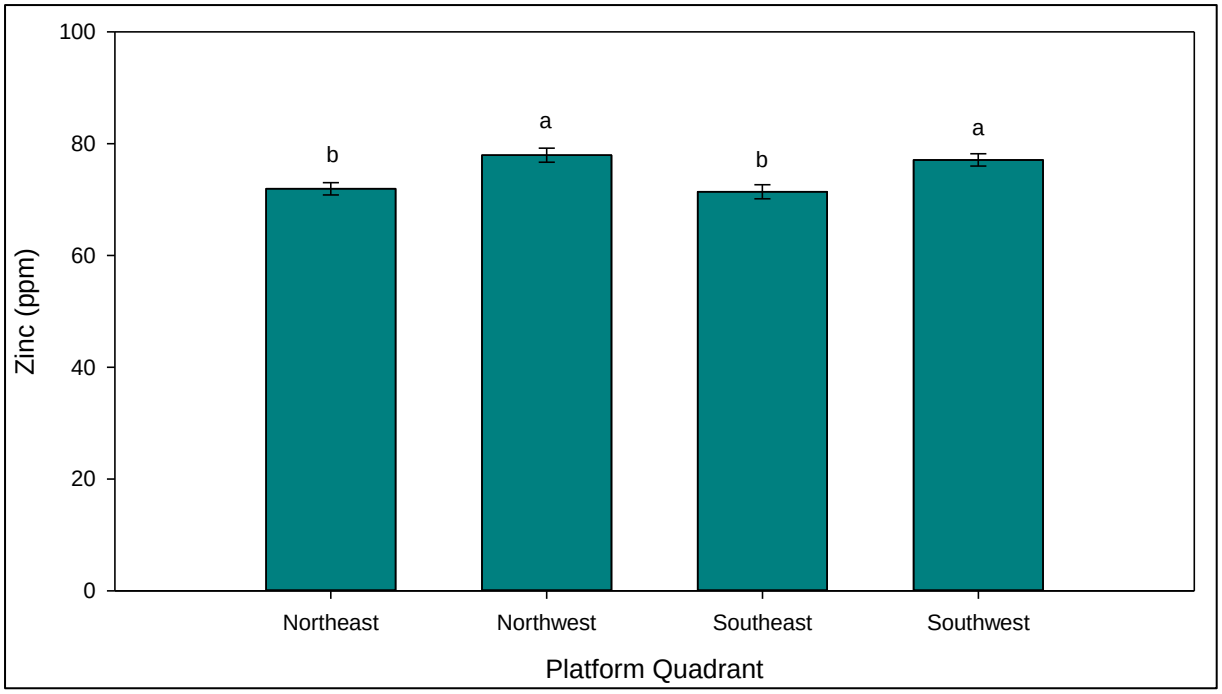


Figure 37. Statistical least square means (± standard error) of zinc concentrations (parts per million [ppm]) analyzed for significant differences among directional strata (platform quadrants) as computed by the analysis of variance (ANOVA) model. Different letters indicate statistical significance at P <0.05 using a post-hoc Tukey Multiple Means Comparison Test.

Table 31. Post-hoc Tukey's Multiple Means Comparison Test results for differences in metals concentrations among directional strata (platform quadrants). Only metals that had a significant difference among platform quadrants are shown. t-values and degrees of freedom are provided for reference.

Metal	Platform Quadrant Comparison			
	Northwest		Southwest	
	Northeast	Southeast	Northeast	Southeast
Chromium	t_{88} = 2.78; P = 0.03	t_{88} = 4.21; P = 0.0004	t_{88} = 3.18; P = 0.01	t_{88} = 4.66; P < 0.0001
Copper	t_{88} = 4.92; P < 0.0001	t_{88} = 4.96; P < 0.0001	t_{88} = 3.95; P = 0.001	t_{88} = 4.04; P = 0.0007
Iron	t_{88} = 5.08; P < 0.0001	t_{88} = 3.67; P = 0.002	t_{88} = 4.38; P = 0.0002	t_{88} = 2.91; P = 0.02
Nickel	t_{88} = 4.98; P < 0.0001	t_{88} = 5.13; P < 0.0001	t_{88} = 4.34; P = 0.0002	t_{88} = 4.52; P = 0.0001
Zinc	t_{88} = 3.60; P = 0.003	t_{88} = 3.68; P = 0.002	t_{88} = 3.32; P = 0.007	t_{88} = 3.40; P = 0.005

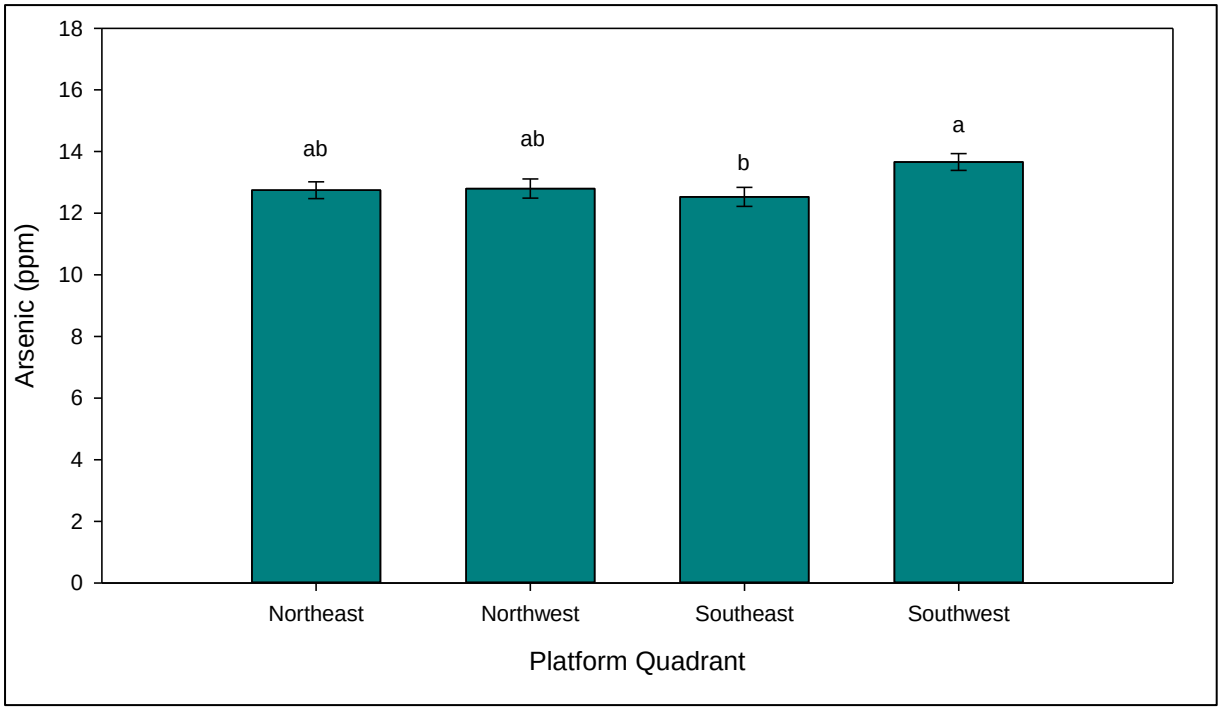


Figure 38. Statistical least square means (± standard error) of arsenic concentrations (parts per million [ppm]) analyzed for significant differences among directional strata (platform quadrants) as computed by the analysis of variance (ANOVA) model. Different letters indicate statistical significance at P <0.05 using a post-hoc Tukey Multiple Means Comparison Test.

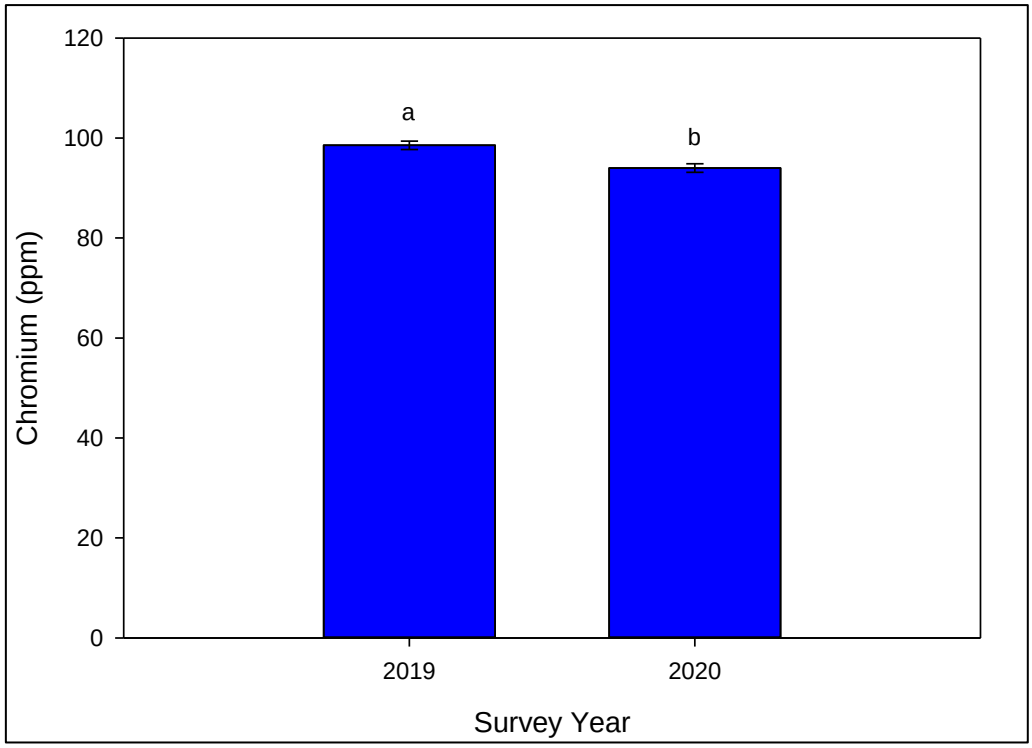


Figure 39. Statistical least square means (± standard error) of chromium concentrations (parts per million [ppm]) analyzed for significant differences among survey years as computed by the analysis of variance (ANOVA) model. Different letters indicate statistical significance at P <0.05 using a post-hoc Tukey Multiple Means Comparison Test.

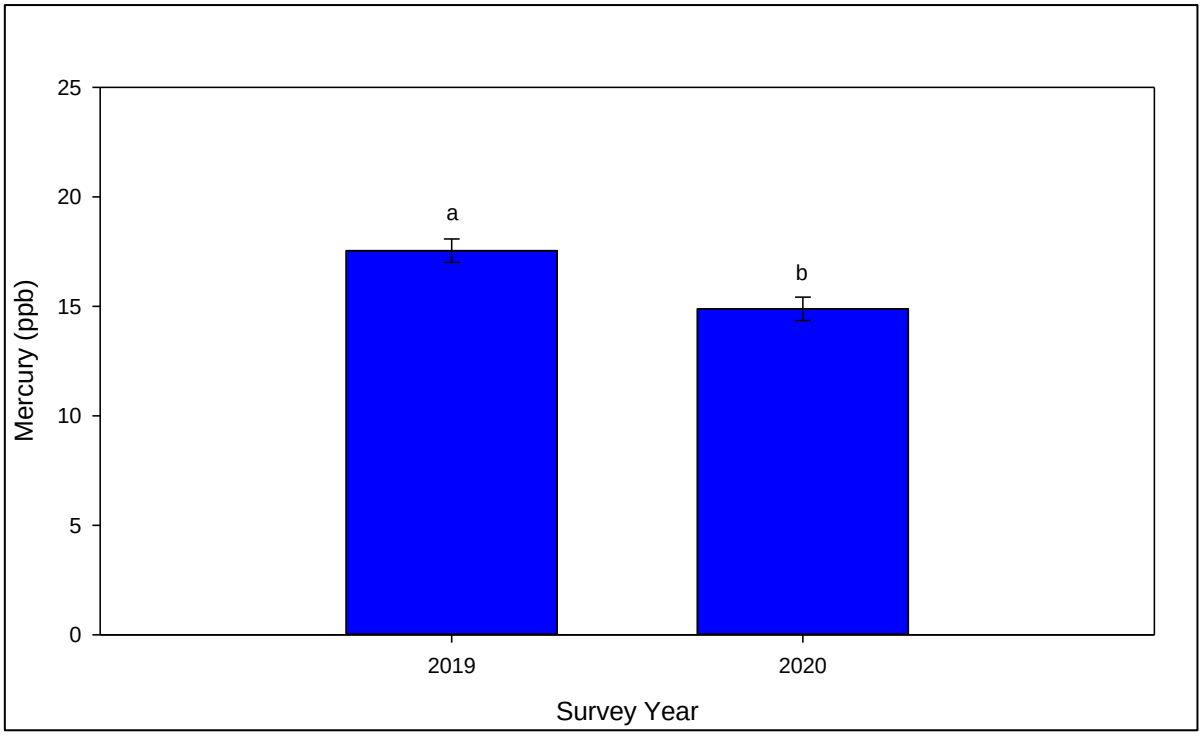


Figure 40. Statistical least square means (± standard error) of mercury concentrations (parts per billion [ppb]) analyzed for significant differences among survey years as computed by the analysis of variance (ANOVA) model. Different letters indicate statistical significance at P <0.05 using a post-hoc Tukey Multiple Means Comparison Test.

Statistical Summary

Concentrations of all metals, including those that have statistically significant differences around the LPP, are not elevated above natural field conditions as measured during the 2014 Leviathan Field Development EBS (**Table 27**). Additionally, at the concentrations reported (**Tables 27** and **28**), statistical differences in metals concentrations do not indicate environmental changes between distance strata, survey years, or platform quadrants that are likely to be biologically relevant.

The statistical findings do indicate, however, that concentrations of some metals within the Near-Platform strata (i.e., arsenic, copper, nickel, and zinc) and from the overall survey area (i.e., mercury, chromium) were lower in samples collected during the 2020 LPP EMS than in samples collected during the 2019 LPP EBS. In no instance was there an indication of any significant increase in any metal concentrations within the 2020 LPP EMS samples. The statistical findings also indicate that several sediment metals concentrations (i.e., chromium, copper, iron, nickel, and zinc) were higher on the western regions of the survey area compared to the eastern regions of the survey area regardless of survey year or distance strata. Additionally, barium concentrations were highest in samples collected from within the Near-Platform strata regardless of survey year or direction.

It is difficult to attribute these statistical differences, with the possible exception of barium, to LPP operations; especially since most of the data indicates a decrease in metals concentrations between the survey years, and even then, mostly only within the Near-Platform stratum. It is worth noting the differences in some metal concentrations between the eastern and western regions of the survey area, although given the relatively small-scale (but still statistically significant) differences in concentrations, it is too early within the monitoring program to determine if differences in these particular metal concentrations will either become more pronounced, remain the same, or continue to persist at all.

5.4.4 Hydrocarbons

Analytical laboratory datasheets for TPH, PAHs, VOCs, and phenols in sediment are provided in **Appendix L**. TPH concentrations ranged from 14 to 26 µg g^{-1} (**Tables 32** and **33**) with an overall average of 19.6 ± 3.3 µg g^{-1}. Balthis et al. (2016) compared sediment contamination and benthic infaunal data. It was concluded that TPH concentrations of less than 606 µg g^{-1} resulted in a low likelihood (<20%) of impacts to benthic macrofauna and meiofauna communities. All TPH concentrations from the 2020 LPP EMS were well below this threshold and no impacts on benthic communities are expected.

Total PAH concentrations ranged from 44.3 to 188 ng g^{-1} with an overall mean of 80.9 ± 28.0 ng g^{-1} which was nearly identical to the 2019 LPP EBS overall mean (79.5 ± 60.9 ng g^{-1}) and the 2014 Leviathan Field Development EBS overall mean (77.2 ± 4.6 ng g^{-1}) (**Tables 32** and **33**). Individual PAHs from the USEPA's 16 priority PAH list are presented in **Table 34** for each sample. All concentrations were less than the ERLs, where applicable.

Concentration of phenols were below the laboratory's MRL for all samples except one (0.44 µg kg^{-1} at Station MF-SE-19) (**Table 32**). During the 2020 LPP EMS, all VOC concentrations were below the laboratory's MRL, although several were above the MDL. All VOCs were below the laboratory's MRL for all samples during the 2019 LPP EBS. VOCs and phenols were not analyzed from samples collected in the 2014 Leviathan Field Development EBS.

Table 32. Hydrocarbon concentrations in sediment samples collected during the 2020 Leviathan Production Platform Environmental Monitoring Survey.

Station	Distance Strata	Directional Strata	TPH (µg g^{-1})	Total PAHs (ng g^{-1})	Phenols (mg kg^{-1})
NP-NE-43	Near-Platform	Northeast	17	63.7	ND
NP-NW-44		Northwest	18	86.9	ND
NP-SW-45		Southwest	15	58.8	ND
NP-SE-46		Southeast	16	64.4	ND
NF-NE-1	Near-Field	Northeast	17	84.3	ND
NF-NE-2			21	68.4	ND
NF-NE-3			19	74.9	ND
NF-NW-4		Northwest	20	77.9	ND
NF-NW-5			19	84.0	ND
NF-NW-6			19	92.6	ND
NF-SE-7		Southeast	19	102	ND
NF-SE-8			19	77.6	ND
NF-SE-9			19	170	ND
NF-SW-10		Southwest	18	75.5	ND
NF-SW-11			22	81.1	ND
NF-SW-12			20	67.3	ND
MF-NE-13	Mid-Field	Northeast	20	188	ND
MF-NE-14			24	92.4	ND
MF-NE-15			26	144	ND
MF-NW-16		Northwest	18	101	ND
MF-NW-17			25	92.8	ND
MF-NW-18			26	98.2	ND
MF-SE-19		Southeast	24	81.0	0.44
MF-SE-20			22	96.2	ND
MF-SE-21			23	87.1	ND
MF-SW-22		Southwest	27	109	ND
MF-SW-23			24	76.8	ND
MF-SW-24			16	74.4	ND
FF-NE-25	Far-Field	Northeast	17	52.2	ND
FF-NE-26			13	56.8	ND
FF-NE-27			16	65.6	ND
FF-NW-28		Northwest	21	86.6	ND
FF-NW-29			14	58.5	ND
FF-NW-30			21	81.4	ND
FF-SE-31		Southeast	14	57.2	ND
FF-SE-32			20	53.4	ND
FF-SE-33			16	56.0	ND
FF-SW-34		Southwest	24	76.8	ND
FF-SW-35			20	68.8	ND
FF-SW-36			21	76.4	ND
REF-NE-37	Reference	Northeast	20	63.0	ND
REF-NE-38			19	65.4	ND
REF-NE-39			17	54.1	ND
REF-SW-40		Southwest	21	55.2	ND
REF-SW-41			17	44.3	ND
REF-SW-42			18	79.2	ND
2020 LPP EMS Overall Mean (± SD)			19.6 ± 3.3	80.9 ± 28.0	--
2019 LPP EBS Mean (± SD)			32.7 ± 5.8	79.5 ± 60.9	--
2014 Leviathan Field Development EBS Mean (± SD)			14.1 ± 4.4	77.2 ± 4.6	N/A
Method Detection Limit			1.4	--	0.12-0.19
ERL			--	4,022	--
ERM			--	44,792	--

EBS = Environmental Baseline Survey; ERL = effects range low; ERM = effects range median; LPP = Leviathan Production Platform; N/A = not applicable; ND = not detected; "--" = no value established or no value calculated; PAH = polycyclic aromatic hydrocarbons; SD = Standard Deviation; TPH = total petroleum hydrocarbons.

Table 33. Mean (± standard deviation) total petroleum hydrocarbons (TPH) and total polycyclic aromatic hydrocarbon (PAHs) concentrations by distance and directional strata in sediment samples collected during the 2020 Leviathan Production Platform Environmental Monitoring Survey.

Strata Type	Strata	TPH (µg g^{-1})	Total PAHs (ng g^{-1})
Distance Strata	Near-Platform	16.5 ± 1.3	68.5 ± 12.5
	Near-Field	19.3 ± 1.3	88.0 ± 27.6
	Mid-Field	22.9 ± 3.4	103 ± 32.3
	Far-Field	18.1 ± 3.5	64.8 ± 11.9
	Reference	18.7 ± 1.6	60.2 ± 11.9
Directional Strata	Northeast Quadrant	18.9 ± 3.4	82.5 ± 42.9
	Northwest Quadrant	20.1 ± 3.5	86.0 ± 12.1
	Southeast Quadrant	19.2 ± 3.2	84.5 ± 34.6
	Southwest Quadrant	20.2 ± 3.5	72.6 ± 15.4
2020 LPP EMS Overall Mean (± SD)		19.6 ± 3.3	80.9 ± 28.0
2019 LPP EBS Mean (± SD)		32.7 ± 5.8	79.5 ± 60.9
2014 Leviathan Field Development EBS Mean (± SD)		14.1 ± 4.4	77.2 ± 4.6[1]
ERL		--	4,022
ERM		--	44,792

EBS = environmental baseline survey; EMS = environmental monitoring survey; ERL = effects range low; ERM = effects range median; LPP = Leviathan Production Platform; SD = standard deviation.
--= no data.

Table 34. Individual polycyclic aromatic hydrocarbon concentrations in sediment samples during the 2020 Leviathan Production Platform Environmental Monitoring Survey. Units are ng g^{-1}.

Station	Distance Strata	Directional Strata	Naphthalene	Acenaphthylene	Acenaphthene	Fluorene	Phenanthrene	Anthracene	Fluoranthene	Pyrene	Benzo[a] anthracene	Chrysene	Benzo[b] fluoranthene	Benzo[k,j] fluoranthene	Benzo[a] pyrene	Benzo[g,h,i] perylene	Dibenzo[a,h] anthracene	Indeno[1,2,3-c,d]pyrene
NP-NE-43	Near-Platform	Northeast	1.43	0.122	0.256	0.513	1.52	0.279	2.12	2.09	1.41	1.97	2.15	1.86	1.54	1.51	0.300	1.37
NP-NW-44		Northwest	1.86	0.183	0.113	0.704	2.63	0.490	2.95	2.86	1.73	2.22	2.79	2.45	1.98	2.20	0.119	1.88
NP-SW-45		Southwest	1.27	<0.041	<0.103	0.438	1.85	0.304	2.24	2.07	1.38	2.22	1.69	1.52	1.35	1.22	0.069	1.11
NP-SE-46		Southeast	0.929	<0.041	<0.103	0.318	2.36	0.427	4.15	3.53	2.32	2.65	2.47	2.40	2.13	1.67	0.104	1.54
NF-NE-1	Near-Field	Northeast	1.37	0.158	0.177	0.441	2.98	0.732	5.60	4.96	2.75	3.21	2.97	2.87	2.83	2.37	0.134	2.03
NF-NE-2			1.73	0.032	0.067	<0.183	1.64	0.308	1.54	1.54	0.901	1.26	1.56	1.28	0.887	1.31	0.043	1.06
NF-NE-3			2.23	<0.041	0.083	0.709	2.13	0.297	1.57	1.54	0.927	1.27	1.49	1.26	0.903	1.25	0.046	0.994
NF-NW-4		Northwest	1.91	0.151	0.152	0.773	2.76	0.450	2.27	2.26	1.33	1.74	2.18	1.79	1.25	1.65	0.066	1.34
NF-NW-5			2.05	0.322	0.471	0.700	1.98	0.339	1.88	1.93	1.12	1.56	2.29	1.49	1.10	1.77	0.111	1.93
NF-NW-6			2.35	0.144	0.612	0.992	2.93	0.356	2.30	2.33	1.22	1.64	2.53	1.37	1.25	1.56	<0.064	1.71
NF-SE-7		Southeast	2.14	0.131	0.428	0.668	2.05	0.367	3.17	2.94	1.67	2.12	2.90	1.95	1.75	1.87	0.152	2.13
NF-SE-8			2.38	0.100	0.380	0.629	1.66	0.307	1.72	1.84	1.03	1.35	1.67	1.45	1.09	1.33	<0.064	1.43
NF-SE-9			2.07	0.174	0.720	1.07	9.98	1.54	14.5	11.1	7.30	8.09	8.13	6.58	6.52	4.18	<0.064	5.35
NF-SW-10		Southwest	1.94	<0.041	0.403	0.545	1.67	0.263	1.78	1.76	1.01	1.39	2.01	1.24	0.927	1.29	<0.064	1.46
NF-SW-11			2.03	0.142	0.411	0.747	1.91	0.299	1.72	1.95	1.04	1.53	1.97	1.62	1.03	1.52	<0.064	1.62
NF-SW-12			2.07	0.142	0.340	0.520	1.37	0.221	1.41	1.57	0.856	1.22	1.65	1.43	0.839	1.23	<0.064	1.42
MF-NE-13	Mid-Field	Northeast	2.22	0.205	0.433	0.549	2.62	0.832	10.4	9.57	9.32	9.84	14.1	11.8	11.78	9.03	0.615	11.1
MF-NE-14			2.23	0.228	0.400	0.622	1.78	0.319	2.18	2.22	1.22	1.70	3.06	2.09	1.67	1.91	0.214	2.25
MF-NE-15			2.47	0.157	0.650	0.979	4.35	0.713	6.78	5.37	3.57	4.33	5.02	4.50	3.39	3.07	0.219	3.78
MF-NW-16		Northwest	2.30	0.181	0.401	0.708	2.00	0.330	2.72	2.62	1.77	2.31	3.22	2.23	1.75	1.86	0.098	2.13
MF-NW-17			2.21	0.099	0.379	0.637	1.79	0.349	2.30	2.38	1.37	1.83	2.64	1.86	1.35	1.87	0.132	2.12
MF-NW-18			2.40	0.247	0.405	0.657	2.15	0.390	3.03	2.90	1.63	2.13	3.15	2.02	1.58	1.86	0.126	2.20
MF-SE-19		Southeast	2.04	0.165	0.374	0.555	1.44	0.259	1.61	1.64	0.999	1.43	2.65	1.64	1.17	1.66	0.082	1.93
MF-SE-20			2.02	0.114	0.380	0.636	1.55	0.266	1.67	1.66	0.922	1.35	2.27	1.38	0.930	1.49	0.072	1.57
MF-SE-21			1.97	0.187	0.353	0.534	1.61	0.308	2.21	2.07	1.23	1.63	3.12	1.95	1.14	1.84	0.101	2.11
MF-SW-22		Southwest	2.07	0.176	0.398	0.708	2.42	0.468	3.66	3.48	2.09	2.68	4.90	3.67	2.34	3.08	0.211	3.55
MF-SW-23			1.69	0.108	0.334	0.540	1.48	0.278	1.81	1.83	1.04	1.57	2.52	2.14	1.00	1.76	0.052	1.96
MF-SW-24			1.84	0.100	0.083	0.493	1.77	0.356	2.73	2.67	1.61	2.09	2.40	1.93	1.63	1.85	0.078	1.56
FF-NE-25	Far-Field	Northeast	1.36	<0.041	<0.103	0.445	1.60	0.380	1.92	1.74	1.20	1.54	1.78	1.36	0.988	1.25	<0.064	1.01
FF-NE-26			1.50	0.100	0.109	0.122	1.87	0.426	2.73	2.55	1.60	1.94	1.90	1.57	1.48	1.44	0.079	1.27
FF-NE-27			1.52	0.145	0.099	0.179	2.01	0.466	2.62	2.52	1.56	1.94	2.06	1.87	1.35	1.54	0.067	1.31
FF-NW-28		Northwest	1.93	0.110	0.162	0.331	3.23	0.572	4.03	3.47	2.30	2.90	2.68	2.46	2.04	1.88	0.091	1.68
FF-NW-29			1.51	0.139	0.080	0.179	1.95	0.425	2.17	2.21	1.38	1.84	1.96	1.65	1.14	1.29	0.072	1.08
FF-NW-30			2.15	0.155	0.063	0.221	2.07	0.429	2.37	2.41	1.55	2.23	2.74	2.45	1.81	2.35	0.127	2.06

Table 34. (Continued).

Station	Distance Strata	Directional Strata	Naphthalene	Acenaphthylene	Acenaphthene	Fluorene	Phenanthrene	Anthracene	Fluoranthene	Pyrene	Benzo[a] anthracene	Chrysene	Benzo[b] fluoranthene	Benzo[k,j] fluoranthene	Benzo[a] pyrene	Benzo[g,h,i] perylene	Dibenzo[a,h] anthracene	Indeno[1,2,3-c,d]pyrene
FF-SE-31	Far-Field (cont'd)	Southeast	1.76	0.096	0.032	0.136	1.20	0.255	1.28	1.31	0.861	1.15	1.38	1.19	0.802	1.17	<0.064	0.945
FF-SE-32			1.21	<0.041	<0.103	0.133	1.38	0.318	1.54	1.55	1.05	1.35	1.67	1.21	0.902	1.27	<0.064	1.01
FF-SE-33			1.92	0.034	0.091	<0.183	1.51	0.290	1.45	1.43	0.877	1.17	1.44	1.22	0.862	1.11	<0.064	0.888
FF-SW-34		Southwest	1.77	<0.041	0.106	0.285	2.00	0.391	2.40	2.38	1.44	1.95	2.37	2.07	1.34	1.82	0.095	1.51
FF-SW-35			1.93	<0.041	0.058	0.188	1.74	0.372	1.75	1.68	1.05	1.48	1.75	1.46	0.936	1.42	0.063	1.15
FF-SW-36			2.27	0.039	0.088	0.610	2.16	0.404	2.57	2.37	1.53	2.05	2.25	1.94	1.37	1.67	0.079	1.44
REF-NE-37	Reference	Northeast	1.80	<0.041	0.066	0.199	1.66	0.339	1.72	1.72	1.07	1.42	1.72	1.47	0.940	1.32	0.053	1.12
REF-NE-38			1.80	<0.041	<0.103	0.150	1.59	0.303	2.65	2.35	1.60	1.84	2.19	1.83	1.55	1.63	0.090	1.40
REF-NE-39			1.40	0.091	0.051	0.376	1.40	0.285	1.67	1.60	1.08	1.33	1.56	1.35	1.01	1.20	0.065	1.02
REF-SW-40		Southwest	1.60	<0.041	<0.103	0.182	1.33	0.272	1.25	1.34	0.760	1.12	1.44	1.16	0.738	1.17	<0.064	0.936
REF-SW-41			0.938	0.119	0.033	0.094	1.44	0.323	1.72	1.84	1.03	1.48	1.98	1.68	1.02	1.47	0.058	1.25
REF-SW-42			1.57	<0.041	0.102	<0.183	2.57	0.544	3.36	3.43	1.96	2.56	2.85	2.58	2.06	1.93	0.113	1.67
2020 LPP EMS Mean (± SD)			1.85 ± 0.38	--	0.246 ± 0.19*	0.467 ± 0.26*	2.15 ± 1.3	0.405 ± 0.21	2.85 ± 2.4	2.67 ± 1.9	1.71 ± 1.5	2.17 ± 1.6	2.72 ± 2.1	2.18 ± 1.7	1.73 ± 1.8	1.87 ± 1.2	0.100 ± 0.10*	1.90 ± 1.6
2019 LPP EBS Mean (± SD)			1.18 ± 0.23	0.183 ± 0.05	0.237 ± 0.33	0.790 ± 0.37	3.66 ± 2.6	0.533 ± 0.31	4.03 ± 6.4	3.62 ± 4.8	2.18 ± 3.6	2.83 ± 4.9	3.11 ± 4.5	2.68 ± 4.3	2.16 ± 3.9	2.49 ± 2.9	0.533 ± 0.99	2.04 ± 2.9
2014 Leviathan Field Development EBS Mean (± SD)			2.25 ± 0.10	0.24 ± 0.02	0.39 ± 0.10	1.49 ± 0.34	7.74 ± 1.22	0.66 ± 0.06	3.59 ± 0.48	2.99 ± 0.42	1.37 ± 0.08	1.72 ± 0.16	1.09 ± 0.85	1.09 ± 0.08	1.36 ± 0.11	1.52 ± 0.05	0.40 ± 0.03	1.32 ± 0.12
MDL			0.342	0.041	0.103	0.183	0.208	0.115	0.333	0.136	0.192	0.116	0.203	0.098	0.101	0.088	0.064	0.050
ERL			160	44	16	19	240	85.3	600	665	261	384	--	--	--	--	--	--
ERM			2,100	640	500	540	1,500	1,100	5,100	2,600	1,600	2,800	--	--	--	--	--	--

EBS = environmental baseline survey; EMS = environmental monitoring survey; ERL = effects range low; ERM = effects range median; LPP = Leviathan Production Platform; MDL = Method Detection Limit; SD = Standard Deviation.

-- = not calculable. More than 25% of samples were less than the laboratory's MDL.

* = One half the MDL was used to calculate averages for samples that were less than the MDL.

Hydrocarbons Statistical Analyses

There was no significant three-way interactive effect among distance, direction, and survey year for sediment TPH concentrations ($F_{10,56} = 1.24$; $P = 0.29$). There were also no significant two-way interactive effects between distance and direction ($F_{10,56} = 1.60$; $P = 0.13$) or direction and survey year ($F_{3,56} = 0.84$; $P = 0.48$). There was, however, a significant interactive effect for distance and survey year ($F_{4,82} = 4.76$; $P = 0.002$). During the 2019 LPP EBS, survey samples collected from the Near-Platform strata had a significantly higher TPH concentrations than samples collected from within the Near-Field strata ($t_{8,2} = 3.34$; $P = 0.04$). During the 2020 LPP EMS, there were no significant differences in TPH concentrations among distance strata. Additionally, all sediment samples collected around the LPP during the 2020 LPP EMS had significantly lower concentrations of TPH than samples collected from around the LPP during the 2019 LPP EBS (**Table 35**; **Figure 41**).

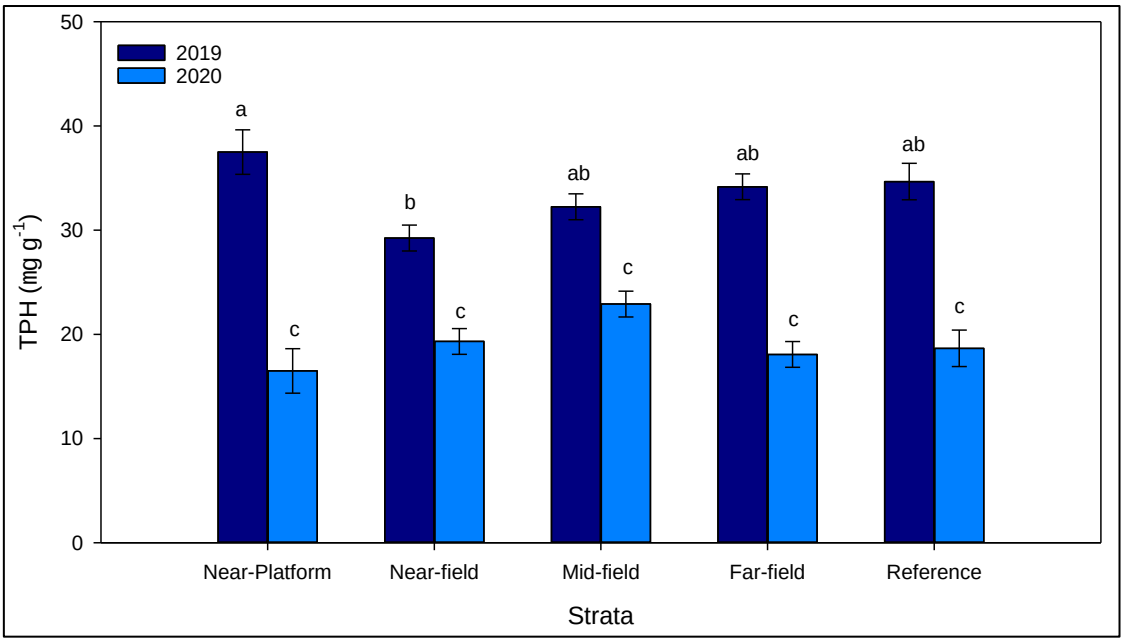


Figure 41. Statistical least square means (± standard error) of sediment total petroleum hydrocarbon concentration (µg g^{-1}) within the significant survey year by distance strata interaction as computed by the analysis of variance (ANOVA) model. Different letters indicate statistical significance at P <0.05.

Table 35. Post-hoc Tukey's Multiple Means Comparison Test result matrix for differences in total petroleum hydrocarbons for the interactive effect of distance strata × survey year specific to the comparisons between 2019 (column) and 2020 (row) survey results. All results below indicate a significant difference.

2019 LPP EBS	2020 LPP EMS				
	Near-Platform	Near-Field	Mid-Field	Far-Field	Reference
Near-Platform	$t_{82} = 6.93$; P < 0.001	$t_{82} = 7.34$; P < 0.001	$t_{82} = 5.90$; P < 0.001	$t_{82} = 5.90$; P < 0.001	$t_{82} = 6.81$; P < 0.001
Near-Field	$t_{82} = 5.15$; P < 0.001	$t_{82} = 5.67$; P < 0.001	$t_{82} = 3.62$; P = 0.017	$t_{82} = 6.32$; P < 0.001	$t_{82} = 4.94$; P = 0.0002
Mid-Field	$t_{82} = 6.37$; P < 0.001	$t_{82} = 7.38$; P < 0.001	$t_{82} = 5.34$; P < 0.001	$t_{82} = 8.10$; P < 0.001	$t_{82} = 6.34$; P < 0.001
Far-Field	$t_{82} = 7.14$; P < 0.001	$t_{82} = 8.48$; P < 0.001	$t_{82} = 6.43$; P < 0.001	$t_{82} = 9.19$; P < 0.001	$t_{82} = 7.24$; P < 0.001
Reference	$t_{82} = 6.93$; P < 0.001	$t_{82} = 5.15$; P < 0.001	$t_{82} = 5.48$; P < 0.001	$t_{82} = 7.74$; P < 0.001	$t_{82} = 6.47$; P < 0.001

EBS = environmental baseline survey; EMS = environmental monitoring survey; LPP = Leviathan Production Platform.

There was no significant three-way interactive effect among distance, direction, and survey year for sediment total PAH concentrations ($F_{10,56} = 1.20$; P = 0.31). There were also no significant two-way interactive effects between distance and direction ($F_{10,56} = 0.77$; P = 0.66), direction and survey year ($F_{3,56} = 0.56$; P = 0.64), or distance and survey year ($F_{4,56} = 0.45$; P = 0.77). Because there were no significant interactions for sediment total PAH concentrations, it was possible to investigate the overall main effects of distance, direction, and survey year. There were no significant differences among distance strata ($F_{4,83} = 2.24$; P = 0.07), directional strata ($F_{3,83} = 0.55$; P = 0.65), or survey year ($F_{1,83} = 0.02$; P = 0.89). These results indicate that total PAH concentrations are statistically similar within the region surrounding the LPP both spatially (i.e., distance and direction) and temporally (i.e., survey year).

5.4.5 Radionuclides

Analytical laboratory datasheets for radionuclides in sediment are provided in **Appendix M**. Results are presented in **Table 36** for the 2020 LPP EMS. Results are presented as the analytical value ± the total propagated analytical uncertainty (TPU). Ambient radium concentrations in most soils and rocks are approximately 0.5 to 5.0 pCi g^{-1} (18.5 to 185 Bq kg^{-1}) (U.S. Geological Survey, 1999). Ambient concentrations of thorium 228 in sediments range from 0.36 to 1.93 pCi g^{-1} (13.3 to 71.4 Bq kg^{-1}) (Agency for Toxic Substances and Disease Registry, 1990). The USEPA (1998) established a protective health-based level for radium and thorium of 5 pCi g^{-1} (185 Bq kg^{-1}) at the sediment surface as a threshold for the clean-up of the top 15 cm of soil from contaminated U.S. Superfund sites.

All concentrations of radium and thorium from the 2020 LPP EMS were below the laboratory's MRL and well below the USEPA protective health-based levels (**Table 36**). Because most of the reported values by the concentrations reported by the analytical laboratory were below the MRL, no averages by distance or direction are presented, and no statistical analyses were performed. During the 2019 LPP EBS, all concentrations of radium and thorium were below the laboratory's MRL except for a single concentration of ^{228}Ra at one station which was slightly above the MRL. Samples for radionuclide analysis were not collected in the vicinity of the LPP during the 2014 Leviathan Field Development EBS.

Table 36. Radioactive compound concentrations (pCi g^{-1}) in sediment samples collected during the 2020 Leviathan Production Platform Environmental Monitoring Survey.

Station	^{226}Ra	^{228}Ra	^{228}Th
NP-NE-43	0.72 ± 0.27	0.38 ± 0.43	0.55 ± 0.12
NP-NW-44	0.46 ± 0.19	0.69 ± 0.39	0.53 ± 0.11
NP-SW-45	0.62 ± 0.26	0.15 ± 0.49	0.54 ± 0.11
NP-SE-46	0.48 ± 0.23	0.35 ± 0.49	0.42 ± 0.10
NF-NE-1	0.63 ± 0.21	0.47 ± 0.35	0.46 ± 0.10
NF-NW-4	0.60 ± 0.18	0.12 ± 0.36	0.69 ± 0.14
NF-SE-8	0.54 ± 0.26	0.55 ± 0.56	0.58 ± 0.12
NF-SW-11	0.60 ± 0.20	0.46 ± 0.28	0.62 ± 0.12
MF-NE-14	0.75 ± 0.26	0.30 ± 0.54	0.62 ± 0.13
MF-NW-16	0.70 ± 0.20	0.59 ± 0.48	0.64 ± 0.13
MF-SE-20	0.046 ± 0.021	0.039 ± 0.044	0.61 ± 0.13
MF-SW-23	0.53 ± 0.24	0.63 ± 0.35	0.62 ± 0.13
FF-NE-27	0.73 ± 0.25	0.49 ± 0.34	0.61 ± 0.13
FF-NW-30	0.68 ± 0.25	0.58 ± 0.51	0.68 ± 0.13
FF-SE-33	0.60 ± 0.18	0.69 ± 0.36	0.56 ± 0.11
FF-SW-34	0.62 ± 0.28	0.10 ± 0.48	0.68 ± 0.14
REF-NE-39	0.55 ± 0.20	0.86 ± 0.43	0.66 ± 0.13
REF-SW-42	0.59 ± 0.27	0.84 ± 0.65	0.64 ± 0.12
Method Reporting Limit (MRL)	1	1	1
Ambient Concentrations	0.5–5.0[1]		0.36–1.93[2]

^{226}Ra = Radium 226; ^{228}Ra = Radium 228; ^{228Th} = Thorium 228.
[1] From: U.S. Geological Survey, 1999.
[2] From: Agency for Toxic Substances and Disease Registry, 1990.

5.5 VIDEO ANALYSIS

5.5.1 Fouling Community

Identification of Taxa

A list of the organisms which comprised the fouling community observed on the legs of the LPP is presented in **Table 37**. As mentioned in **Section 4.5.1**, several species could not be identified to a sufficiently low taxonomic level and were therefore classified as "morphospecies" according to visible morphological characteristics.

Porifera, Bryozoa, Chordata (Class: Ascidiacea) and Mollusca (Class: Bivalvia) were the most diverse phyla encountered. Three species of ascidians were documented: *Didemnum* sp., *Herdmania momus* and *Phallusia nigra*. Several species of bivalves were documented, of which three were identified to the genus or species level: *Malleus regula*, *Spondylus spinosus*/*Chama pacifica* bivalve complex and *Chlamys* sp. Three species of Porifera and three species of Bryozoa were documented, however, due to the difficulty to taxonomically identify species from still images, and with no physical sample in hand to confirm potential classification, it is likely that several additional species were present but not identified. Arthropoda, Annelida and Cnidaria were represented by only one or two species each (**Table 37**). Documented Annelida taxa included the sedentary worm families Serpulidae (**Image 6**) and Sabellidae, and the invasive fire worm *Hermodice carunculata* (**Image 7**). Documented Cnidaria taxa included unidentified species of Hydrozoa and Hexacorallia. All documented Arthropoda taxa were barnacles (Infraclass: Cirripedia). No macroalgae were documented during the survey.

Table 37. Taxonomic list of the fouling community identified organisms from the Leviathan Production Platform (LPP) northeast and southeast legs during the 2020 LPP Environmental Monitoring Survey.

[1]Origin	Phylum	Class	Taxonomic Identification
Invasive	Annelida	Polychaeta	*Hermodice carunculata*
Local			Sabellidae
Local			Serpulidae
Unknown	Arthropoda	Maxillopoda	Unidentified Cirripedia (barnacles)
Unknown	Bryozoa	Gymnolaemata	Bryozoa Morphospecies 1 - dark red
Unknown			Bryozoa Morphospecies 2 - branching
Unknown			Bryozoa Morphospecies 3 - white
Both	Chordata	Ascidiacea	*Didemnum* sp.
Invasive			*Herdmania momus*
Invasive			*Phallusia nigra*
Unknown	Cnidaria	Hydrozoa	Unidentified Hydrozoa spp.
Unknown		Anthozoa	Unidentified Hexacorallia spp.
Local	Echinodermata	Crinoidea	*Antedon mediterranea*
Invasive		Echinoidea	*Arbacia lixula*
Invasive			*Diadema* sp.
Invasive	Mollusca	Bivalvia	*Chama pacifica*/*Spondylus spinosus* bivalve complex
Both			*Chlamys* sp.
Invasive			*Malleus regula*
Unknown			Unidentified Bivalvia spp.
Local	Porifera	Calcarea	*Leucosolenida* sp.
Local		Demospongiae	Demospongiae morphospecies 1 - orange
Local			Demospongiae morphospecies 2 - red
Local			Demospongiae morphospecies 3 - white

[1] Taxa origin (local/invasive) was determined based on documented records of the taxonomic identification and peer reviewed publications which provide information on the distribution of higher taxonomic levels along the Israeli coastline and the Levantine basin region. Data was cross referenced with marinespecies.com website database. Taxa with both local and invasive representatives were labelled "Both".

Depth Distribution

The vertical distribution of taxa across the different sampling depths was generally similar at all platform legs. **Figures 42** and **43** display the vertical distribution of taxa for both platform sides (northeast and southwest). Serpulids, bivalves (**Image 6**), and a form of branching bryozoan (morphospecies 1) (**Image 8**) were prevalent and found at all depths. The encrusting ascidian *Didemnum* sp. (**Image 6**) was also prevalent and found from 10 to 60 m depth, while the solitary ascidian *Herdmania momus* (**Image 7**) was found from 15 to 70 meters depth, and the solitary ascidian *Phallusia nigra* was found sporadically down to a maximum depth of 50 m. Various sponge species of the class Demospongiae (**Image 9**) were found from 10 m depth down to the bottom of the platform legs while calcareous sponge species of the order *Leucosolenida* sp. (**Image 9**) occurred between 15 m and 60 m depth. Hydroids and barnacles were found at the shallow end of the water column on the northeastern side (maximum 40 m and 20 m depth, respectively) while at the southwest side both groups extended their range further down the water column.

Motile Fauna

Of the motile fauna, the crinoid *Antedon mediterranea* (**Image 10**) was the most abundant and occurred from a depth of 40 m down to 80 m with the highest density found at 60 m on the northeastern side – an average of 42 ± 26 individuals m^{-2} (**Figure 44**). The echinoid *Arbacia lixula* (**Image 10**) was found intermittently across all depths, and the echinoid *Diadema* sp. (**Image 10**) was only sighted twice, on the northeastern side of the platform (**Figure 45**).

Sessile Fauna

Sessile fauna from the phyla Annelida, Arthropoda, Chordata, Porifera, Mollusca (Class: Bivalvia) and Cnidaria were documented on both sides of the platform legs. Bryozoans had highest cover of all documented sessile fauna on both sides of the platform legs, particularly between 30 m and 60 m depth, and reaching greatest percent cover (32.6% ± 0 %) at the southwestern side of the platform at 40 and 50 m depth (**Figure 46**, **Image 8**). Bivalvia were also ubiquitous on all platform legs and their greatest percent cover was 17.7% ± 21 % at both 70 and 80 m depth on the southwestern side (**Figure 47**). The encrusting ascidian *Didemnum* sp. was prominent from 10 m down to a depth of 60 m and the highest percent cover it presented was 16.3% ± 23%, at 40 m depth on the southwestern side of the platform (**Figure 46**). Calcareous tubeworms were prevalent on both sides of the platform, presenting higher percent cover at depth, with the highest percent cover, 10.6% ± 5.2 %, recorded at 70 m depth on the Northeastern side of the platform (**Figure 48**). Poriferans of the class Demospongiae were recorded at all depths on the northeastern side and most depths on the southwestern side (all but 20 m and 70 m depth), but overall percent cover for these species was low, with a maximum of 2.81% ± 0 % at 10 and 15 m depth on the southwestern side (**Figure 49**).

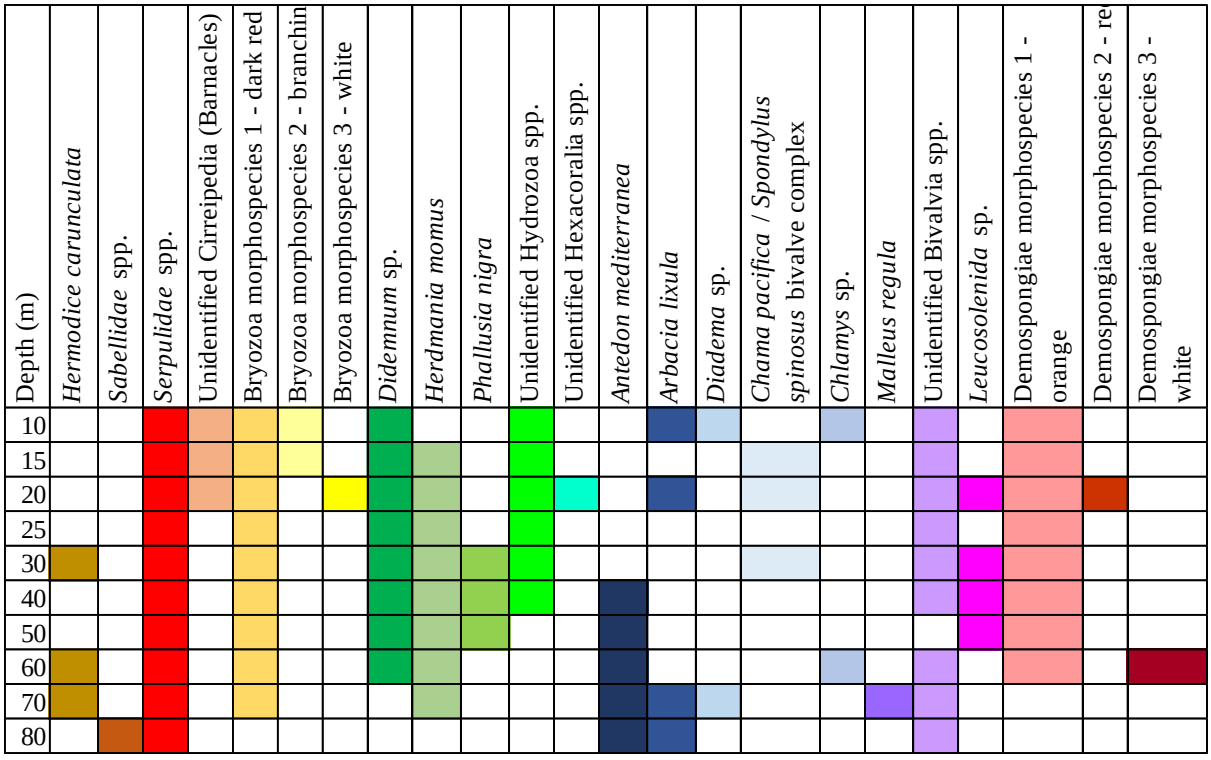


Figure 42. Mean depth distribution of taxa identified from the video survey on the northeastern side of the Leviathan Production Platform. This depth distribution represents presence or absence of taxa from all legs investigated. Colored cells indicate the species was observed within that depth stratum.

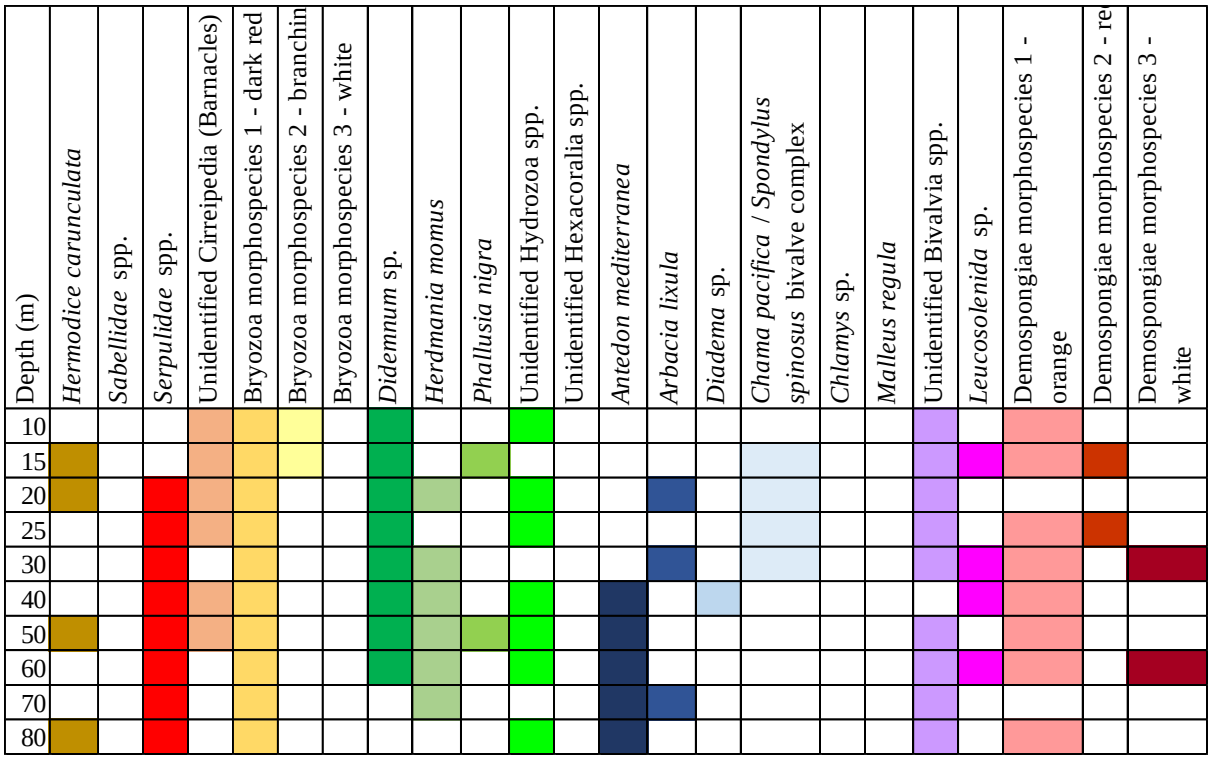


Figure 43. Mean depth distribution of taxa identified from the video survey on the southeastern side of the Leviathan Production Platform. This depth distribution represents presence or absence of taxa from all legs investigated. Colored cells indicate the species was observed within that depth stratum.



Image 6. Representative image of organisms found on the northeastern side of the Leviathan Production Platform legs. Round forms were all unidentified bivalves and elongated white forms were all annelids from the family Serpulidae. Horizontal field of view = 1.2 m.



Image 7. Representative organisms (red circles) found on the northeastern side of the Leviathan Production Platform legs. A = *Herdmania momus*; B = *Hermodice carunculata*. Horizontal field of view = 1.2 m.



Image 8. Representative organisms found on the northeastern side of the Leviathan Production Platform legs. A = Bryozoa morphospecies 1; B = Bryozoa morphospecies 2.; C = *Didemnum* sp. Horizontal field of view = 1.2 m.

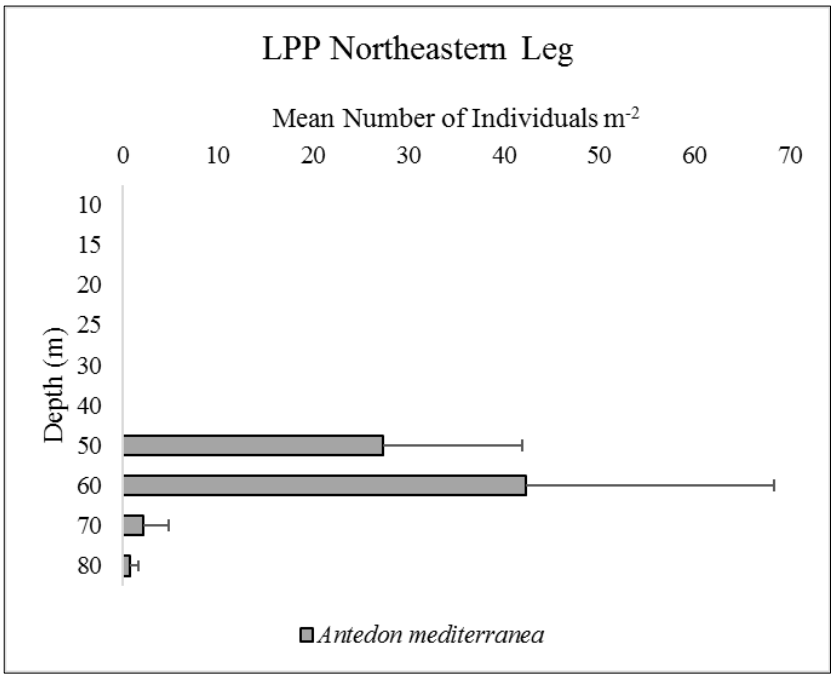


Image 9. Representative organisms (red circles) found on the northeastern side of the Leviathan Production Platform legs. A = Demospongiae morphospecies 1; B = *Leucosolenida* sp. Horizontal field of view = 1.2 m.



Image 10. Representative organisms (red arrows) found on the northeastern side of the Leviathan Production Platform legs. A =*Arbacia lixula*; B = *Diadema* sp.; C = *Antedon mediterranea*. Horizontal field of view = 1.2 m.

A



B

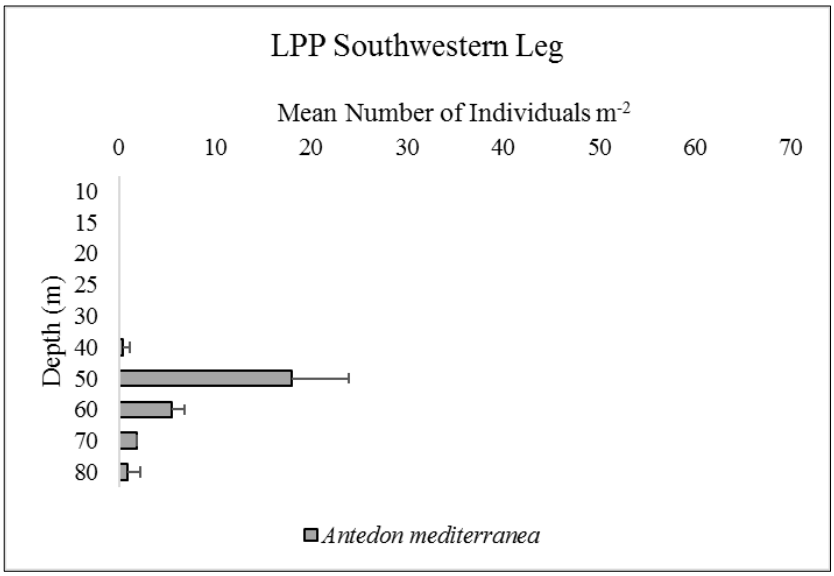
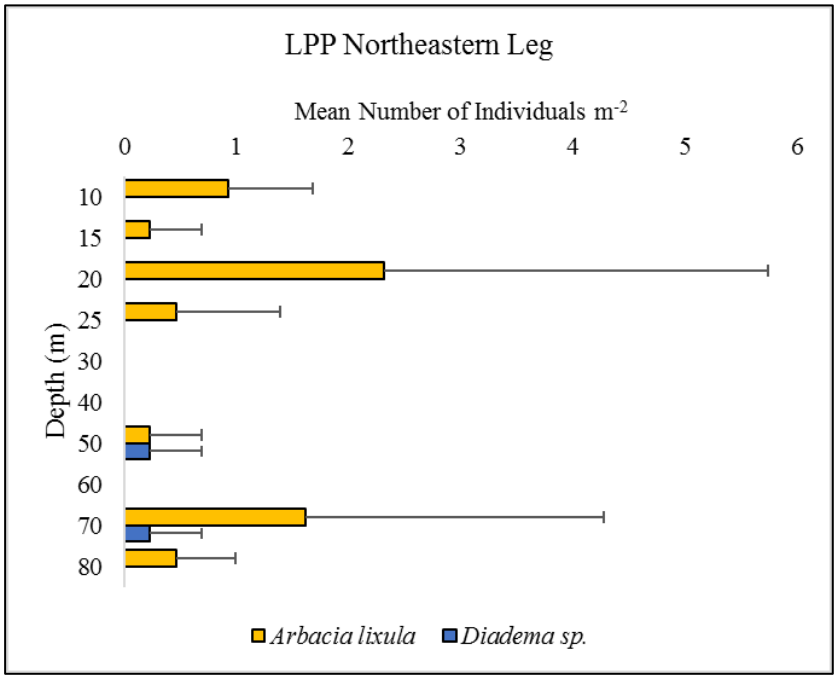


Figure 44. Mean number of *Antedon mediterranea* individuals m^{-2} (± standard deviation), at each sampling depth on the (A) northeastern side and (B) southwestern side of the Leviathan Production Platform. For means where standard deviation = 0, no error bar is shown.

A



B

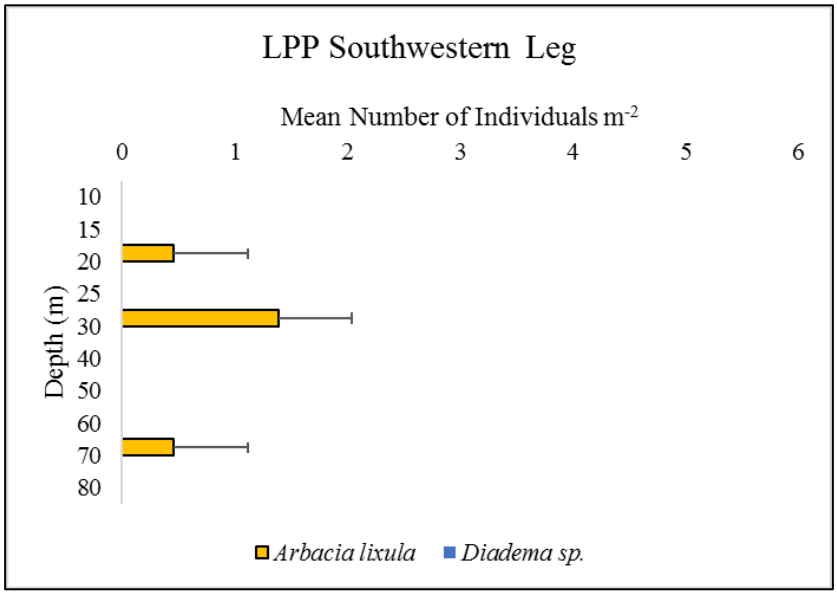
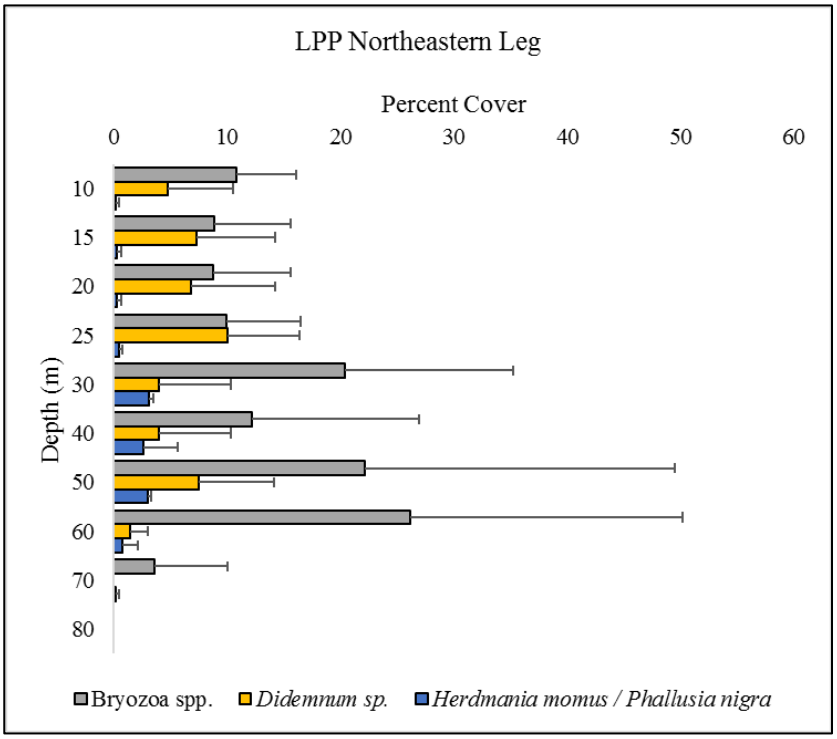


Figure 45. Mean number of *Arbacia lixula* and *Diadema* sp. individuals m^{-2} (± standard deviation), at each sampling depth on the (A) Northeastern side and (B) Southwestern side of the Leviathan Production Platform.

A



B

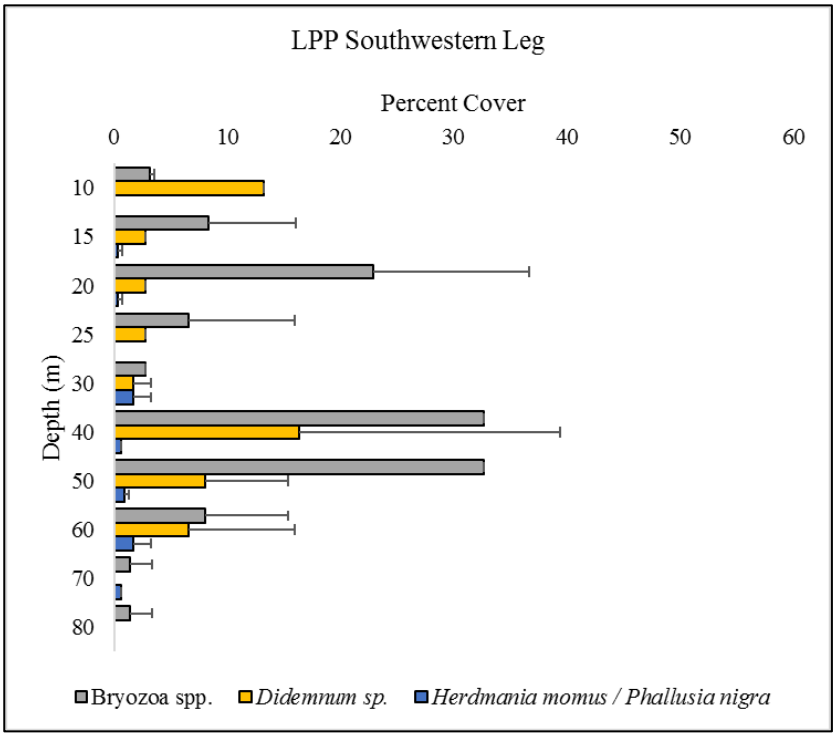
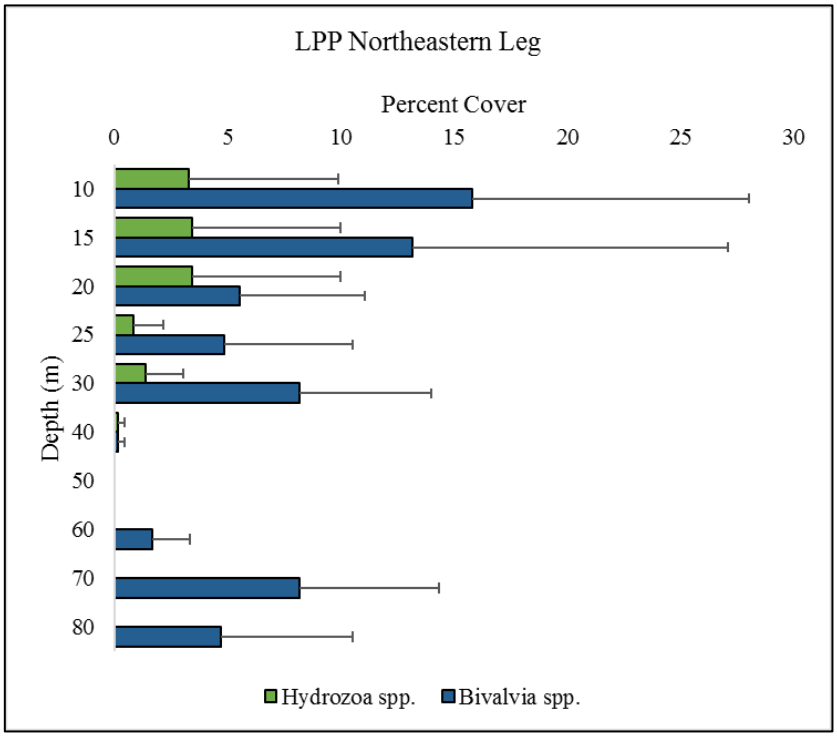


Figure 46. Mean percent cover of Bryozoa, encrusting Ascidia (*Didemnum* sp.) and Solitary Ascidia (*Herdmania momus* / *Phallusia nigra*) from all sampling depths recorded on the (A) northeastern side and (B) northwestern side of the Leviathan Production Platform. For means where standard deviation = 0, no error bar is shown.

A



B

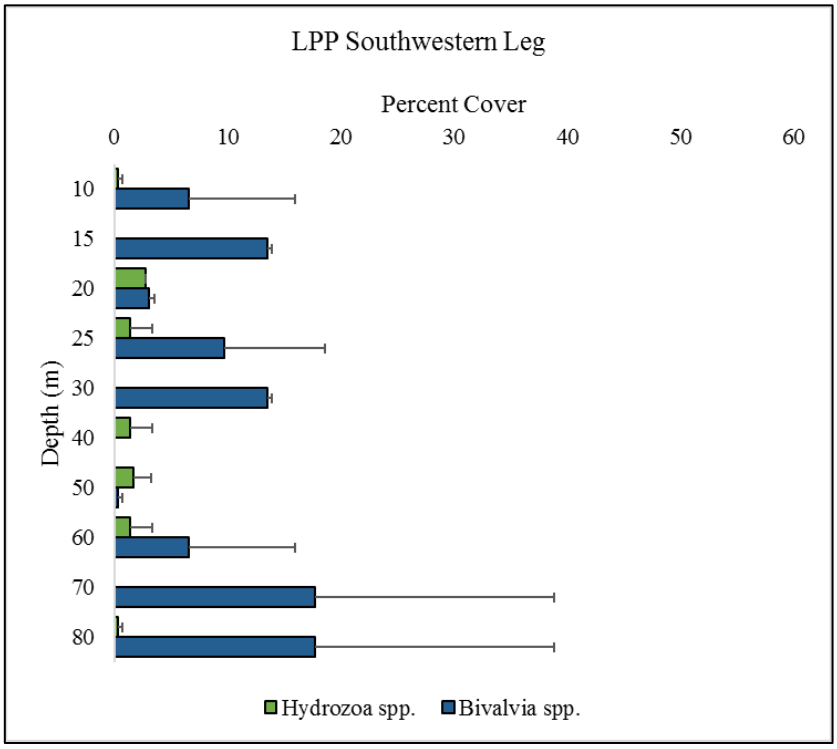
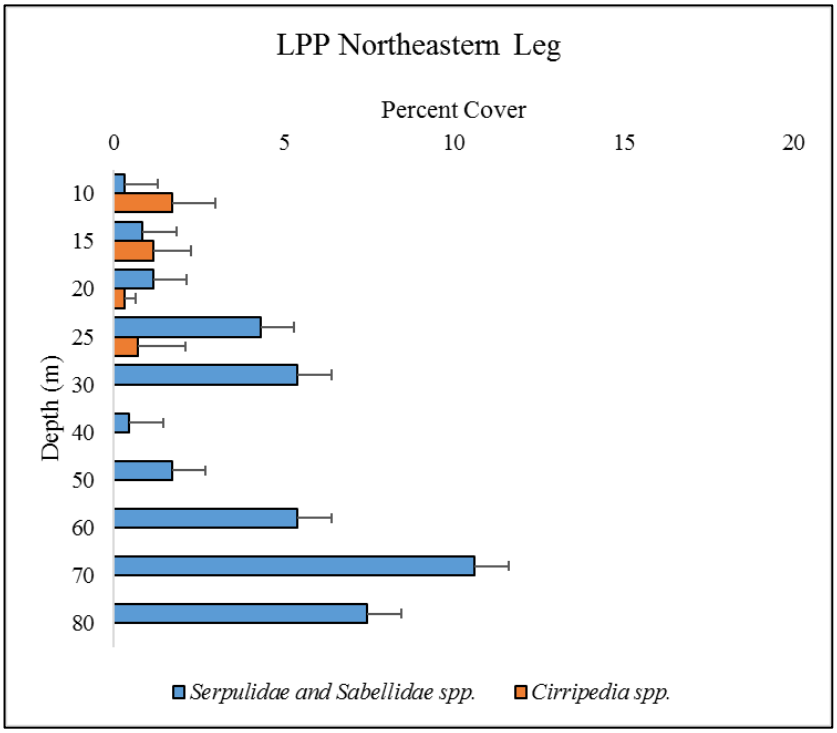


Figure 47. Mean percent cover of Hydrozoa and Bivalvia from all sampling depths recorded on the (A) northeastern side and (B) southwestern side of the Leviathan Production Platform. For means where standard deviation = 0, no error bar is shown.

A



B

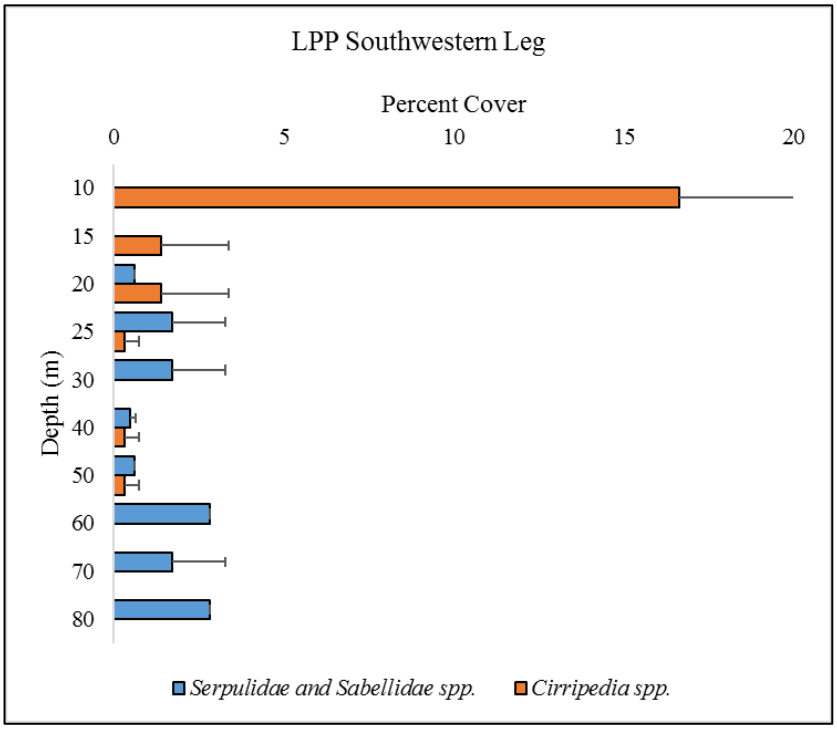
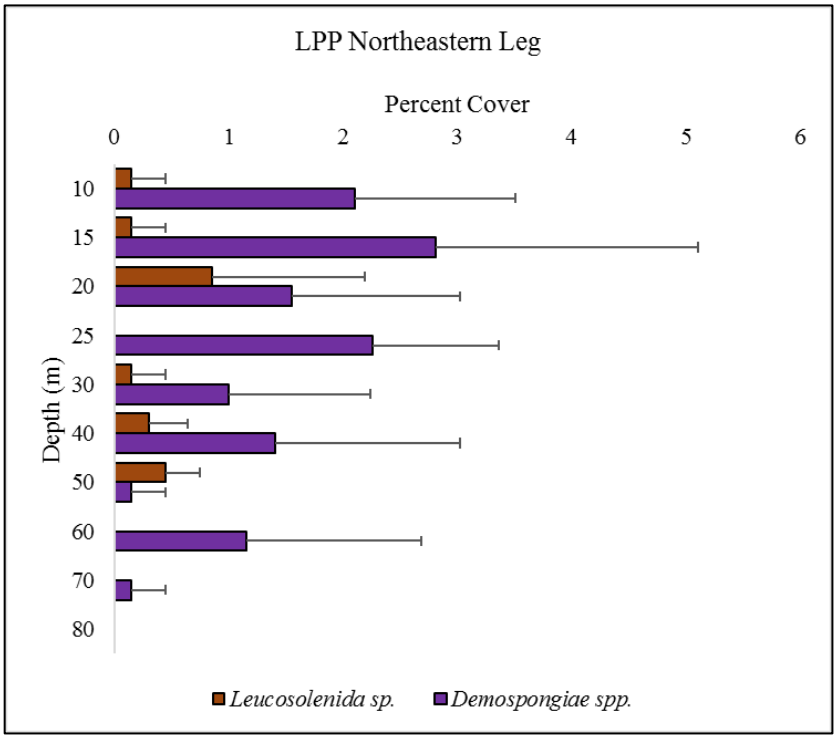


Figure 48. Mean percent cover of tube worms (Families: *Serpulidae* and *Sabelidae*) and barnacles (Infraclass: Cirripedia) from all sampling depths recorded on the (A) northeastern side and (B) southwestern side of the Leviathan Production Platform. For means where standard deviation = 0, no error bar is shown.

A



B

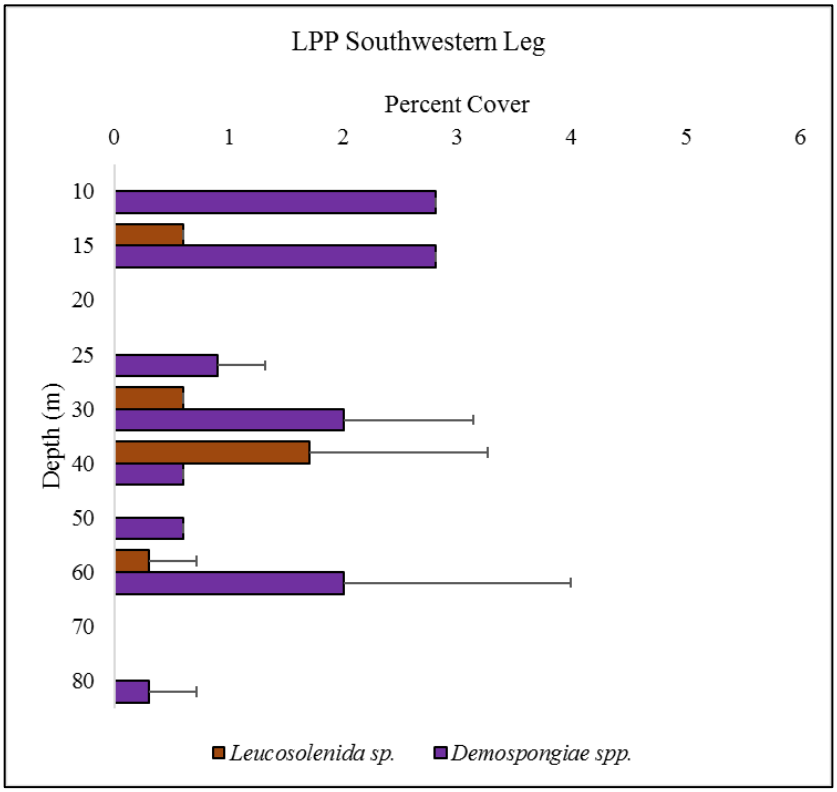


Figure 49. Mean percent cover of Porifera from the classes Calcarea (Order: Leucosolenida) and Demospongiae from all sampling depths recorded on the (A) northeastern side and (B) southwestern side of the Leviathan Production Platform. For means where standard deviation = 0, no error bar is shown.

Overall, the taxonomic richness and percent cover of the sessile fouling community (and density of motile invertebrates) was similar between both the northeastern and southwestern sides of the platform, although the southwestern side had lower percent cover of tube worms (*Serpulidae* spp.) and patchier cover of sponges (Porifera). This mild variation is likely due to a different number of legs surveyed on each side (four at the northeast and two at the southwest). Prevailing current conditions at the area may also account for differences in epibenthic communities' composition between the two sides of the LPP, although these were not readily discernable during the 2020 LPP EMS and may only be discernable after additional future visual assessments of the LPP fouling communities. In addition, based on data collected, the LPP discharge point at the southwestern side did not seem to have an effect on the fouling communities' composition.

Due to the location of the LPP, a considerable distance away from typical sources of colonizing species, the recruitment timeline for fouling communities is expected to be considerably longer for both sessile and motile invertebrates in comparison with nearshore infrastructures or natural hardbottom environments. During the current survey, 22 invertebrate taxa were observed at the LPP. By comparison, 24 taxa were observed on the Mari-B and Tamar Platforms during 2016, and 34 taxa during 2019, demonstrating that additional species typically settle on submerged structures over time (MVI, 2019a). While the LPP (10 km offshore) is approximately 14 km closer to shore as compared to the Mari-B and Tamar platforms (located nearly 24 km offshore), the latter platforms were installed in 2003 and 2012, respectively, and have therefore, been introduced with many additional species which colonized the submerged structure during this time period. It is likely that the LPP fouling community is still in a process of succession and that future surveys will reveal additional species that have yet to colonize the platform legs and increased epibenthic coverage.

5.5.2 Fish Community

Analysis of the videos from the LPP yielded a total of eight documented fish species (**Table 38**). Six of the eight species were observed at the northeast side and were distributed among the surveyed strata along the vertical extent of the platform (**Figure 50**). No fish were observed at the 40 m and 50 m depths. The shallow water depths (10 m to 30 m) were numerically dominated by the blue runner (*Caranx crysos*) and white trevally (*Pseudocaranx dentex)*. White trevally fishes were the most ubiquitous, found among half of the strata, ranging from 10 m to 30 m dept, and amassing the greatest abundance overall on the northeast side with 18 individuals (**Image 11**). Two fish taxa from the Serranidae family were documented: an unidentified grouper (*Epinephelus* sp.) and a comber (*Serranus cabrilla*) (**Images 12** and **13**), with three observed individuals each. The two taxa were recorded near the bottom of the platform legs, between 60 m and 80 m depth. The unidentified grouper individuals were not close enough to the ROV for visual identification to the species level.

Analysis of the videos from the southwest side of the LPP yielded four fish species (**Table 38**; **Figure 51**), including two of those observed on the northeast side: *Epinephelus* sp., and the invasive lionfish (*Pterois miles*) (**Image 14**). All identified fish were documented near the bottom of the water column, between 50 m and 80 m depth. A large school of greater amberjack (*Seriola dumerili*) (**Image 15**) with approximately 20 individuals, was present near the bottom of the platform legs, at 80 m depth, making this the most abundant species at the southwest side, and followed by the gray triggerfish (*Balistes capriscus*) (**Image 16**), of which six individuals were documented at 60 m depth. The fourth fish taxa documented at the southwest side was *Scorpaena* sp. (**Image 17**), of which one individual was documented at 50 m depth and another at 70 m depth.

Table 38. Taxonomic list of fish identified from the Leviathan Production Platform (LPP) northeast and southwest legs during the 2020 LPP Environmental Monitoring Survey (names follow Carpenter and De Angelis, 2016). Scientific taxonomy is followed by English common name.

[1]Origin	Family	Species	Common Name	Northeast	Southwest
Local	Balistidae	*Balistes capriscus*	Grey triggerfish	+	+
Local	Carangidae	*Caranx crysos*	Blue runner	+	
Local	Carangidae	*Pseudocaranx dentex*	White trevally	+	
Local	Carangidae	*Seriola dumerili*	Greater amberjack		+
Invasive	Scorpaenidae	*Pterois miles*	Common lionfish	+	+
Both	Scorpaenidae	*Scorpaena* sp.	Unidentified scorpionfish		+
Local	Serranidae	*Epinephelus* sp.	Unidentified grouper	+	
Local	Serranidae	*Serranus cabrilla*	Comber	+	

+ = species present.
[1] Taxa origin (local/invasive) was determined based on documented records of the taxonomic identification and peer reviewed publications which provide information on the distribution of higher taxonomic levels along the Israeli coastline and the Levantine basin region. Data was cross referenced with marinespecies.com website database. Taxa with both local and invasive representatives were labelled "Both".

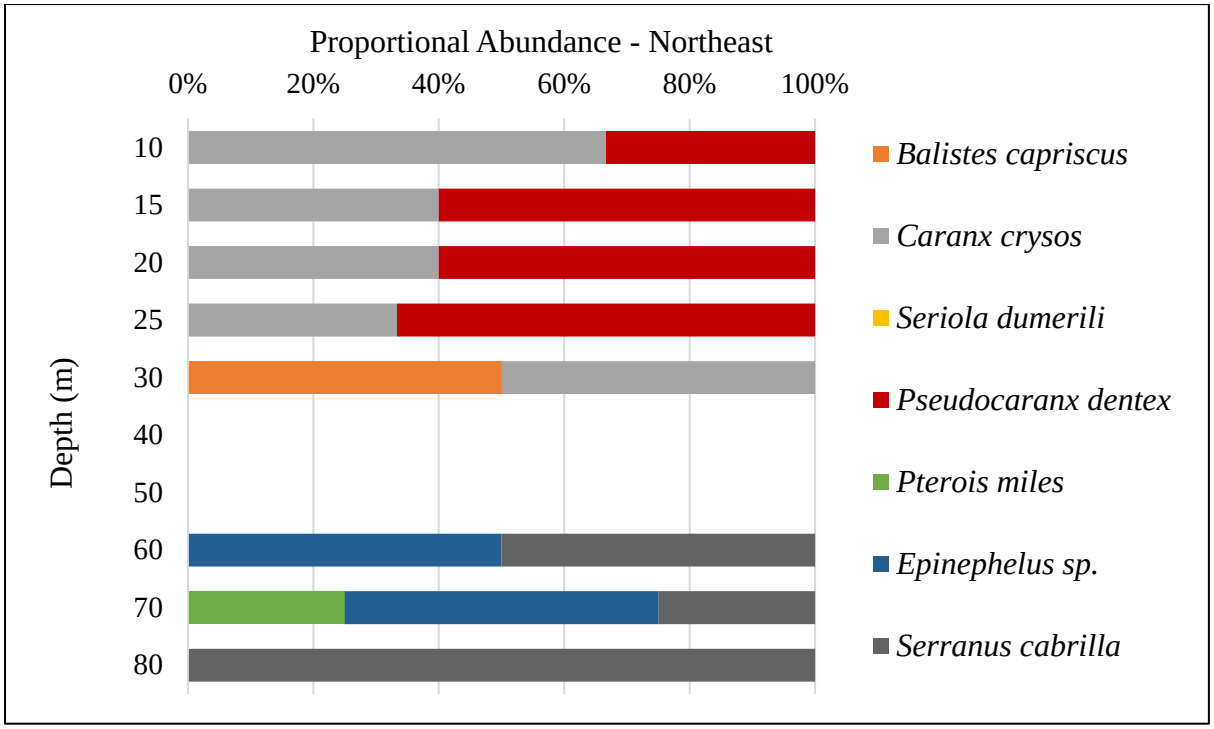


Figure 50. Proportional abundance and depth distribution of fish species found at the northeast side of the Leviathan Production Platform.

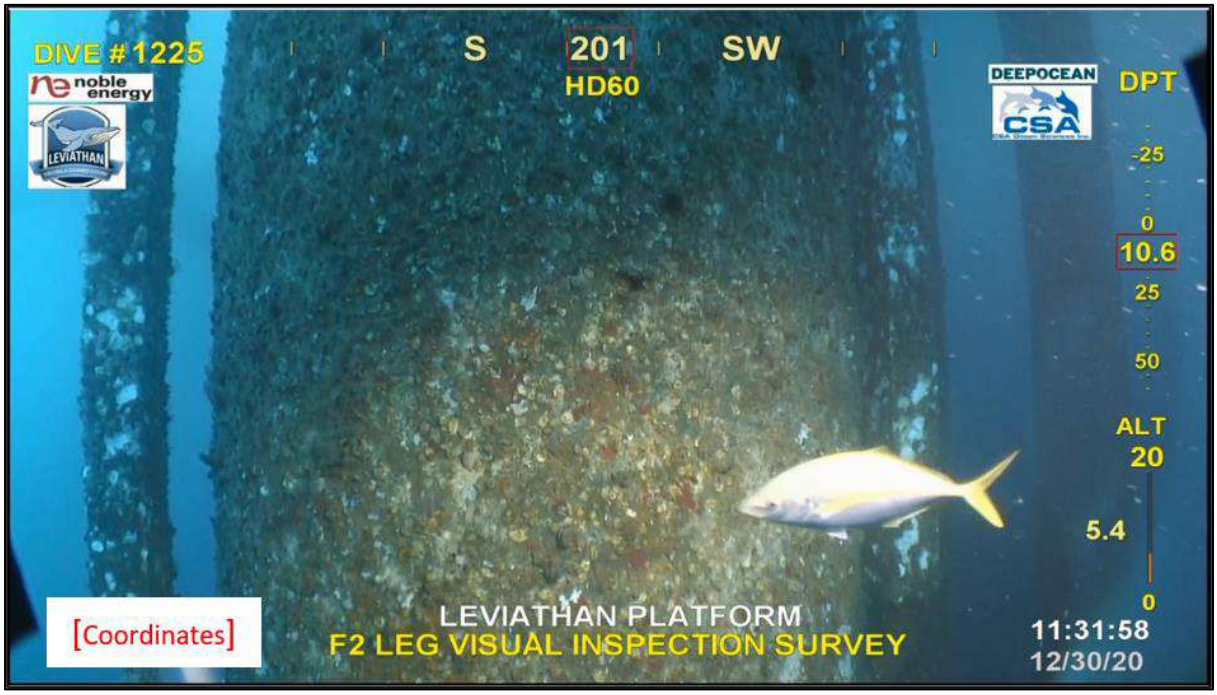


Image 11. White trevally, *Pseudocaranx dentex* at 10 m water depth on the Leviathan Production Platform's F-2 northeastern leg. Length of fish is approximately 15 cm.

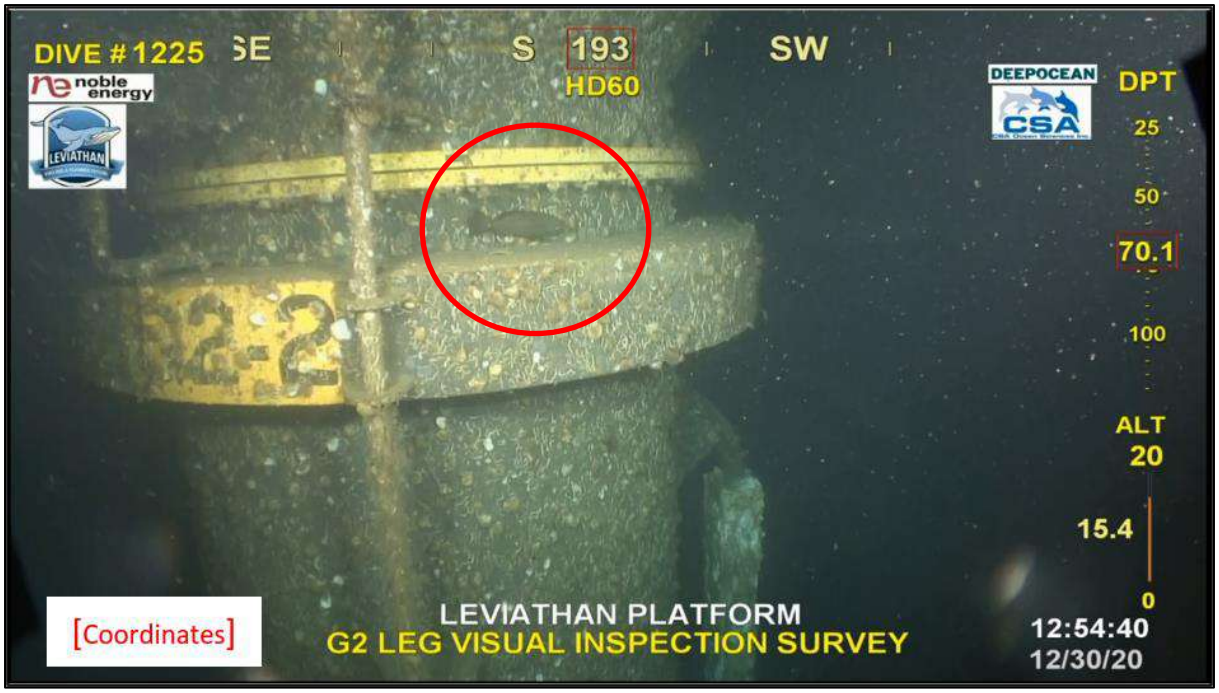


Image 12. An unidentified grouper (red circle), *Epinephelus* sp., *at* 70 m water depth on the Leviathan Production Platform's G-2 northeastern leg. Length of fish is approximately 10 cm.



Image 13. A comber, *Serranus cabrilla*, at 80 m water depth on the Leviathan Production Platform's C-2 northeastern leg. Length of fish is approximately 15 cm.

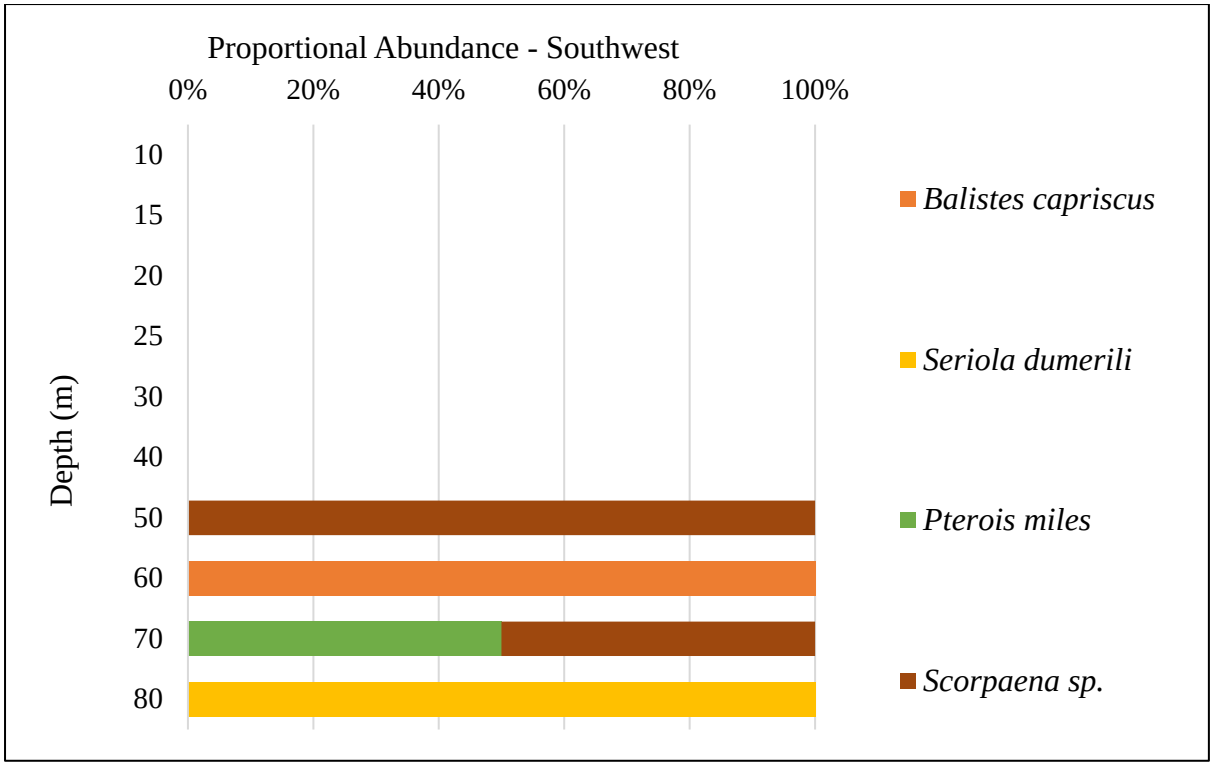


Figure 51. Proportional abundance and depth distribution of fish species found at the southwest side of the Leviathan Production Platform.



Image 14. A lionfish, *Pterois miles*, at 70 m water depth on the Leviathan Production Platform's F-2 northeastern leg. Length of fish is approximately 10 cm.

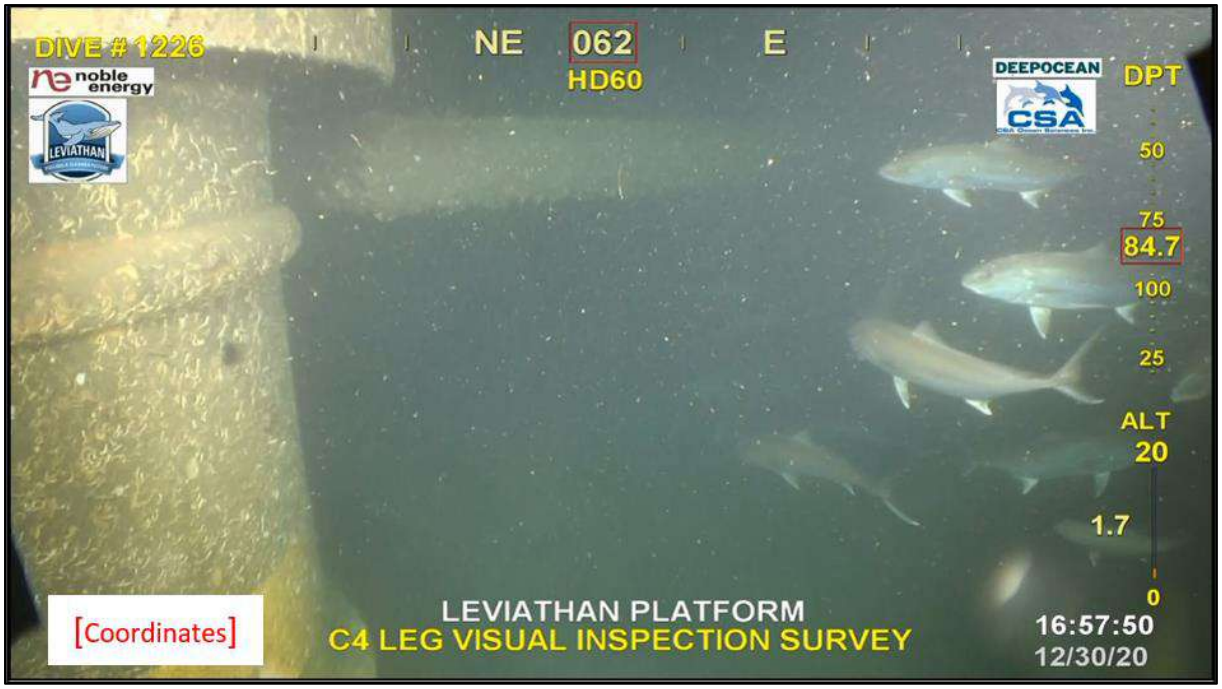


Image 15. A school of greater amberjack (*Seriola dumerili*) near 80 m water depth on the Leviathan Production Platform's C-4 northeastern leg. Length of fish are approximately 50 cm.



Image 16. A gray triggerfish (red circle), *Balistes capriscus*, at 60 m water depth on the Leviathan Production Platform's B-4 southwestern leg. Length of fish is approximately 20 cm.



Image 17. A scorpionfish (red circle) (*Scoropaena* sp.) at 70 m water depth on the Leviathan Production Platform's C-4 southwestern leg. The dual laser beams (red ovals) (10 cm apart) are displayed for size reference.

The fish species observed at the LPP were typical of those found in the region and within the habitat preferences (temperature, clarity, depth) of individual species. The entire fouling and fish communities survey was conducted during daytime with only the survey of leg C-4 ending shortly after sunset. The majority of the fish species observed were diurnal.

The relatively low taxonomic diversity, compared to other water bodies, is likely a result of the generally low Levantine Basin taxonomic diversity as well as the short timespan since the installation of the platform in mid-2019, which has thus not completed the process of colonization by both fouling organisms and fish alike.

Four of the eight species identified (greater amberjack, *Scorpaena* sp., *Epinephelus* sp., and comber) were also observed during similar surveys conducted by MVI/CSA at the Tamar and Mari-B Platforms, located approximately 120 km south of the LPP (MVI, 2019c). Several common reef-associated fishes such as rainbow wrasse (*Coris julis*), ornate wrasse (*Thalassoma pavo*), *Chromis* sp., and swallowtail sea perch (*Anthias anthias*) have been identified at the Tamar and Mari-B platforms, though not at the LPP. These species presumably colonized the platforms as planktonic larvae transported from distant spawning grounds and their absence at the LPP, which is nearer to shore by nearly14 km in comparison with the Tamar and Mari-B Platforms, is an indication that colonization of the LPP is only partially complete. In contrast, the larger species, such as

groupers, greater amberjacks, and triggerfish are capable of swimming considerable distances and likely migrated to the platforms from other locations as fully mature adults.

Several of the species observed at the LPP have also been recorded from other oil and gas platforms in the greater region. Amberjacks are present throughout the Mediterranean Sea and are well known to associate with platforms in the Adriatic and Ionian seas (Fabi et al., 2002, Fabi et al., 2004, Scarcella et al., 2011, Consoli et al., 2013). Aside from amberjacks, platforms in the Ionian Sea and Adriatic Sea also supported three more of the taxa found on the LPP platform: gray triggerfish, *Scorpaena* sp. and comber (Consoli et al., 2013). The invasive lionfish was first observed in the Mediterranean Sea, in Israel, in 1992 (Golani & Sonin, 1992) and has since been documented in increasing abundance and geographic range across both the eastern and western basins of the Mediterranean Sea (Azzurro et al., 2017, Kletou et al., 2016, Özbek et al., 2017, Zenetos et al., 2005).

One unique aspect of oil and gas platforms as fish habitat is their vertical extent, which spans from the seafloor to the surface and therefore supports species with a range of depth preferences. Fishes associated with the LPP illustrated this principle by segregating among the sampling depths. Generally, blue runner and white trevally were concentrated within the upper 30 m, while *Epinephelus* sp., comber and common lionfish were found in depths of 60 m and below. The vertical structure provides shelter at small scales (m to cm) for smaller species such as comber and cryptic species such as *Scorpaena* sp. which associates with the fouling community on the legs as well as shelter to protect from larger predator fish such as groupers and amberjacks.

The fish community varied between the northeast and the southwest faces of the platform structure. This variation may be due to several factors including number of legs surveyed (four on the northeast face and two on the southwest), the prevailing current in the area being to the southwest, the platform discharge point located adjacent to the southwest legs and the time of day during which the survey was conducted (with the northeast legs surveyed from morning to early afternoon while the southwest legs were surveyed from late afternoon to sunset).

This survey presents the initial results from a fish community assessment during the first survey conducted at the LPP since its installation and commissioning. While all fish observed are typical of the eastern Mediterranean, it is likely that fish diversity and abundance will increase in the following surveys with the continuation of colonization along this structure.

5.5.3 Hardbottom Analysis

5.5.3.1 Environmental Conditions

The environmental conditions at the hardbottom survey area were characterized by a weak near-bottom south-westerly current (up to 0.3 knots, based on ROV observations), and poor near-bottom visibility conditions (5 to 7 m) compared with the pre- and post-installation surveys conducted in 2018 and 2019. As noted in the pre- and post-installation hardbottom visual reports (MVI, 2018; 2019c) strong current speeds at the seafloor are sufficient to resuspend sediment particles from the surrounding soft bottom and to impact near-bottom visibility and re-settle on the exposed kurkar hardbottom formations. It was assumed that the biological assemblages associated with these kurkar hardbottom formations are most likely acclimated to these natural conditions and dominated by sediment tolerant biota. The premise that this high sedimentation is a chronic (and hence part of the natural variability) phenomenon was, and still is, supported by the observations of generally higher biological coverage and occurrence of less sediment tolerant biota (e.g., corals) established on more vertical and under overhanging features of the hardbottom (**Image 18**). In respect to repeated occurrences and observations of benthic invertebrates across the kurkar hardbottom environment, both on horizontal and vertical features, reduced sediment cover at some of the inspected kurkar hardbottom features during the 2020 LPP EMS allowed a corroboration of this premise.

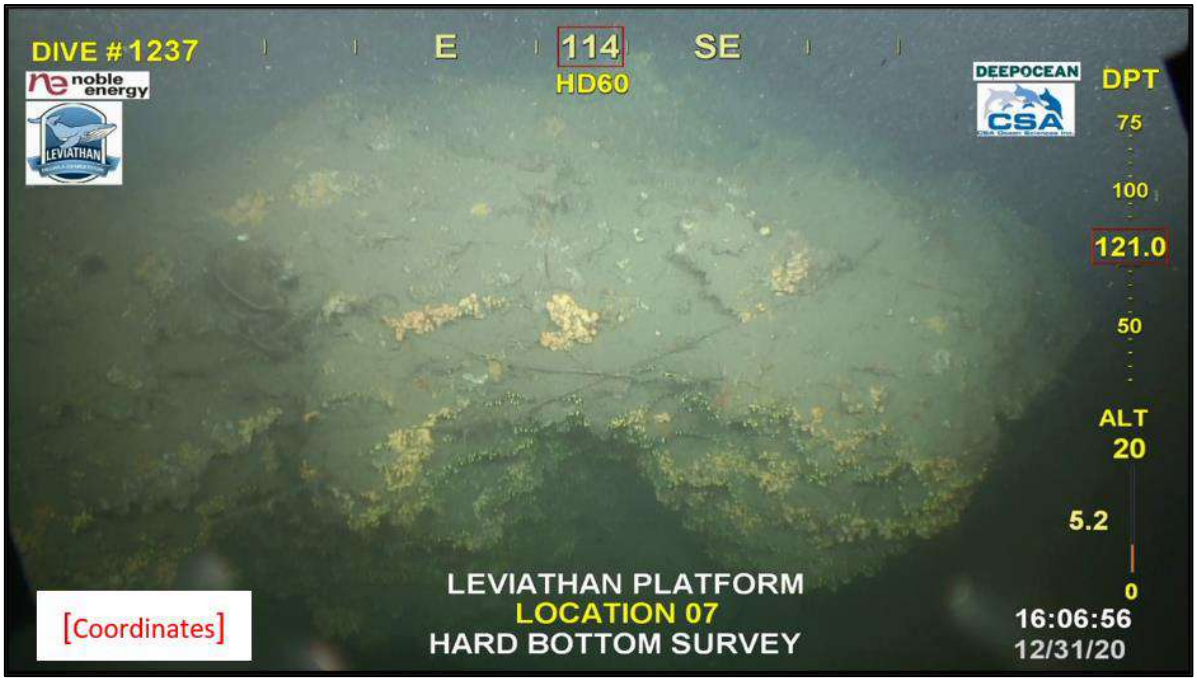


Image 18. The more vertical and underside of overhanging features of the hardbottom appears to support generally higher biological coverage and occurrence of less sediment tolerant biota (e.g. corals). Image was taken during the 2020 Leviathan Production Platform Environmental Monitoring Survey at Location 7 approximately 3.9-km from the LPP.

5.5.3.2 Anthropogenic Debris

A large amount of anthropogenic debris was observed within the survey area. The debris, primarily related to commercial fishing (**Image 19**), included monofilament line, steel cables, weighted nets, warp wires, and bridles; other anthropogenic debris of unknown origin was observed during this survey as they were observed as well during the pre- and post-installation surveys. It is important to note that although the LPP is in active production of natural gas, fishing trawlers can continue to operate in this offshore area as the LPP exclusion zone boundaries are limited to approximately 3-kilometer radius around the platform. Although there was an official government decision made on regional banning of fishing activities north of Dor-HaBonim area at all water depths within the Israeli territorial waters (2016 update to fishing regulations) trawling vessels are still sighted around the LPP deploying nets and potentially causing additional damages to these kurkar hardbottom formations and the associated benthic communities (author's personal observations). Trawl fishing activities with potential impacts including direct contact with hardbottom, disruption of surface sediment binding by microbiota, and localized resuspension of sediments, could confound an assessment of any impact potentially caused by the LPP.

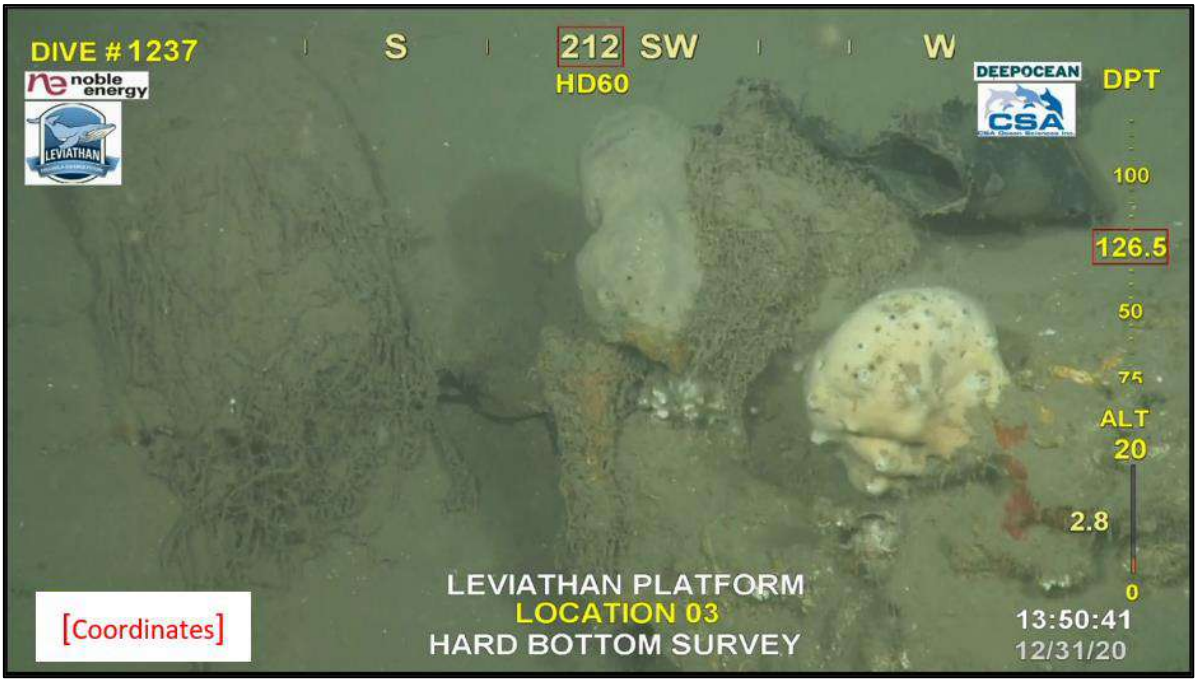
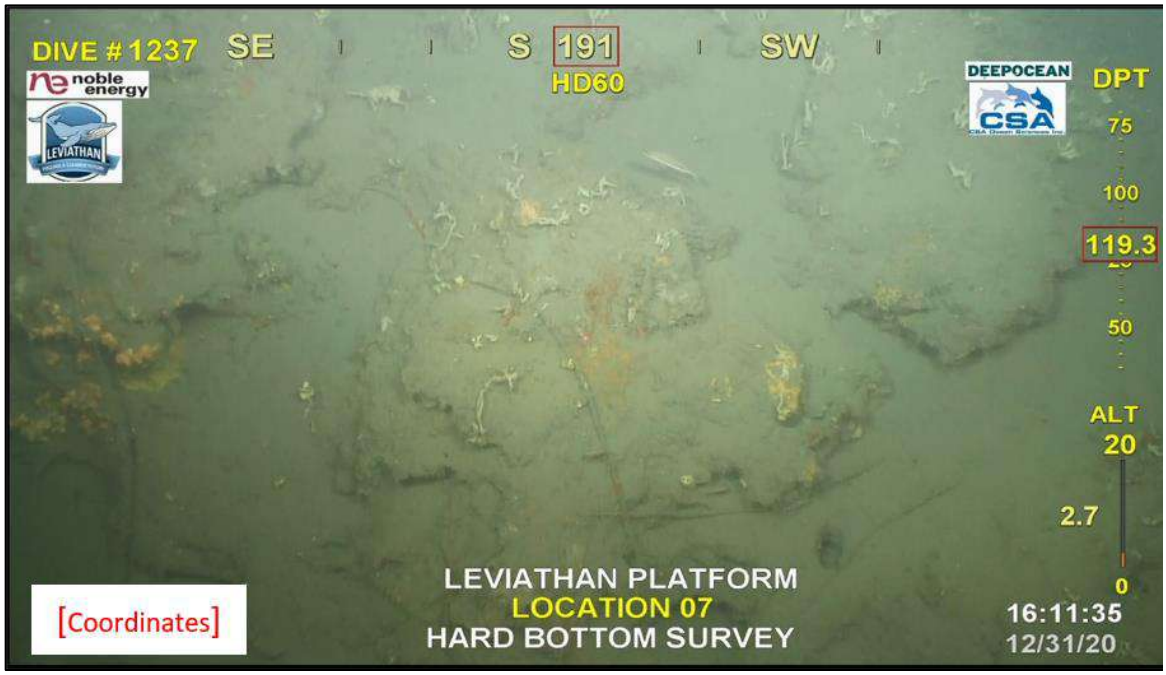


Image 19. Anthropogenic debris, primarily related to commercial fishing, was commonly observed during the 2020 Leviathan Production Platform Environmental Monitoring Survey. Image was taken approximately 3.5 km north of the LPP.

5.5.3.3 Benthic and Ichthyofaunal Assemblages

As seen in the pre- and post-installation surveys, the monitored hardbottom formations had relatively variable biological coverage qualitatively estimated to range from <1% up to 25% for horizontal surface/topsides (**Image 20a**) and up to 75% in some of the vertical surfaces/overhangs (**Image 20b**). Reduced sediment cover on several of the horizontal surfaces of the kurkar hardbottom features resulted in biological cover qualitatively estimated at the higher end of this range. Biological coverage was mainly composed of encrusting/boring, erecting, and bulky sponges (**Image 21a**, **21b,** and **21c**); other visual prominent biota included Cnidarians (corals, sea anemones, and hydroids; **Images 22a**, **22b**, and **22c**), Annelida (polychaete, serpulid and sabellid worms; **Image 23a** and **23b**), Echinodermata (sea urchins and starfishes; **Images 24a** and **24b**), Bryozoans, and Decapoda (shrimp and lobsters). *Caulerp*a sp. was the only documented floral taxon (**Image 25**), which was also observed during the post-installation survey. The composition of the hardbottom benthic assemblage appears to be temporally consistent with no visually detectable proliferation or loss of prominent biota. There were no new visibly documented benthos compared with those observed during the pre- and post-installation surveys. Lists of previously documented marine fauna within the kurkar hardbottom environment can be found in previously submitted visual surveys reports (MVI, 2018; 2019b).

a)

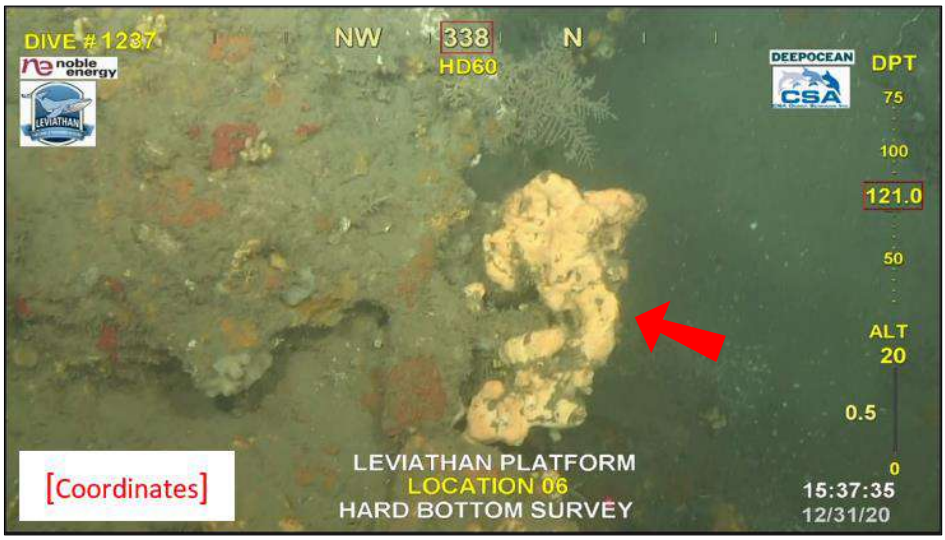


b)

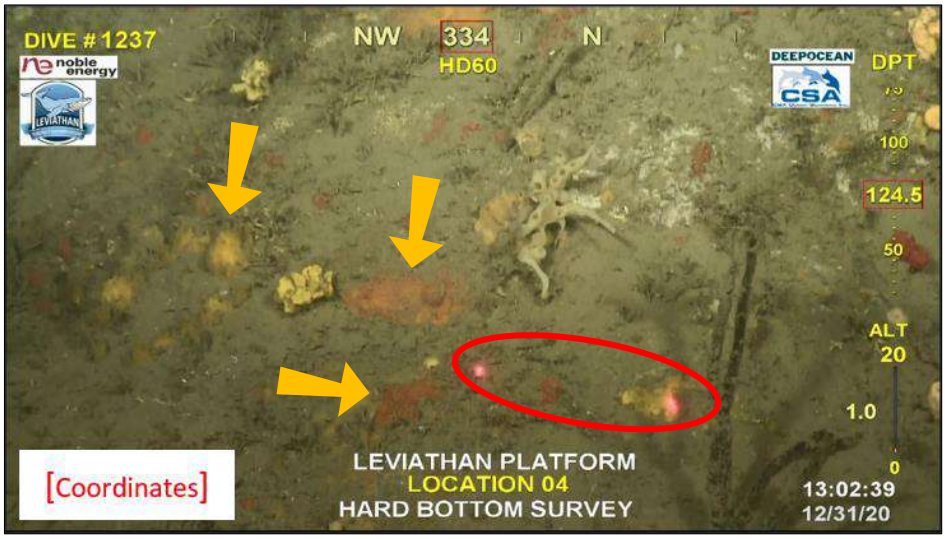


Image 20. Faces of the kurkar hardbottom features.
a) horizontal surface (topside) of kurkar hardbottom feature showing biological coverage of up to 25% from Location 7. b) Vertical surface (overhangs) of kurkar hardbottom feature showing biological coverage of up to 75% from Location 8. Vertical surfaces were void of most sediment cover that characterized the topsides of the kurkar hardbottom features.

a)



b)



c)

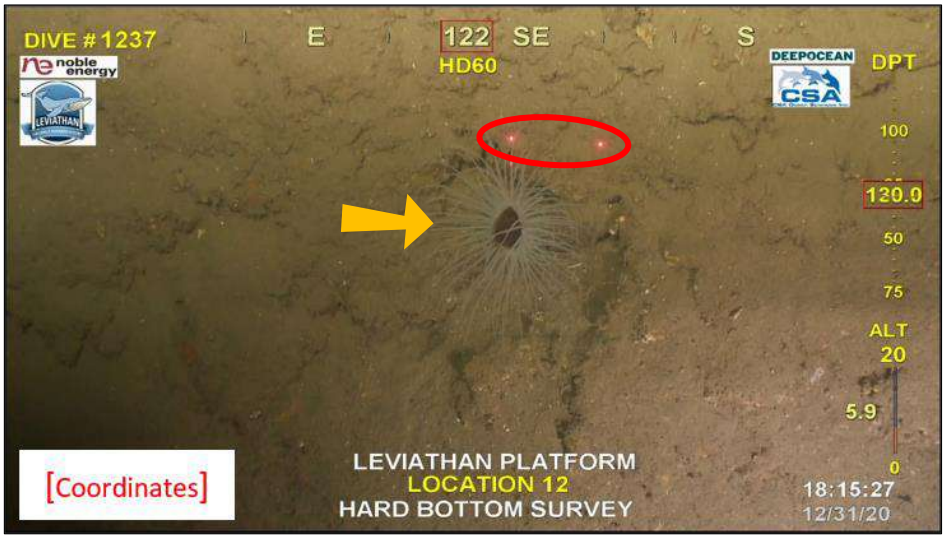


Image 21. Some of the sponge morphologies observed across the kurkar hardbottom features. a) bulky sponge (red arrow) from Location 6, b) encrusting sponges (orange arrows) from Location 4, and c) erecting sponge (blue arrow) from Location 7. The dual laser beams (red ovals) (10 cm apart) are displayed for size reference.

a)



b)



c)

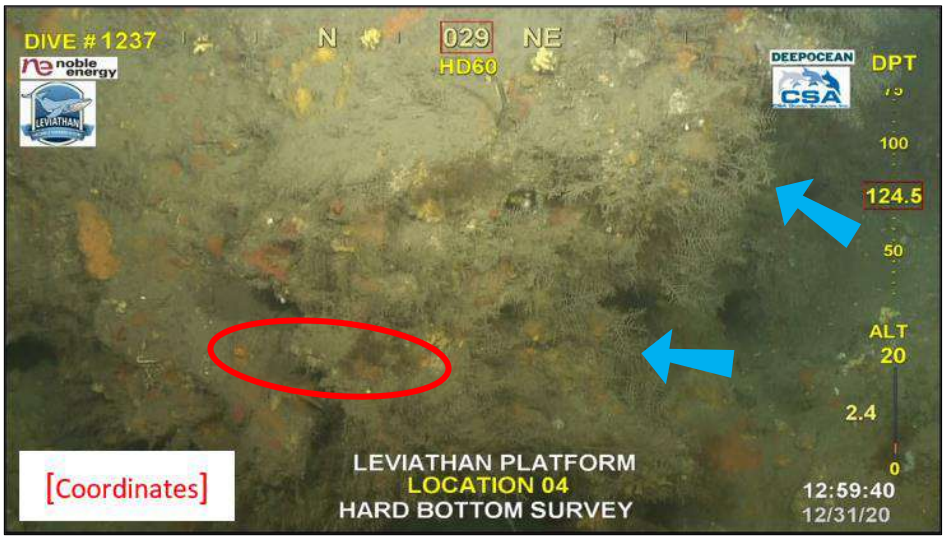
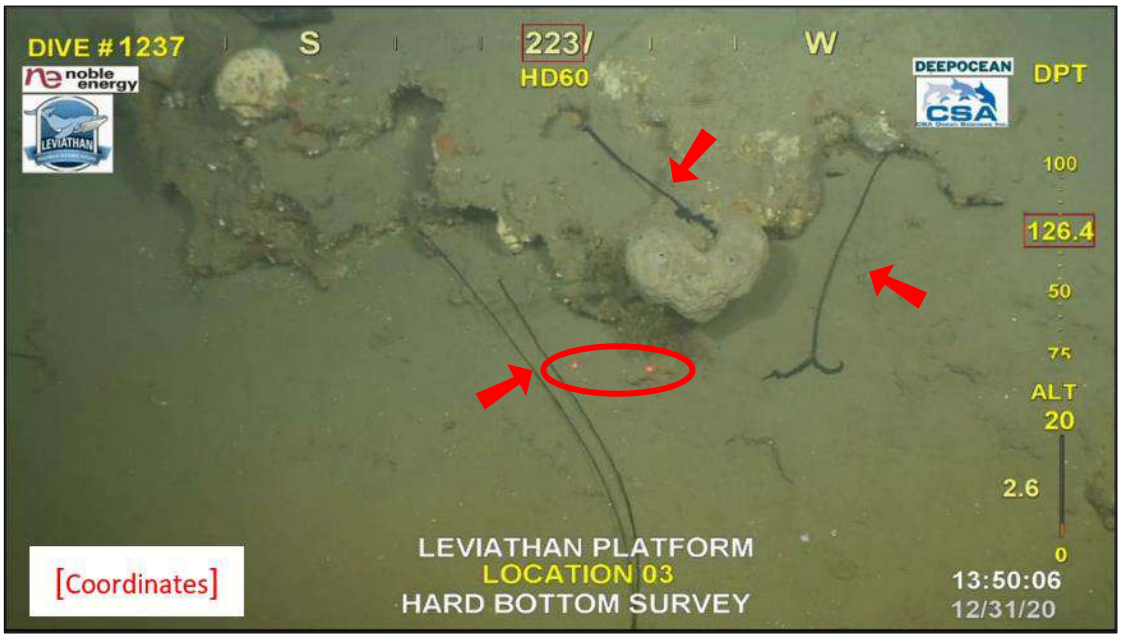


Image 22. Cnidarians observed across the kurkar hardbottom features.
a) cup corals (red arrows) from Location 8, b) sea anemone (orange arrow) from Location 12, and c) hydroids (blue arrows) from Location 4. The dual laser beams (red ovals) (10 cm apart) are displayed for size reference.

a)



b)

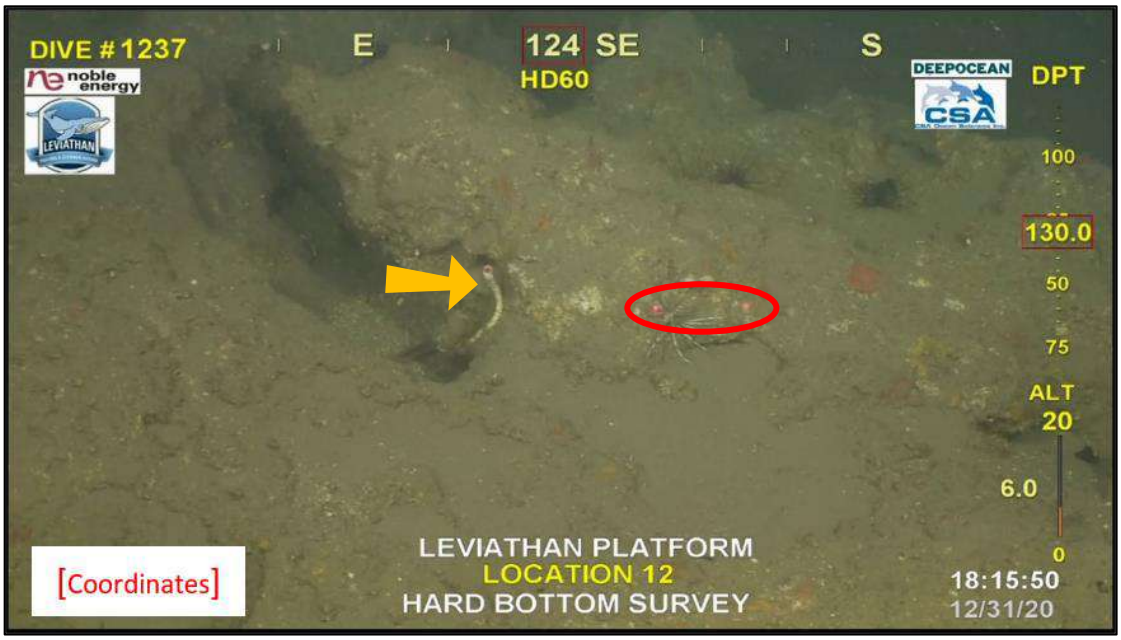
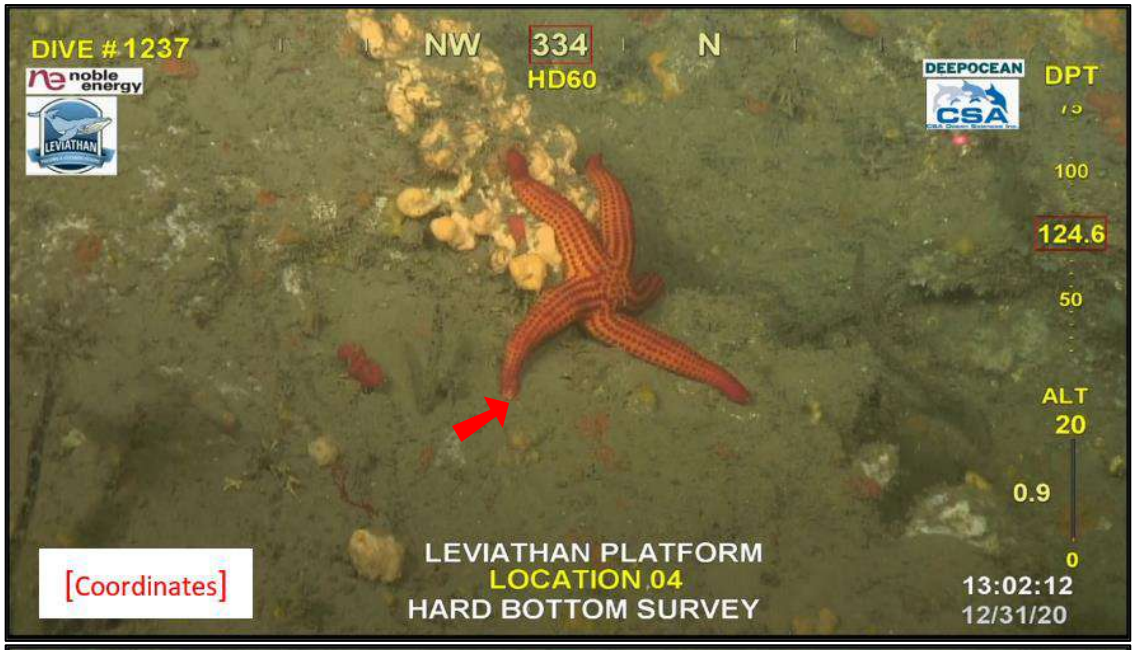


Image 23. Annelida taxa observed across the kurkar hardbottom features.
a) spoon worms (Polychaeta: *Bonellia viridis*) (red arrows) from Location 3, and b) tube worms (Serpulidae) (orange arrow) from Location 12. The dual laser beams (red ovals) (10 cm apart) are displayed for size reference.

a)



b)

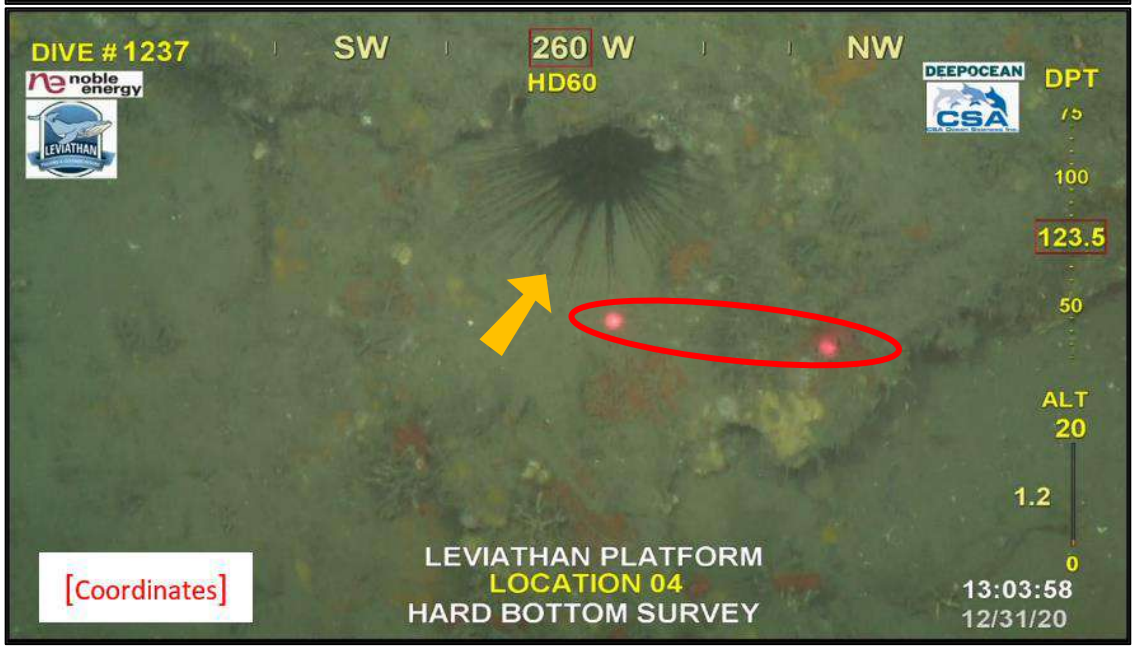


Image 24. Echinodermata taxa observed across the kurkar hardbottom features.
a) Sea star (Asterroidea: *Echinaster sepositus*) (red arrow), and b) sea urchin (Echinoidea: *Centrostephanus longispinus*) (orange arrow). The dual laser beams (red oval) (10 cm apart) are displayed for size reference.

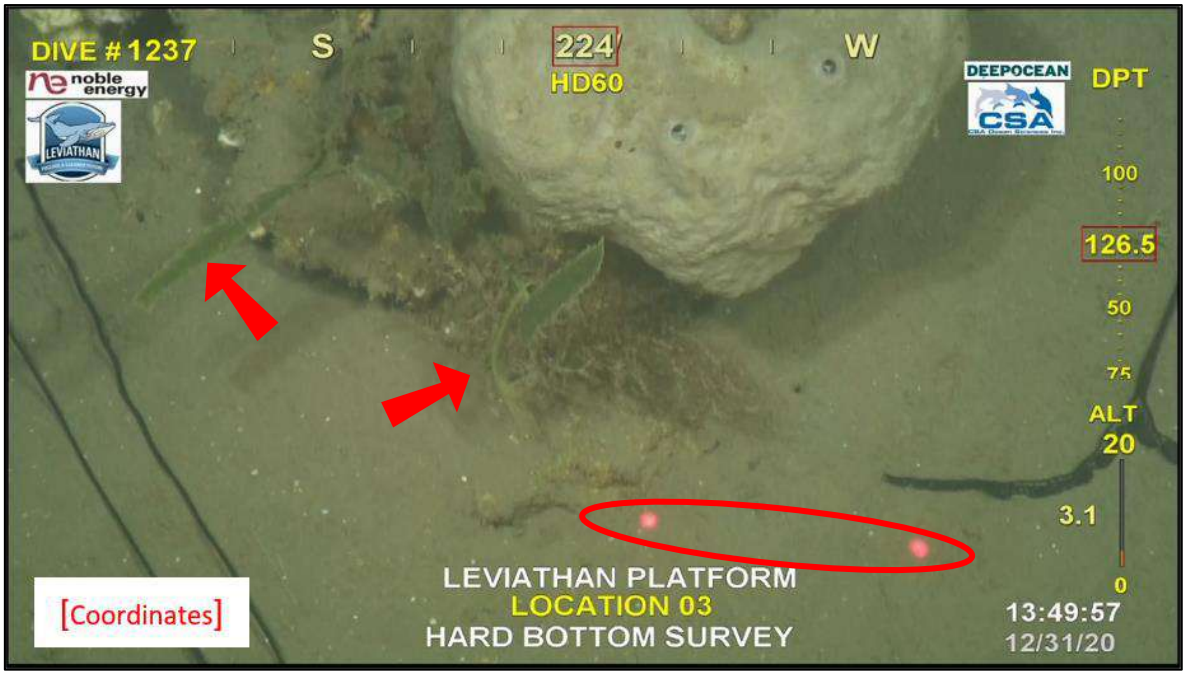


Image 25. The green algae, *Caulerpa* sp. (red arrows). The dual laser beams (red oval) (10 cm apart) in are displayed for size reference.

It should be noted that the visual observation methodology was different between the pre-installation and subsequent surveys. Observations during the pre-installation survey were made using ROV transects to identify hardbottom areas, while observations during all later surveys used 360° inspections to characterize known areas of hardbottom.

The ichthyofauna within the survey area was visually estimated to be quite similar to the pre- and post-installation surveys and included observations of planktivorous fishes (**Image 26**), leopard spotted gobies (**Image 27**), common lion fishes (**Image 11**), Mediterranean rainbow wrasses (**Image 9**), red porgies (**Image 29**), groupers (*Epinephelus* spp.), greater amberjacks (**Image 30**), the Large-scaled scorpionfish (**Image 31**), the Mediterranean moray eel (**Image 32**), and the European conger eel (**Image 33**). Schools of juvenile and adult fish were commonly observed in association with the hardbottom formations. The low near-bottom visibility precluded the collection of continuous long-range observations of hardbottom associated fish.

Based on the qualitative visual data (still and video imagery) collected during the 2020 LPP EMS, there was no visually detectable negative temporal changes to the hardbottom benthic environment in relatively close proximity to the LPP from the two previous survey events (pre- and post-installation) conducted in 2018-2019.

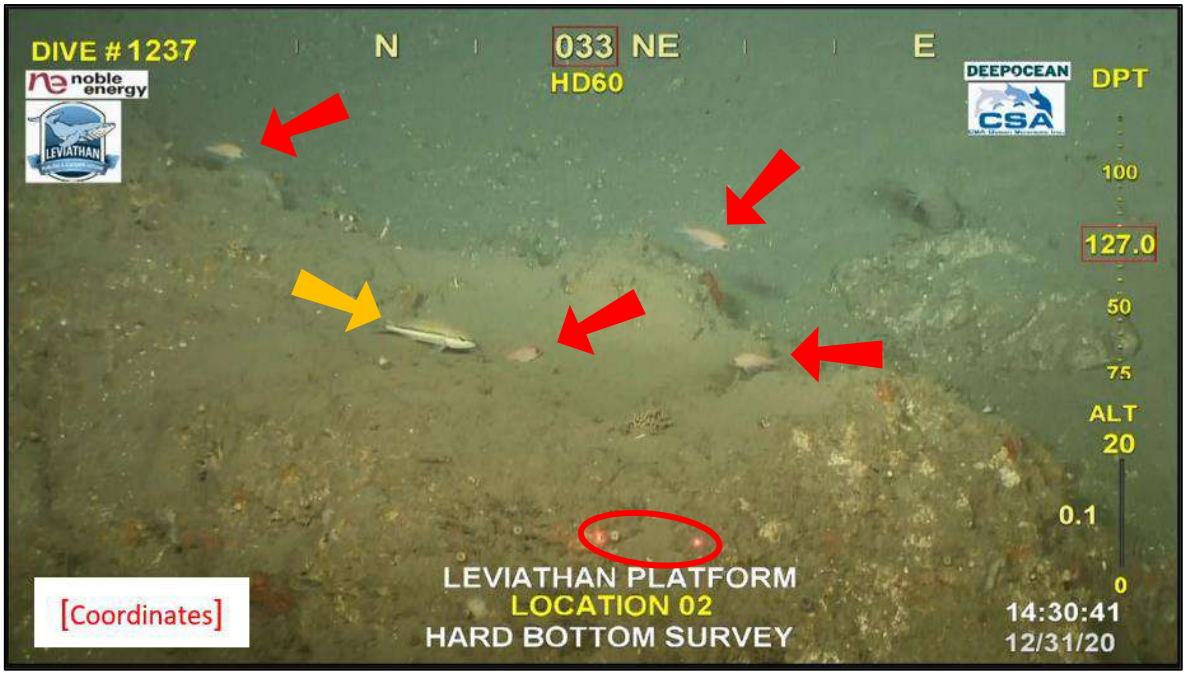


Image 26. Planktivorous fishes (*Anthias* sp.) (red arrows), and Mediterranean rainbow wrasses (*Coris julis*) (orange arrow). The dual laser beams (red oval) (10 cm apart) are displayed for size reference.

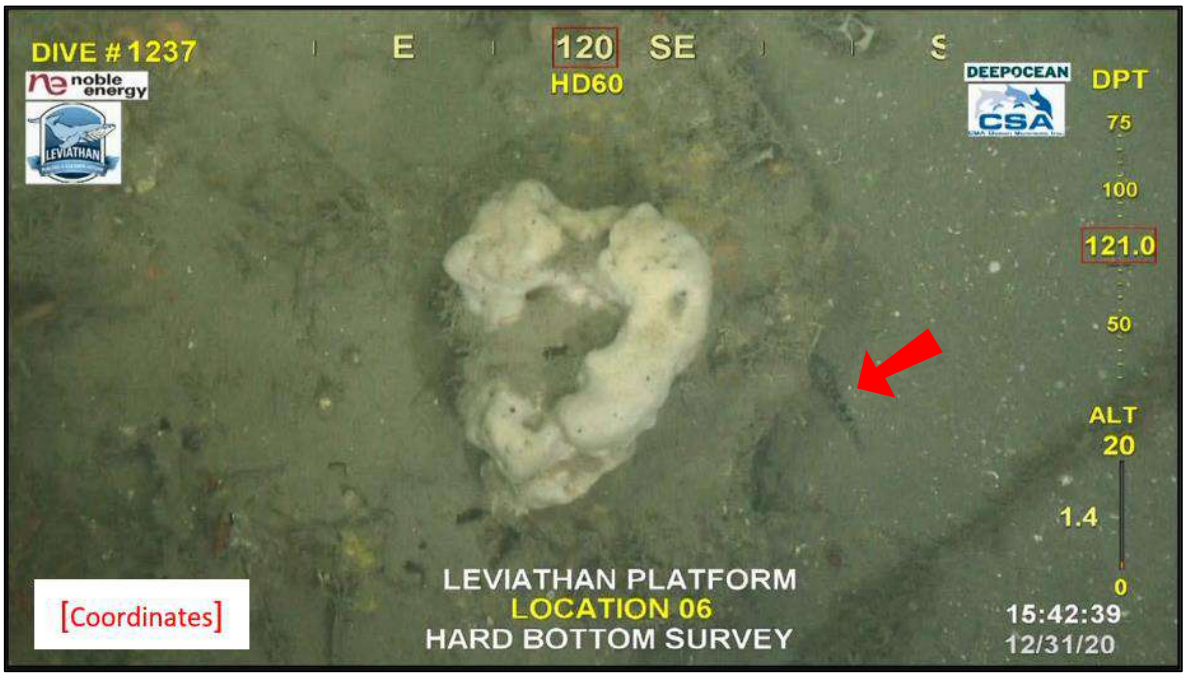


Image 27. A leopard spotted goby (*Thorogobius ephippiatus*) (red arrow).

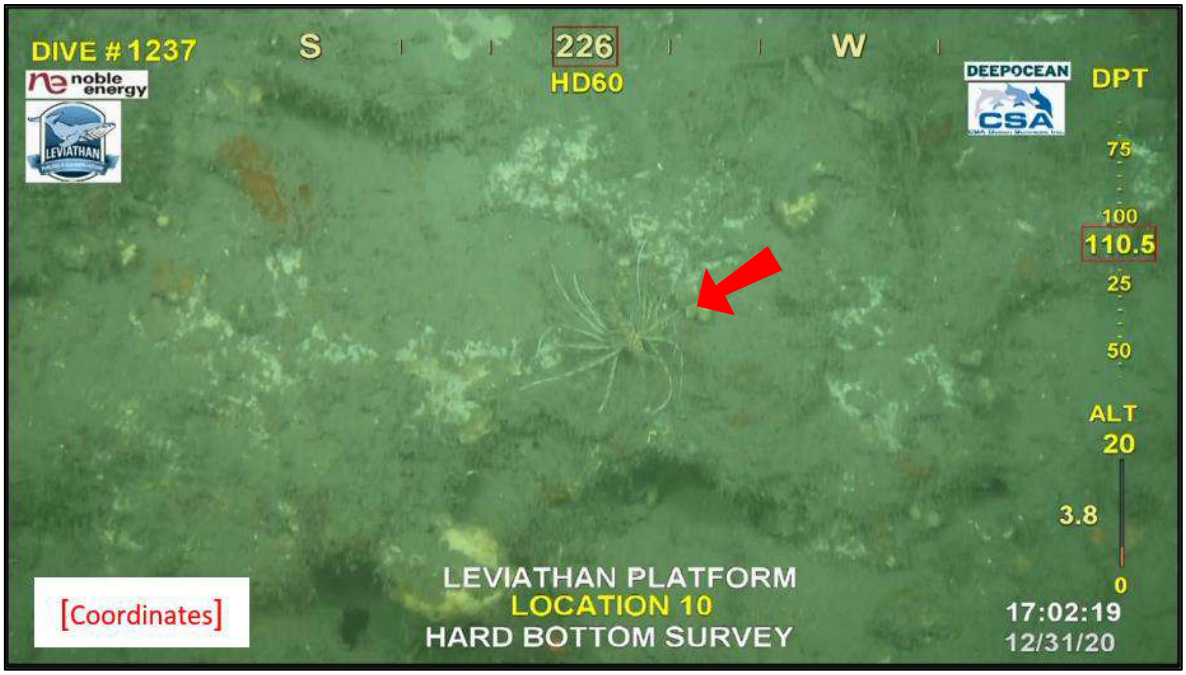


Image 28. A common lionfish (*Pterois miles*) (red arrow).

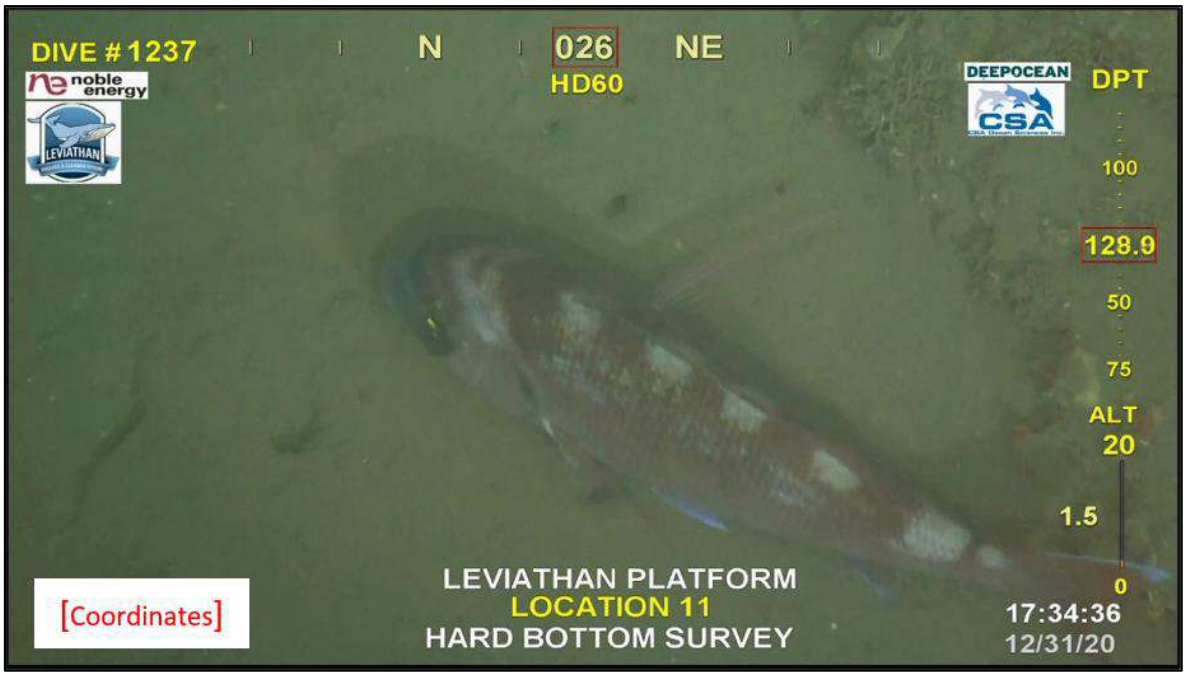


Image 29. A red porgy (*Pagrus pagrus*).

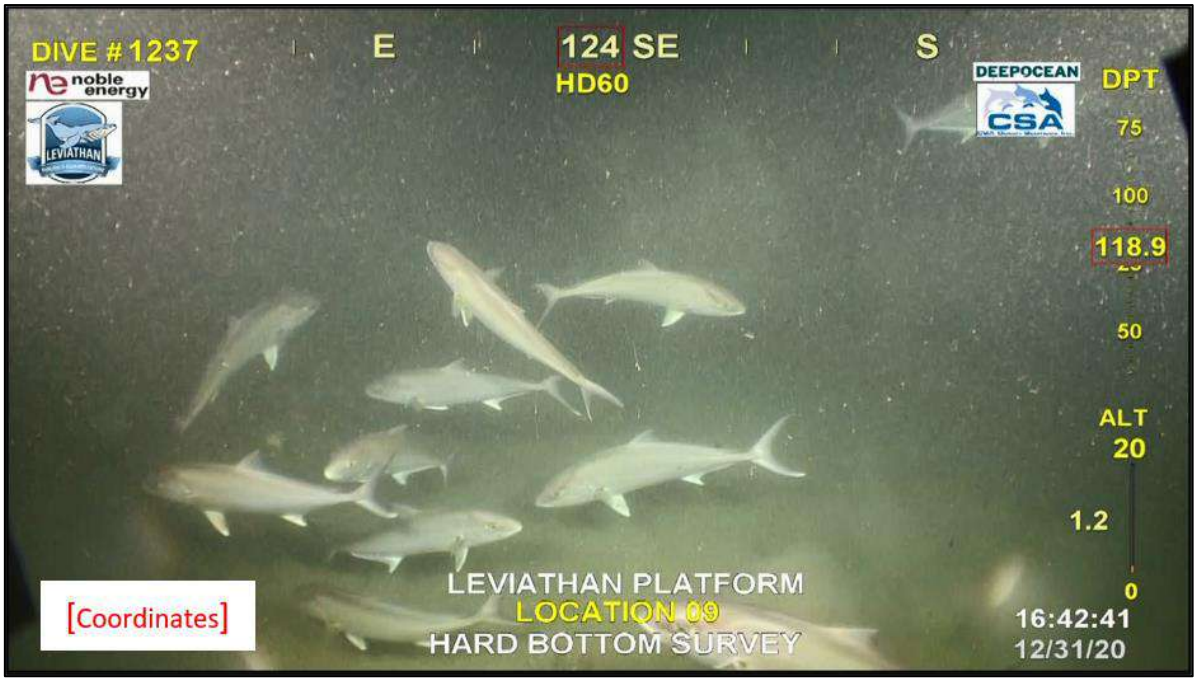


Image 30. Greater amberjacks (*Seriola dumerili*). As can be seen in the image, the amberjacks were responsible for suspending sediments from the seafloor and increasing turbidity at this location, as well as at several other locations.

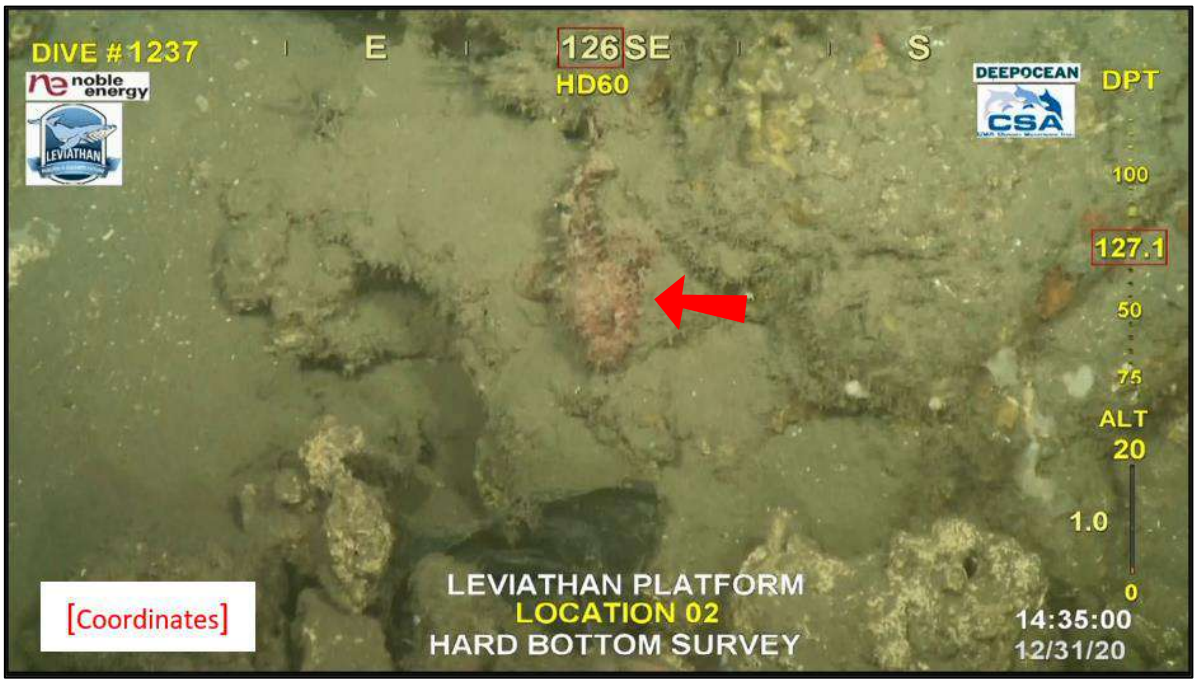


Image 31. The large-scaled scorpionfish (*Scorpaena scrofa*) (red arrow).

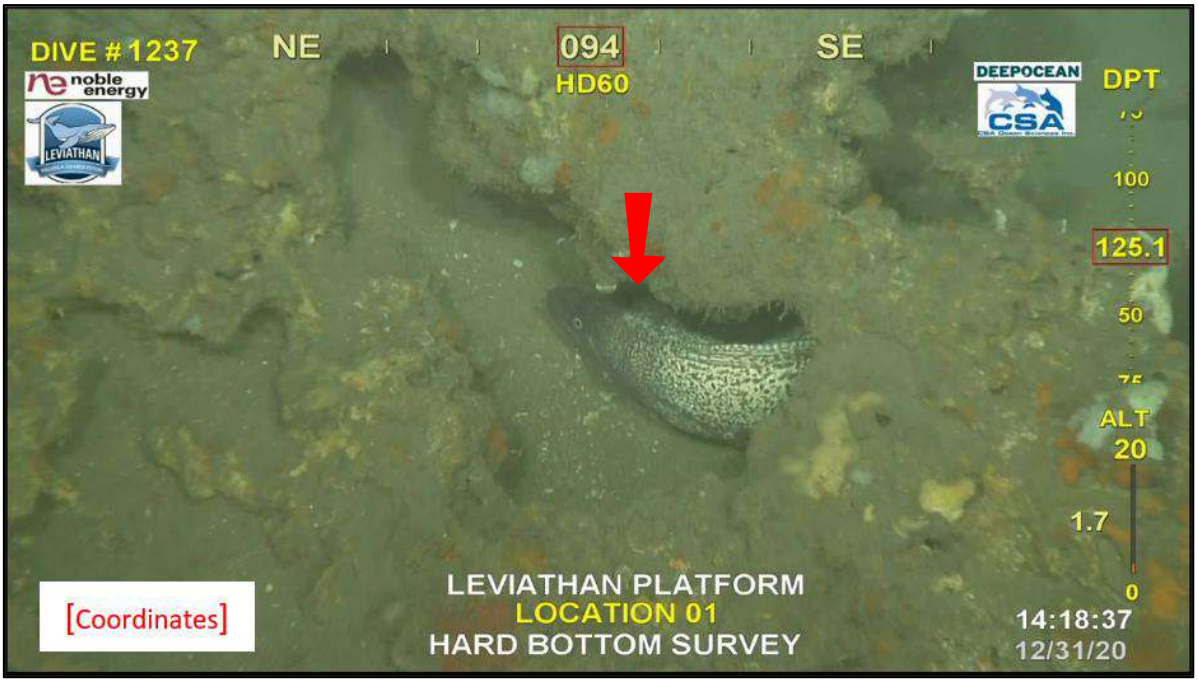


Image 32. The Mediterranean moray eel (*Muraena helenae*) (red arrow).

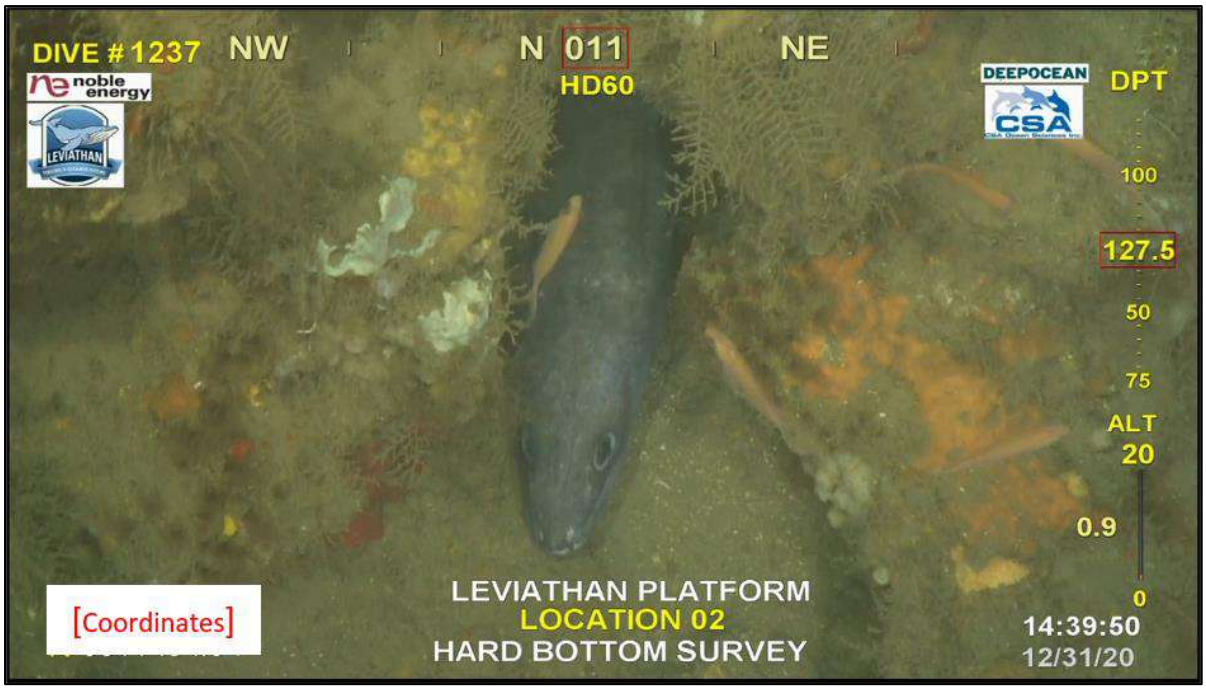
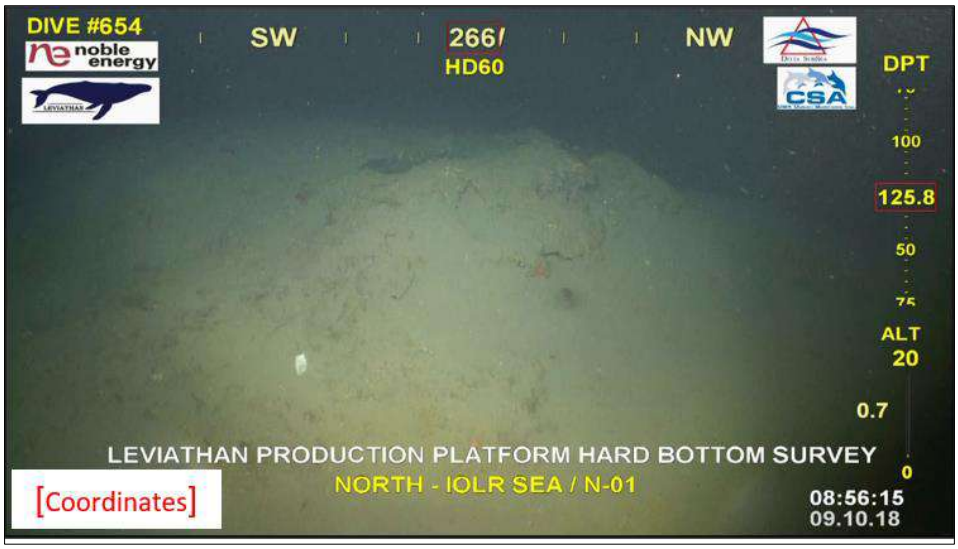


Image 33. The European conger eel (*Conger conger*).

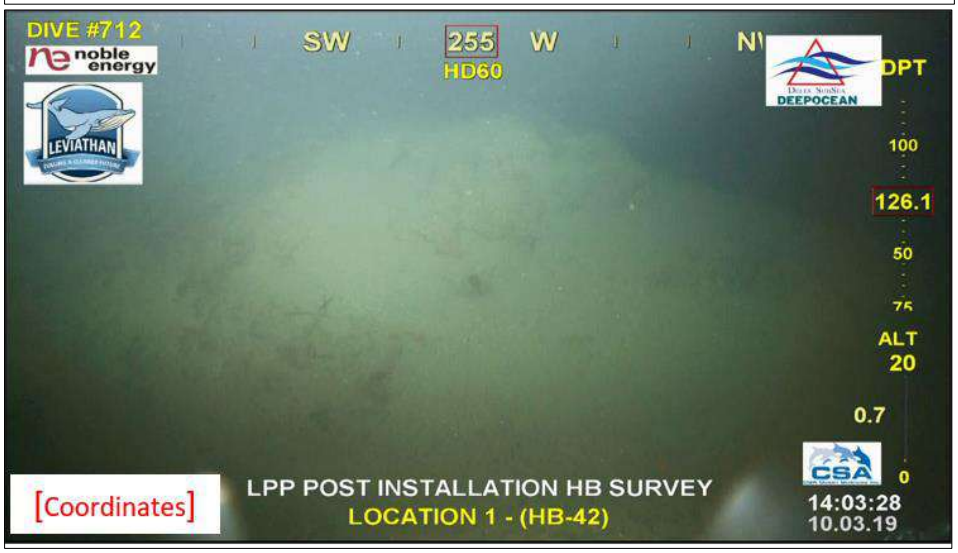
5.5.3.4 Comparative Imagery

Comparative images (Images 34 through 45) for each of the 12 monitoring locations are presented for the pre-installation and post-installation hardbottom survey, and the 2020 LPP EMS. Each triplet of images shows the same view of each hardbottom feature from the pre- and post-installation surveys (2018-2019) and the 2020 LPP EMS. These images can be considered as representative of observed features at each of the selected monitoring locations. Murky near-bottom visibility during the 2019 post-installation survey is evident throughout the images of this survey. Conversely, improved visibility during the 2020 LPP EMS and reduced sediment cover on the horizontal kurkar features are evident throughout the images of this survey. Some images show increased turbidity and murkiness; however, those were caused by nearby amberjacks that swam around the ROV and suspended sediments off the seafloor (**Image 30**).

a)



b)



c)

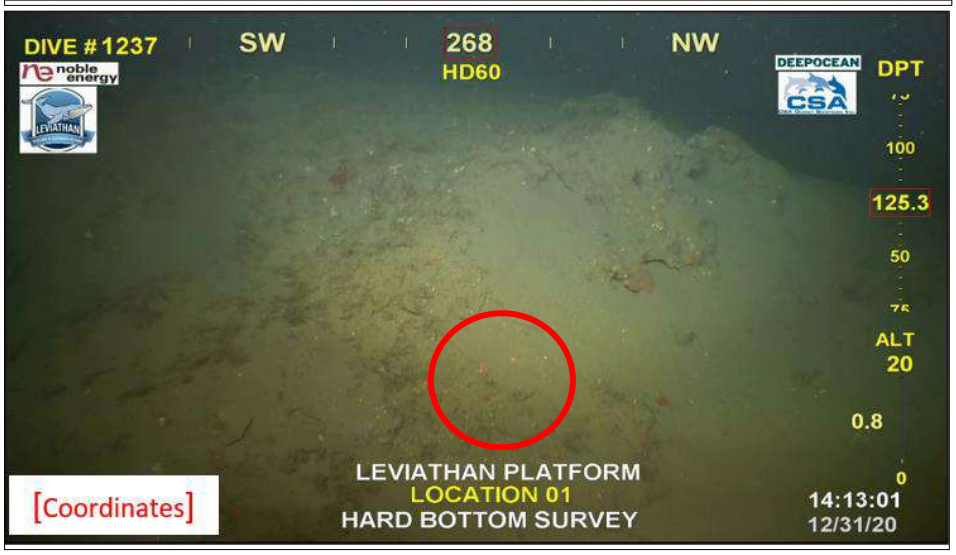
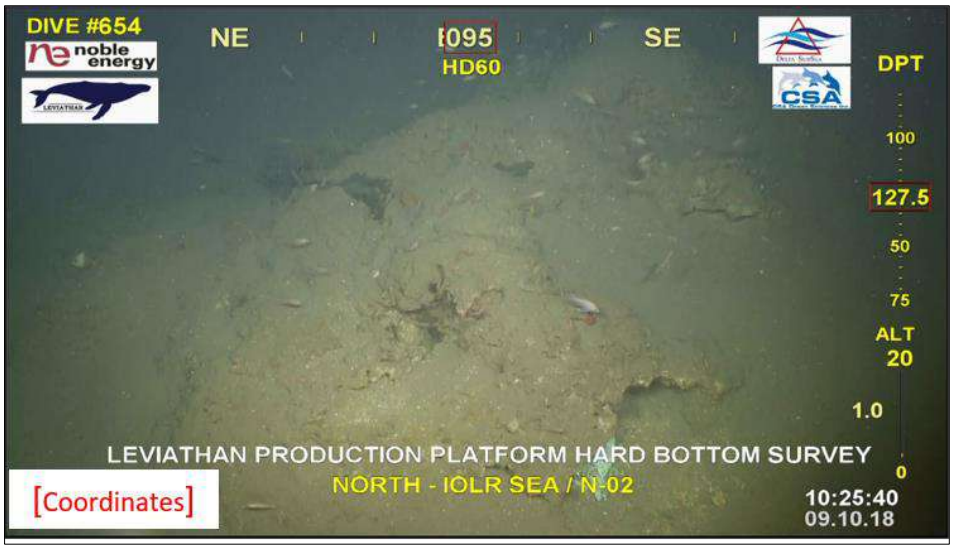


Image 34. A comparative view of the seafloor at Location 1 with a) taken during the pre-installation survey, b) taken during the post-installation survey, and c) taken during the 2020 Leviathan Platform Environmental Monitoring Survey. The dual laser beams (red circle) (10 cm apart) are displayed for size reference.

a)



b)



c)

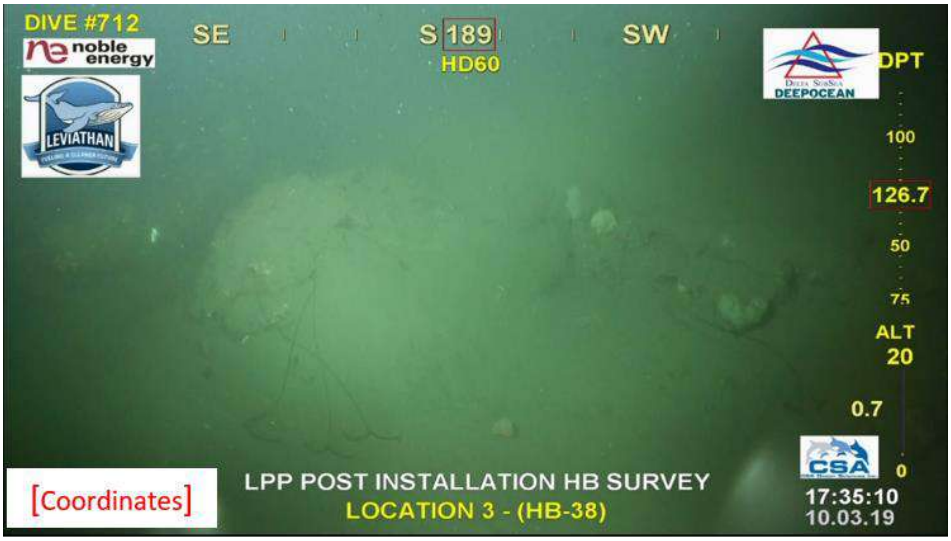


Image 35. A comparative view of the seafloor at Location 2 with a) taken during the pre-installation survey, b) taken during the post-installation survey, and c) taken during the 2020 Leviathan Platform Environmental Monitoring Survey. The dual laser beams (red circle) (10 cm apart) are displayed for size reference.

a)



b)



c)

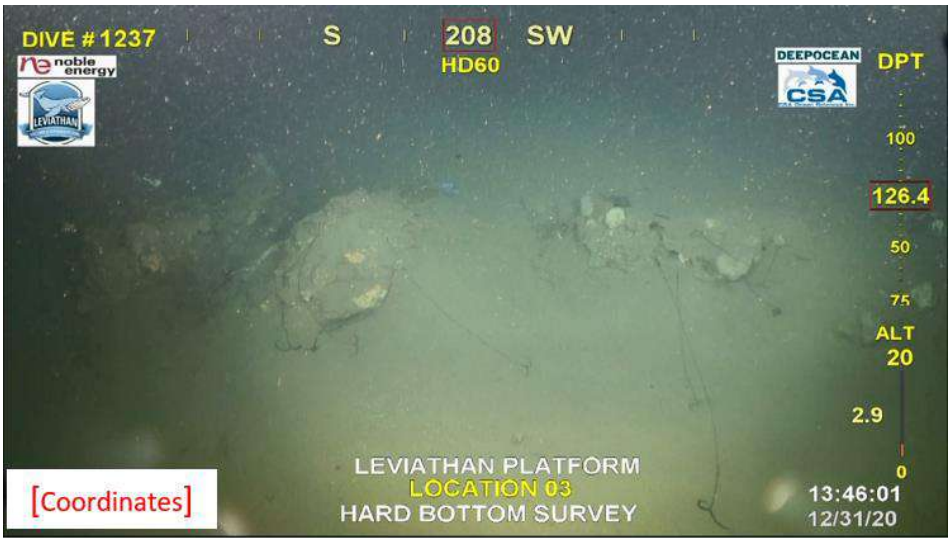
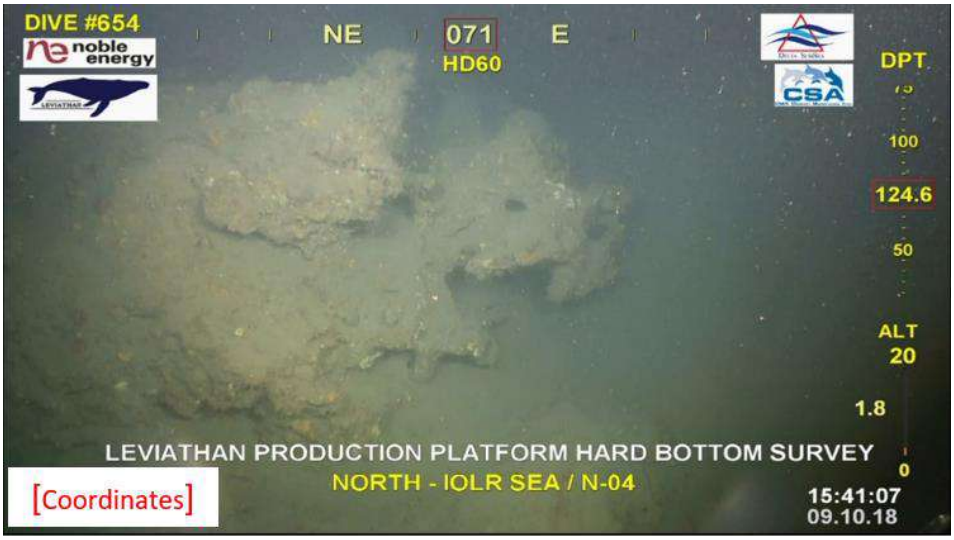


Image 36. A comparative view of the seafloor at Location 3 with a) taken during the pre-installation survey, b) taken during the post-installation survey, and c) taken during the 2020 Leviathan Platform Environmental Monitoring Survey.

a)



b)



c)

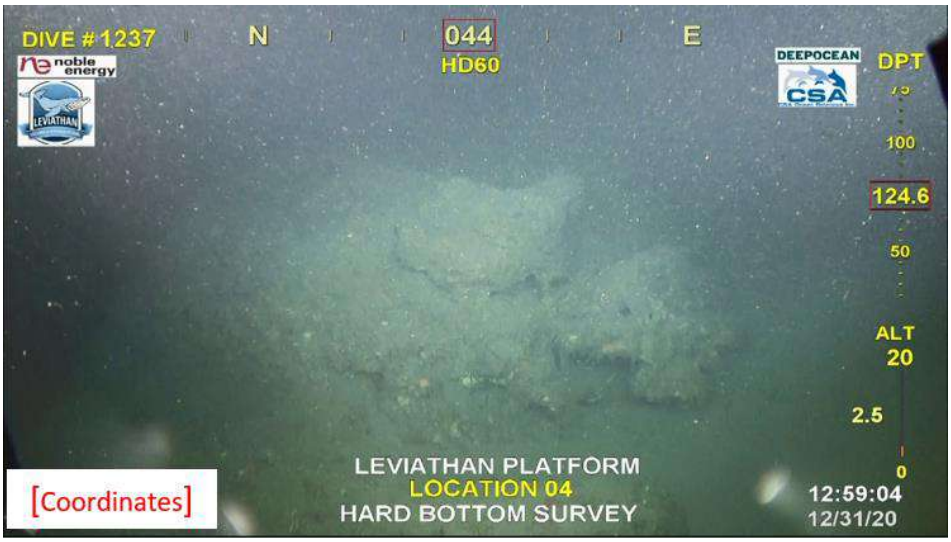
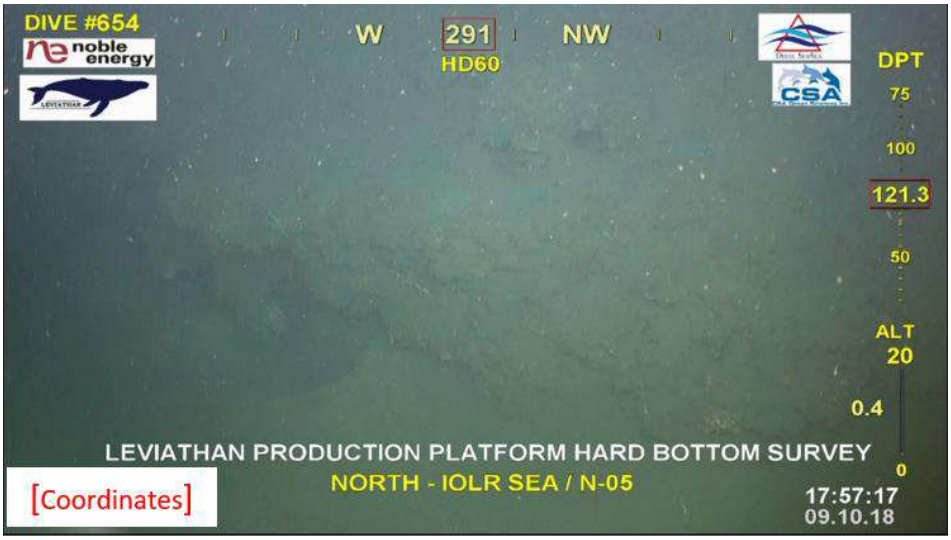


Image 37. A comparative view of the seafloor at Location 4 with a) taken during the pre-installation survey, b) taken during the post-installation survey, and c) taken during the 2020 Leviathan Platform Environmental Monitoring Survey.

a)



b)



c)

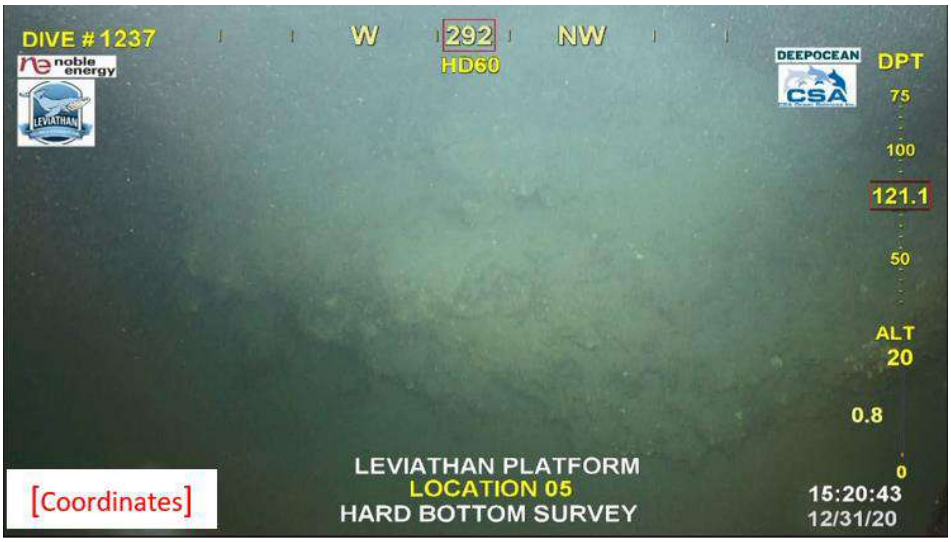
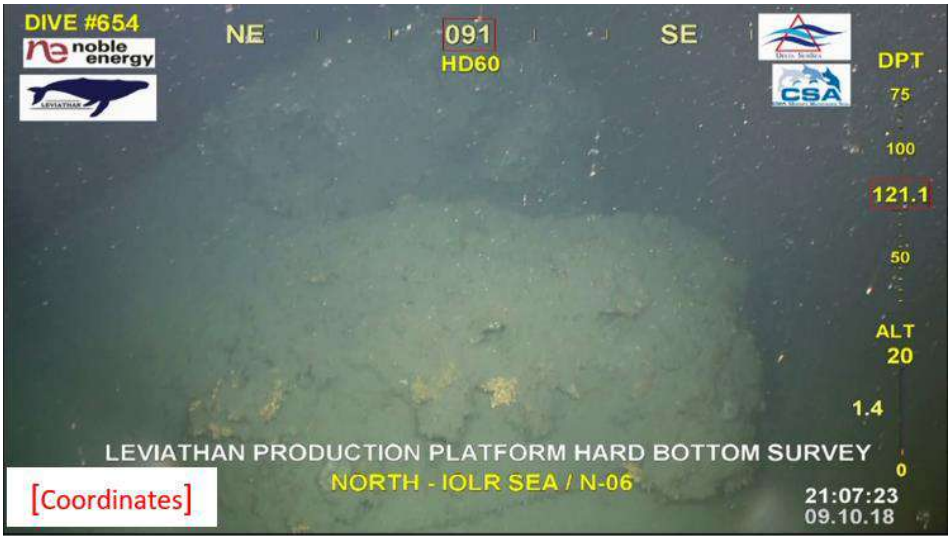
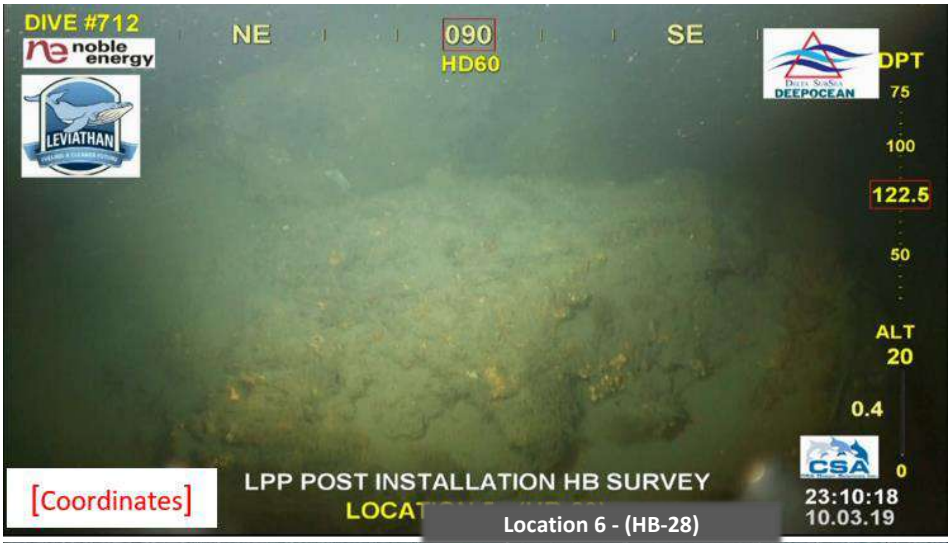


Image 38. A comparative view of the seafloor at Location 5 with a) taken during the pre-installation survey, b) taken during the post-installation survey, and c) taken during the 2020 Leviathan Platform Environmental Monitoring Survey.

a)



b)



c)

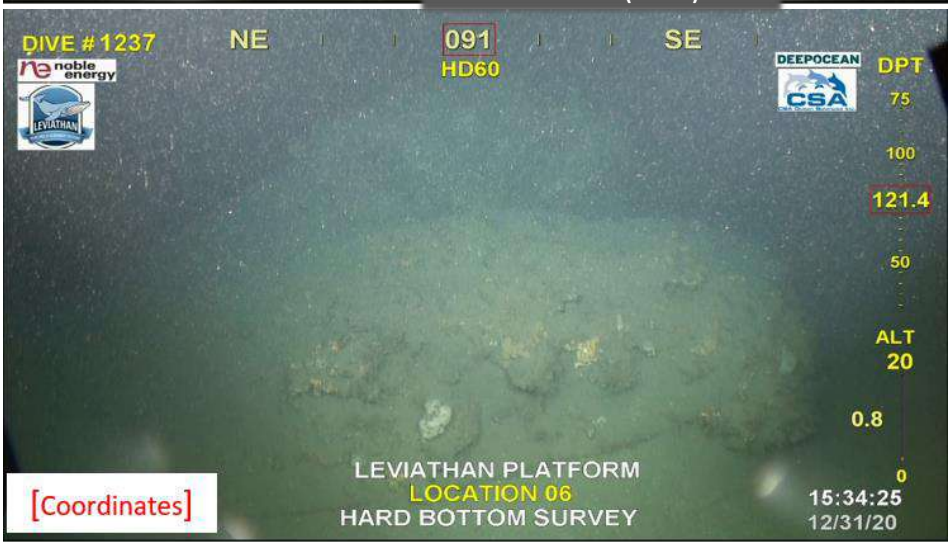
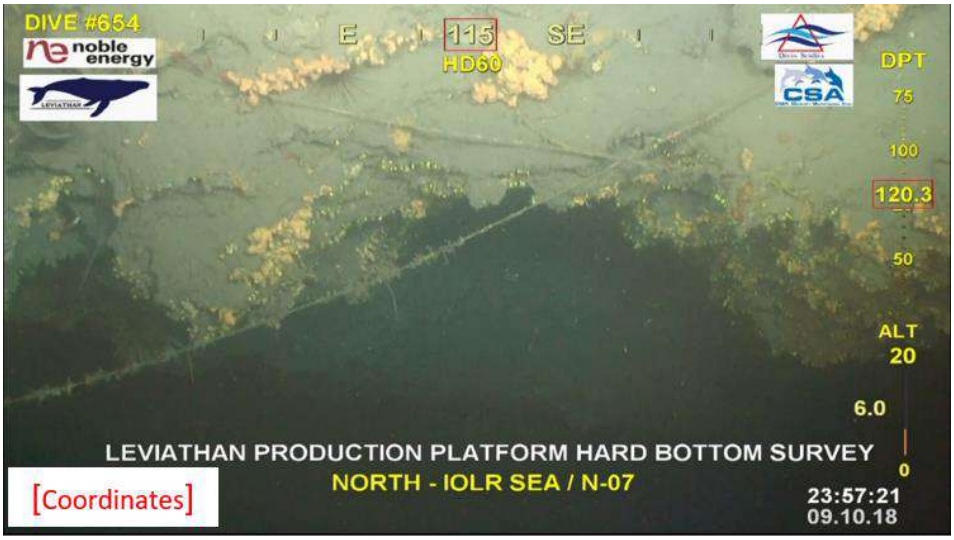


Image 39. A comparative view of the seafloor at Location 6 with a) taken during the pre-installation survey, b) taken during the post-installation survey, and c) taken during the 2020 Leviathan Platform Environmental Monitoring Survey.

a)



b)



c)

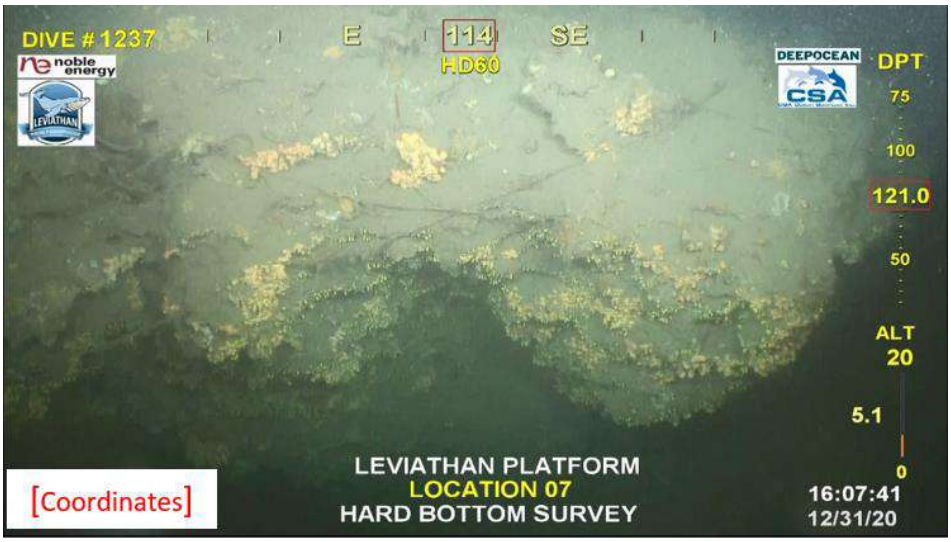
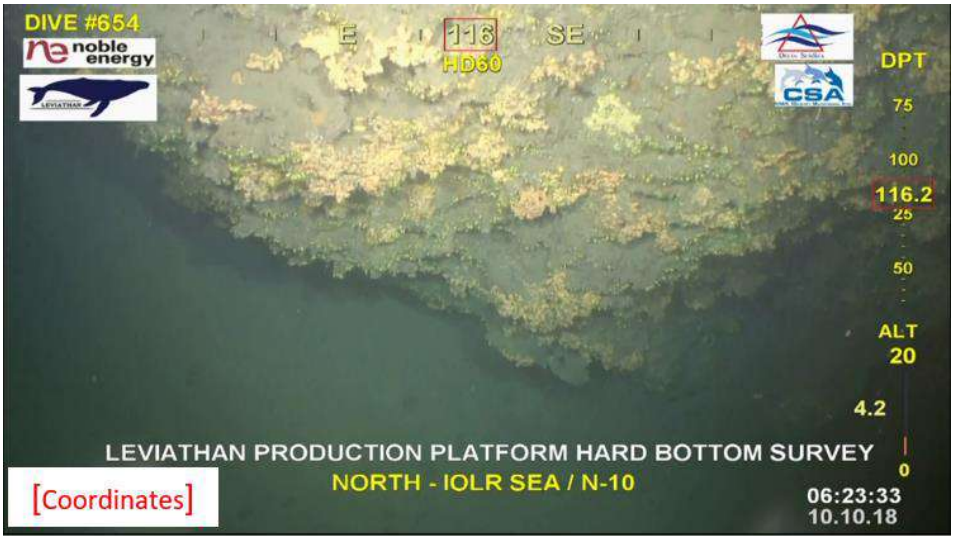


Image 40. A comparative view of the seafloor at Location 7 with a) taken during the pre-installation survey, b) taken during the post-installation survey, and c) taken during the 2020 Leviathan Platform Environmental Monitoring Survey.

a)



b)

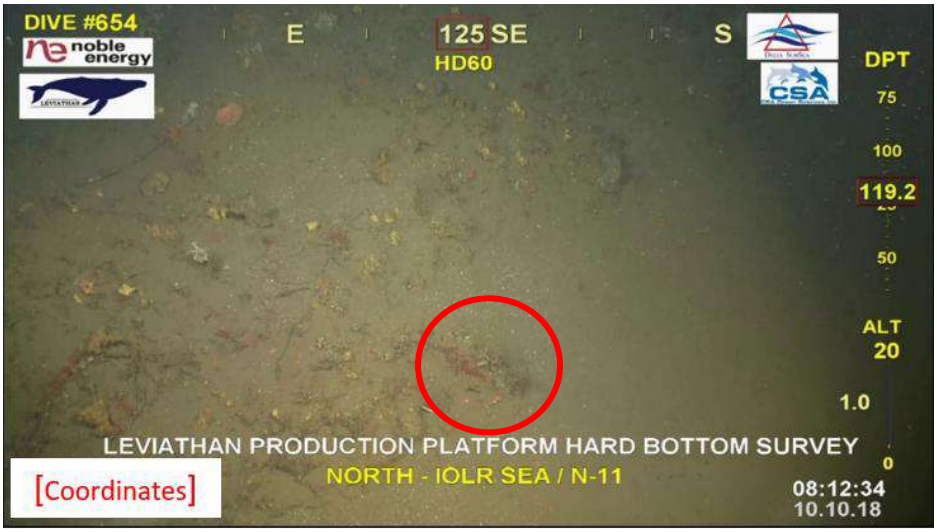


c)

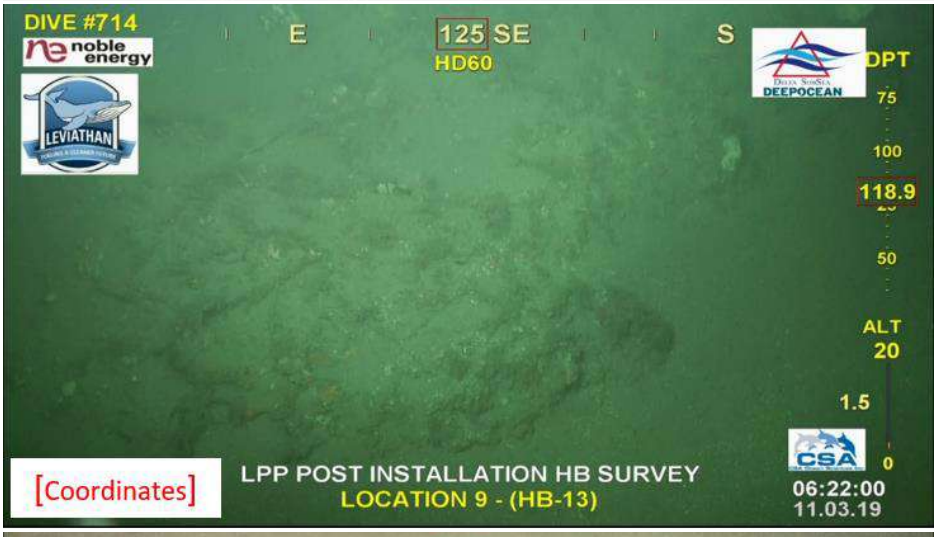


Image 41. A comparative view of the seafloor at Location 8 with a) taken during the pre-installation survey, b) taken during the post-installation survey, and c) taken during the 2020 Leviathan Platform Environmental Monitoring Survey.

a)



b)

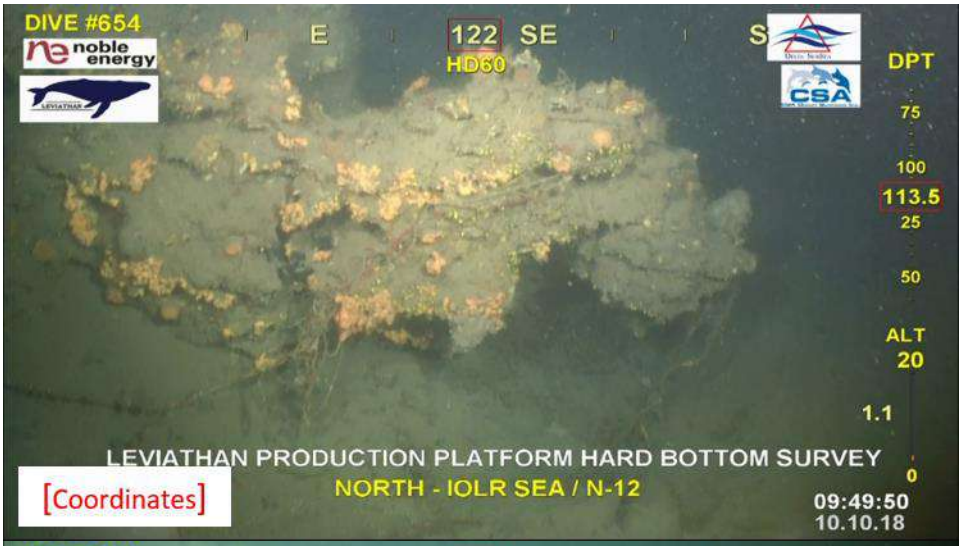


c)



Image 42. A comparative view of the seafloor at Location 9 with a) taken during the pre-installation survey, b) taken during the post-installation survey, and c) taken during the 2020 Leviathan Platform Environmental Monitoring Survey. The dual laser beams (red circle) (10 cm apart) are displayed for size reference. Increased turbidity in **Image 42c** was caused by amberjack fish swimming around the ROV and suspending sediment off the seafloor.

a)



b)



c)

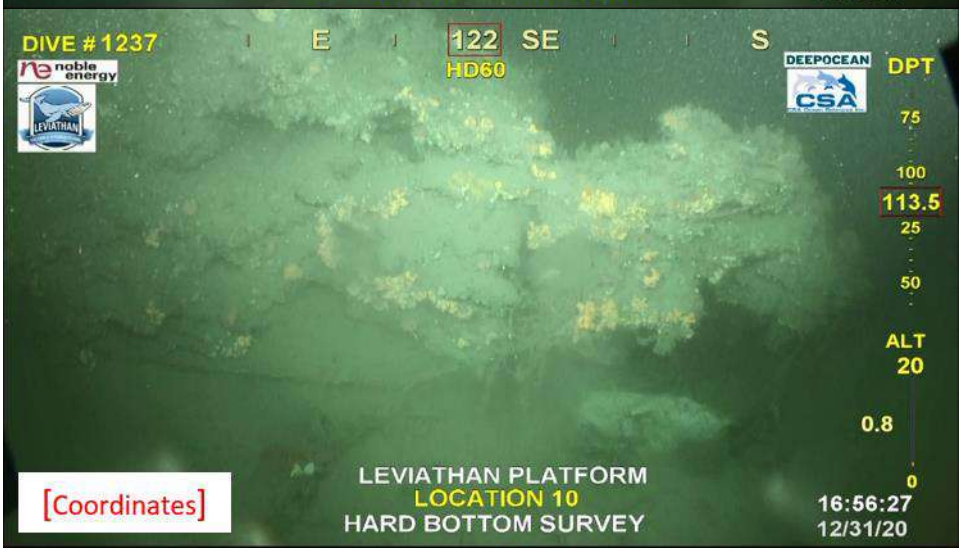
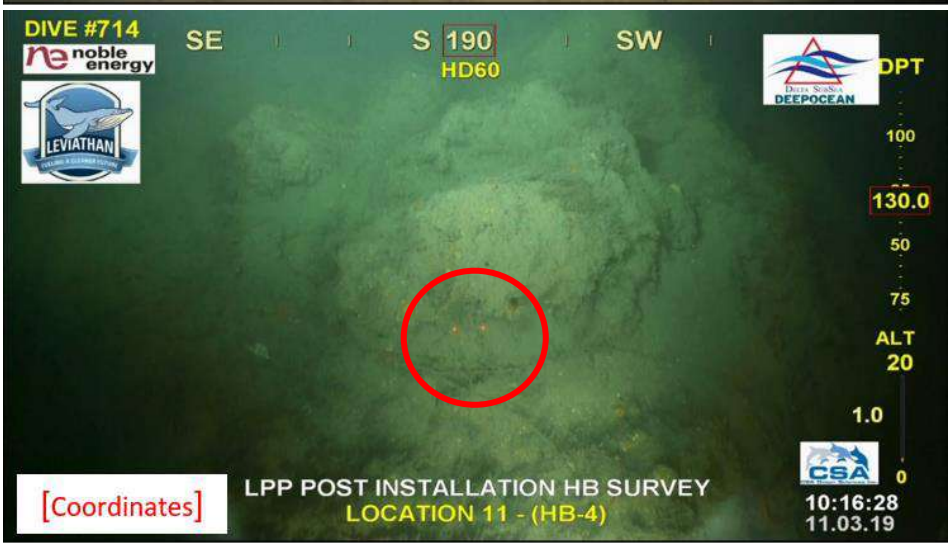


Image 43. A comparative view of the seafloor at Location 10 with a) taken during the pre-installation survey, b) taken during the post-installation survey, and c) taken during the 2020 Leviathan Platform Environmental Monitoring Survey. The persistence of the biota and anthropogenic debris is evident from the image.

a)



b)



c)

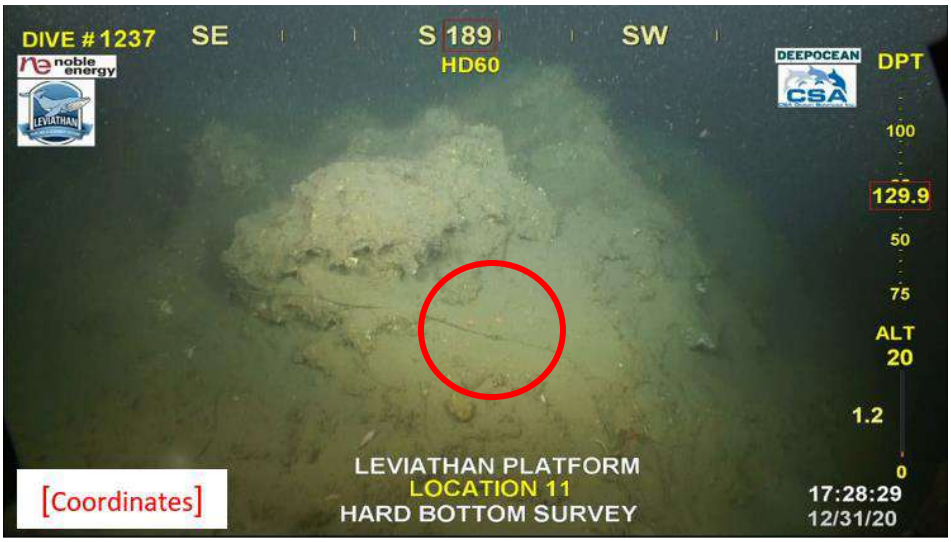


Image 44. A comparative view of the seafloor at Location 11 with a) taken during the pre-installation survey, b) taken during the post-installation survey, and c) taken during the 2020 Leviathan Platform Environmental Monitoring Survey. The dual laser beams (red circles) (10 cm apart) in are displayed for size reference.

a)



b)



c)

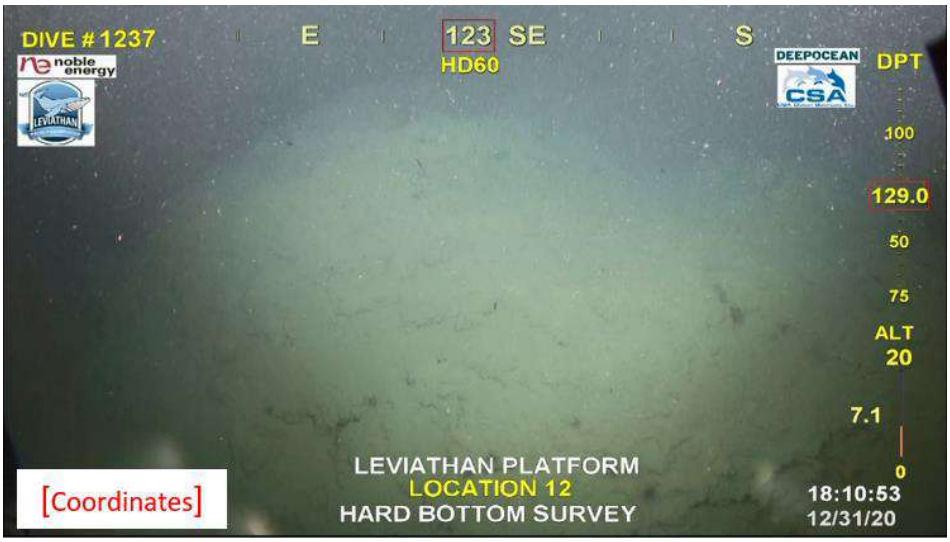


Image 45. A comparative view of the seafloor at Location 12 with a) taken during the pre-installation survey, b) taken during the post-installation survey, and c) taken during the 2020 Leviathan Platform Environmental Monitoring Survey. The dual laser beams (red circles) (10 cm apart) are displayed for size reference.

5.6 INFAUNA ANALYSIS

Analytical laboratory datasheets for infauna are provided in **Appendix N**. Benthic grab samples were collected from 46 stations during the 2020 LPP EMS using a stainless steel 0.5-meter × 0.5-meter modified Gray O'Hara box corer. The number of individuals, density, and diversity metrics were calculated for each benthic grab sample (**Table 39**). The 46 samples yielded a total of 74,573 individuals from 264 taxa. Abundance was high at all stations and ranged from 516 individuals at Station NP-NE-43 to 3,039 individuals at Station NF-NE-1 with an overall impact station average of 1,705 ± 715 individuals per station and overall reference station average of 1,056 ± 429 individuals per station. Infauna density varied greatly and ranged from 2,752 to 16,208 individuals m^{-2}.

Overall, identified taxa included individuals from the phyla Annelida, Arthropoda, Chordata, Cnidaria, Echinodermata, Hemichordata, Mollusca, Nematoda, Nemertea, Phoronida, Platyhelminthes, Porifera, and Sipuncula. The most numerically dominant taxa were the phyla Nematoda (n = 39,172), followed by the Polychaeta family Nephtyidae (n = 4,918) and Polychaeta taxa *Prionospio* sp. (n = 4,201). Averages and standard deviations for the 2014 Leviathan Field Development EBS and 2019 LPP EBS samples were provided to broaden the overall context results from the 2020 LPP EMS. While all infauna metrics between the 2014 and 2019 surveys were similar; it should be noted that the 2014, 2019, and 2020 surveys each had a different number of infauna samples (n=6, n=17, and n=46, respectively).

Taxa richness was moderate at all stations, ranging from 43 to 107 taxa per station. Margalef's diversity index (D) can be used as a simple indicator of species diversity (Margalef, 1958). The index is weighted toward species richness and is a measure of the total number of species for a given number of individuals. The index values are unbounded since it is determined by the theoretically unlimited number of species and individuals in a community. D values in highly diverse, species rich areas such as tropical rainforests may exceed 10 (Naidu and Kumar, 2016). D values from stations in the 2020 LPP EMS survey area were high, ranging from 6.7 at Station NP-NE-43 to 13.2 at Station NF-NE-1, with an average at impacts stations of 10.5 ± 1.4 and average at reference stations of 10.7 ± 1.0 (**Table 38**). D values were generally similar across distance and directional strata (**Table 40**). Mean D values were slightly lower in the 2020 LPP EMS as compared with the 2014 and 2019 surveys, likely due to the high abundance of nematodes in many stations.

Table 39. Diversity metrics for benthic infauna collected during the 2020 Leviathan Production Platform (LPP) Environmental Monitoring Survey.

Station	Distance Strata	Directional Strata	Abundance	Density (Individuals m^{-2})	Taxa Richness (S)	Margalef's Diversity (D)	Shannon-Wiener Diversity (H')	Pielou's Evenness (J')
NP-NE-43	Near-Platform	Northeast	516	2,752	43	6.72	1.77	0.47
NP-NW-44		Northwest	2,114	11,275	81	10.45	1.97	0.45
NP-SW-45		Southwest	1,439	7,675	81	11.00	2.38	0.54
NP-SE-46		Southeast	1,450	7,733	67	9.07	1.79	0.43
NF-NE-1	Near-Field	Northeast	3,039	16,208	107	13.22	2.28	0.49
NF-NE-2			1,401	7,472	87	11.87	2.39	0.53
NF-NE-3			1,194	6,368	80	11.15	2.06	0.47
NF-NW-4		Northwest	1,389	7,408	82	11.19	2.85	0.65
NF-NW-5			1,484	7,915	72	9.72	2.51	0.59
NF-NW-6			2,625	14,000	94	11.81	2.23	0.49
NF-SE-7		Southeast	1,302	6,944	83	11.43	2.47	0.56
NF-SE-8			2,872	15,317	91	11.30	1.91	0.42
NF-SE-9			1,291	6,885	73	10.05	2.11	0.49
NF-SW-10		Southwest	1,071	5,712	77	10.89	2.45	0.56
NF-SW-11			1,434	7,648	79	10.73	2.38	0.55
NF-SW-12			2,400	12,800	86	10.92	2.42	0.54

Table 39. (Continued).

Station	Distance Strata	Directional Strata	Abundance	Density (Individuals m^{-2})	Taxa Richness (S)	Margalef's Diversity (D)	Shannon-Wiener Diversity (H')	Pielou's Evenness (J')
MF-NE-13	Mid-Field	Northeast	2,216	11,819	97	12.46	2.13	0.47
MF-NE-14			2,377	12,677	84	10.68	2.18	0.49
MF-NE-15			1,603	8,549	80	10.71	2.56	0.58
MF-NW-16		Northwest	2,732	14,571	93	11.63	2.45	0.54
MF-NW-17			2,859	15,248	100	12.44	2.33	0.51
MF-NW-18			2,272	12,117	80	10.22	2.40	0.55
MF-SE-19		Southeast	994	5,301	65	9.27	2.16	0.52
MF-SE-20			1,061	5,659	72	10.19	2.40	0.56
MF-SE-21			2,951	15,739	97	12.02	2.41	0.53
MF-SW-22		Southwest	1,762	9,397	70	9.23	2.11	0.50
MF-SW-23			1,297	6,917	73	10.04	2.25	0.52
MF-SW-24			2,021	10,779	89	11.56	2.71	0.60
FF-NE-25	Far-Field	Northeast	2,476	13,205	85	10.75	1.73	0.39
FF-NE-26			865	4,613	65	9.46	1.92	0.46
FF-NE-27			1,027	5,477	77	10.96	2.63	0.61
FF-NW-28		Northwest	1,071	5,712	78	11.04	2.80	0.64
FF-NW-29			831	4,432	58	8.48	1.71	0.42
FF-NW-30			1,360	7,253	71	9.70	2.61	0.61
FF-SE-31		Southeast	2,623	13,989	75	9.40	1.81	0.42
FF-SE-32			2,077	11,077	68	8.77	1.39	0.33
FF-SE-33			1,393	7,429	86	11.74	2.46	0.55
FF-SW-34		Southwest	721	3,845	74	11.09	2.75	0.64
FF-SW-35			1,972	10,517	88	11.47	2.63	0.59
FF-SW-36			658	3,509	45	6.78	1.75	0.46
2020 LPP EMS Impact Stations Mean (± SD)			1,706 ± 715	9,999 ± 3,813	79 ± 13	10.5 ± 1.4	2.26 ± 0.34	0.52 ± 0.07
REF-NE-37	Reference	Northeast	761	4,059	77	11.46	2.76	0.64
REF-NE-38			1,610	8,587	73	9.75	1.83	0.43
REF-NE-39			1,054	5,621	71	10.06	2.80	0.66
REF-SW-40		Southwest	1,549	8,261	90	12.12	2.36	0.52
REF-SW-41			656	3,499	73	11.10	2.99	0.70
REF-SW-42			703	3,749	64	9.61	2.56	0.62
2020 LPP EMS Reference Stations Mean (± SD)			1,056 ± 429	5,629 ± 2,290	75 ± 8.6	10.7 ± 1.0	2.55 ± 0.41	0.60 ± 0.10
2019 LPP EBS Overall Mean (± SD)			946 ± 298	5,045 ± 1,591	101 ± 13.2	14.65 ± 1.37	3.75 ± 0.14	0.81 ± 0.03
2014 Leviathan Field Development EBS Mean (± SD)			475 ± 229	3,880 ± 1,869	75 ± 15	12.11 ± 1.51	3.61 ± 0.14	0.96 ± 0.01

EBS = environmental baseline survey; EMS = Environmental Monitoring Survey; SD = standard deviation.

Table 40. Mean (± standard deviation) infauna diversity metrics by distance and directional strata in sediment samples collected during the 2020 Leviathan Production Platform Environmental Monitoring Survey.

Strata Type	Strata	Abundance	Density (Individuals m^{-2})	Taxa Richness (S)	Margalef's Diversity (D)	Shannon-Wiener Diversity (H')	Pielou's Evenness (J')
Distance	Near-Platform	1,380 ± 657	7,359 ± 3,502	68 ± 18	9.31 ± 1.91	1.98 ± 0.28	0.47 ± 0.05
	Near-Field	1,792 ± 719	9,556 ± 3,836	84 ± 10	11.2 ± 0.90	2.34 ± 0.25	0.53 ± 0.06
	Mid-Field	2,012 ± 677	10,731 ± 3,611	83 ± 12	10.9 ± 1.14	2.34 ± 0.18	0.53 ± 0.04
	Far-Field	1,422 ± 694	7,588 ± 3,703	73 ± 12	9.97 ± 1.47	2.18 ± 0.51	0.51 ± 0.11
	Reference	1,056 ± 429	5,629 ± 2,290	75 ± 9	10.7 ± 1.02	2.55 ± 0.41	0.59 ± 0.10
Directional	Northeast	1,594 ± 737	8,262 ± 3,930	79 ± 15	10.7 ± 1.53	2.23 ± 0.39	0.51 ± 0.09
	Northwest	1,874 ± 736	9,993 ± 3,923	81 ± 12	10.7 ± 1.19	2.39 ± 0.35	0.54 ± 0.08
	Southeast	1,801 ± 762	9,607 ± 4,061	78 ± 11	10.3 ± 1.21	2.09 ± 0.36	0.48 ± 0.08
	Southwest	1,360 ± 710	7,255 ± 3,785	76 ± 13	10.5 ± 1.40	2.44 ± 0.30	0.56 ± 0.06

Evenness is a measurement of the homogeneity of a community or sample. Pielou's Evenness (J') compares the diversity value (e.g., Shannon-Wiener Index [H]') to the maximum possible H' value when all species are equally abundant. This calculation is constrained between 0 and 1, with higher values representing a more even community. J' values are highly dependent on sample size, and due to the high abundance of individuals found in all stations during the 2020 LPP EMS, J' values are likely a good interpretation of actual community evenness. Calculated J' values were variable, ranging from 0.33 at Station FF-SE-32 to 0.70 at Station REF-SW-41, with an average at impacts stations of 0.52 ± 0.07 and average at reference stations of 0.60 ± 0.10 (**Table 39**). The low J' values at several individual stations are a result of unidentified nematodes (which are counted as a single taxa) numerically dominating the sample make-up at those stations. Similarly, the lower mean J' values during the 2020 LPP EMS as compared to the 2019 LPP EBS and the 2014 Leviathan Field Development EBS are due to the very high abundances of nematodes present in the current survey which were not previously present in such high abundances (2019 LPP EBS) or absent entirely (2014 Leviathan Field Development EBS). Mean J' values were generally similar across distance and directional strata (**Table 40**).

Species richness measures do not account for the relative abundances within different taxa. Species diversity metrics, such as H' account for both species richness and species evenness. Values of H' can vary from 0 to 5 (with higher values representing higher diversity communities), with values typically range from 1.5 to 3.5 in most communities. H' values in samples from the 2020 LPP EMS were moderate, ranging from 1.39 at Station FF-SE-32 to 2.99 at Station REF-SW-41 (**Table 39**), with an average at impact stations of 2.26 ± 0.34 and average at reference stations of 2.55 ± 0.41 (**Table 39**). These results indicate that the infauna community in the vicinity of the LPP have moderate diversity. However, it should be noted that H' values are likely skewed too low given the index considers the numerically dominant unidentified nematodes as a single species. For comparison, if all nematodes are removed, H' values range from 2.9 to 3.6 with an overall average of 3.35 ± 0.15, which is much more comparable with the mean H' value of 3.75 ± 0.14 observed during the 2019 LPP EBS (**Table 39**). For the 2020 LPP EMS, mean H' values were generally similar across distance and directional strata (**Table 40**).

5.6.1 Taxonomy

A comparison of the most numerically dominant phyla for the 2014 Leviathan Field Development EBS, the 2019 LPP EBS, and the 2020 LPP EMS is presented in **Figure 52**. These results show that the fraction of annelids and arthropods sharply decreased between 2019 and 2020, corresponding to the rise in the fraction of nematodes observed during the 2020 LPP EBS. Nematodes were rare in the 2019 LPP EBS, and completely absent during the 2014 Leviathan Field Development EBS. As previously noted, there were different number of infauna samples collected during each survey (n=6 [2014], n=17 [2019], and n=46 [2020]). The low sample sizes in 2014 and 2019 make it difficult to ascertain if the results present a true representation of infauna community structure during those years.

During the 2020 LPP EMS, numerically dominant phyla were generally similar between impact stations and reference stations (**Figure 52**). The fraction of annelids was slightly higher at the reference stations (39.8% of all individuals) as compared with the impact stations (36.2% of all individuals), and the fraction of nematodes was slightly smaller at the reference stations (48.4% of all individuals) as compared to the impact stations (52.9% of all individuals). It should be noted that there were relatively few reference stations (n=6) as compared with impact stations (n=40).

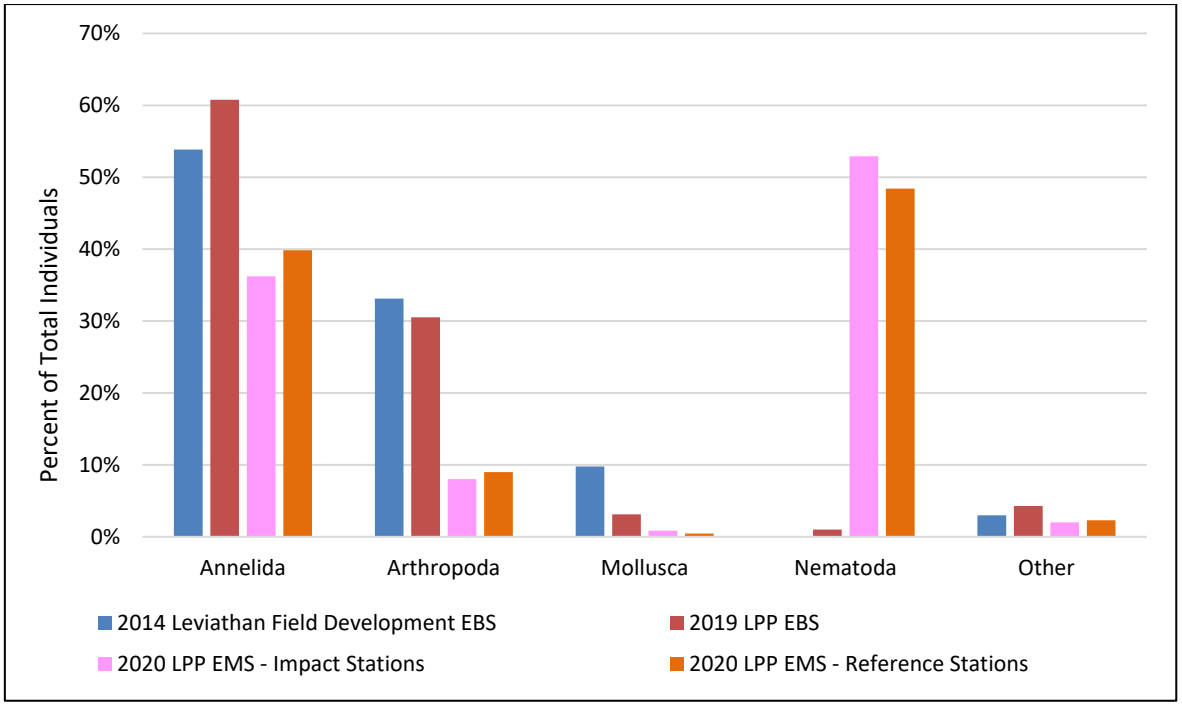


Figure 52. Percentage of total individuals within each of the dominant phyla collected during the 2014 Leviathan Field Development Environmental Baseline Survey (EBS), the 2019 Leviathan Production Platform EBS, and the 2020 Leviathan Production Platform Environmental Monitoring Survey (EMS).

The following subsections present taxonomic details, where applicable, of each of the three most abundant phyla during the 2020 LPP EMS.

5.6.1.1 Annelida

During the 2020 LPP EMS, nearly all identified annelids belonged to the class Polychaeta (99.5% of all annelids at impact stations and 99.4% of all annelids at the reference stations). The remaining annelids belonged to the class Clitellata. The most abundant families from the impact stations were Nephytidae, Syllidae, and Spionidae. Nephytidae had an abundance of 115 ± 83 individuals per station, comprising 6.7% of all annelids at impact stations, Syllidae had an abundance of 106 ± 72 individuals per station, comprising 6.2% of all annelids at impact stations, and Spionidae had an abundance of 103 ± 52 individuals per station, comprising 6.1% of all annelids at impact stations.

At reference stations, the most abundant families were Spionidae, Cirratulidae, and Nephytidae. Spionidae had an abundance of 105 ± 56 individuals per station, comprising 10.0% of all annelids at reference stations, Cirratulidae had an abundance of 56.8 ± 24.5 individuals per station, comprising 5.4% of all annelids at reference stations, and Nephytidae had an abundance of 56.3 ± 33.7 individuals per station, comprising 5.3% of all annelids at reference stations. Other notably abundant families at both impact and reference stations were Ampharetidae, Capitellidae, Lumbrineridae, Magelonidae, Opheliidae, Pilargidae, Paraonidae, and Sabellidae.

5.6.1.2 Arthropoda

During the 2020 LPP EMS, nearly all identified arthropods belonged to the class Malacostraca (97.4% of all arthropods at impact stations and 94.0% of all arthropods at the reference stations). The remaining arthropods belonged to Arachnida, Ostracoda and Pycnogonida families. The most abundant families from the impact stations were Typhlotanaidae, Agathatanaidae, and Phoxocephalidae. Typhlotanaidae had an abundance of 70.1 ± 24 individuals per station, comprising 19.2% of all arthropods at impact stations, Agathatanaidae had an abundance of 23.1 ± 25.5 individuals per station, comprising 15.9% of all annelids at impact stations, and Phoxocephalidae had an abundance of 13.1 ± 10.8 individuals per station, comprising 9.3% of all annelids at impact stations.

At reference stations, the most abundant families were Phoxocephalidae, Typhlotanaidae, and Agathatanaidae. Phoxocephalidae had an abundance of 16.2 ± 8.0 individuals per station, comprising 17.0% of all arthropods at reference stations, Typhlotanaidae had an abundance of 15.2 ± 12.5 individuals per station, comprising 15.9% of all annelids at reference stations, and Agathatanaidae had an abundance of 9.5 ± 10.8 individuals per station, comprising 10.0% of all annelids at reference stations. Other notably abundant families at both impact and reference stations were Ampeliscidae, Corophiidae, Gnathiidae, Leptocheliidae, Leuconidae, Pasiphaeidae, and Pseudotanaidae.

Individuals from the family Ostracoda were not identified to family level, and there were 1,246 individuals from the family Malacostraca that could only be identified to the class level from impact stations and 97 individuals from the family Malacostraca that could only be identified to the class level from the reference stations.

5.6.1.3 Mollusca

During the 2020 LPP EMS, molluscs were nearly evenly split between the classes Bivalvia (48.6% of all molluscs at impact stations) and Gastropoda (43.0% of all molluscs at impact stations). At reference stations, a similar trend was observed, with bivalves comprising 41.3% of all molluscs and gastropods comprising 48.2% of all molluscs. It should be noted that the total number of molluscs found at reference stations was low (n=29). The remaining molluscs belonged to the classes Aplacophora, Caudofoveata, Scaphopoda, and Solenogastres. The most abundant family at the impact stations was Philinidae (39.1% of all molluscs at impact stations). It should be noted however, that a large fraction of all molluscs at impact stations (39.5%) could not be identified to the family level.

At reference stations, the majority of molluscs (69%) could not be identified to family level. Taxa that were identified to family level included seven individuals from the family Hederodonta, and single individuals from the families Chaetodermomorpha and Protobranchia.

Mollusca abundance seems to have declined since the 2014 Leviathan Field Development EBS; the reasons for this apparent decline are unknown. However, it should be noted that the number of infaunal samples greatly differed among surveys, with just six samples collected during the 2014 Leviathan Field Development EBS in the vicinity of the LPP. Future monitoring efforts and infauna analyses will further reveal whether Mollusca abundance is continuing to decline or if the trend observed between 2014 and 2020 is an artifact of sampling size.

5.6.1.4 Nematoda

Nematodes were the most dominant phyla at both the impact stations and reference stations during the 2020 LPP EMS. However, the infauna analytical laboratory did not identify the nematodes past the phyla level, so no detailed taxonomic analysis could be performed.

5.6.2 Infauna Statistical Analysis

A MDS ordination plot was created using PRIMER v6 software (Clarke and Gorely, 2006). MDS is an ordination technique that provides a 2D projection of inter-sample relationships in abstract high dimensional space. Samples that are most similar in terms of species composition and proportional abundance will cluster near one another in a 2D ordination diagram. This data matrix was analyzed by square-root transformation of the raw numbers and then applied to the Bray-Curtis similarity index (Bray and Curtis, 1957) to construct the sample similarity matrix.

The MDS plot for infauna showed no distinct clustering by distance or directional strata (**Figures 53** and **54**). One station (Station NP-NE-43) was somewhat of an outlier and slightly removed from the main cluster. Upon examination of the raw data, this station had substantially fewer taxa (n=43) than the overall impact stations mean (79 ± 15), and a substantially fewer number of individuals (n=516) as compared to the overall impact stations mean (1,706 ± 715). The difference in the number of individuals was partially driven by the relative lack of nematodes at this station (n=317), whereas the overall average number of nematodes per station was 852 ± 430. The reasons for the relatively low number of species at this station is unknown, although it should be noted that its location within the Near-Platform strata and downstream of the LPP (i.e., the northeast quadrant).

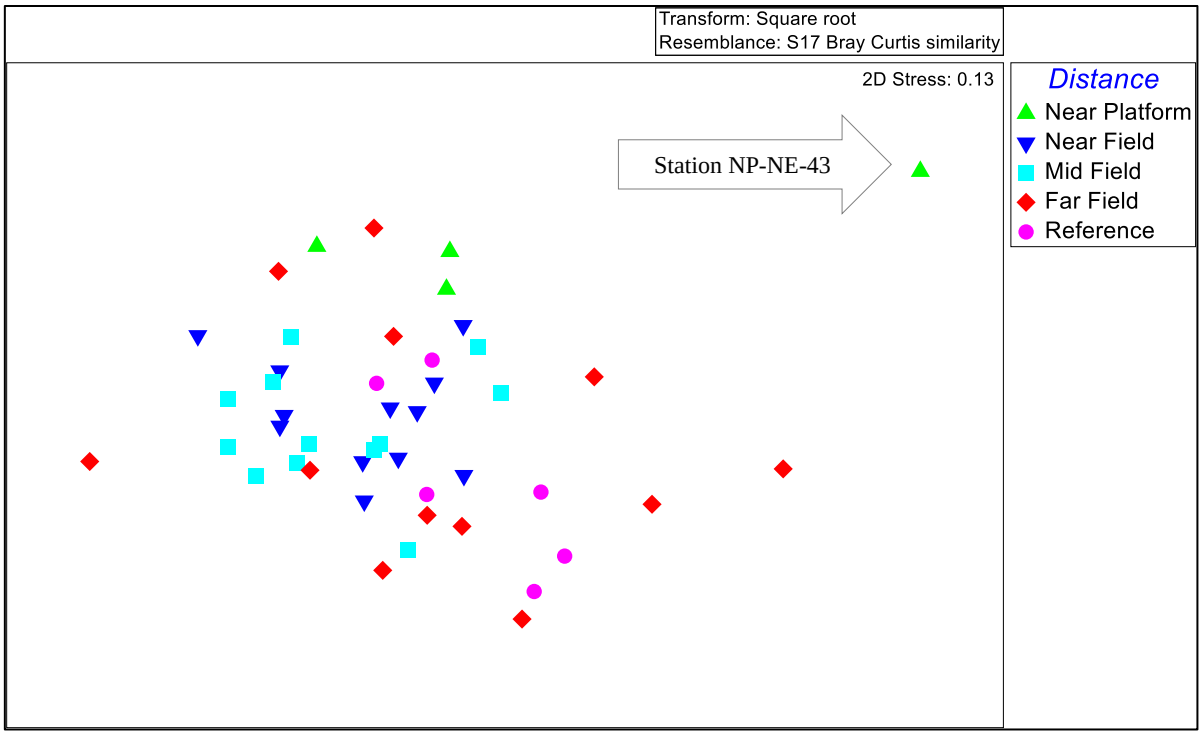


Figure 53. Multi-dimensional scaling ordination of infauna samples by distance during the 2020 Leviathan Production Platform Environmental Monitoring Survey.

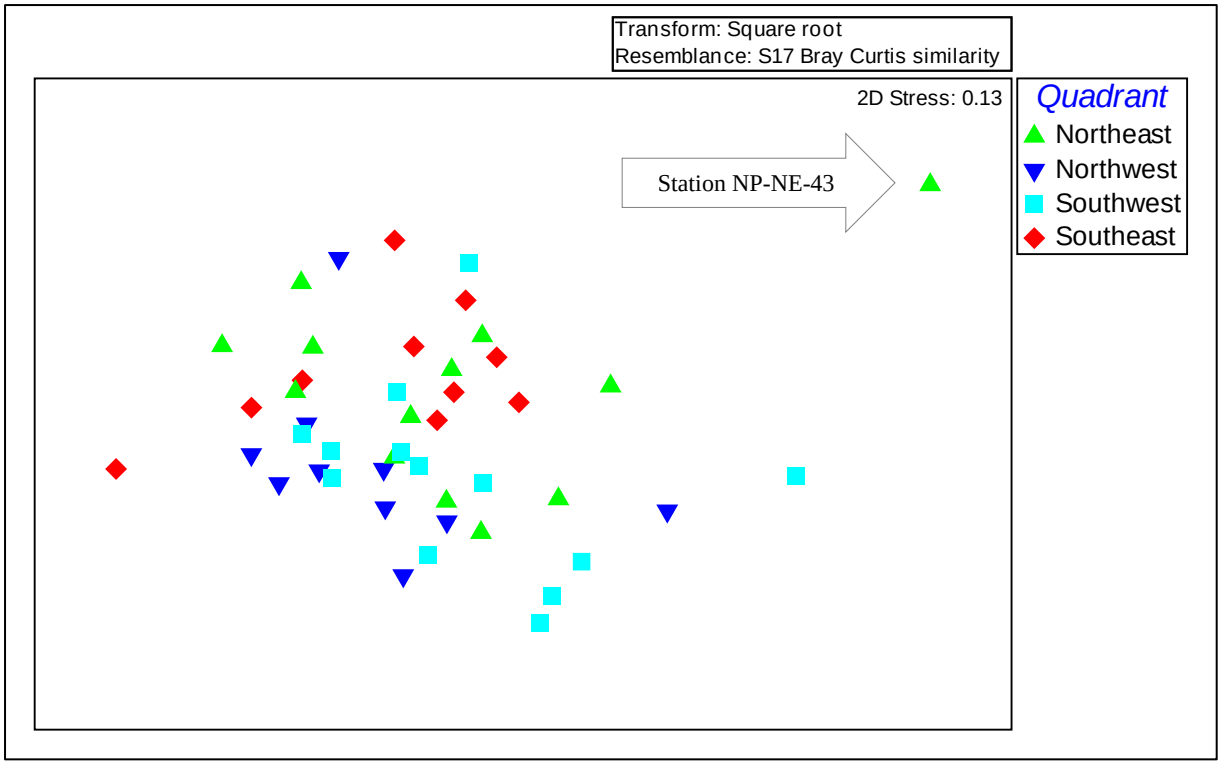


Figure 54. Multi-dimensional scaling ordination of infauna samples by direction (quadrant) during the 2020 Leviathan Production Platform Environmental Monitoring Survey.

A second MDS plot was created to compare infaunal community by survey (**Figure 55**). As expected, the MDS plot showed distinct clustering by survey, indicating the infaunal community is changing over time. A SIMPER analysis was conducted in Primer to determine the overall dissimilarity between surveys and to assess the contribution of individual taxa to the overall dissimilarity between the survey year clusters. The SIMPER analysis revealed that the 2019 LPP EBS and 2020 LPP EMS were less dissimilar to each other (overall 56.8% dissimilarity) than the 2014 Leviathan Field Development EBS and the 2019 LPP EBS and the (overall 73.3% dissimilarity) and the 2014 Leviathan Field Development EBS and the 2020 LPP EMS (overall 75.8% dissimilarity). These results are logical, given the smaller time lapse (approximately 1 year) between the 2019 LPP EBS and the 2020 LPP EMS as compared with the 5-to-6-year lapse from the 2014 Leviathan Field Development EBS and the 2019 LPP EMS and 2020 LPP EMS, along with the difference in season between surveys. Additionally, the difference in the number of infauna samples between surveys also may have contributed to the overall dissimilarity.

The SIMPER analysis also revealed that nematodes, serpulid annelids, and nephtyid polychaetes were the largest contributor to the dissimilarity between surveys. Between the 2014 Leviathan Field Development EBS and the 2019 LPP EBS, annelids of the family Serpulidae were the largest contributor to the dissimilarity; it is important to note that nematodes were absent in 2014 and relatively rare in 2019. Between the 2014 Leviathan Field Development EBS and the 2020 LPP EBS, nematodes were by far the largest contributor to dissimilarity, contributing 10.2%. The taxa with the next highest contribution to dissimilarity were polychaetes of the family Nephtyidae, contributing just 3.4%. Between the 2019 LPP EBS and the 2020 LPP EMS, nematodes were again by far the largest contributor to dissimilarity (10.0%), with serpulid annelids contributing 2.1%.

The reason for the dramatic increase in the number of nematodes between 2014 and 2019 is unknown but could be the result of natural infaunal community succession over time. It is also possible that the disturbance caused by the installation of the LPP displaced sensitive species, making habitat available for pioneer species to colonize the newly disturbed area. However, nematode abundance was also

high in the Reference strata far from the LPP where no disturbance from installation occurred. Sample collection from future surveys in the vicinity of the LPP will continue to analyze infauna taxonomic structure (especially regarding nematode abundance) to determine the nature of infauna succession in the area.

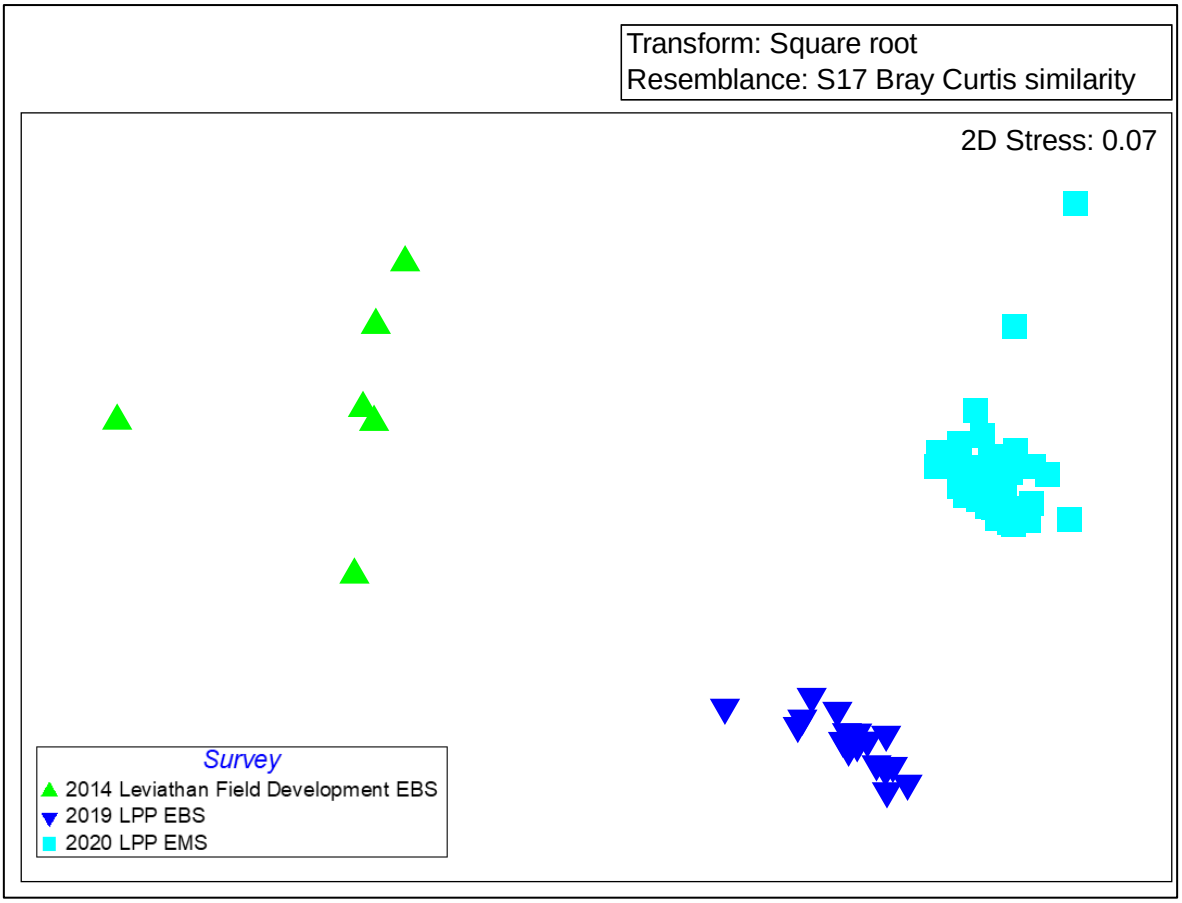


Figure 55. Multi-dimensional scaling ordination of infauna samples by survey.

5.7 BIOACCUMULATION PASSIVE SAMPLING DEVICES ANALYSIS

5.7.1 Metals – DGT Samplers

Masses of each targeted metal that accumulated on the DGT sampler during the 43-day deployment are presented in **Table 41**; raw datasheets from the laboratory are presented in **Appendix O**. Chromium, cadmium, and lead were below the laboratory's detection limit for all samples. Nickel was detected only in two of the Near-Platform samplers, and zinc was detected in a single Far-Field sampler. Mercury and manganese were detected in all samples. The mean accumulated masses (where calculable) are presented in **Table 42** and graphically in **Figures 56** and **57**. No metal other than mercury was detected on the DGT blanks; mercury was present on the blanks in approximately half the concentration found on the deployed samplers suggesting the true amount of bioavailable mercury at the deployment locations may be roughly half of the values presented below. Manganese masses were generally similar among the five deployment locations. Mean mercury mass was noticeably higher at the Near-Platform deployment location (143 ± 10 ng), whereas means from other deployment locations ranged from 102 ± 16 µg (Mid-Field) to 117 ± 19 / 117 ± 16 µg (Hardbottom and Far-Field respectively) (**Table 42**).

Table 41. Measured mass of metals from the DGT samplers after a 43-day deployment near the Leviathan Production Platform. Units are in micrograms (µg) unless otherwise noted.

DGT Sampler	Chromium	Cadmium	Mercury (ng)	Lead	Manganese	Nickel	Zinc
NP-200m-1	ND	ND	131	ND	1.09	ND	ND
NP-200m-2	ND	ND	146	ND	1.28	0.25	ND
NP-200m-3	ND	ND	151	ND	2.01	0.21	ND
MF-500m-1	ND	ND	115	ND	1.41	ND	ND
MF-500m-2	ND	ND	84.5	ND	1.52	ND	ND
MF-500m-3	ND	ND	105	ND	0.86	ND	ND
FF-1000m-1	ND	ND	116	ND	1.90	ND	0.51
FF-1000m-2	ND	ND	133	ND	0.766	ND	ND
FF-1000m-3	ND	ND	101	ND	0.568	ND	ND
HB-3.5km-1	ND	ND	98.1	ND	0.275	ND	ND
HB-3.5km-2	ND	ND	137	ND	0.858	ND	ND
HB-3.5km-3	ND	ND	117	ND	2.39	ND	ND
REF-3.5km-1	ND	ND	121	ND	1.02	ND	ND
REF-3.5km-2	ND	ND	119	ND	1.22	ND	ND
REF-3.5km-3	ND	ND	106	ND	3.20	ND	ND
Seawater Blank	ND	ND	60.7	ND	ND	ND	ND
Fabrication Blank	ND	ND	52.5	ND	ND	ND	ND
Air Blank	ND	ND	51.7	ND	ND	ND	ND
Deployed DGT Sampler Mean ± SD	--	--	119 ± 30	--	1.36 ± 0.76	--	--
MRL	0.20	0.020	0.10	0.05	0.05	0.20	0.50

DGT = diffuse gradient in thin film; FF = far-field; HB = hardbottom; MF = mid-field; MRL = method reporting limit; ND = not detected; ng = nanogram; NP = near platform; REF = reference; SD = standard deviation; "--"= not calculable.

Table 42. Mean metals mass by deployment location on DGT samplers after a 43-day deployment near the Leviathan Production Platform.

DGT Sampler	Mercury (ng)	Manganese (µg)	Nickel (µg)
Near Platform Mean ± SD	143 ± 10	1.5 ± 0.5	0.23 ± 0.03 [1]
Mid-Field Mean ± SD	102 ± 16	1.3 ± 0.4	--
Far-Field Mean ± SD	117 ± 16	1.1 ± 0.7	--
Hardbottom Mean ± SD	117 ± 19	1.2 ± 1.1	--
Reference Mean ± SD	115 ± 8	1.8 ± 1.2	--
MRL	0.1	0.05	0.20

[1] Value calculated from two samples only. DGT = diffuse gradient in thin film; µg = microgram; ng = nanogram; MRL = method reporting limit; SD = standard deviation; "--" = not calculable.

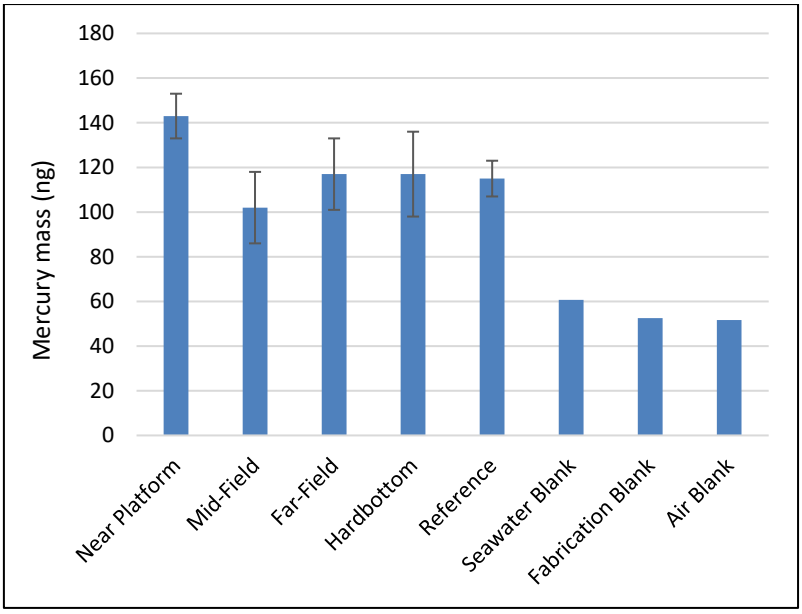


Figure 56. Average (± standard deviation [SD]) accumulated mercury mass on the diffuse gradient in thin film sampler devices by deployment location and blank devices after the 43-day deployment near the Leviathan Production Platform. ng = nanograms.

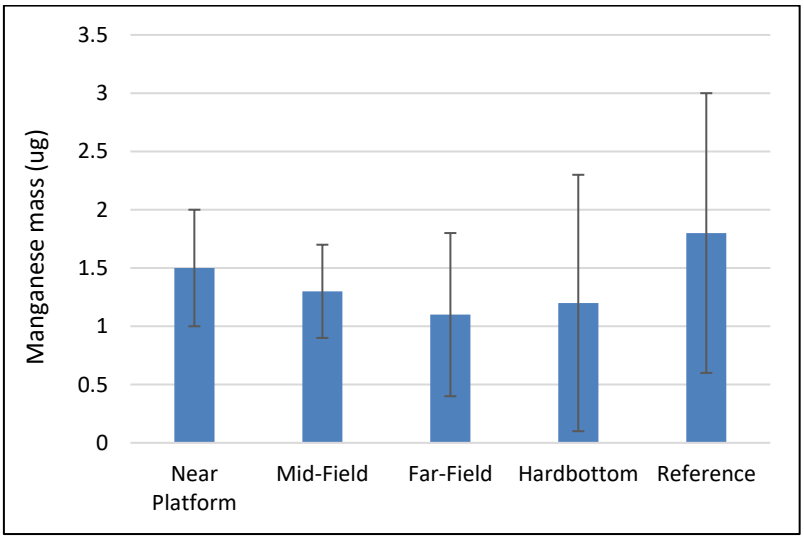


Figure 57. Average (± standard deviation [SD]) accumulated manganese mass on the diffuse gradient in thin film sampler devices by deployment location after the 43-day deployment near the Leviathan Production Platform. µg = micrograms.

As outlined in **Section 4.6.1**, the TWAC for each metal that was detected by the analytical laboratory was calculated; results are presented in **Table 43**. Chromium, cadmium and lead are excluded from **Table 43** because all metal masses were less than the laboratory's detection limit and therefore no TWAC could be calculated. Mercury TWACs ranged from 0.098 to 0.175 ng mL^{-1}, with an overall average of 0.138 ± 0.02 ng mL^{-1}. The mean TWAC of the three samplers deployed at the Near Platform deployment area (0.165 ± 0.05 ng mL^{-1}) was slightly elevated as compared with other deployment areas, indicating that more bioavailable mercury may be available at this area.

Mean manganese TWACs were similar across deployment locations, ranging from 1.71 ± 1.14 ng mL^{-1} (Far-Field) to 2.87 ± 1.91 ng mL^{-1} (Reference) with an overall average of 2.16 ± 1.2 ng mL^{-1}. Manganese TWACs showed no obvious trend by deployment location. Nickel

was only detected on two of the Near Platform DGT samplers (**Table 41**), and therefore nickel TWACs could only be calculated for those two samplers. The nickel TWAC was similar on the two samplers (0.337 and 0.401 ng mL^{-1}). Zinc was only detected on a single DGT sampler at the Far-Field deployment location. The TWAC for that sample was calculated to be 0.777 ng mL^{-1} (**Table 43**).

Table 43. Calculated time-weighted average concentrations for selected metals (ng mL^{-1}) on deployed DGT samplers during a 43-day deployment near the Leviathan Production Platform.

DGT Sampler	Mercury	Manganese	Nickel	Zinc
NP-200m-1	0.152	1.73	--	--
NP-200m-2	0.169	2.03	0.401	--
NP-200m-3	0.175	3.18	0.337	--
MF-500m-1	0.133	2.23	--	--
MF-500m-2	0.098	2.41	--	--
MF-500m-3	0.122	1.36	--	--
FF-1000m-1	0.134	3.01	--	0.777
FF-1000m-2	0.154	1.21	--	--
FF-1000m-3	0.117	0.90	--	--
HB-3.5km-1	0.117	0.45	--	--
HB-3.5km-2	0.163	1.40	--	--
HB-3.5km-3	0.139	3.89	--	--
REF-3.5km-1	0.140	1.61	--	--
REF-3.5km-2	0.138	1.93	--	--
REF-3.5km-3	0.123	5.07	--	--
Overall Mean ± SD	0.138 ± 0.02	2.16 ± 1.2	--	--
Near Platform Mean ± SD	0.165 ± 0.01	2.31 ± 0.77	0.369 ± 0.05[1]	--
Mid-Field Mean ± SD	0.118 ± 0.02	2.00 ± 0.56	--	--
Far-Field Mean ± SD	0.135 ± 0.02	1.71 ± 1.14	--	--
Hardbottom Mean ± SD	0.140 ± 0.02	1.91 ± 1.78	--	--
Reference Mean ± SD	0.134 ± 0.01	2.87 ± 1.91	--	--

[1] Mean calculated using two values only. -- = not calculable. DGT = diffuse gradient in thin film; FF = far-field; HB = hardbottom; MF = mid-field; NP = near platform; REF = reference; SD = standard deviation; "--" = not calculable.

No known studies have utilized DGT samplers to measure bioavailable metals in the eastern Mediterranean. MVI/CSA deployed a different type of PSD to measure metals in 2019 (Chemcatchers), but TWACs were not calculable because the samplers were not specifically designed by the manufacturer to be deployed in seawater and diffusion coefficients were therefore unavailable.

Several studies have utilized DGT samplers in estuarine and marine water. Wallner-Kersnach et al. (2009) deployed DGT samplers in Patos Lagoon (Brazil). While it should be noted that some metal species' diffusion is sensitive to changes in pH (and pH may change rapidly in estuarine settings due to freshwater inflow), after a 10-day deployment, TWACs of manganese (ranging from approximately 4 to 6 ng mL^{-1}), nickel (approximately 0.2 ng mL^{-1}), and zinc (approximately 0.5 ng mL^{-1}) were generally similar to values calculated in the present study. Wallner-Kersnach et al. (2009) did not measure mercury.

In Israel, IOLR has monitored metal concentrations in tissue samples of marine biota off the coast of Israel for over two decades (IOLR, 2017; 2020), including during the years 2016 and 2018 when various metals concentrations were measured in the gastropods *Cellana* sp. and *Patella* sp. and in the bivalve *Donax* sp. (2016 survey only). Arsenic, cadmium, copper, iron, lead, manganese, mercury, and zinc were all detected in samples from both surveys (except arsenic which was not measured during the 2016 survey), indicating that bioavailable species of these metals were present at the sampling locations.

It should be noted that direct measurements of bioaccumulated metals in biotic tissue (as conducted by IOLR) is not directly comparable to the TWAC values calculated for the current study. The TWAC values identify the concentration of metal that is bioavailable, as compared with direct sampling that measures a concentration that has accumulated in tissue. Each species is likely to accumulate metals at different rates as well as accumulate different metals at different rates. The IOLR studies confirm that bioaccumulation of heavy metals is occurring in marine organisms offshore Israel and lends support to the continued use of PSDs near the LPP to measure the bioavailability of metals.

5.7.2 Hydrocarbons – SPMD Samplers

Seventy-six PAH compounds were analyzed for accumulation on the SPMDs (**Table 44**); raw datasheets from the analytical laboratory are included as **Appendix P**. The average total PAH mass of all samples (excluding blanks) was 934 ± 70.4 ng. Excluding the PRC spikes (these PAHs were artificially added and are not part of the ambient concentrations), the total accumulated mass on the fabrication blank was 509 ng, the total accumulated mass on the air blank was 968 ng, and the total accumulated mass on the seawater blank was 3,434 ng. The reason for the extremely elevated PAH mass on the seawater blank is unknown. The seawater blank was attached to the ROV during each deployment and retrieval of the deployed SPMDs and it is possible that the SPMD sampler came into contact with ROV-related hydrocarbons such as hydraulic fluid, lubrication grease, etc.

Mean total PAH masses were slightly higher at the Near Platform (1,028 ± 28 ng) and Hardbottom location (977 ± 38) as compared to the other deployment locations, which ranged from 852 ± 40 ng (Reference) to 914 ± 41 ng (Mid-Field) (**Figure 58**). It is important to note that while there were triplicate SPMDs deployed at each location, these were not independent samples (i.e., they were deployed on the same monopod) and therefore it is possible to calculate within-station variability, the means among deployment locations cannot be statistically compared and a qualitative comparison must be used. PAHs were not detected in produced water discharges at the LPP from June to December 2020 (see **Table 4**) and therefore it is unlikely that the higher PAH masses seen at the Near Platform deployment location were caused by the LPP discharges. It is possible that the differences are a result of natural localized differences in PAH concentrations based on localized currents, differences in depths, or other oceanographic metrics.

Table 44. The accumulated masses of polycyclic aromatic hydrocarbons (PAHs) on the semi-permeable passive membrane devices (SPMDs) after the 43-day deployment near the Leviathan Production Platform. Gray shaded rows indicate the 16 United States Environmental Protection Agency priority PAHs. Blue shaded rows are the performance reference compound spikes. Units are in nanograms (ng).

Compound	NP-200m-1	NP-200m-2	NP-200m-3	MF-500m-1	MF-500m-2	MF-500m-3	FF-1000m-1	FF-1000m-2	FF-1000m-3	HB-3.5km-1	HB-3.5km-2	HB-3.5km-3	REF-3.5km-1	REF-3.5km-2	REF-3.5km-3	Seawater Blank	Fabrication Blank	Air Blank
Naphthalene	19.3	19	19.6	20.4	19.6	15.4	16.6	17	19.5	19	21.2	21.9	21.7	19.1	17.3	171	45.3	50.8
Acenaphthylene	0	0	1.27	1.22	0	1.14	0	1.31	0	0	0	0	0	0	0	35.7	0	0
Acenaphthene	8.16	8.44	7.62	10.5	7.48	8.14	7.1	10.4	8.45	7.42	8.89	6.95	4.83	5.55	5.77	17.2	4.71	5.82
2-Methylfluorene	5.87	6.78	6.69	4.94	6.42	5.74	5.13	4.39	4.88	11.1	9.27	7.11	5.08	4.55	5.08	0	0	0
C2 Phenanthrenes/Anthracenes	27.4	31.6	34.2	33	32.7	29.2	30.3	28.5	32.2	24.8	26.2	25.1	31.1	26.5	28.1	28.5	6.89	11.2
Fluorene	11.3	61.4	12.3	11.1	11.8	10.5	12.5	13.9	10.4	10.5	10.6	10.9	10.6	9.68	10.1	20.1	7.42	8.2
Phenanthrene	61.8	59.7	63.2	60.7	62	56.1	56.7	66.3	60.7	52	49.7	50.9	51.8	54.7	52	124	40	42
Anthracene	0	1.55	0	1.84	2.01	1.49	0.878	1.65	1.31	1.42	0	1.16	0	0	1.19	7.58	1.39	1.91
C1 Phenanthrenes/Anthracenes	42.5	40.6	43.2	38.7	45.8	41.9	42	41.9	44.3	36.3	34.5	34.8	40	39.7	41.2	61.9	13.7	18.5
Fluoranthene	49.2	50.8	53.9	51.2	55.8	50.6	51	52.8	55.7	43	43.8	41.8	49.1	49.2	45.1	44.2	8.37	7.34
Pyrene	16.7	16.2	16.6	14.8	17.2	14.9	16.1	14.3	15.9	14.3	12.8	12.9	15	15	14	32.7	4.66	3.8
Benz[a]anthracene	0.502	0.442	0	0	0.842	0	0	0.907	0.678	0	0.475	0	0	0	0	1.12	0	0
Chrysene	13.1	14.5	14.5	14.6	15.2	16.6	13.6	16.9	15.7	11.3	12	11.4	12.3	13.1	14.7	3.99	0	0
Benzo[b]fluoranthene	1.37	2.97	1.21	2.51	1.64	2.81	1.26	2.15	2.81	1.06	1.92	1.54	2.17	2.44	2.71	1.85	0	0
Benzo[j,k]fluoranthenes	0.958	1.38	1.31	0	2.04	1.52	2.52	0	1.94	0	0	0	0	0	0	0	0	0
Benzo[e]pyrene	0	1.48	2.02	1.66	2.31	0	1.33	0	1.73	0	1.54	0	2	1.68	0	1.55	0	0
Benzo[a]pyrene	0	0	0	0	0	0	0	0	0	0	0	0	0	0	0	1.93	0	0
Perylene	4.37	3.22	4.25	4.5	4.84	4.7	3.87	3.88	2.88	4.03	3.56	4.79	3.94	5.61	3.28	0	0	0
Dibenz[a,h]anthracene	0	0	0	0	0	0	0	0	0	0	0	0	0	0	0	0	0	0
Indeno[1,2,3-cd]pyrene	1.35	0	0	0	0	0	0	0	0	0	0	0	0	0	0	2.09	0	0
Benzo[g,h,i]perylene	0	0	0	0	0	0	0	0	0	0	0	0	0	0	0	3.96	0	0
2-Methylnaphthalene	12.2	11.9	11.6	12	11.4	11.6	11.2	11.8	11.5	23	23.6	23.2	16.9	15.7	15.4	254	42	90.4
1-Methylnaphthalene	7.64	8.47	7.86	8.34	7.59	8.05	7.85	7.54	8.08	14.7	14.4	14.6	11.2	11.7	10.5	152	21.8	50.8
C1-Naphthalenes	19.9	20.4	19.5	20.3	19	19.6	19	19.3	19.6	37.7	38	37.8	28.1	27.4	25.9	406	63.8	141
Biphenyl	9.3	10.5	10.2	9.5	9.68	9.32	8.94	9.09	9.01	9.37	9.29	8.72	10	9.67	8.82	32.3	12.1	14
C1-Biphenyls	9.97	10.2	10.5	11.7	10.4	9.01	9.69	8.64	10.8	10	11	9.14	10.3	10.8	7.72	44.9	10.9	20.3
C2-Biphenyls	28.5	28	33.2	33.5	28.4	22.8	23.2	20	32.6	25.8	28.6	21.2	29.8	27.2	17.6	73.9	21.5	28.6
C2-Naphthalenes	54.2	52.3	51.8	55.5	53.7	55.2	48.6	49.7	51	65.3	71.7	66.2	61.9	58.8	58.9	642	62	176

Table 44. (Continued).

Compound	NP-200m-1	NP-200m-2	NP-200m-3	MF-500m-1	MF-500m-2	MF-500m-3	FF-1000m-1	FF-1000m-2	FF-1000m-3	HB-3.5km-1	HB-3.5km-2	HB-3.5km-3	REF-3.5km-1	REF-3.5km-2	REF-3.5km-3	Seawater Blank	Fabrication Blank	Air Blank
1,2-Dimethylnaphthalene	0	0	0	0	0	3.43	0	0	0	0	5.27	0	0	0	0	39.8	0	10.3
2,6-Dimethylnaphthalene	8.82	9.77	9.35	9.2	9.96	10.1	10.4	8.54	9.27	13.4	13.6	13.9	12.2	10.7	11.5	170	13.1	42.9
C3-Naphthalenes	67.3	60.3	72.7	55.6	56.4	56.7	56.8	56	61.3	68.6	61.2	68.9	66.6	66.9	59.7	372	36	91.6
2,3,6-Trimethylnaphthalene	16.3	15.5	16.9	14	16.3	14.8	15.4	13.9	15.8	16.7	15.6	16.1	17	18.5	16.2	105	10.4	25.3
2,3,5-Trimethylnaphthalene	11	11.7	12.7	9.95	12.2	9.21	11.4	10.8	12	12	12.2	11.7	11.3	12.7	12	75.7	8.61	18.3
C4-Naphthalenes	43.7	48.2	53	35.9	39.3	38	39.2	33.5	38.1	38.8	37.2	31.4	40.3	37.9	28	138	10.6	29.5
C1-Acenaphthenes	0	0	0	0	0	0	0	0	0	0	0	0	0	0	0	3.7	0	0
C1-Fluorenes	20.1	22.1	19.7	17.6	21.6	19.4	21.5	21.7	20.6	24.8	22.9	22.8	18.8	19.2	20	26.5	4.84	8.75
1,7-Dimethylfluorene	1.91	3.84	3.07	0	0	3.71	3.3	0	0	0	0	0	0	0	0	0	0	0
C2-Fluorenes	39.2	39.6	41.1	36.5	40.6	50.9	51.1	39.3	44.5	32.5	34.3	40.7	32.2	37.7	39.5	38.3	5.91	12.1
C3-Fluorenes	29	32	47.3	33.6	41.3	43	44.7	40.4	35.8	33.3	25.6	35	27.5	23.6	25	48	10.6	3.65
Dibenzothiophene	5.77	5.75	5.53	5.74	6.52	5.65	5.16	5.83	5.96	4.86	4.54	4.68	4.74	4.85	5.08	10.4	3.91	4.65
C1-Dibenzothiophenes	8.37	8.3	8.83	9.13	7.01	8.1	12.5	13.2	12.7	5.38	4.87	5.57	5.83	7.93	6.27	11.5	0	2.35
2/3-Methyldibenzothiophenes	4.9	5.15	5.04	3.31	5.25	4.41	3.87	4.1	3.55	6.72	7.23	5.78	4.4	4.29	3.88	3.81	0	0
C2-Dibenzothiophenes	31.2	29.2	32.4	27.3	29.4	28.7	27.2	26.7	27.6	43	49.8	36.9	28	25.1	25.5	40	10	11.8
2,4-Dimethyldibenzothiophene	5.84	5.38	5.12	0	0	3.06	0	0	0	0	6.48	6.84	0	3.39	0	0	2.29	0
4,6-Dimethyldibenzothiophene	4.99	4.11	5.29	0	0	4.46	4.15	4.39	0	0	0	0	0	3.92	0	6.83	0	0
C3-Dibenzothiophenes	20.2	20.9	19.3	17.9	18.9	22.1	19.9	19.7	18.7	16.7	20.5	20.5	14.1	16.8	13.8	26.4	9.45	9.17
C4-Dibenzothiophenes	13.8	29.8	17.6	6.29	5.38	8.17	2.93	7.66	5.71	7	8.76	6.43	3.23	2.23	2.09	13.3	0	0
3-Methylphenanthrene	10.4	9.39	10.2	9.08	10.2	9.92	10	10.1	10.3	8.36	7.58	8.36	9.14	9.78	9.36	16	3.65	5.79
2-Methylphenanthrene	15.6	14.4	16	14.1	16.7	15.8	15.3	14.6	16.6	12.9	12.5	12.7	13.9	14.2	15.8	21.4	4.96	6.49
2-Methylanthracene	2.68	3.11	2.43	2.96	3.63	3.48	3.94	3.62	4.13	3.05	4.27	2.88	2.75	3.28	2.77	2.4	0	0
9/4-Methylphenanthrene	7.96	8.29	8.62	7.85	9	8.59	8.76	8.52	8.83	7.61	6.87	6.96	8.28	8.48	8.4	12.3	2.57	3.41
1-Methylphenanthrene	8.55	8.52	8.35	7.65	9.82	7.6	7.95	8.77	8.55	7.48	7.56	6.85	8.7	7.22	7.6	9.77	2.52	2.83
3,6-Dimethylphenanthrene	2.85	3.16	4.04	3.46	0	3.47	3.48	3.26	3.91	2.85	2.61	2.74	2.99	3.52	3.4	4.2	0	0
2,6-Dimethylphenanthrene	3.18	3.43	4.02	3.6	0	3.74	2.59	2.77	0	0	3.83	3.31	4.07	3.73	3.15	4.57	0	0
1,7-Dimethylphenanthrene	4.22	5.08	4.88	4.38	5.95	4.48	4.7	4.46	5.39	3.98	3.89	3.61	4.37	4.58	4.46	3.27	1.02	
1,8-Dimethylphenanthrene	0	2.59	3.26	2.57	0	0	0	0	0	0	0	0	0	0	0	0	1.49	3.47
C3-Phenanthrenes/Anthracenes	19.9	12.5	18.3	17	22.8	23.8	21.1	14.7	17.5	8.75	17.1	8.47	15	13	18.4	19.3	0	0
1,2,6-Trimethylphenanthrene	0	0	0	0	0	0	0	0	0	0	0	0	0	0	0	0	0	0

Table 44. (Continued).

Compound	NP-200m-1	NP-200m-2	NP-200m-3	MF-500m-1	MF-500m-2	MF-500m-3	FF-1000m-1	FF-1000m-2	FF-1000m-3	HB-3.5km-1	HB-3.5km-2	HB-3.5km-3	REF-3.5km-1	REF-3.5km-2	REF-3.5km-3	Seawater Blank	Fabrication Blank	Air Blank
Retene	24.6	24.1	18.7	6.63	8.39	7.65	6.7	7.99	8.04	45.3	28.9	20.7	17.6	8.06	7.12	0	0	0
C4-Phenanthrenes/Anthracenes	128	99.8	113	46.6	69.5	86.4	73.3	53.8	54.6	127	105	87.2	72.5	46.9	54.4	14.9	0	4.59
C1-Fluoranthenes/Pyrenes	12.9	13.3	12.3	13.6	14.9	13.2	12.5	12.4	15.9	10.6	11.9	12	11.5	11.2	10.5	9.35	0.877	
3-Methylfluoranthene/Benzo[a]fluorene	6.86	7.76	7.73	7.31	9.26	8	7.8	7.16	7.7	5.81	6.54	5.27	7.14	6.65	6.3	3.99	0	0
C2-Fluoranthenes/Pyrenes	7.94	9.45	12.2	8.87	10.9	9.2	8.47	5.8	9.59	7.64	9.87	6.77	5.92	4.86	2.79	2.88	0	0
C3-Fluoranthenes/Pyrenes	0	0	0	1.55	0	0	0	0	0	0	0	2.07	0	0	0	0	0	0
C4-Fluoranthenes/Pyrenes	0	0	0	0	0	0	0	0	0	0.885	0	0	0	0	0	0	0	0
C1-Benzo[a]anthracenes/Chrysenes	2.32	2.74	1.99	2.57	3.38	2.65	3.28	3.21	2.51	1.67	2.4	1.59	2	2.48	2.28	0	0	0
5/6-Methylchrysene	0	0.736	0	0	0.73	0	0	0	0	0	0	0	0	0	0	0	0	0
1-Methylchrysene	0	0	0	0	1.03	0.842	0	0	0	0	0.531	0	0	0	0	0	0	0
C2-Benzo[a]anthracenes/Chrysenes	0	0	0	0	0	0	0	0	0	0	0	0	0	0	0	0	0	0
5,9-Dimethylchrysene	0	0	0	0	0	0	0	0	0	0	0	0	0	0	0	0	0	0
C3-Benzo[a]anthracenes/Chrysenes	0	0	0	0	0	0	0	0	0	0	0	0	0	0	0	0	0	0
C4-Benzo[a]anthracenes/Chrysenes	0	0	0	0	0	0	0	0	0	0	0	0	0	0	0	0	0	0
C1-Benzofluoranthenes/Benzopyrenes	0	0	0	0	0	0	0	0	0	0	0	0	0	0	0	0	0	0
7-Methylbenzo[a]pyrene	0	0	0	0	0	0	0	0	0	0	0	0	0	0	0	0	0	0
C2-Benzofluoranthenes/Benzopyrenes	0	0	0	0	0	0	0	0	0	0	0	0	0	0	0	0	0	0
1,4,6,7-Tetramethylnaphthalene	0	0	0	2.83	0	2.71	0	2.54	3.32	2.83	0	2.92	0	3.95	0	16	0	0
Fluoranthene d-10	6,090	6,030	5,770	6,050	5,620	7,060	6,090	6,490	5,710	6,300	5,980	6,660	5,920	6,240	8,120	9,110	9,970	9,780
Dibenzo[a,h]anthracene d-14	906	888	876	871	858	851	878	873	888	892	867	900	881	888	813	876	814	901
Anthracene d-10	2,240	2,040	1,940	2,280	1,900	1,900	2,110	1,800	1,870	2,110	1,960	2,330	2,090	2,220	1,960	8,500	8,750	8,970
Accumulated Total PAHs	**996**	**1,042**	**1,047**	**867**	**934**	**942**	**909**	**872**	**910**	**1,003**	**994**	**934**	**890**	**856**	**811**	**3,434**	**509**	**968**

FF = far-field; HB = hardbottom; MF = mid-field; NP = near platform; REF = reference.

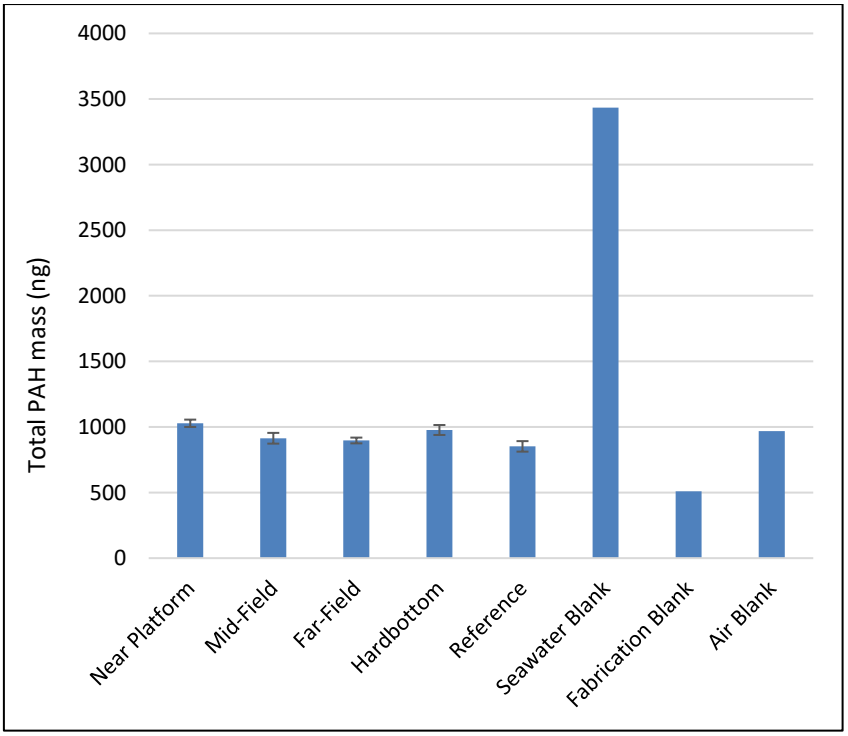


Figure 58. Average (± standard deviation [SD]) accumulated total polycyclic aromatic hydrocarbon (PAH) mass on the semi-permeable passive membrane devices by deployment location after the 43-day deployment near the Leviathan Production Platform. ng = nanograms.

Of the 16 USEPA priority PAHs, phenanthrene and fluoranthene were found with the highest mean mass (57.2 ± 5.2 and 49.5 ± 4.4 ng, respectively) across all deployment locations. This result is the same as was observed during a 2019 deployment of SPMDs at the LPP location prior to commencement of operations at the LPP (MVI, 2020). Three of the 16 USEPA priority PAHs were not detected on any of the three SPMDs (Dibenz(a,h)anthracene, Benzo(a)pyrene, and Benzo(g,h,i)perylene). Indeno(1,2,3,c,d)pyrene was only detected on one of the Near Platform SPMDs. These results are generally consistent with previous SPMD deployment (MVI, 2020) and spot-sampling conducted in the eastern Mediterranean by MVI/CSA during surveys which generally found undetectable or very low PAH concentrations in seawater (e.g., the Tamar Reservoir baseline survey conducted in 2013) (CSA Ocean Sciences Inc., 2014b). However, when detected, previous spot-sampling has generally found naphthalene to be the PAH with the highest concentrations in seawater. These results are consistent with results from the current study where the naphthalenes (including naphthalene, C1-naphthalenes, C2-naphthalenes, C3-naphthalenes, and C4-naphthalense) had some of the highest concentrations of the detected PAHs. Other PAHs included in the 16 USEPA priority list have almost always been undetected in spot sampling. Some of those PAHs (e.g., Benz(a)anthracene, Benzo(j,k)fluoranthene) were detected in low concentrations during the current study, but it must be noted that the SPMDs accumulated PAHs over a 43-day period as opposed to spot sampling which only analyzes an in-situ sample. The general agreement between previous SPMD sampling, spot-sampling and the current SPMD sampling supports the reliability of the SPMD results.

Of the USEPA 16 priority PAHs (gray-shaded in **Table 44**), naphthalene was present in the blanks at many times the mass observed in the deployed SPMDs (**Table 44**). The seawater blank in particular, had a naphthalene mass of 171 ng, as compared with an average of 19.1 ± 1.9 ng across all deployed SPMDs. Previous studies that utilized SPMDs in offshore waters have reported similar results for naphthalene with regards to elevated masses in blanks (e.g., Harman et al., 2010; Boehm et al., 2005). Therefore, considering the precedent of previous studies, naphthalene results from the deployed SPMDs are nonetheless included in the following discussion but these results should not be considered reliable. On the fabrication and air blanks, with the exception of anthracene, the remaining

PAHs (of the USEPA 16 priority PAHs) were either not detected on the blanks (10 PAHs) or were detected in amounts substantially lower than on the deployed SPMDs. The reasons for contamination of the blanks is unknown, but could be some combination of contamination due to vessel exhaust or other sources of hydrocarbons on the vessel (air blank only), or contamination during laboratory analysis or during shipping for the fabrication and air blanks. It should be noted that during both the deployment and recovery field efforts the MVI/CSA team was consistent in following scientific sampling procedures that included, among the rest, use of nitrile gloves when dealing with SPMD samplers, working up wind on the ROV deck to avoid contamination from vessel exhaust, and adherence to strict environmental exposure protocols of the air and seawater blanks. Nevertheless, it is possible that the SPMD were sensitive enough to pick up trace concentrations of hydrocarbons which would result in the reported PAH values.

The accumulated mass for each of the 16 USEPA priority PAH on each SPMD as measured following the deployment (see gray-shaded rows in **Table 44**) was inserted into the USGS (2016) spreadsheet to determine R_s for each targeted analyte and the overall concentration of each analyte in the water column using the PRC data to make appropriate adjustments in the R_s constant. It should be noted that R_s is calculable even if a particular PAH is not detected in the SPMD because R_s is only dependent on the volume of the SPMD sampler, the SPMD water partitioning coefficient and release rate constant for each PRC (see **Section 4.5.2**). R_s values for each of the 16 USEPA priority PAHs for each SPMD is shown in **Table 45**, despite that for SPMDs where any particular PAH was not detected, no concentration is calculable (**Table 46**). **Table 46** presents the calculated seawater concentration of each targeted USEPA priority PAH after the PRC adjustment for each deployed SPMD.

Table 45. Calculated sampling rates of the 16 United States Environmental Protection Agency priority polycyclic aromatic hydrocarbons for each of the 15 deployed semi-permeable passive membrane devices.

Compound	Sampling Rate (R_s; L d^{-1})														
	NP-200m-1	NP-200m-2	NP-200m-3	MF-500m-1	MF-500m-2	MF-500m-3	FF-1000m-1	FF-1000m-2	FF-1000m-3	HB-3.5km-1	HB-3.5km-2	HB-3.5km-3	REF-3.5km-1	REF-3.5km-2	REF-3.5km-3
Naphthalene	2.9	3.2	3.5	3.3	3.7	3.2	3.3	3.3	3.4	3.0	3.5	2.8	3.3	3.1	2.9
Acenaphthylene	5.3	5.8	6.2	5.9	6.7	5.8	5.9	5.9	6.1	5.5	6.2	5.0	6.0	5.6	5.2
Acenaphthene	5.8	6.3	6.8	6.5	7.3	6.3	6.5	6.5	6.7	6.0	6.8	5.5	6.5	6.1	5.7
Fluorene	6.3	6.9	7.5	7.1	8.0	6.9	7.0	7.0	7.3	6.6	7.5	6.0	7.1	6.6	6.3
Phenanthrene	6.6	7.2	7.7	7.4	8.3	7.1	7.3	7.3	7.6	6.8	7.7	6.2	7.4	6.9	6.5
Anthracene	6.8	7.4	8.0	7.6	8.6	7.4	7.6	7.6	7.8	7.0	8.0	6.4	7.6	7.1	6.7
Fluoranthene	7.7	8.4	9.0	8.6	9.7	8.3	8.5	8.5	8.8	7.9	9.0	7.3	8.6	8.0	7.6
Pyrene	7.7	8.4	9.0	8.6	9.6	8.3	8.5	8.5	8.8	7.9	9.0	7.3	8.6	8.0	7.5
Benz[a]anthracene	6.8	7.4	8.0	7.6	8.5	7.3	7.5	7.5	7.8	7.0	8.0	6.4	7.6	7.1	6.7
Chrysene	7.3	8.0	8.8	8.2	9.3	8.0	8.2	8.2	8.5	7.6	8.7	7.0	8.3	7.7	7.2
Benzo[b]fluoranthene	7.1	7.7	8.3	7.9	8.9	7.6	7.8	7.8	8.1	7.3	8.3	6.7	7.9	7.4	7.0
Benzo[k]fluoranthene	6.1	6.6	7.1	6.8	7.6	6.6	6.7	6.7	7.0	6.3	7.1	5.7	6.8	6.3	6.0
Benzo[a]pyrene	5.6	6.2	6.6	6.3	7.1	6.1	6.3	6.3	6.5	5.8	6.7	5.4	6.3	5.9	5.6
Dibenz[a,h]anthracene	5.2	5.7	6.1	5.8	6.6	5.6	5.8	5.8	6.0	5.4	6.1	4.9	5.8	5.5	5.1
Indeno[1,2,3-cd]pyrene	4.5	5.0	5.3	5.1	5.7	4.9	5.0	5.0	5.2	4.7	5.3	4.3	5.1	4.8	4.5
Benzo[g,h,i]perylene	4.1	4.5	4.9	4.6	5.2	4.5	4.6	4.6	4.8	4.3	4.9	3.9	4.6	4.3	4.1

FF = far-field; HB = hardbottom; MF = mid-field; NP = near platform; REF = reference; R_s = Sampling rate.

Table 46. Calculated seawater concentrations of the 16 United States Environmental Protection Agency priority polycyclic aromatic hydrocarbons for each of the 15 deployed semi-permeable passive membrane devices.

Compound	Concentration (ng L^{-1})														
	NP-200m-1	NP-200m-2	NP-200m-3	MF-500m-1	MF-500m-2	MF-500m-3	FF-1000m-1	FF-1000m-2	FF-1000m-3	HB-3.5km-1	HB-3.5km-2	HB-3.5km-3	REF-3.5km-1	REF-3.5km-2	REF-3.5km-3
Naphthalene	1.366	1.345	1.387	1.444	1.387	1.090	1.175	1.203	1.380	1.380	1.500	1.550	1.536	1.352	1.225
Acenaphthylene	--	--	0.019	0.018	--	0.017	--	0.019	--	--	--	--	--	--	--
Acenaphthene	0.092	0.093	0.083	0.116	0.081	0.090	0.078	0.115	0.093	0.095	0.097	0.079	0.053	0.062	0.065
Fluorene	0.097	0.511	0.100	0.092	0.095	0.088	0.104	0.115	0.085	0.088	0.087	0.095	0.088	0.082	0.087
Phenanthrene	0.467	0.438	0.453	0.442	0.436	0.413	0.414	0.484	0.438	0.453	0.356	0.393	0.377	0.407	0.395
Anthracene	--	0.010	--	0.012	0.013	0.010	0.006	0.011	0.008	0.009	--	0.008	--	--	0.008
Fluoranthene	0.196	0.189	0.191	0.188	0.188	0.190	0.188	0.194	0.200	0.216	0.155	0.173	0.179	0.189	0.181
Pyrene	0.064	0.058	0.057	0.052	0.056	0.054	0.057	0.051	0.055	0.060	0.044	0.052	0.053	0.056	0.055
Benz[a]anthracene	0.002	0.002	--	--	0.003	--	--	0.003	0.002	0.003	0.002	--	--	--	--
Chrysene	0.048	0.050	0.046	0.049	0.046	0.057	0.046	0.057	0.052	0.041	0.039	0.044	0.041	0.047	0.055
Benzo[b]fluoranthene	0.005	0.010	0.004	0.009	0.005	0.010	0.004	0.007	0.009	0.010	0.006	0.006	0.007	0.009	0.010
Benzo[k]fluoranthene	0.004	0.005	0.005	0.000	0.007	0.006	0.010	--	0.007	0.008	--	--	--	--	--
Benzo[a]pyrene	--	--	--	--	--	--	--	--	--	--	--	--	--	--	--
Dibenz[a,h]anthracene	--	--	--	--	--	--	--	--	--	--	--	--	--	--	--
Indeno[1,2,3-cd]pyrene	0.007	--	--	--	--	--	--	--	--	--	--	--	--	--	--
Benzo[g,h,i]perylene	--	--	--	--	--	--	--	--	--	--	--	--	--	--	--

-- = not calculable because PAH mass on SPMD was not detected. FF = far-field; HB = hardbottom; MF = mid-field; NP = near platform; REF = reference.

Figure 59 presents a graphic representation of the seven PAHs with the highest calculated concentrations as detected by the SPMDs. There were no obvious trends in PAH concentrations by deployment location except for a small spike in fluorene in the Near Platform deployment location. Upon inspection of the laboratory's data, this data point was qualified in analysis of this sample, a peak was detected but it was outside quantification limits and the reported value was an estimate of the highest possible PAH mass. Therefore, it is likely that the fluorene mass reported for this sample (61.4 ng) is overestimated and is not a true representation of fluorene at the Near Platform deployment location. The fluorene mass values at the other two SPMDs deployed at the Near Platform location (11.3 and 12.3 ng) were much lower and likely a more accurate representation of true values.

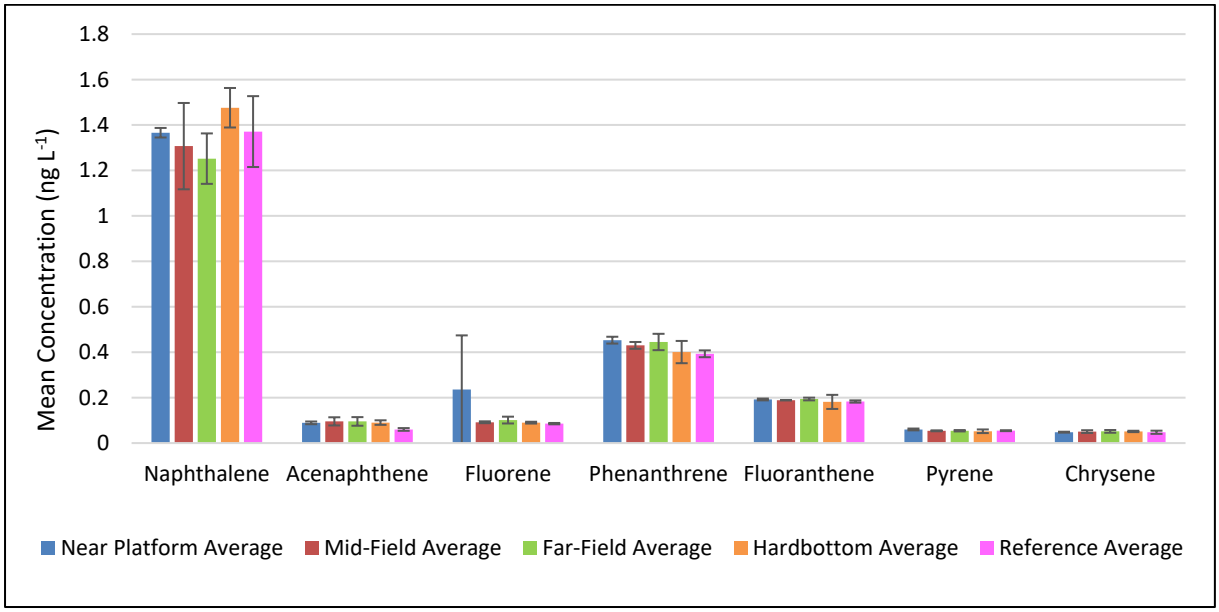


Figure 59. Average (± standard deviation [SD]) calculated concentrations (ng L^{-1}) of the seven highest-concentration PAHs as detected by the semi-permeable passive membrane devices after the 43-day deployment near the Leviathan Production Platform. ng = nanograms.

Table 47 presents the PRC-adjusted mean concentration (among the triplicates at each deployment location) for each of the 16 USEPA priority PAHs compared with previous studies that utilized SPMDs to measure PAH concentrations. Other than the previous MVI/CSA deployment of SPMDs near the LPP location for Noble in 2019 (MVI, 2020), there are no known studies which have utilized SPMDs to measure PAH concentrations in the eastern Mediterranean Sea, although Marrucci et al. (2013) used SPMDs to monitor PAH concentrations offshore of Sardinia in the western Mediterranean and David et al. (2010) used SPMDs to compare PAH concentrations in passive samplers and mussels in French lagoons. Values from these studies are not included in **Table 47** because the studies were conducted in very shallow coastal lagoons and embayments and are not considered to be equitable with the current study.

The concentrations from the published studies presented in **Table 47** are from reference locations presumed to be free of contamination from anthropogenic sources. It should be noted that three of the reference concentrations presented in **Table 47** are from studies in the North Sea and did not use PRCs to calculate *Rs* (Durrell et al., 2006; Harman et al., 2009; and Harman et al., 2011), while the calculations from the present study and MVI (2020) did use PRCs. The studies from the North Sea utilized *Rs* values from previously published laboratory studies (i.e., Huckins et al., 2006).

Table 47. Calculated mean seawater concentrations (± standard deviation) of the 16 United States Environmental Protection Agency priority polycyclic aromatic hydrocarbons for each of the 15 deployed semi-permeable passive membrane devices (SPMDs) and reference concentrations of PAHs in seawater taken from three published literature sources and MVI (2020).

Compound	2020 Deployment Mean Concentration ± SD (ng L^{-1})					Published/Gray Literature Reference Concentrations			
	Near Platform Mean ± SD	Mid-Field Mean ± SD	Far-Field Mean ± SD	Hardbottom Mean ± SD	Reference Mean ± SD	Mean Reference Concentration (n=2) (ng L^{-1}) From: Durrell et al. (2006)	Reference Concentration (ng L^{-1}) From: Harman et al. (2009)	Reference Concentration (ng L^{-1}) From: Harman et al. (2011)	Mean Reference Concentration ± SD (ng L^{-1}) From: MVI (2020)
Naphthalene	1.37 ± 0.02	1.31 ± 0.19	1.25 ± 0.11	1.48 ± 0.09	1.37 ± 0.16	6.11	1.1	[a]	0.833 ± 0.10
Acenaphthylene	0.006 ± 0.01	0.012 ± 0.01	0.006 ± 0.01	0	0	0.02	ND	0.038	0
Acenaphthene	0.089 ± 0.01	0.096 ± 0.018	0.095 ± 0.02	0.090 ± 0.01	0.060 ± 0.006	0.07	0.2	--	0.059 ± 0.02
Fluorene	0.236 ± 0.24	0.092 ± 0.004	0.101 ± 0.02	0.090 ± 0.004	0.086 ± 0.003	0.405	0.5	0.390	0.058 ± 0.03
Phenanthrene	0.453 ± 0.02	0.430 ± 0.015	0.445 ± 0.036	0.401 ± 0.049	0.393 ± 0.015	0.485	1.3	0.270	0.0357 ± 0.07
Anthracene	0.003 ± 0.01	0.012 ± 0.002	0.008 ± 0.003	0.006 ± 0.005	0.003 ± 0.005	0.005	0.1	0.196	0.003 ± 0.005
Fluoranthene	0.192 ± 0.004	0.189 ± 0.001	0.194 ± 0.006	0.181 ± 0.031	0.183 ± 0.005	0.425	--	0.385	0.141 ± 0.02
Pyrene	0.06 ± 0.004	0.054 ± 0.002	0.054 ± 0.003	0.052 ± 0.008	0.055 ± 0.002	0.03	0.3	0.119	0.050 ± 0.005
Chrysene	0.048 ± 0.002	0.051 ± 0.006	0.052 ± 0.006	0.041 ± 0.03	0.048 ± 0.007	0.135	--	0.032	0.026 ± 0.006
Benz[a]anthracene	0.001 ± 0.001	0.001 ± 0.002	0.002 ± 0.002	0.002 ± 0.002	0	0.015	--	0.011	0
Benzo[b]fluoranthene	0.006 ± 0.003	0.008 ± 0.003	0.007 ± 0.003	0.007 ± 0.002	0.009 ± 0.002	0.03	--	0.008	0
Benzo[k]fluoranthene	0.005 ± 0.001	0.004 ± 0.004	0.006 ± 0.005	0.003 ± 0.005	0	0.025	--	0.004	0
Benzo[a]pyrene	0	0	0	0	0	0.005	--	0.001	0
Dibenz[a,h]anthracene	0	0	0	0	0	0	--	<0.031	0
Indeno[1,2,3-cd]pyrene	0.45 ± 0.78	0	0	0	0	0.01	--	<0.021	0
Benzo[g,h,i]perylene	0	0	0	0	0	0.02	--	<0.034	0

As depicted in **Table 47,** PAH concentrations as measured by SPMDs during the 2020 deployment are generally similar to or lower than the reference concentrations in the North Sea published by Harman et al. (2009; 2011) and Durrell et al. (2006). These papers, among others (e.g., Huckins et el., 2002), compared SPMD results with *in situ* bioaccumulation of PAHs in biota (namely mussels and fish). Overall, published literature concurs that the use of SPMDs or other passive samplers are generally a good proxy for the estimation of bioaccumulation of up to four-ring PAHs in fish and mussels.

Mean concentrations across all deployment locations were also similar to MVI (2020) reported concentrations, with the exception of naphthalene which was somewhat higher during the current study (**Figure 60**). However, the naphthalene concentration is still substantially lower than the reference concentration reported by Durrell et al. (2006), and roughly equivalent to the reference values reported by Harman et al. (2009; 2011) (**Table 47**). It should also be noted that only three SPMDs were deployed during the MVI (2020) study and they were located in a different location than the deployment locations for the current study.

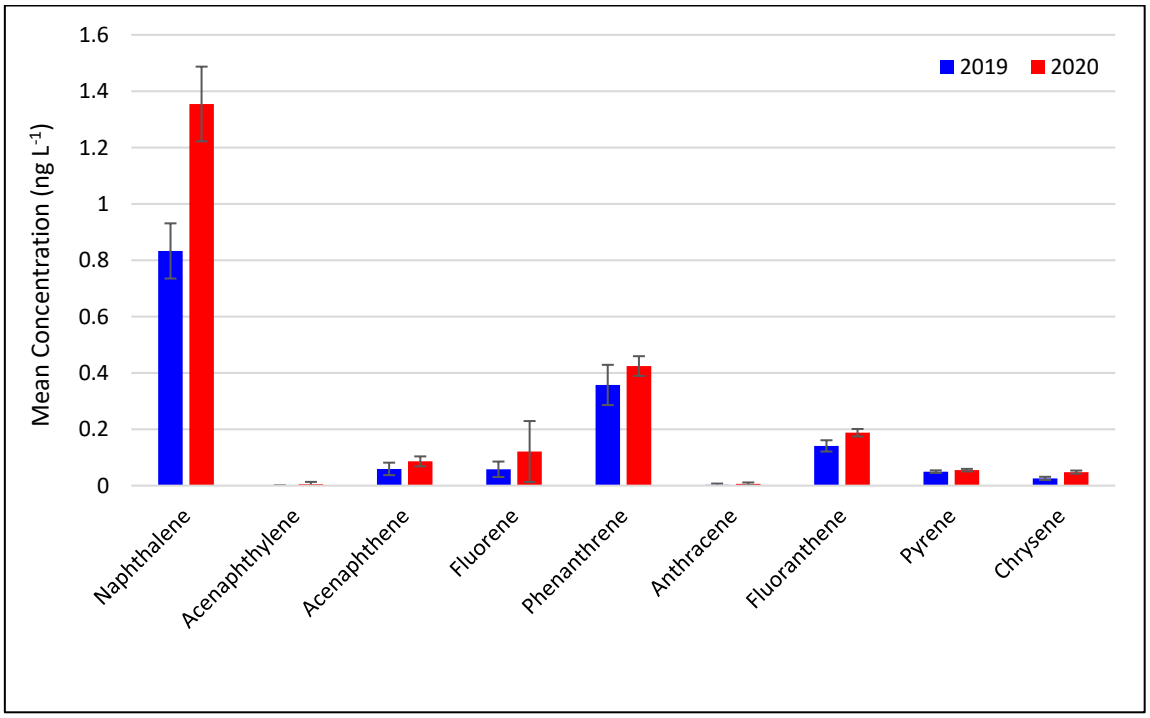


Figure 60. Average (± standard deviation [SD]) calculated concentrations (ng L^{-1}) of the seven highest-concentration PAHs as detected by the semi-permeable passive membrane devices during the 2019 and 2020 deployments in the vicinity of the Leviathan Production Platform.

It is important to note that the calculated seawater concentrations from the SPMDs are the result of the sum of the accumulated PAH mass over the 43-day deployment and are not directly comparable to results from an *in situ* spot-sample. However, all PAH concentrations were well below the European Commission Environmental Quality Standard's annual average concentration (2,000 ng L^{-1}) and the lowest marine Criterion Continuous Concentration (an estimate of the highest concentration of a material in water that an aquatic community can be exposed to indefinitely without resulting in unacceptable adverse effects) of 1,400 ng L^{-1} for naphthalene (Buchman, 2008). Overall, the bioavailable concentrations of PAHs in seawater in the vicinity of the LPP are consistent with concentrations in previously published literature and are likely indicative of unpolluted conditions.

6 References

Agency for Toxic Substances and Disease Registry. 1990. Toxicological profile for thorium. www.atsdr.cdc.gov/toxprofiles/tp147.pdf.

Ajemian, M.J., Wetz, J.J., and Shipley, J.B. 2015. An analysis of artificial reef fish community structure along the northwestern Gulf of Mexico shelf: Potential impacts of "rigs-to-reefs" programs. PLoS One 10. e0126354.

Alvarez, D. 2010. Guidelines for the use of the semipermeable membrane device (SPMD) and the polar organic chemical integrative sampler (POCIS) in environmental monitoring studies. U.S. Geological Survey, Techniques and Methods 1-D4. Reston, Virginia. 28 p.

Alvarez, D. 2019. Passive sampling devices for environmental monitoring: Tips for a successful study. Webinar presented by the National Water Quality Monitoring Council. 16 April 2019. https://acwi.gov/monitoring/webinars/index.html

Azzurro, E., B. Stancanelli, V. Di Martino, and M. Bariche. 2017. Range expansion of the common lionfish *Pterois miles* (Bennett, 1828) in the Mediterranean Sea: an unwanted new guest for Italian waters. BioInvasions Records 6(2): 95-98.

Balthis, W.L., J.L. Hyland, C. Cooksey, P.A. Montagna, J.G. Baguley, R. W. Ricker, and C. Lewis. 2016. Sediment quality benchmarks for assessing oil-related impacts to the deep-sea benthos. Integrated Environmental Assessment and Management 13(5): 840-851.

Boehm, P.D., D.S. Page, J.S. Brown, J.M. Neff, and A.E. Bence. 2005. Comparison of mussels and semi-permeable membrane devices as intertidal monitors of polycyclic aromatic hydrocarbons at oil spill sites. Marine Pollution Bulletin 50(7): 740-750.

Booij, K., H.M. Sleiderink, and F. Smedes. 1998. Calibrating the uptake kinetics of semipermeable membrane devices using exposure standards. Environmental Toxicology and Chemistry 17: 1236-1245.

Bray, J.R. and J.T. Curtis. 1957. An ordination of the upland forest communities of southern Wisconsin. Ecological Monographs 29(1):325-349.

Braun-Blanquet, J. 1964. Pflanzensoziologie, Grundzüge der Vegetationskunde. 3rd edition. Vienna, Austria, Springer. 865 pp.

Buchman, M.F. 2008. Screening quick reference tables. NOAA Office of Response and Restoration. NOAA OR&R Report 08-1. 34 pp.

Carpenter, C. and N. De Angelis (eds.). 2016. The Living Marine Resources of the Eastern Central Atlantic. Vol. 3: Bone Fishes Prt 1 (*Elopiformes* to *Scorpaeniformes*). FAO Species Identification Guide for Fishery Purposes. Rome, Italy. pp. 1,511-2,350.

Clarke, K.R. 1993. Non-parametric multivariate analyses of changes in community structure. Australian Journal of Ecology 18:117-143.

Clarke, K.R. and R.N. Gorley. 2006. PRIMER version 6. User manual/Tutorial. Primer-E Ltd: Plymouth, U.K. 190 pp.

CSA Ocean Sciences Inc. 2014a. Leviathan Field Development Environmental Baseline Survey. Prepared for Noble Energy Mediterranean Ltd.

CSA Ocean Sciences Inc. 2014b. Tamar Field background monitoring survey report. Prepared for Noble Energy Mediterranean Ltd. Document No. CSA-Noble-FL-14-2650-06-REP-VER02.

Consoli, P., T. Romeo, M. Ferraro, G. Sarà, and F. Andaloro. 2013. Factors affecting fish assemblages associated with gas platforms in the Mediterranean Sea. Journal of Sea Research 77:45-52.

David, A., E. Gomez, S. Aïm-Aïssa, M. Bachelot, D. Rosain, C. Casellas, and H. Fenet. 2010. Monitoring organic contaminants in small French coastal lagoons: comparison of levels in mussel, passive sampler and sediment. Journal of Environmental Monitoring 12: 1,471-,1481.

Davison, W. Ed. 2016. Diffusive Gradients in Thin-Films for Environmental Measures. Cambridge University Press, Cambridge, United Kingdom.

DGT Research Ltd. (DGT). nd. General Guide for Using DGT Passive Samplers in Waters. https://www.dgtresearch.com/wp-content/uploads/2020/11/waters-181120.pdf.

Docekalová, H. and P. Divis. 2005. Application of diffusive gradient in thin films technique (DGT) to measurement of mercury in aquatic systems. Talanta 65(5):1,174-1,178.

Durell, G., T.R. Utvik, S. Johnsen, T. Frost, and J. Neff. 2006. Oil well produced water discharges to the North Sea. Part I: Comparison of deployed mussels (*Mytilus edulis*), semi-permeable membrane devices, and the DREAM model predictions to estimate dispersion of polycyclic aromatic hydrocarbons. Marine Environmental Research 62:194-223.

English, S., C. Wilkinson, and V. Baker. 1997. Survey manual for tropical marine resources, 2nd ed. Australian Institute of Marine Science, Townsville. 390 pp.

Fabi, G., F. Grati, A. Lucchetti, and L. Trovarelli. 2002. Evolution of the fish assemblage around a gas platform in the northern Adriatic Sea. ICES Journal of Marine Science 59:S309–S315.

Fabi, G., F. Grati, M. Puletti, and G. Scarcella. 2004. Effects on fish community induced by installation of two gas platforms in the Adriatic Sea. Marine Ecology Progress Series 273:187–197.

Folk, R.L. 1954. The distinction between grain size and mineral composition in sedimentary rock nomenclature. Journal of Geology 62(4):344-359.

Folk, R.L. 1974. The petrology of sedimentary rocks. Austin, TX, Hemphill Publishing Co. 182 pp.

Fugro Global Environmental & Ocean Sciences Ltd. 2001. Metocean data for the Mari-B Platform Fugro GEOS Reference No: C56021\2195\F0.

Gert-Jan de Maagd, P. 2009. Bioaccumulation tests applied in whole effluent assessment: A review. Environmental Toxicology and Chemistry 19(1): 25-35.

Golani, D., and O. Sonin. 1992. New records of the Red Sea fishes, *Pterois miles* (Scorpaenidae) and *Pteragogus pelycus* (Labridae) from the eastern Mediterranean Sea. Japanese Journal of Ichthyology 39(2):167-169.

Green, D.R., J.K. Stull, and T. H. Heesen. 1986. Determination of chlorinated hydrocarbons in coastal waters using a moored *in situ* sampler and transplanted live mussels. Marine Pollution Bulletin 176(7): 324-329.

Hale, S.E., A.M.P. Oen, G. Cornelissen, M.T.O. Jonker, I.K. Waarum, and E. Eek. 2016. The role of passive sampling in monitoring the environmental impacts of produced water discharges from the Norwegian oil and gas industry. Marine Pollution Bulletin 111: 33-40.

Harman, C., K. Hylland, T.F. Holth, and K.V. Thomas. 2009. Relationship between polycyclic aromatic hydrocarbon (PAH) accumulation in semipermeable membrane devices and PAH bile metabolite levels in Atlantic cod (*Gadus morhua*). Journal of Toxicology and Environmental Health, Part A 72(3): 234-243.

Harman, C., K.E. Tollefsen, and E. Farmen. 2010. Monitoring North Sea oil production discharges using passive sampling devices coupled with in vitro bioassay techniques. Journal of Environmental Monitoring 12: 1699-1708.

Harman, C., S. Brooks, R.C. Sundt, S. Meier, and M. Grung. 2011. Field comparison of passive sampling and biological approaches for measuring exposure to PAH and alkylphenols from offshore produced water discharges. Marine Pollution Bulletin 63(5-12): 141-148.

Herut, B. and A. Sandler. 2006. Normalization methods for pollutants in marine sediments: review and recommendations for the Mediterranean. Israel Oceanographic and Limnological Research (IOLR). Haifa, Israel. Report H18/2006. 23 pp.

Huckins, J.N., G.K. Manuweera, J.D. Petty, D. Mackay, and J.A. Lebo. 1993. Lipid-containing semipermeable membrane devices for monitoring organic contaminants in water. Environmental Science and Technology 27: 2489-2496.

Huckins, J.N., J.D. Petty, J.A. Lebo, F.V. Almeida, K. Booij, D.A. Alvarez, W.L. Cranor, R.C. Clark, and B.B. Morgensen. 2002. Development of the permeability/performance reference compound approach for an in situ calibration of semipermeable membrane devices. Environmental Science and Technology 36: 85-91.

Huckins, J.N., J.D. Petty, and K. Booij. 2006. Monitors of organic chemicals in the environment: semipermeable membrane devices. Springer, New York, New York. 223 p.

Israel Oceanographic and Limnological Research Institute (IOLR). 2017. The National Monitoring Program of Israel's Mediterranean Waters, Scientific Report for 2016, Part III: Sea Pollution Monitoring. Israel Oceanographic and Limnological Research Ltd. IOLR Report H38C/2017.

Israel Oceanographic and Limnological Research Institute (IOLR). 2020. The National Monitoring Program of Israel's Mediterranean Waters, Scientific Report for 2018-2019 Part III: Sea Pollution Monitoring. Israel Oceanographic and Limnological Research Ltd. IOLR Report H8/2020.

Kim, M.S., M.S. Choi, and C.K. Kim. 2016. Monitoring trace metals in seawater using diffusive gradient in thin film probe in Ulsan Bay, East Sea, Korea: Comparison with transplanted mussels. Ocean Science Journal 51: 169-182.

Kletou, D., J.M. Hall-Spencer, and P. Kleitou. 2016. A lionfish (*Pterois miles*) invasion has begun in the Mediterranean Sea. Marine Biodiversity Records 9(1):46.

Long, E.R. and L.G. Morgan. 1990. The potential for biological effects of sediment-sorbed contaminants tested in the National Status and Trends Program. U.S. National Oceanic and Atmospheric Administration. Seattle, WA. NOAA Technical Memorandum NOS OMA 52. 233 pp.

Margalef, R. 1958. Information theory in ecology. General Systems 3:36-71.

Marine Ventures International, Inc. (MVI). 2018. Leviathan Production Platform Visual Reconnaissance Survey Report, ROV Survey for Suspected Hardbottom. Prepared for Noble Energy Mediterranean Ltd. 32 pp. + apps.

Marine Ventures International, Inc. (MVI). 2019a. Environmental Monitoring Program, Leviathan Production Platform, Offshore Israel. July/August 2019 Marine Environmental Baseline Survey Report. Prepared for Noble Energy Mediterranean Ltd.

Marine Ventures International, Inc. (MVI). 2019b. Mari-B/Tamar Production Platforms Environmental Monitoring Program, Offshore Israel. January/February 2019 Platform Survey. Prepared for Noble Energy Mediterranean Ltd.

Marine Ventures International, Inc (MVI). 2019c. Leviathan Production Platform Post-Installation Qualitative Survey Report, ROV Hardbottom Survey. Prepared for Noble Energy Mediterranean Ltd. 32 pp. + apps.

Marrucci, A., B. Marras, S.S. Campisi, and M. Schintu. 2013. Using SPMDs to monitor seawater concentrations of PAHs and PCBs in marine protected areas (Western Mediterranean). Marine Pollution Bulletin 75:69-75.

Ministry of the Environment. 2002. Environmental Quality Standards for the Mediterranean Sea in Israel. State of Israel. Ministry of the Environment. Marine and Coastal Environment Division 36 pp.

Naidu, M. and O. Kumar. 2016. Tree diversity, stand structure, and community composition of tropical forests in eastern Ghats of Andrha Pradesh, India. Journal of Asia-Pacific Biodiversity 9(3):328-334.

Oliver, I. and A.J. Beattie. 1996. Invertebrate morphospecies as surrogates for species: a case study. Conservation Biology 10(1):99-109.

Özbek, E. Ö., S. Mavruk, İ. Saygu, and B. Öztürk. 2017. Lionfish distribution in the eastern Mediterranean coast of Turkey. Journal of the Black Sea/Mediterranean Environment 23:1-16.

Roper, J.M., D.S. Cherry, D.S., J.W. Simmers, and H.E. Tatem. 1997.. Bioaccumulation of PAHs in the Zebra Mussel at Times Beach, Buffalo, New York. Environmental Monitoring and Assessment 46: 267–277.

Rosen, S.D., L. Raskin, and B. Galanti. 2013. Long-term characteristics of sea level, wave, wind, and current at central Mediterranean coast of Israel from 20 years of data at Gloss Station Hadera. 40th CIESM Congress, Marseille, France. Volume 40:157. October 2013.

Salazar, S. and S. Salazar. 1995. *In-Situ* bioassays using transplanted mussels: I. Estimating chemical exposure and bioeffects with bioaccumulation and grow. In: *Environmental Toxicology and Risk Assessment: Third Volume,* eds. J. Hughes, G. Biddinger, and E. Mones. West Conshohocken, Pennsylvania.

Scarcella, G., F. Grati, and G. Fabi. 2011. Temporal and spatial variation of the fish assemblage around a gas platform in the northern Adriatic Sea, Italy. Turkish Journal of Fisheries and Aquatic Sciences 11:433-444.

Schintu, M., B. Marras, L. Durante, P. Meloni, and A. Contu. 2009. Macroalgae and DGT as indicators of available trace metals in marine coastal waters near a lead-zinc smelter. Environmental Monitoring and Assessment 167(1-4): 653-661.

Shepard, F.P. 1954. Nomenclature based on sediment: H-clay ratios. Journal of Sedimentary Petrology 24:151-158.

Stanley, D.R. and C.A. Wilson. 2000. Seasonal and Spatial Variation in the Biomass and Size Frequency Distribution of the Fish Associated With Oil and Gas Platforms in the Northern Gulf of Mexico. U.S. Department of Commerce. Minerals Management Service. New Orleans, LA. OCS Study MMS 2000-005. 252 pp.

Sugimura, Y. and Y. Suzuki. 1988. A high temperature catalytic oxidation method for the determination of non-volatile dissolved organic carbon in seawater by direct injection of a liquid sample. Marine Chemistry 24:105-131.

Trefry, J.H., K.H. Dunton, R.P. Trocine, S.V. Schonberg, N.D. McTigue, E.S. Hersh, and T.J. McDonald. 2013. Chemical and biological assessment of two offshore drilling sites in the Alaskan Arctic. Marine Environmental Research 86:35-45.

Trefry, J.H., R.D. Rember, R.P. Trocine, and J.S. Brown. 2003. Trace metals in sediments near offshore oil exploration and production sites in the Alaskan Arctic. Environmental Geology 45:149-160.

University of Haifa. 2021. University of Haifa – Eastern Mediterranean Observatory (THEMO) Project. http://themo.haifa.ac.il/#.

U.S. Environmental Protection Agency. 1992. Specifications and guidance for contaminant-free sample containers. EPA Publication 9410.0-05A. Office of Solids Waste and Emergency Response, Washington, DC, USA.

U.S. Environmental Protection Agency. 1998. Memorandum on Use of Soil Cleanup Criteria in 40 CFR Part 192 as Remediation Goals for CERCLA Sites. Directive No. 9200.4-25.

U.S. Environmental Protection Agency. 2001. Methods for collection, storage and manipulation of sediments for chemical and toxicological analysis. EPA-823-B-01-002. Office of Water, Washington, DC, USA. 208 pp.

U.S. Geological Survey (USGS). 1999. Naturally occurring radioactive materials (NORM) in produced water and oil field equipment - An issue for the energy industry. http://pubs.usgs.gov/fs/fs-0142-99/fs-0142-99.pdf. USGS Fact Sheet FS–142–99.

U.S. Geological Survey (USGS). 2000. Interagency Field Manual for the Collection of Water-Quality Data. Open-File Report 00-213. Compiled by D.L. Lurry and C.M. Kolbe. U.S. Geological Survey, in cooperation with the U.S. Environmental Protection Agency, Austin, TX. 77 pp.

U.S. Geological Survey (USGS). 2016. Estimated water concentration calculator from SPMD data using PRCs. https://www.usgs.gov/centers/cerc/science/passive-sampling-using-spmds-and-pocis?qt-science_center_objects=0#qt-science_center_objects.

Veil, J.A., T.A. Kimmell, and A.C. Rechner. 2005. Characteristics of produced water discharged to the Gulf of Mexico hypoxic zone. ANL/EAD/05-3. 76 pp.

Wallner-Kersanach, M., C.F.F. de Andrade, H. Zhang, M.R. Milani, and L.F.H. Niencheski. 2009. *In situ* measurement of trace metals in estuarine waters of Patos Lagoos using diffusive gradients in thin films (DGT). Journal of the Brazilian Chemical Society 20(2): 333-340.

Wilson, C.A., M.W. Miller, Y.C. Allen, K.M. Boswell, and D.L. Nieland. 2006. Effects of Depth, Location, and Habitat Type on Relative Abundance and Species Composition of Fishes Associated with Petroleum Platforms and Sonnier Bank in the Northern Gulf of Mexico. U.S. Department of Commerce. Minerals Management Service. New Orleans, LA. OCS Study MMS 2006-037. 85 pp.

Wirtz, P. and H. Debelius. 2003. Mediterranean and Atlantic Invertebrate Guide. Hollywood Import & Export, Inc. Gainesville, FL. 304 pp.

Zenetos, A., M.E. Çinar, M.A. Pancucci-Papadopoulou, J.G. Harmelin, G. Furnari, F. Andaloro, N. Bellou, N. Streftaris, and H. Zibrowius. 2005. Annotated list of marine alien species in the Mediterranean with records of the worst invasive species. Mediterranean Marine Science 6(2):63-118.

Appendices

Appendix A

2019 Leviathan Production Platform Environmental Baseline Survey Scope of Work

Appendix B

Discharge Reports

Appendix C

Sampling Station Geographic Coordinates

Appendix D

Nor Naomi Vessel Specifications

Appendix E

Water Column Profiles

Appendix F

Analytical Datasheets: Seawater Hydrocarbons

Appendix G

Analytical Datasheets: Seawater Total Nitrogen, Total Phosphorous, Total Organic Carbon, Nutrients and Total Suspended Solids

Appendix H

Analytical Datasheets: Seawater Radionuclides

Appendix I

Analytical Datasheets: Sediment Grain Size

Appendix J

Analytical Datasheets: Sediment Total Organic Carbon

Appendix K

Analytical Datasheets: Sediment Metals

Appendix L

Analytical Datasheets: Sediment Hydrocarbons

Appendix M

Analytical Datasheets: Sediment Radionuclides

Appendix N

Analytical Datasheets: Infauna

Appendix O

Analytical Datasheets: DGT Samplers

Appendix P

Analytical Datasheets: SPMD Samplers